

**MODELING OF DYNAMIC FRICTION, IMPACT BACKLASH AND  
ELASTIC COMPLIANCE NONLINEARITIES IN MACHINE TOOLS,  
WITH APPLICATIONS TO ASYMMETRIC VISCOUS AND  
KINETIC FRICTION IDENTIFICATION**

by

Julian Andrew de Marchi

A Thesis Submitted to the Graduate Faculty  
of Rensselær Polytechnic Institute

in Partial Fulfillment of the Requirements for the Degree of  
**DOCTOR OF PHILOSOPHY**

Major Subject: Mechanical Engineering

The original of the complete thesis is on file  
in the Rensselær Polytechnic Institute Library

Examining Committee:

Kevin C. Craig, Thesis advisor

C. James Li, Member

Daniel F. Walczyk, Member

James J. Napolitano, Member

Rensselær Polytechnic Institute  
Troy, New York

December 1998

*The original of this thesis is printed on 20% recycled archival flax.*

© Copyright 1998  
by  
Julian Andrew de Marchi  
All Rights Reserved

# Contents

LIST OF TABLES . . . . .	viii
LIST OF FIGURES . . . . .	ix
Personal Acknowledgments . . . . .	x
Professional Acknowledgments . . . . .	xiii
Preface . . . . .	xiv
Abstract . . . . .	xvii
Abbreviations and Nomenclature . . . . .	xix
0.1 Mathematical Nomenclature . . . . .	xix
0.2 Acronyms . . . . .	xix
0.3 Regarding Representation of the Friction Forces and Torques. . . . .	xx
1. Introduction and Historical Review. . . . .	1
1.1 A Discussion of the Three Basic Drive Nonlinearities. . . . .	1
1.1.1 Friction. . . . .	1
1.1.1.1 What Exactly is Friction? . . . . .	2
1.1.1.2 The Classical Friction Model: Static + Dynamic + Viscous Frictions. . . . .	4
1.1.1.3 The Modern Friction Model: Rolling, Stribeck, Stick-Slip, and Hydraulic Frictions. . . . .	10
1.1.2 Backlash. . . . .	19
1.1.2.1 What is Backlash? . . . . .	20
1.1.2.2 The Classical Backlash Model. . . . .	20
1.1.2.3 The Modern Backlash Model. . . . .	22
1.1.3 Compliance. . . . .	22
1.1.3.1 What is Compliance? . . . . .	23
1.1.3.2 The Classical Compliance Model. . . . .	24
1.1.3.3 The Modern Compliance Model. . . . .	25
1.1.4 Motivation for the Study of Friction, Backlash and Compliance. . . . .	27
1.1.4.1 Understanding Friction. . . . .	28
1.1.4.2 Understanding Backlash. . . . .	28
1.1.4.3 Understanding Compliance. . . . .	29
1.2 Current Trends in Nonlinear Drive Research. . . . .	29
1.2.1 Shortcomings in Current Research and Technology. . . . .	30

1.2.1.1	Social, Economic and Political Factors. . . . .	30
1.2.1.2	Scientific Factors. . . . .	32
1.2.2	Trends in Friction Research. . . . .	33
1.2.2.1	Transdisciplinary Trends in Machine Lubrication, Material Surface Science, Nanotribology and Wear Modeling. . . . .	34
1.2.2.2	Trends in Macroscopic Friction Modeling. . . . .	35
1.2.2.3	Trends Towards the Controllability of Friction. . . . .	36
1.2.3	Trends in Backlash Research. . . . .	38
1.2.4	Trends in Compliance Research. . . . .	38
1.2.5	Composite Models for Friction, Backlash and Compliance. . . . .	39
1.2.6	The Problem as it Pertains to Machine Tool Technology. . . . .	41
1.2.7	Trends in Machine Tool Research. . . . .	44
1.2.7.1	How are National Research Institutions Addressing the Problem? . . . . .	44
1.2.7.2	How is Rensselær Addressing the Problem? . . . . .	44
1.2.8	Mechatronic Solutions for Drive Nonlinearity. . . . .	46
1.3	Unique Contributions of This Work. . . . .	48
2.	Theory. . . . .	52
2.1	Models for Drive Nonlinearities. . . . .	52
2.1.1	The State-of-the-Art Friction Model. . . . .	52
2.1.1.1	The Stribeck Effect. . . . .	53
2.1.1.2	Rising and Stick-Slip Frictions. . . . .	57
2.1.1.3	Frictional Memory. . . . .	60
2.1.1.4	Presliding Displacement. . . . .	61
2.1.1.5	“Normal” Friction. . . . .	64
2.1.1.6	Full Dynamic Friction Model. . . . .	66
2.1.2	The State-of-the-Art Backlash Model. . . . .	68
2.1.2.1	Deadband Model. . . . .	68
2.1.2.2	Impact Model. . . . .	70
2.1.2.3	Duration of Impact. . . . .	77
2.1.3	The State-of-the-Art Compliance Model. . . . .	80
2.1.3.1	Summed Normal Mode Approximation. . . . .	81
2.1.3.2	Proportional Damping. . . . .	83
2.1.3.3	Shaft Boundary Conditions. . . . .	84
2.1.3.4	Nonlinear Fundamental Mode Approximation. . . . .	85
2.1.4	A Lumped Model for Drive Nonlinearities. . . . .	86
2.1.4.1	Drive Motor Subsystem. . . . .	87
2.1.4.2	Shaft Subsystem. . . . .	91

2.1.4.3	Transmission Subsystem. . . . .	96
2.2	Identification of Drive Nonlinearities. . . . .	98
2.2.1	System Identification Methods. . . . .	98
2.2.2	Simple Harmonic Motion . . . . .	100
2.2.3	Transient (Unforced) Harmonic Oscillation . . . . .	101
2.2.3.1	Overdamped Response . . . . .	102
2.2.3.2	Critically-damped Response . . . . .	102
2.2.3.3	Underdamped Response . . . . .	103
2.2.4	Asymmetric Harmonic Motion . . . . .	103
2.2.5	The Logarithmic Decrement Method . . . . .	104
2.2.5.1	The Logarithmic Decrement . . . . .	104
2.2.5.2	Asymmetric Friction Estimation . . . . .	105
2.2.5.3	Identification Procedure . . . . .	107
2.2.6	Forced Harmonic Oscillation . . . . .	108
2.2.7	Parametric Harmonic Oscillation Using PD Feedback . . . . .	108
2.2.7.1	(Pseudo-) Free Parametric Harmonic Oscillation . . . . .	110
2.2.7.2	Forced Parametric Harmonic Oscillation . . . . .	112
2.2.8	Analytic Signals and Describing Functions. . . . .	112
2.2.9	Hilbert Transform. . . . .	114
2.2.9.1	Evaluation of the Instantaneous Amplitude and Phase . . . . .	118
2.2.9.2	Application to Linear and Quasi-Linear Second-Order Systems . . . . .	118
2.2.10	Wavelet Transformation. . . . .	119
2.2.10.1	The Morlet Wavelet . . . . .	119
2.2.10.2	The Morlet Wavelet Transformation . . . . .	120
2.2.11	Wavelet Transformation of an Analytic Signal . . . . .	122
2.3	Summary . . . . .	123
3.	Experimental Apparata. . . . .	125
3.1	Hardware. . . . .	125
3.1.1	Equipment. . . . .	126
3.1.2	Hardware Interface. . . . .	126
3.1.3	Signal Wiring. . . . .	127
3.2	Software. . . . .	127
3.2.1	Data Acquisition Interface. . . . .	127
3.2.2	Simulation. . . . .	128

4. Method of Procedure. . . . .	129
4.1 System Identification Methodology. . . . .	129
4.2 Procedural Motivation. . . . .	130
4.3 Verification of the Proposed Identification Techniques. . . . .	131
5. Experimental Results. . . . .	132
5.1 System ID Results from the Mechanical Positioning Test Bed. . . . .	135
5.2 System ID Results from the Inverted Pendulum System. . . . .	137
6. Discussion and Conclusions. . . . .	139
6.1 Recommended Future Work. . . . .	140
References. . . . .	142
Appendices.	
A. A Timeline of the History of Friction . . . . .	169
B. Software Code. . . . .	170
B.1 How to Obtain and Use the Software. . . . .	170
B.2 Simulation Code. . . . .	170
B.2.1 Description. . . . .	170
B.2.2 Instructions for Use. . . . .	170
B.2.3 Dynamics Analysis Code (AutoLev <sup>TM</sup> ). . . . .	171
B.2.4 Simulation Code (ANSI c). . . . .	171
B.3 Data Acquisition Code (c). . . . .	171
B.3.1 Description. . . . .	171
B.3.2 Instructions for Use. . . . .	173
B.3.3 Data Acquisition Code. . . . .	175
B.4 c Support Code Listings. . . . .	175
B.4.1 Data-Acquisition Header Files. . . . .	175
B.4.2 System Header Files. . . . .	175
B.5 Data Analysis Code (Matlab <sup>®</sup> ). . . . .	176
B.5.1 Description. . . . .	176
B.5.2 Instructions for Use. . . . .	176
B.5.3 Friction Analysis Code. . . . .	176
B.6 Matlab <sup>®</sup> Support Code Listings. . . . .	177
B.6.1 Control System Design Utilities. . . . .	177
B.6.2 General Functions. . . . .	177

B.6.3	Math Functions. . . . .	177
B.6.4	Plotting Functions. . . . .	177
B.6.5	Signal Processing Functions. . . . .	178
C.	Test Bed Counterbalance Modifications. . . . .	179

## List of Tables

5.1	Simulation: Log-Decrement Identification. . . . .	134
5.2	Experiment: Test Bed System Identification . . . . .	137
5.3	Experiment: Pendulum System Identification . . . . .	138

## List of Figures

1.1	The classical static + kinetic + viscous friction model. . . . .	9
1.2	The static + Stribeck + viscous friction model. . . . .	19
1.3	The classical deadband backlash model. . . . .	21
1.4	The deadband + impact backlash model. . . . .	23
1.5	The classical fundamental mode compliance approximation. . . . .	24
1.6	Summed modal compliance approximation. . . . .	26
1.7	The mechanical positioning test bed at Rensselær. . . . .	45
1.8	The interdisciplinary roots of mechatronic design. . . . .	47
1.9	Drift caused by asymmetric friction. . . . .	49
2.1	A comparison of modern dynamic friction models. . . . .	57
2.2	Rising static friction. . . . .	58
2.3	Frictional memory. . . . .	62
2.4	Presliding displacement. . . . .	63
2.5	Normal friction. . . . .	65
2.6	Deadband/deadzone model of backlash. . . . .	69
2.7	Impact with material resonance and damping. . . . .	71
2.8	Impulse phenomenon at the instant of contact. . . . .	78
2.9	Total system block diagramme. . . . .	88
3.1	The linear inverted pendulum system at Rensselær. . . . .	126
3.2	Equipment Wiring Diagramme. . . . .	127
5.1	A Representative Parametric Harmonic Oscillation. . . . .	132
5.2	Time Delay in the PHO Feedback Loop. . . . .	133
5.3	Negative Viscous Damping in the Presence of Kinetic Friction. . . . .	136
A.1	A timeline of the history of friction. . . . .	169

## Personal Acknowledgments

Much of the intensity of my experience at Rensselaer, and the invaluable measures of achievement I can now be so proud of, will be remembered by a close circle of people whom I would like to recognise first and foremost.

Prof. Dr. Kevin Craig's unwavering support of my studies at Rensselaer over the past five years has made this work possible. I am utterly unable to express in words the depth of my appreciation for this man's kind friendship, his academic support and also financial support throughout my Master's and Doctorate careers. His unequivocal faith and devotion helped me through some of the most trying moments of personal and professional growth I have experienced during my studies with the Department of Mechanical Engineering, Aeronautical Engineering & Mechanics. It is with great humility and encomium that herewith I dedicate this pinnacle of my achievements to you, Kevin. Thank you so much.

My parents, Wilhelmina Jannetje and Neil Barry together, in spite of circumstances, are naturally largely responsible for any of this happening to me in the first place. I love you both dearly, and I hope to make you proud.

Within our excellent mechatronics research group there are certain individuals who influenced and supported me greatly, with whom I shared moments of triumph and devastation, philosophical and technical inquiry, and numerous talks over good and frothy ales.<sup>1</sup> In chronological order of my acquainting them, these folk would include: Robert S. Hirsch, whose entrepreneurial spirit and tenacity I will always recall as an emblem of freedom in this crazy economic world; Abu Islam, a voice of patience and reason to my wild initial endeavours in the lab; Kwaku-Oppong Prakah-Asante, whose flag of determination and methodology remains an almost archetypal inspiration to the meaning of success itself; Andrew B. Wright, a fellow of strong opinion to say the least, yet, for the most part, consistently amiable and understanding, quick in wit and happy to oblige, a good conversationalist and a rigorous researcher, a solid programmer and technician, not to mention a fellow southerner and school bus driver—in my memory I will remember him as a close friend in '1209 over the years we shared at RPI, and a meticulous mirror of my own image in many unexpected ways; James Fairweather, co-creative funk-ed-up punker homeslice with a bent for individualism testing the tolerances and redefining the limits of expectation, a lad of synchronous ilk as together we reconciled our flavour of the fantastic with the norms of highest formal education; Michael Chen, whose emblematic Chinese happiness in smile and

---

<sup>1</sup>The American micro-brew revolution over the past few years has definitely kept me sane in this hole of a dungeon.

laughter, and warm helpfulness in all manners, always made my visits to '1034 the most convivial; and Scott A. Green, the most vivid and dynamic of us all, Mr. Presentation-Man, but uncompromising in his ideals and collaborative vision of an ethically and socially sound career in engineering. To all of you I extend deep respect and the best wishes for a bright future in our unique field, whether improving the function and quality of life between communities or teaching subsequent generations of people with an inspired and light-hearted hand.

Close associates of “the lab” include my ex-girlfriend Nicole Farkas, who bestowed me with personal blessings and emotional support for a significant number of months. I will be ever grateful for the friendship we shared during this time. I must also, despite his reluctance for professional association with the author, thank my friend Laurent Chazeau, for all the caffeine, communality, and the invaluable collaboration on geeky tracts of equations in the Clubhouse Pub, and terraces around the globe (at least in concept, anyway). His inimitable French edge is indubitably what helped me gain the upper hand over my twilight hours of research mayhem.

There are others who have played strongly in my rise to this substantial achievement whom I wish to recognise formally, and express thanks and wonder again. In their influence upon my academic life, these actors, each nudging me forward with words of encouragement and selflessly passing me to the next, have truly prepared me to accept the many different responsibilities associated with this start of what I hope to be a very fruitful career: Marjorie Lancaster, my English teacher at Chapel Hill High School, cared singularly in spite of the difficulties of my age and brood, and made it possible for me to even hope for what I have now, and with her I wish to share the deepest of thanks for sharing that hope with me—you *are* a stellar teacher in every sense of the description; Burt Brody at good old Bard College, who encouraged my fascination with electronics, philosophically reconciled environmental responsibility with professional deed with admirably exemplary subtlety, and always had the best intent of helping me to further my endeavours, even if he only let onto that a little at a time as I earned it; Zeita-Marion Lobleby, who was like a mother to us at Columbia University during our grueling 3-2 programme and lent so much of her charming wit and strength in our darkest hours there, she I will always remember as the true embodiment of *Alma Mater*; of course my doctoral thesis adviser, Kevin Craig, who helped me actualise a promising and exciting career in what I always wanted to pursue but didn't even know could possibly be, and unlike any other professor in this rigorous field of study whom I have known, has played the lightest and friendliest and most supportive of any adviser under whose direction and concern I might even have dreamed to have had the great opportunity to study; Burt Swersey, whose daughter was my lovely next-door neighbour my sophomore

year back at Bard, and inspired me to continue pursuing creative endeavours throughout my academic pursuits at Rensselær, without compromise; and finally John Tichy, whose mysterious travels from Commander Cody to ME, AE & M Chair are as elusive as his kindness and high expectations are strong, who plays a mean guitar, pays respect to WRPI beyond the call of duty, and has always been one of the best guys to know both personally and professionally in this Department.<sup>2</sup>

And to that tune, I would lastly like to thank the many people at WRPI 91.5 F.M. Stereo, Troy New York, for enriching my personal and creative life, and my interpersonal and managerial skills so wonderfully. You all know who you are. Verb.

As for the contrary, my final word is a very special message to the designers of the Jonsson Engineering Center, who for some crazy reason felt that people who work on experiments in the basement laboratories wouldn't particularly need any natural sunlight, since engineers are just a bunch of troglodytes anyway: *"Thanks for nothing!"*

I can say much more of my architect friend Susanna Takfen Chan, with whom I believe building a positive future with many windows and vistas, is as intrinsic as the brightest Sunshine. My memories of our all-hours KaffeHaus in the Moon-splashed lobby of the JEC will be my fondest of all the time I have spent pursuing this silly Ph.D. thing, Süßē. *Jawohl, ik ben zeker.*<sup>3</sup>

---

<sup>2</sup>His memorably famous, parting kernel of wisdom: *"Never trust the data!"*

<sup>3</sup>(So what exactly *does* "Ilium" mean, anyway?!?)

## Professional Acknowledgments

The author wishes to thank the National Science Foundation for their sustained support of our research in mechatronics for machine tools at Rensselaer, under NSF grant No. GER-9354913 [73], which the work in this thesis is a contribution towards.

I would also like to thank the following individuals for their invaluable contributions and assistance during my work:

Firstly, my Doctoral Committee: My advisor, Prof. Kevin Craig, of course, to whom I am deeply indebted with gratitude; Prof. Dan Walczyk, without whose work my research would have been impossible; and Profs. James Napolitano and C. James Li for the helpful critique of the final thesis manuscript. To Prof. Li in particular: first for introducing me to Columbia University SEAS as a prospective 3-2 student, and now for also being the final member of my examination committee at Rensselaer to sign off on my manuscript, a fitting thank you.

Also, thanks to Prof. Simon S. Braun, for his assistance in gathering information on the Hilbert Transform method of system identification; Laurent Chazeau, for his assistance in corroborating numerous equations and proofing the flow of the articles spawned by this work; Bill (and Prof. Brian) Feeny for his cartoons on friction which I used for my thesis defence presentation;<sup>4</sup> Mr. Hill of Hill's Stationary in downtown Troy for his generous assistance in acquiring and cutting the paper used to print this thesis; and (finally!), especial thanks to Mr. Dennis Gornic of the Graduate School for his truly *interminably* good graces (pew!).

---

<sup>4</sup>You may be able to find the cartoons on Brian Feeny's Michigan State University homepage at [www.egr.msu.edu/ME/htdocs/faculty/feeny/cartoons.html](http://www.egr.msu.edu/ME/htdocs/faculty/feeny/cartoons.html).

## Preface

In preparing this thesis, I found a particular group of references especially helpful. These are listed separately in the Bibliography as preparation materials, but I would like to point out their significance here for the reference of others.

In specifying the thesis format, the Rensselaer Graduate School's *Thesis Writing* was a necessary reference. This document is somewhat sparsely (but sufficiently) detailed, and is readily available through the Graduate School. [297]

I used  $\text{\LaTeX} 2_{\epsilon}$  to typeset the document itself. This was at first a big challenge, but soon enough it became a real pleasure. To help me on the learning curve, Dr. Selahattin Özçelik was very forthcoming with personal assistance. Also, the thesis templates made available to all Rensselaer students by Harriet Borton of the Rensselaer Voorhees Computing Center, was most useful in getting it all started. Lastly, kudos to Donald Knuth, Leslie Lamport & co. for making it so easy, despite the initial enigma. I strongly recommend using  $\text{\LaTeX} 2_{\epsilon}$  [143, 201] for any serious document preparation, even well above pursuing a thesis with expertise in Microsoft Word<sup>®</sup> or Adobe FrameMaker<sup>®</sup> or PageMaker<sup>®</sup>. Firstly, it's free, secondly, it's 100% portable, and thirdly, typing those long equations in is pretty much just like writing it in English — and just as fast and easy to change. It's a bit of a challenge to change your paradigm from WYSIWYG, but well worth it for the snazzy type-setting results you get!

The paper this thesis is printed on is from Mohawk Paper Mill's Vellum & Satin, high-opacity white line of papers.<sup>5</sup> The paper is called Flax Vellum 70 Text (104g/m<sup>2</sup>), a 20

- it is a recycled paper;
- it has a nice feel and looks great;
- Mohawk is a local company;
- it duplicates without producing black specks on the photocopy.

I selected this paper after trying several other samples from different distributors and mills. It was the best-quality recycled paper I could choose out of the 20 or so I examined. It also satisfies all the requirements of Rensselaer's graduate school.<sup>6</sup> The paper was only available

---

<sup>5</sup>Mohawk is located in Cohoes, New York and may be reached at 800.THE.MILL

<sup>6</sup>If you wish to use recycled paper too you should bring a sample to the Graduate School to see that it meets their requirements.

in press size (23" x 35") or larger as a vellum in this weight, so I had it cut into 8.5" x 11" sheets. Hill's Stationary ordered and cut the paper for me at a reasonable price.

The broad yet complete survey paper by Brian Armstrong-Hélouvry, Pierre E. Dupont and Carlos Canudas de Wit helped me get a quick grasp of what friction is all about, a field so inundated with good and bad papers that the sheer magnitude of research involved nearly had my mind quite boggled down. The paper was timely, accurate, informative and comprehensive yet succinct (insofar possible!), and above all, extremely helpful in navigating the imbroglio of loosely coordinated (if at all) world-wide research on the subject. In this regard, of course, the seminal work of Ernest Rabinowicz on friction and wear was a solid reference as well, particularly his recently updated edition.

On backlash, the dedicated studies of Gang Tao and Petar V. Kokotović in this regard, recently summarised in a new text on hysteretic nonlinearities in identification and control, has proved most useful. I was lucky their complete view on the subject was published just in time for my thesis work, helping me to tie together the scattered works within their various proceedings and journal papers on the subject over the past decade or so.

The biographical references are nearly all culled from Cajori on physicists [57], Boyer and Merzbach on mathematicians [49], and MacCurdy on da Vinci in particular [217]. These are all excellent references on the history of science.

The main technical references I used were Max Kurtz' handbook [198] and Mary Boas' excellent, broadly-scoped text on applied mathematics [45]. John Dettman's book on complex variables aided with my breaking open the Riemann Space [87].

I would also like to introduce a criticism of the current paradigm within scientific publishing. In my investigation I encountered a good number of published articles with little more reason for existence than political motivations. Though the everyday researcher or academic is usually not to blame for this, since their funding likely depends on some "show" of "progress", not once did I in my career as a graduate student encounter any researcher here or in my travels who admitted to this popular charade of scientific production. Personally I am grateful for the funding I received as a graduate student, and believe I understand some of the stress associated with acquiring such funding, myself having had to play by the same rules as part of the team. But I sincerely wish those with the purse strings knew that in the end, publishing merely for the sake of doing it only helps produce mounds of extra garbage to have to sift through on the way to getting some real results out of the available literature. To hell with it. I would generally prefer to read less material with greater useful and applicable content than inflating my *curriculum vitae* with embarrassingly prosaic treatments slopped out the door with such rushed prolificacy.

I hope that contrary to the rampant generalisation of the preceding argument you will

find this thesis work a relatively good read, and that it's useful for whatever endeavours you're attempting in the way of nonlinear identification and control. I tried to present a balanced picture of the historical and technological context within which this subject is rooted and currently operates. These are fundamental issues of importance to all mechanical engineers, and as such enjoy a certain timelessness. Perhaps this compiled reference may endure the rapid changes in technology for a while; if so, I hope it assists with your understanding of it all in some small manner.

Interested readers are encouraged to visit the mechatronics web site to download Matlab<sup>®</sup> tools implementing the wavelet algorithms presented here, and/or to send e-mail with any comments or questions:

- <http://www.meche.rpi.edu/research/mechatronics>
- [dema1@rpi.edu](mailto:dema1@rpi.edu) or [mechatronics@rpi.edu](mailto:mechatronics@rpi.edu)

Julian A. de Marchi      Troy, New York  
October 1998

## Abstract

This work reports on methods for identifying arbitrary combinations of friction, backlash and compliance in mechanical drive mechanisms. Such methods are necessary to suppress drive nonlinearities contributing to mechanical positioning errors in, for example, machine tools. Backlash, friction and joint compliance are traditional nemeses of precision tooling and a traditional study in mechanical engineering. To date, our understanding of these phenomena remains limited, as does our ability to control them. Friction, backlash and compliance are each presented here in sufficient detail to characterise the nonlinearities affecting machine tools in detailed analytical form. The dynamic coupling between the three nonlinear elements is highlighted as being particularly important to improving the precision and accuracy of machine tools and quality of the workpiece product. The main practical contributions of this thesis are a strong theoretical development of the nonlinearities present in machine tools, and easy-to-apply system identification techniques for asymmetric or nonlinear friction and compliance estimation, as well as strategies for identifying backlash with impact.

The nonlinearities present in a drive are to some degree well-understood: the majority of observed nonlinear effects can be modeled as a combination of damping (energy loss), hysteresis (dead band), and vibration (impact and oscillation). Using a model allows the nonlinearities to be represented and analysed using well-developed mathematical foundations. The model provides a structure allowing simple interpretation of and reaction to the approximate behaviour of the drive nonlinearities. These nonlinearities have been studied in depth, and models are available in a range of complexities addressing a variety of their salient behaviours. It is possible to construct a model with any finite degree of precision, but real-time digital implementation typically confines the degree of complexity remaining tractable. Fortunately, most established models for friction, backlash and compliance are mathematically simple to describe, and yield useful approximations of the overall nonlinear behaviour of a drive mechanism. The work herein therefore takes an analytical (model-based) approach to the problem of identifying and controlling these nonlinearities. In particular, the combination of viscous and kinetic friction prevalent in machine tool-like drive trains is examined.

A detailed overall analysis is given of dynamic friction, backlash with impact, and multi-modal elastic compliance as they operate interactively in a realistic dynamic environment. It is shown that interaction between these otherwise standard nonlinear elements is a crucial component of successful machine tool controllability. The results are important

to the improved mechatronic design of future machine tools as well as the retrofitting of existing tools with better-informed software control. The work has applications to many dynamic systems in general, and especially in the field of robotics. The three basic nonlinearities are examined individually and as components in a complete system. The scheme is first developed analytically, then simulated, and the friction identification methodology is actually tested on two systems mimicking the nonlinearities of a typical machine tool.

Unique contributions include a backlash model with viscoelastic impact properties, and extension of the traditional time-domain identification technique known as the *logarithmic decrement* method to include estimation of asymmetric kinetic and viscous friction for linear, second-order oscillations with time-invariant system parameters. The method may be applied to any such free vibration response, using only the time history of displacement data. Moreover, a novel technique called *parametric harmonic oscillation* is introduced, whereby even highly overdamped systems can be made to mimic underdamped free harmonic vibration, allowing one to apply the extended log decrement method to all second-order systems exhibiting asymmetric kinetic and/or viscous friction. The parametric harmonic oscillation method reveals the actual physical mass, and hence the friction and stiffness parameters of a system, in addition to the usual mass-dimensionalised frequency and damping values. The techniques are demonstrated in theory and simulation, and subsequently verified on two real second-order systems with asymmetric friction. Identification techniques for nonlinear (time-varying) friction and (multimodal) stiffness are also explored.

## Abbreviations and Nomenclature

### 0.1 Mathematical Nomenclature

The mathematical notation follows one of the widely accepted conventions, as follows:

- constants are denoted using plain serif typeface;
- *scalars* are denoted using italic serif typeface;
- **vectors** are denoted using bold serif lowercase typeface;
- **MATRICES** are denoted using bold serif uppercase typeface;
- *indices* are denoted using italic subscript;
- description of a variable's type is denoted using upright sans serif subscript;
- SET membership is denoted using “blackboard” superscript;
- the complex conjugate of a number is denoted by a superscript asterisk (\*);
- the transpose of a matrix is denoted by a superscript “T”;
- the real component of a complex variable is denoted by a superscript “ $\Re$ ”;
- the imaginary component of a complex variable is denoted by a superscript “ $\Im$ ”;
- equivalences valid for all values of the relevant variables are denoted by “ $\equiv$ ”;
- defining equations are denoted by the symbol “ $\triangleq$ ”;
- other special notational symbols are used in accordance with common nomenclature.

### 0.2 Acronyms

The following acronyms appear in the text, and are summarised here for the sake of convenience:

DC	Direct Current
HT	Hilbert Transform
ID	Identification
NSF	National Science Foundation (USA)
PHO	Parametric Harmonic Oscillation

RPI            Rensselaer Polytechnic Institute (USA)  
WT            Wavelet Transformation

### 0.3    Regarding Representation of the Friction Forces and Torques.

Note that the nomenclature denoting the various components of dynamic friction (static, kinetic *et cetera*) do *not* follow the traditional notation. Traditionally, the Greek letter  $\mu$ , with appropriate subscripts, is used to denote the relevant friction coefficient, a dimensionless correlation between normal contact force (load) and the resulting tangential friction force. In this study, a more contemporary notation is used where the friction force itself is denoted by  $\mu$ , because in the context of dynamic friction there is no one particular “coefficient” of friction to speak of, and furthermore, this both highlights the type of friction while clarifying the equations by elimination of repetitive subscripts. Also, the viscous friction is interchangeably represented both by the traditional tribological variable  $\nu$  and also the traditional mechanics-of-vibrations variable  $c$ . The author apologises for any confusion surrounding this selection of variables departing from the norms which the reader may be more familiar with.

## Chapter 1

### Introduction and Historical Review.

#### 1.1 A Discussion of the Three Basic Drive Nonlinearities.

Three basic drive nonlinearities dominate empirical observation of machine behaviour, and these are friction, backlash and compliance. The term friction is used loosely to indicate any speed- or force-dependent energy dissipations in the machine. Backlash connotes mechanical hysteresis as well as multibody impactation. Compliance is really just the opposite of stiffness, and regards the elastic transmission components of a machine. The literature examines these effects individually or in combinations of two, whereas this thesis describes all three acting in concert to deride the precision of machine tools, and how to identify the contributions of each under such circumstances. Perfect machines portray none of these nonlinearities, but the world is certainly not perfect, especially when perfection costs more money. One might go so far as to say that the simultaneous identification of these three basic effects—which encompass the fields of lubrication, tribology, multibody dynamics, thermodynamics, vibration, and machine design—would, out of all the conducted research so far, be the most applicable and useful, and carry the most potential benefit for industry.

The history of each of these topics in engineering is outlined below as an introduction to the current state of the art pertaining to industrial application of the available technology.<sup>7</sup>

##### 1.1.1 Friction.

*Friction* is a word traceable to 15<sup>th</sup>-century English, denoting “the force that resists relative motion between two bodies in contact,” [227] and derives from the Latin word *fricare*, “to rub”. Friction is of interest to scientists because it a universal phenomenon affecting our everyday lives—for example, it allows us to traverse the earth, air and water! Mechanical engineers are concerned with the effect of friction on the behaviour of machines. Friction allows us to slow or stop the motion of machines using brakes; it causes heating between frictional elements in motion; and it also allows machines to start and accelerate their motions. It can be used to positive effect in some part of a machine’s function, whilst in other parts producing a confounding effect. In all forms friction is a fundamental physical phenomenon intrinsic to all machines and mechanical processes. The field of friction itself dates back more than three millenia! [276]

---

<sup>7</sup>A timeline delineating significant achievements in the history of friction research is given in Appendix A on page 169.

Every student when studying college physics for the first time comes to regard the subject of friction with mixed feelings. [S]he finds that the motion of one surface over another is always opposed by a force due to friction irrespective of the direction of movement, hence the efficiency of any mechanical device is reduced because of the friction of its moving parts. Corrections have to be applied in order to make calculated results agree with experience. This is a nuisance. Yet, without friction, [s]he finds that nails, screws, and moving belts would be useless; trains and automobiles would not start, but if going, could not stop without a smashup; and [her] own ability to walk to [her] classroom would be lost. Thus, whether friction plays the part of devil or of angel, it exercises an influence upon everything that moves; it springs into action the instant a sliding force is applied; it may prevent motion that would otherwise occur (as when a body is at rest upon a plane inclined to the horizontal at a small angle). [251, p.181]

During the course of daily life we only occasionally encounter structures that have little or no damping, and hence we rarely have the opportunity to observe the absence of a phenomenon that we take almost completely for granted. When a structure possesses no damping, no mechanism exists to remove the vibrational energy in it, implying that any vibratory motion, once set up, will continue for ever. Clearly this can never happen in the real world. [236, p.45]

In fact, the energy “lost” to friction can be expressed in a number of different ways, depending on the level of detail desired; considering that friction and wear are inextricably linked (more on this later), the loss of material from a system must accompany a really specific model, for example. Factors of mass loss and interactions between the subsystems rubbing against one another may be cast purely in the sense of exchanged energies, though superficially speaking this may at first seem somewhat philosophical [290].

#### 1.1.1.1 What Exactly is Friction?

In science—one art aiming to elucidate the mysteries of friction—the dissipative effect of friction is observed by the Second Law of Thermodynamics [299, 365], a theorem postulated on the basis of consistent experimental observation. Lord Kelvin (née William Thomson, physicist, 1824–1907) and Max K. E. L. Planck (physicist, 1858–1947) recognised the Second Law in terms of heat engines. Rudolph J. E. Clausius (physicist, 1822–1888) extended this notion with the definition of entropy of an isolated thermal cycle, which never decreases; this resolved the ambiguity between initial and final states of a thermodynamic cycle, both of which often share similar, and thus indistinguishable, equilibrium properties.

Entropy, which a fundamental system state, can remain constant only for an isolated, fully reversible process; otherwise it increases with the process. Irreversible system cycles are the norm, and include those where work is “lost” to uncontrollable factors like friction—for example, during the full stroke of a piston which rubs against its cylinder. Assuming the Universe of our experience (which naturally includes all such machines and cycles) is an isolated system—in accordance with our common observation<sup>8</sup>—this leads to the well-known *principle of increasing entropy*, which basically states that since not all processes are fully reversible, entropy must, to some extent, always be increasing. Friction is a particularly common example of such “lost energy” in mechanical cycles; in fact it was a friction experiment between churning paddles and water by James Prescott Joule (entrepreneurial brewer, 1818–1889) which first proved the equivalence of mechanical and thermal energies [57, 246].

Control systems theory provides a similar account for losses due to friction through the concept of *dissipation* [371]. Reflecting the principle of increasing entropy, friction can be described as the “loss” or dissipation of energy from the cycle or machine under investigation, into its surroundings. Hence a system is described as *dissipative* if it dissipates energy—when “the outgoing energy is less than or equal to the incoming energy.” [93]

The energy lost over one cycle is defined as the line integral of dissipation along the path of action. In thermodynamics this is the line integral of entropy change over the path from some state  $A$  to some other state  $B$  and then back to  $A$ . In mechanics it is the line integral of friction loss over the path from some displacement  $A$  to some other displacement  $B$  and back to  $A$ . If the paths happen to be equivalent both back and forth, then the cyclic process is said to be *reversible*, and no energy is “lost”. Typically, though the path of action is often stationary (stable in both directions), it will differ in either direction of traversal, because realistic system behaviour varies with temperature, frequency and amplitude of cyclic oscillation, and other properties. In this case, the path of action will describe a hysteresis curve, and the area bounded by this curve will be the value of the line integral (for example, the energy “lost” to friction).<sup>9</sup>

This mathematical description accounts for commonly observed behaviours such as a flexible beam or oscillating pendulum under free vibration coming to an eventual standstill because of frictional energy dissipation. In the pendulum example, friction manifests itself in the pendulum’s hinge, whereas in the vibrating beam, the friction is largely contained within the structure itself—dissipative forces exist between the beam’s molecular layers as they “rub” and stretch alongside one another on a microscopic scale, giving rise to a macroscopically-observable effect. This distinction between micro- and macroscopic

---

<sup>8</sup>Yet this is by no means a closed issue in physics or philosophy!

<sup>9</sup>If the dissipation is proportional to the square of the amplitude of the cycle (*linear damping*), the hysteresis curve will be elliptic.

frictional behaviour gives rise to the distinguishing terms *internal*, *molecular* or *vibrational* friction and *external* or *macroscopic* friction, respectively, though often the type under current discussion is determined simply within the context of the problem at hand.

*Friction constants* or *damping coefficients* are used to distinguish the frictional properties of different materials. Depending on their scaling with respect to the range of various materials under consideration, different mathematical conveniences may be obtained. The frictional behaviour of a material is rarely, if ever, constant, and typically depends not only on the material itself, but the environment in which it is used. However, it is common for frictional properties to be modeled as constant within some small specified tolerance, over the anticipated range of useful operation. These factors are the special domain of spring manufacturers and others who conduct extensive research and tests to determine the validity of constant damping. The ranges of validity are then specified with the final product.

Friction may be expressed in a number of different ways. Internal friction is often constant over a wide range of frequencies of vibration, and proportional to the squared amplitude of vibration: such friction is called *linear*, *structural* or *solid* damping, and has units of **force versus displacement**. Other materials and systems may exhibit *viscous* damping, where the frictional force is proportional to the velocity of cyclical motion—in this case the friction is greatest at the natural frequencies of the system. Other types of damping can be expressed in terms of an *equivalent* viscous damping, by equating the energy loss during an arbitrary stationary cycle (stable, but forced at various different frequencies simultaneously) with that which would be lost under pure harmonic excitation (forced by a single frequency). External friction is usually denoted by the *damping ratio*, a non-dimensional number proportional to the energy loss per cycle of work (*specific damping capacity* or *loss coefficient*). Generally, internal friction is used to specify the behaviour of flexible machine parts, and external friction to specify that of rigid links connected by kinematic joints or supported by surface contacts or contours [346].

The work presented herein will address both types of friction. The following section will concentrate on the frictional interactions in joints between rigid bodies. Internal friction will be discussed further on within the context of elastic compliance.

### 1.1.1.2 The Classical Friction Model:

#### Static + Dynamic + Viscous Frictions.

*Coulomb damping* is used to describe the friction between two dry, clean rubbing surfaces, as in a joint, and is named after Charles Augustin Coulomb (experimental physicist, 1736–1806). This definition should actually be attributed to Leonardo da Vinci (artist and

scientist extraordinaire, 1452–1519), who observed that the phenomenon of friction was a force independent of contact area. Among da Vinci’s pontifications on the subject one may find the following prose on impetus (the “instantaneousness” of force):<sup>10</sup>

When the friction of the moveable thing over the place where it is moved is of slight density, the power of the mover will be united for so great a space with the movable thing, since this is separated from the mover in proportion as the friction is of less density [217, p.429].<sup>11</sup>

Friction is divided into three parts: these are simple, compound and disordered. Simple friction is that made by the thing moved upon the place where it is dragged [kinetic friction]. Compound is that which the thing moved makes between two immovable things [static friction]. Irregular is that made by corners of different sides [friction at a point contact]. [217, p.527]<sup>12</sup>

If you desire true knowledge of the quantity of the weight required to move [a] hundred pounds over [a] sloping road, it is necessary to know the nature of the contact which this weight has with the smooth surface where it produces friction by its movement, because different bodies have different kinds of friction; because if there shall be two bodies with different surfaces, that is, that one is soft and polished and well greased or soaped, and it is moved upon a smooth surface of a similar kind, it will move much more easily than that which has been made rough by the use of lime or a rasping-file [217, p.596–597].<sup>13</sup>

All things and everything whatsoever however thin it be which is interposed in the middle between objects that rub together lighten the difficulty of this friction. [217, p.601]<sup>14</sup>

[Furthermore,] friction produces double the amount of effort if the weight be doubled. [217, p.607]<sup>15</sup>

In 1699, da Vinci’s ideas were independently rediscovered by Guillaume Amontons (physicist, 1663–1705), who is credited for first phrasing friction in “modern” terms [15]. Amontons was convinced that this friction was the result of the inter-penetration of two surfaces; in other words, their contact pressure, a view further advanced by Coulomb

---

<sup>10</sup>da Vinci’s nebulous prose is indicative of his philosophical insights into everyday mechanisms, unlike the later work of Newton; although both men concluded much the same about the laws of physics, da Vinci postulated upon fascinating observations whereas Newton abstracted the same into divinely precise “laws of nature”.

<sup>11</sup>*Quod vide* Codice Atlantico 161v.a.

<sup>12</sup>*Quod vide* La Bibliothèque de l’Institut de France, notebook E 35 r.

<sup>13</sup>*Quod vide* the Victoria and Albert Museum of London, Forster Bequest Manuscripts II 87 r. and 86 v.

<sup>14</sup>*Quod vide* Forster Manuscripts II 133 r. and 132 v.

<sup>15</sup>*Quod vide* Forster Manuscript III 72 r.

later on [67,68]. In fact, da Vinci was already a step ahead of Amontons the whole way through: unlike Amontons, the ever-curious Renaissance Italian had quickly recognised that blocks sliding on inclined planes exhibited frictional resistance not only proportional to their weight, but in connection with their angle of “repose”, complete with sketches of supporting experiments to boot [251].

The significance of the angle of repose was rediscovered by Antoine Parent (mathematician, 1666–1716) in 1704 [256], and further elaborated by Leonhard Euler (great mathematician, 1707–1783) in 1748 in the form and notation which now appears in our textbooks [111].<sup>16</sup> The latter also says: ‘Everyone is agreed that friction depends upon load only and not upon the extent or shape of the surfaces. One would think that, since friction is caused by asperities, the larger the surfaces, the greater the friction because there would be more asperities, but this is not the case.’ He states that the force of static friction is greater than that of kinetic, and gives an equation for each in terms of the angle of repose. [251, p.184]

Unwavering since da Vinci’s recorded ruminations, this view became known as the “roughness hypothesis.” [276]

Indeed all of the authors who have written of the unstable forces, there is perhaps not one who has paid sufficient attention to the effect of friction in machines, and of the resistance caused by the stiffness of ropes, nor who has given us the rules for understanding the one and the other, and for reducing them to calculation. [15, p.206]<sup>17</sup>

Enter Coulomb, who was later able to quantify rules of friction for various materials, and verified that, in accordance with Amontons’ observation, the friction is directly proportional to the interfacial pressure shared between two surfaces. When a block of some material slides upon a surface, it is therefore the weight distributed over the area of contact of the block which determines this pressure. Coulomb defined a coefficient of friction  $\mu$ , independent of the velocity of sliding (once sliding is initiated), but whose action counters all directions of sliding.<sup>18</sup>

[Coulomb in 1785 concluded some important] determinations of the factor

---

<sup>16</sup>See equation (1.1) on page 8.

<sup>17</sup>Translation by Frederic Palmer, *quod vide* [251, p.182]

<sup>18</sup>Neither Coulomb nor Amontons had any idea that da Vinci had already scribbled all this information into his notebooks, a whole three centuries earlier!

that control the force in static friction as distinct from those that control that of kinetic friction [67]:<sup>19</sup>

1. in both cases, Amontons' laws concerning load and contact area . . . are valid over the range tested;
2. in both cases, the force of friction depends upon the nature of the materials in contact and their coatings;
3. the force of static friction depends upon the length of time during which the surfaces have been in contact;
4. the force of kinetic friction is independent of the velocity;
5. at least part of the frictional force may be ascribed to cohesion of the molecules at the sliding surfaces.

So, although the *laws* of friction seemed stable, there was still some question as to what exactly the *mechanisms* of friction really were. Coulomb also stated that friction was independent of speed, but his experimental observations indicated that friction increased with speed for some materials, while for others it decreased [251].

Subsequently, Arthur Jules Morin (applied mathematician, 1795-1880) discovered that friction was in fact independent of speed when sliding, in a series of experiments from 1831 to 1834 [231]. Morin, in contrast to Coulomb, executed numerous meticulous experimental measurements of friction over a wide range of materials and conditions – 631 of them in all [251]. Morin conclusively reported that his results proved dry friction was independent of velocity. However, Coulomb had nonetheless proposed the interesting idea that the friction might likely be caused by a dynamic spring-like mechanism between surface asperities, literally brushing against one another, proposing a possible explanation for the actual mechanism of friction.<sup>20</sup> Coulomb, whose more memorable contributions to physics are electrostatically oriented, devised a theory of electronic interaction of the interfacial molecules across two rubbing surfaces, an idea simultaneously suggested by S. Vince in England (the phenomenon known as *triboelectrification*) [251]. Nonetheless the evidence gathered into the turn of this century still left much in question as to the real operating mechanisms of friction.

In spite of all this debate, the basic empirical observations of friction are usually lumped into one convenient mathematical equation commonly known as either *Amonton's*

---

<sup>19</sup>Translation by Frederic Palmer, *quod vide* [251, p.184]

<sup>20</sup>This notion is elaborated further by the “bristle” model of the friction phenomenon by Hæssig and Friedland [155], and Canudas de Wit *et alii* [62], presented further on in Chapter 2.

or *Coulomb's law of friction*,<sup>21</sup> describing an arbitrary point contact between two rigid bodies as [181]

$$\mathbf{f} = \mathbf{n} + \mathbf{t} \quad (1.1)$$

where:  $\mathbf{f}$  is the contact force;

$n \triangleq |\mathbf{n}| > 0$  is the normal force;

$t \triangleq |\mathbf{t}| \leq \mu n$  is the tangential shear force opposing the sliding.

This equation can be modified to describe the friction at point or distributed contacts, in linear or rotating joints. During sliding,  $t = \mu_k n$ , and before sliding  $t = \mu_s n$ . Typically  $\mu_s \mu_k$ , where  $\mu_s$  is called the *static* and  $\mu_k$  the *kinetic* coefficient, respectively, of Coulomb friction, and these  $\mu$  are taken to be constant for a given pair of rubbing materials across some range of operation.

The Coulomb friction model of (1.1) above is a good approximation for clean, dry, geometrically regular surfaces sliding together. Coulomb's "law" of sliding friction (as customarily cited in textbooks)" states that the frictional force [251]:

- ... is directly proportional to load, that is, to the total force which acts normal to the sliding surface;
- ... for a constant load is independent of the area of contact;
- ... is independent of the velocity of sliding;
- ... depends upon the nature of the materials in contact.

With the spread of the industrial revolution and high-speed machinery, like shafts rotating on lubricated bearings, it became evident that a new, speed-dependent component of friction existed, called *viscous* friction. The concept of viscous friction was promulgated by the fluid mechanics pioneer M. Osborne Reynolds (engineer, 1842–1912), and is associated with the viscosity of a bearing's lubricating fluid, which typically being non-Newtonian, becomes stiffer at the higher pressures produced by higher speeds [282]. Isaac Newton (physicist, 1642–1727) had proposed laws of motion for what he baroquely termed "perfect" (frictionless) fluids, contemporarily known as *Newtonian* fluids. A number of mathematicians developed Newton's equations into the theory of "hydrodynamics" to solve many hypothetical problems, amongst them Jean Le Rond d'Alembert (mathematician, 1717–1783) who proved the paradox that a body immersed in a frictionless fluid must have zero drag, which naturally was contrary to all observation. Engineers of the day reacted by

---

<sup>21</sup>Coulomb is partially credited because he first committed the laws to paper in mathematical form.

solving their own problems based on empirical evidence instead, developing the science of “hydraulics”. Eventually the theory and practise of fluids research became confluent under the theory of viscous flow, which dominates most engineering problems. It is out of this modern work in fluid mechanics that we can explain the effect of viscous friction. For this reason it is also sometimes called *wet* friction (found in lubricated bearings), to distinguish it from Coulomb friction, in turn sometimes referred to as *dry* friction (as found between dry, rubbing surfaces).

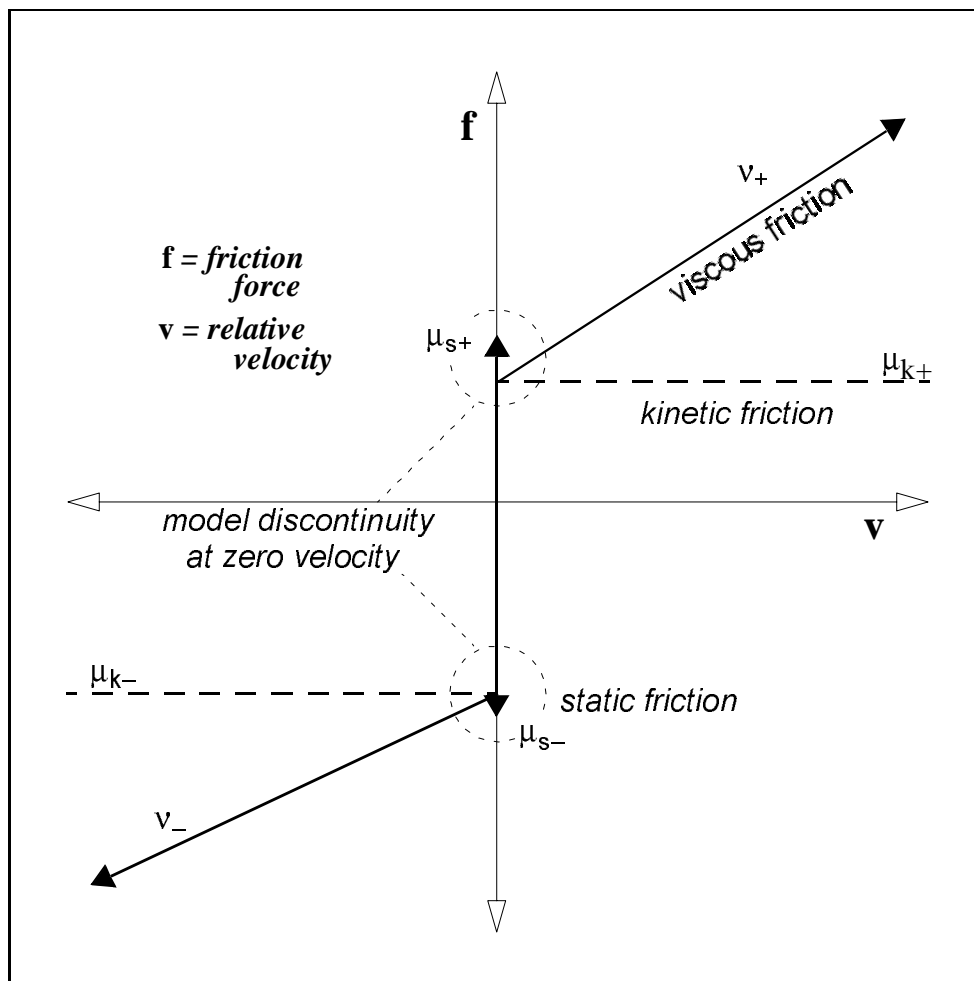


Figure 1.1: The classical static + kinetic + viscous friction model.

For a good while the model of wet+dry friction prevailed in the engineering analysis of machines. A graphic representation of this fairly straightforward model is given in Figure 1.1.

Further than this most students do not go; first, because of a lack of interest since friction is not an exciting topic full of fireworks, like atomic energy; second,

because, even with the requisite interest, an inquiring student will be discouraged to find the answers to [her] questions scattered through the literature rather than brought together in easily available form. [251, p.182]

The tenacity of modern tribologists, however, has prevailed, as will be immediately evident.

### 1.1.1.3 The Modern Friction Model:

#### Rolling, Stribeck, Stick-Slip, and Hydraulic Frictions.

With the advent of the field of *tribology* (after the Greek word *tribos*, “to rub”), which developed in England during the 1920s and ’30s, and brought with it an increasingly better understanding of the molecular forces of friction, a rather different view of friction began to emerge. The classical view held that friction was due to the roughness of the surface contact between two bodies, and that surface asperities and atomic forces were responsible for their “interlocking”, thus resisting motion. Scientists during the Enlightenment toyed with the notion that the surfaces might be electronically adhering to one another, but the idea was reluctantly discarded because it would have required, contrary to empirical evidence, that the friction between rubbing bodies be proportional to their interfacial contact area.

The revised view suggested that the friction really *should* be more explicable via the “adhesion theory”, since further observation, thanks to turn-of-the-century advances in the expertise of surface chemistry, revealed that varying degrees of surface contamination had a significant effect on the adhesion (or friction) of bodies in contact. To wit [252]:

1. The friction of ground glass is *less* than that of plate glass or of glass polished to an “optical face”.
2. The coefficient of friction usually has the same value whether a rider is slid over a freshly prepared surface or in the same visible groove of previous trips.<sup>22</sup>
3. The effect of a spherical contact in bringing about the deceleration of a flywheel leads to the conclusion that friction is independent of surface polish except when the rider is of relatively soft material.
4. The results of more than one thousand friction measurements on each of five different metals were essentially the same whether the surfaces were polished, or rough and torn.

---

<sup>22</sup>Though new evidence suggests that hydrodynamic effects may have a significant erroneous effect on the measured friction over multiple passes (*Quod vide* [224]), probably a manifestation of normal force dependencies (discussed in a later section).

5. Lower frictional resistance and less frictional wear occur in bearings and cylinders in which one of the sliding surfaces is rougher than the other.
6. Steel journals, with varying degrees of polish, turning in lubricated bearings, show no significant differences in frictional torque.

This mounting body of information forced researchers to consider more closely the real meaning of the “actual area” of frictional contact between two bodies. This thought had already been considered by H. Shaw around 1886 [252].<sup>23</sup> As Rabinowicz critically reveals in the opening to one article,

Early workers in the friction field (Amontons, Coulomb, Morin) described the macroscopic phenomena, the ‘laws’ of friction, very accurately... and discussed them very shrewdly. They had no concept of what constitutes a ‘clean’ surface... and hence underestimated the extent and significance of adhesive effects. They paid lip service to one another’s opinion that friction was due to surface roughness, but had an uneasy feeling that adhesion might be the real factor. Modern work has definitely confirmed the adhesion hypothesis as against the roughness hypothesis because, among other reasons, very smooth surfaces almost invariably show as much (sometimes more) friction as do less smooth ones. However, in an attitude reminiscent of Aristotle’s medieval disciples, most authors in mechanics still equate “smooth” surfaces with “frictionless” ones. [275, p.1]

Investigators had discovered that the apparent (macroscopically observed) and the actual (microscopic) areas of contact were completely different! This deduction, based on the role of surface asperities in friction, resolved most of the dispute surrounding the modern adhesion theory. The modern view is now that the interfacial pressure between two bodies in contact deforms local, microscopic surface asperities, increasing the real contact area, thereby explaining the observations of the classical scientists; and the same theory explains why the real interfacial surface area appears to be largely independent of the roughness of contact. Additionally, the “third body” theory has developed out of closer examinations of interfacial rubbing, which considers the likelihood that frictional wear forcefully detaches microscopic material particles which, under certain lubrication conditions, can allow a miniscule “third” particular body to alternately roll or weld itself between the two relatively macroscopic rubbing surfaces. The wear also accounts for a consistent renewal of the rubbing surfaces, whose characteristic roughness will remain fairly constant, while the

---

<sup>23</sup>Palmer attributes the original citation to “Archbutt and Deeley (1912).”

frictional detritus produced during the rubbing becomes compressed between the interfacial surface asperities, thereby increasing the actual contact area. The complete mechanism described by the adhesion theory can be condensed out of the dedicated work of F. P. Bowden and David Tabor in the late 1930s and early 1940s, who meticulously isolated the influence of several variables known to affect the behaviour of friction [252, p.329]:

- The area of actual contact can be measured by employing a simple electrical technique (conductivity).
- The area of actual contact of either moving or stationary surfaces is essentially unaffected by both the shape and the area of apparent contact of these surfaces.
- Under the same load, the area of actual contact of the same metals, whether rough filed or finely polished, is the same.
- At least in the case of metals, frictional force is proportional to the area of actual contact, which is a small fraction of the area of apparent contact.
- Frictional force is *independent* of applied load. The principal effect of an increased load is an increased area of actual contact. [The pressure thus remains constant.]
- Deformation of metals, due to the load, is chiefly plastic. This deformation increases until the area of actual contact is sufficient to support the load; hence [the pressure] is the same whether the surface finish is rough or smooth.
- Since the area of actual contact is very small, even a light load may produce a pressure high enough to cause adhesion (welding) of the points of contact.
- Frictional resistance of metals is due primarily to the shearing of welds at points of contact, and secondarily, to the work of plowing the harder [asperities] through the softer.

Research along these lines continues to pursue a closer observation and understanding of the more microscopic and subtle mechanics of surface chemistry and lubrication than was previously possible [276].

Heinrich Rudolf Hertz (engineer *cum* physicist, 1857–1894), among his more astounding achievements,<sup>24</sup> studied the close contact of spherical ball bearings [157]. *Hertzian* contact mechanics now bear his name, and describe the action of rolling evident in pre-stressed bearings such as those commonly used to fix machine spindles. Whereas previous

---

<sup>24</sup>Hertz succeeded Clausius at Bonn at the age of thirty-two for good reason: he experimentally proved Maxwell's theoretical extensions of Faraday's electromagnetic wave-induced forcefields.

models took rolling to be along the moving point contact between the ball and a plane, which mechanically would result in a pure slip or no-slip condition at the contact point, Hertz exhibited a contact where the ball is pressed onto the surface by the load stress of the machine spindle it bears, deforming locally to produce a more or less circular *area* of contact with the plane it rolls along. Because of this elastic deformation at the interface, the velocity profile over the contact area is non-uniform—hence it is impossible that the true contact would result in either pure slip or no-slip! Depending on this profile, then, there is additional friction produced, since part of the contact surface of the ball will always be rubbing against the plane, one way or another. This friction is therefore called *rolling friction*, and is proportional to the ratio of mean contact slipping to rolling velocities [276]:

$$\mu_r = \frac{\mathbf{v}_{\text{slip}}}{\mathbf{v}_{\text{roll}}}\mu_k \quad (1.2)$$

*where:*  $\mathbf{v}_{\text{slip}}$  is the mean slipping velocity over the contact area, and  
 $\mathbf{v}_{\text{roll}}$  is the mean rolling velocity of the ball across the planar surface.

A similar approach exists for elliptical Hertzian contacts, as in the case of gears “rolling” across one another during contact. It should be noted that similar rolling friction will also take place within the curved “trough” known as the *bearing race*, used to keep ball bearings aligned and more uniformly stressed when assembled [23].<sup>25</sup> An analysis of such elliptical Hertzian contacts may be found in the recent work of J. A. Greenwood of the University of Cambridge [148].

A further small contribution exists which adds to the rolling friction, and this comes from the fact that the deformation at the rolling contact is not entirely elastic in property: some energy is always lost to heat as the leading edge of the rolling ball is first compressed and then released at the trailing edge. For the most part, however, Hertz’ analysis gives a fairly good estimation of measured values in real bearings, where such rolling predominates the overall bearing friction. Ball bearings are otherwise very elegant mechanisms for reducing the friction on rotating spindles or sliding guideways.

R. Stribeck (engineer, ??-??<sup>26</sup>) spent a couple of years at the turn of this century studying the lubricated bearings of machines at the (German) Central Agency for Scientific and Technical Research at Neu-Babelsberg. He conducted a number of tedious experiments, collecting vast amounts of empirical data on the behaviour of rotating shafts and slides on slideways [319–321]. Stribeck describes his motivation [319, p.1341]:<sup>27</sup>

---

<sup>25</sup>The original work is attributed to Eschmann (*quod vide* [110]).

<sup>26</sup>The author was unable to locate any biography of Herr Stribeck.

<sup>27</sup>Translation by the author.

In hindsight of the traditional and expanded use of slideways, the following may come as a surprise. Upon closer inspection one becomes aware that slideways, like various other bearings under heavy use and wear, exhibit similarly devious behaviour from one case to another.

.. One seeking to learn the inner workings of various bearings may not find the solution within the field of lubrication alone, for this teaches one more about lubricants than about the bearing. More important is the installation and operation of shafts within their bearings. Of particular interest is the acceleration phase, where the machine starts at rest and ends at its normal operating speed. This effects of this phase are found in locomotives, machine tools, and other machines with heavy spindles.

Stribeck experimented on both slideways and roller bearings and compared the results for different loading conditions, lubricant temperatures and pressures, and velocities. Without attempting to generalise his results by an exact model, he rather sought to explain qualitatively the possible reasons for his observations. The meticulousness of his experimental methodology<sup>28</sup> elicited a number of interesting results, which to some degree explained the previously enigmatic discontinuity between the static and dynamic friction coefficients. With detailed recordings of spindle movement under applied torques, using a rather ingenuous apparatus to sample the instantaneous temperature and speed of the spindle right at the bearing, he was able to show that the spindle friction dropped rapidly—not instantaneously—from the static value to a minimum kinetic value. The exact minimum depended on spindle velocity, lubricant temperature and pressure, and duration of operation. The friction then rose asymptotically with increasing spindle speeds, eventually conjoining the linear domain of viscous friction. This frictional transition is known as the velocity-dependent *Stribeck effect*, which is shown in the “partial lubrication” phase of Figure 1.2 on page 19.

There is another effect determined by Stribeck which follows almost the same exact pattern of behaviour as the velocity dependence of bearing frictions. This is called the *temporal Stribeck effect* [319, p.1341].

Because the temperature-dependent friction is initially greater than the final friction, the lubricant must first undergo a period of warming. The required time is not merely a few minutes, but hours. The friction during this warming period is almost universally greater than during steady operation. It is therefore important to investigate friction in the start-up, acceleration, warming and

---

<sup>28</sup> ... not to mention patience with his belts occasionally slipping off the spindle, and severe—even catastrophic—wear of the bearings in some experiments!

steady-state phases together. The results show not only the practicalities of determining frictional behaviour, but also the effects of bearing load and the importance of measurement accuracy.<sup>29</sup>

Stribeck shows that friction decreases exponentially with lubricant temperature (lowering the fluid viscosity), which in turn increases exponentially with higher velocities and under longer continuous operation. Steady state is typically only reached after about two hours' continuous operation, at which point the friction levels out asymptotically. He also observes that the viscous friction is more noticeable with smaller bearing loads. Furthermore, Stribeck shows that at low steady-state velocities, the friction decreases with increased bearing load to some minimum, after which it rapidly climbs again [319, p.1345]:<sup>30</sup>

The experience, as strange as at first occurrence it may seem, elucidates itself readily: when with increasing load the friction grows rapidly, this implies that the lubricant thickness becomes less and less sufficient, preventing motion between the spindle and bearing. The lubricant film becomes useless when not enough of it enters the contact interface, yet because some does pass through the interface, we can further conclude: with increased bearing loads, the necessary velocity to draw sufficient lubricant into the interface that the bearing is fully supported on a thick film may never be reached.

Importantly, Stribeck's data shows that the transition from the static to the kinetic and viscous friction régimes is in fact continuous, and that it occurs either over a very small velocity range about standstill (unobservable in the macroscopic sense of the long-term) or over a very lengthy period of time during steady-state operation (unobservable in the microscopic sense of the short-term). This explains why other scientists, who had concentrated on steady-state friction behaviour in short-term experiments, had completely missed the transitory phenomenon describing this change in frictional behaviour at the start and stop of motion. Stribeck notes [319, p.1345–1346]:<sup>31</sup>

Another important observation is expressed in that all the [*friction versus velocity*] curves [comparing various bearing loads] originate at the same [static friction] point. This shows that: the friction coefficient at rest is independent of the bearing load—and, as immediately implied, also virtually independent of the lubricant temperature.

---

<sup>29</sup>Translation by the author.

<sup>30</sup>Translation by the author.

<sup>31</sup>Translation by the author.

For the [small] loads used in this experiment . . . the [static friction] agrees with the friction measured at rest by Morin, who used small [interfacial] pressures and little lubricant. In both cases this friction was determined at the point that motion commenced, as well as by the extrapolated frictional behaviour at very low speeds. When the spindle comes to rest under a load, the lubricant is no longer fed [into the contact interface], and in fact is pressed out of it. What remains of the lubricant is insufficient to prevent the effect of significant friction when attempting to subsequently move the spindle again. The friction at rest naturally must depend on the presence of lubrication, which is restored only seconds after the spindle is again brought into motion. During the start-up time, . . . the friction more or less regained its lower steady-state values.

*Stribeck* friction is sometimes colloquially called *negative* friction, because of this negative dip in the *friction versus velocity* curve.

A. Tustin in 1947 [359] and Armstrong-Hélouvry in 1988 and 1990 [17, 18] both cite this negative-going friction behaviour as forming the prerequisite for the phenomenon called *stick-slip* friction, or simply *stiction*. Stick-slip friction is quite common in everyday life, and is a direct result of the fact that the static friction between two surfaces nearly always supercedes the kinetic friction. This seemingly paradoxical phenomenon is usually accompanied by a familiar shuddering, squeaking or squealing sound. Consider, for example: the squeal of brake pads against a disc in an automobile or locomotive coming to a halt; the squeak of a damp cloth on a freshly-cleaned windowpane; or the shudder of the plumbing when the faucet is nearly turned off.<sup>32</sup> This phenomenon often occurs in steady-state systems which exhibit some degree of compliance (in the otherwise relatively stiff) mechanism between the applied pressure and the relative action of the two bodies. It also occurs in transient systems where the lubrosity of contact is changing, or when the velocity of transition is changing.

*Harmonic* stick-slip is used to describe those situations where the compliance of surface asperities is the main factor over a domain of rubbing speeds which varies depending on the materials in question. The main reason these systems cause noise, which in turn is caused by a relatively high-frequency and high-energy mechanical vibration, is because

---

<sup>32</sup>Frederic Palmer urges us to recall *quod vide* [252, p.334]:

- Did you ever tease your school teacher by the squeeks of your slate-pencil moved in a nearly normal position across the slate?
- Did you ever hear the squeeks of a door, gate or blind rotated upon its hinges?
- Did you ever shudder at that awful noise made by an automobile as it skids to a sudden stop?
- Were you ever bothered by the “chatter” of tools in a lathe?

even a small degree of mechanistic compliance, at small relative velocities, induces a stable oscillation (*limit cycle*) between the states of static and kinetic friction. The frequency of the sound is roughly proportional to the stiffness of the mechanism [47]. In the first example of a locomotive, the mechanism which presses the brake pads against the disc surface is very stiff, but not entirely rigid—yet even this slight flexibility is sufficient to produce an annoying high-frequency noise, as when a railroad car comes to a halt. In the window-wiping example, the noise is simply at a lower frequency, since the mechanism is more flexible. In the plumbing example, the water itself has a very high (but finite) specific stiffness, yet the pipes can be so long that the stiffness of the piping itself may come into play; a very low-frequency shuddering is then produced, which can be predicted analytically. Experience makes it fairly obvious that if such high-energy, state-transiting vibrations don't actually cause severe damage when allowed to cycle indefinitely (which at steady-state they do), then certainly they're a terrible nuisance to one's aural comfort. In fact, with most machines it is the other way around: the nuisance noise is a real symptom of potential interfacial damage in its bearings [276].

*Regular* stick-slip describes a “shuddering” arising from the very sudden yet constantly cyclic change from no movement to very small movement at the surface contact(s). Like harmonic stick-slip, it is related to the difference between static and kinetic frictions; however, unlike harmonic stiction, regular stick-slip is connected with the plasticity of surface asperities.

[Its] operation... has been described essentially as follows. The area of actual contact is very small irrespective of the load, hence pressure and heat are both concentrated in small areas [“hot spots”] rather than dispersed over the apparent contact area. The local result is high load and high temperature. If sliding takes place under these conditions the combination of high pressure and high local temperature forms a weld which holds and prevents further sliding until there is a force sufficient to break it and so to jerk one surface over the other very quickly. Thus heat is generated and the cycle is repeated.

While the surfaces are at rest relative to each other, plastic deformation occurs which allows the macroscopic irregularities of the particles to flow and interlock. This welding and adhesion produces larger coefficients of friction than would be obtained under the same conditions of load and surface smoothness at higher velocities . [252]<sup>33</sup>

Regular stiction usually precedes harmonic stiction, which takes place as the velocity ap-

---

<sup>33</sup>The latter statement is cited by Palmer as *quod vide* [90].

proaches the critical velocity, above which motion is once again smooth [252].

Research has revealed that the static friction is not constant, but in fact is a function of *dwell time*, the time for which a frictional contact remains at rest between successive periods of interfacial motion—the longer a contact is resting, the greater the static friction (also called *rising* friction, since it asymptotically rises to some constant value); the shorter the period of rest, the closer the static friction approaches the kinetic friction [15, 23, 67].<sup>34</sup> When stick-slip occurs, the dwell time takes effect each period of interfacial rest, and this dynamically changes the effective (or instantaneous) static friction. The result is another form of cyclic excitation more irregular than, but similar to, the harmonic stick-slip occurring at high velocities [276].

*Irregular* stick-slip is the most insidious variety, and is caused by partial and inconsistent boundary lubrication over the contact area, and the lubricant composition (mainly the presence of “third body” particulates worn off the interface surfaces). Because such surface dynamics are beyond prediction, irregular stick-slip can cause—usually under extreme conditions of interface pressure or length of continuous operation or inoperation—chaotic frictional behaviour [269, 270]. This behaviour is easily mistaken for measurement noise in machine measurements or controls, and is thus also the most confounding.

Up to Stribeck’s day, scientists held that friction remained constant under changing velocities—

a statement to which authorities have clung like grim death for a hundred and fifty years from the time of Coulomb (1785). Even to this day [1949] our textbooks make this incorrect statement, perhaps because their authors have not had time to sift the mass of conflicting opinion on this point and determine how [Coulomb’s] Law should be restated more in accordance with the facts.

The chaos of conflicting opinion concerning the dependence of frictional force upon speed can be given a semblance of order if the results are grouped according to range of speed, as follows:

1. At very low speeds, frictional force increases with speed.
2. At medium speeds [25 *mm/s* to 30 *cm/s*], frictional force is nearly independent of speed.
3. At high speeds, frictional force decreases with speed.

It is thought that the increase in speed in the high range may lower the frictional force by causing the surfaces to separate from each other by a slight

---

<sup>34</sup>This phenomenon is described with much closer detail in section 2.1.1.2 on Rising Friction.

amount, thus reducing the average of the molecular forces of attraction [or adhesion]. [252]

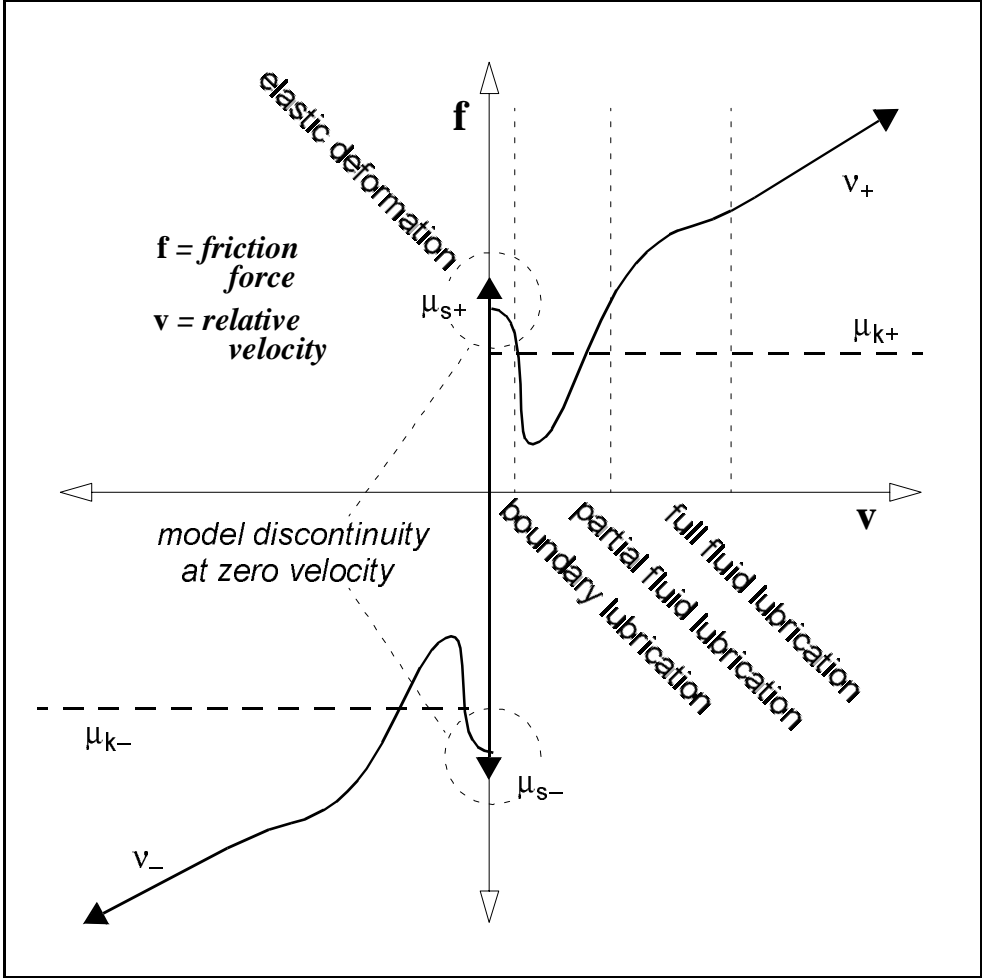


Figure 1.2: The static + Stribeck + viscous friction model.

The Stribeck friction model, incorporating many of the salient effects of friction, is shown in Figure 1.2. This figure represents the transition dynamic of Stribeck friction at low speeds; the three régimes enumerated above refer to general behaviour whereas the figure represents the localised phenomenon. The current state-of-the-art model is divided into separate régimes of operation by velocity, and includes the effects described by the classical model; it is presented in the next chapter with greater detail.

1.1.2 Backlash.

“Backlash” was coined around 1815, and is a compound word denoting a backward lash (violent movement or reaction). In technical circles this has come to mean “the play

between adjacent moveable parts (as in a series of gears),” or “the jar caused by this when the parts are put into action.” [227] Basically, backlash contains a mechanical hysteresis of the type commonly found in geared actuators and sensors, mechanisms employing lead or ball screws, and the like. Gears and screws provide mechanical engineers with a very useful means to adjust the ratio of applied force to resultant action and *vice versa* in machine mechanisms; however, backlash can confound the accuracy of such operations. The component of backlash more familiar to the layperson is gearplay, which many of us are used to dealing with, for example, in the manual steering wheels of automobiles. The less familiar component is that of the “gnashing” of gears when put into sudden motion.

### 1.1.2.1 What is Backlash?

As illustrated by its figurative and literal dictionary definitions, backlash is composed of two salient features. In mechanical engineering terms these are mechanical hysteresis and impact phenomena between two relatively hard surfaces coming into contact. These features are both readily found in old-fashioned geartrains, where the gears fit loosely together and are usually made of a hard metal. Modern geartrains may be made of plastics, which are more pliant and thus impact with less power than do metals ones, and are also more likely to be manufactured and fit together with smaller tolerances (and less freeplay). However, friction and wear can reduce tolerances in any kind of gears and also the axial truth of their spindles, potentially introducing appreciable backlash where originally it might have been negligible. Contrary to friction, backlash is a phenomenon which is fairly well-understood, and can be addressed, with varying degrees of detail, as either a simple deadband or a deadband with impact dynamics, using the established mechanics theory.

### 1.1.2.2 The Classical Backlash Model.

The classical model takes the simpler view of backlash as plainly a deadband centred about a shifted equilibrium. Notice this accounts for no transient impact dynamics, and implicitly takes all impacts to be simply fully plastic. What is missing from this model is of course the entire scope of any *backlash* whatsoever, in the true spirit of the definition. However, in earlier times there was less of a need to account for the transient behaviour in gears than in modern times. A diagramme of the classical model, following the same *reaction versus action* format customarily used to graph the concept of friction, is given in Figure 1.3 on the following page. Note that the slopes and deadbands may differ on either “side” of the nonlinearity due to gearing.

The predominant reasons for this simplification are two-fold: firstly, for the most part, large industrial machines (with relatively large tolerances) which ran at steady state never

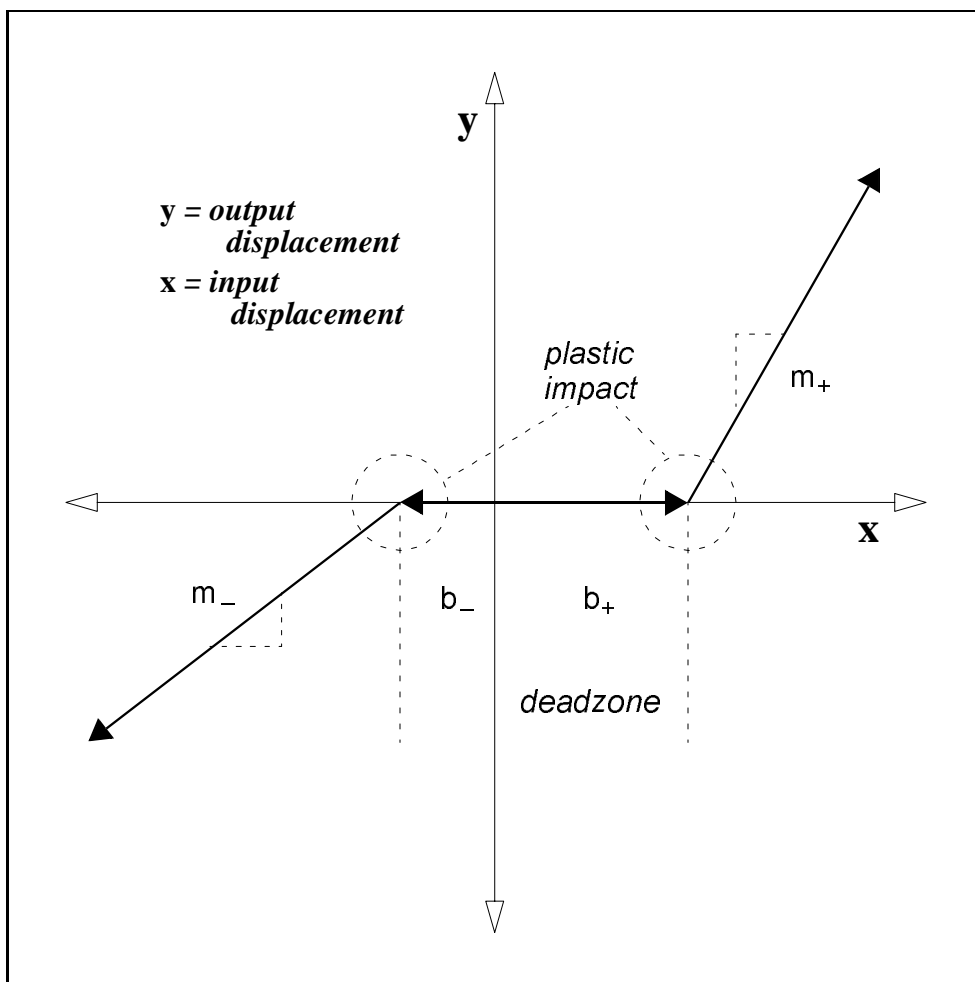


Figure 1.3: The classical deadband backlash model.

reversed direction as an integral part of their usual operation; secondly, smaller machines (such as the famous Swiss pocket watches) had tiny gears with almost no mass, and thus transferred very little impact energy to other gears (watch gears in particular were also lightly spring-loaded to prevent hysteresis). In short, there was originally no pressing need to model the impact dynamics, nor was it a well-understood phenomenon at the time.

The classical backlash model is widely developed in the control theory, and impact too has received plenty of attention from the robotics community (many references are given in section 1.2.3 on Research Trends in Backlash). However, very few people have modeled both effects together. Current industry specifications demand a more detailed model than those previously used.

### 1.1.2.3 The Modern Backlash Model.

Modern machines require greater precision than those a century ago, and the tighter tolerances in their mechanisms are an ongoing challenge to machine technology. Both dynamic aspects of backlash—deadband and impact—have, over time, become significant contributors to machine imprecision, as manufacturing technology now fights to keep up with industry-demanded tolerances. A complete backlash model will include the rigid, multibody, near-elastic impact dynamics in conjunction with the deadband.

Impact between two rigid bodies made of, for example, hard metals, will result in transient vibrations. Lower-frequency vibrations of the mechanism will result in structural positioning errors, whereas higher-frequency vibrations of the components will result in punctuated acoustic emissions. Since the noises caused by backlash are in and of themselves usually not any real hindrance to the usefulness of the machine—nor to its positioning precision—normally only the structural vibrations are considered; but since they constitute a finite part of the energy exchanged during impact, the assumption of purely elastic collision is not exactly correct when the acoustic component is ignored. Fortunately, the acoustic energy produced is under most circumstances relatively small compared with the structural component of vibration, so measuring the collision as purely viscoelastic is a fair approximation for many near-elastic materials.

The modern model may be represented as in Figure 1.4 on the next page. The transient vibrations demonstrate the effect of impact after the deadband is traversed when there is substantial compliance in the mechanism. The source of compliance can be due to either to distributed mechanical compliance(s) or co-located material elasticity in the backlash components. The various characteristics of the model will be discussed in detail in the following chapter.

### 1.1.3 Compliance.

*Compliance* denotes “the ability of an object to yield elastically when subjected to a force.” [227] Like backlash, it is a compound word formed *circa* 1647 from the 14<sup>th</sup>-century word pliant (like the modern plastic) and the prefix com-, which connotes a compounded effect. Compliance is thus an intrinsic property allowing an object to be elastic, and in this sense is synonymous with elasticity.<sup>35</sup>

---

<sup>35</sup>Selection of the terminology to describe this concept in this thesis involved some other factors. The word “elastic” appears in the title to flag computerised search engines, since “compliance” by itself has figurative as well as literal meaning as in engineering. Technically, “elastic” by itself would have been a more accurate choice than “compliance”; however, this was avoided since “elasticity” refers to a whole different field of continuum mechanics engineering which could potentially have obscured the simple element of elasticity presented here.

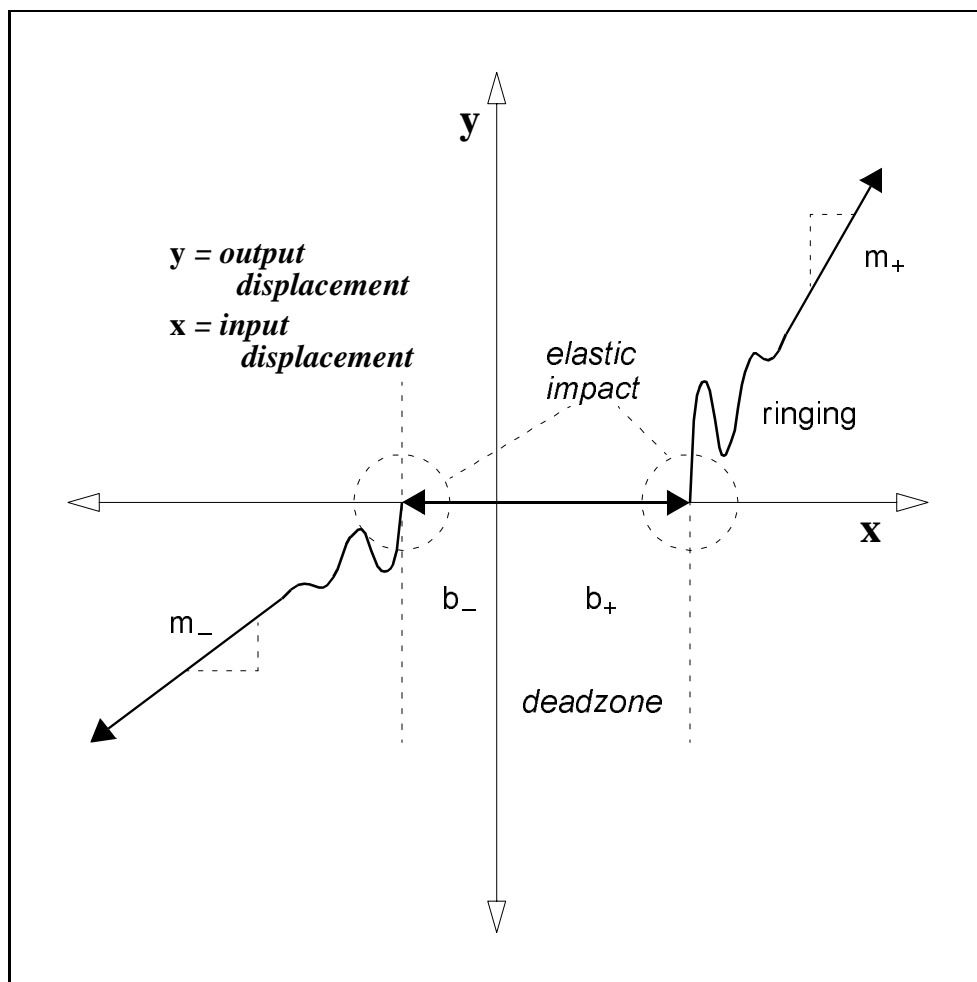


Figure 1.4: The deadband + impact backlash model.

### 1.1.3.1 What is Compliance?

Compliance is the manifestation of elasticity in solid, flexible bodies. Research in compliance extends some hundreds of years. Galileo Galilei (scientist extraordinaire, 1564–1642) first documented the “resistance” of solids in 1638 [135].<sup>36</sup> Robert Hooke (physicist, 1635–1703) in 1660 discovered the proportionality of stress and strain, “that is, the power of any spring is in the same proportion with the tension thereof.” [160]<sup>37</sup> This statement is now known as *Hooke’s Law* [215, p.2]. The question of elasticity was visited by several famous physicists and mathematicians, including Claude Navier (mathematician, 1785–1836), Leonhard Euler (mathematician, 1707–1783), Charles Augustin Coulomb (experimental physi-

<sup>36</sup> *Quod vide* [215, p.1].

<sup>37</sup> Hooke made his discovery at the age of 25 in 1660 but did not publish it for another sixteen years [215, p.2]. His modesty caused him also to miss the fame associated with Newton’s inverse-square law of gravitational attraction, which Hooke, to no avail, claimed to have discovered himself earlier [57, p.68].

cist, 1736–1806), Thomas Young (scientist, 1773–1829), the Bernoullis (mathematicians, 1700s), Siméon-Denis Poisson (mathematician, 1781–1840), Augustin-Louis Cauchy (mathematician, 1789–1857), Gustav Kirchhoff (physicist, 1824–1887), Heinrich Rudolf Hertz (engineer *cum* physicist, 1857–1894), and Lord Rayleigh (née John William Strutt, physicist, 1842–1919) [215, Introduction].

E. A. H. Love gives an excellent and detailed historical survey of all accounts in his book, *A Treatise on the Mathematical Theory of Elasticity* [215].

### 1.1.3.2 The Classical Compliance Model.

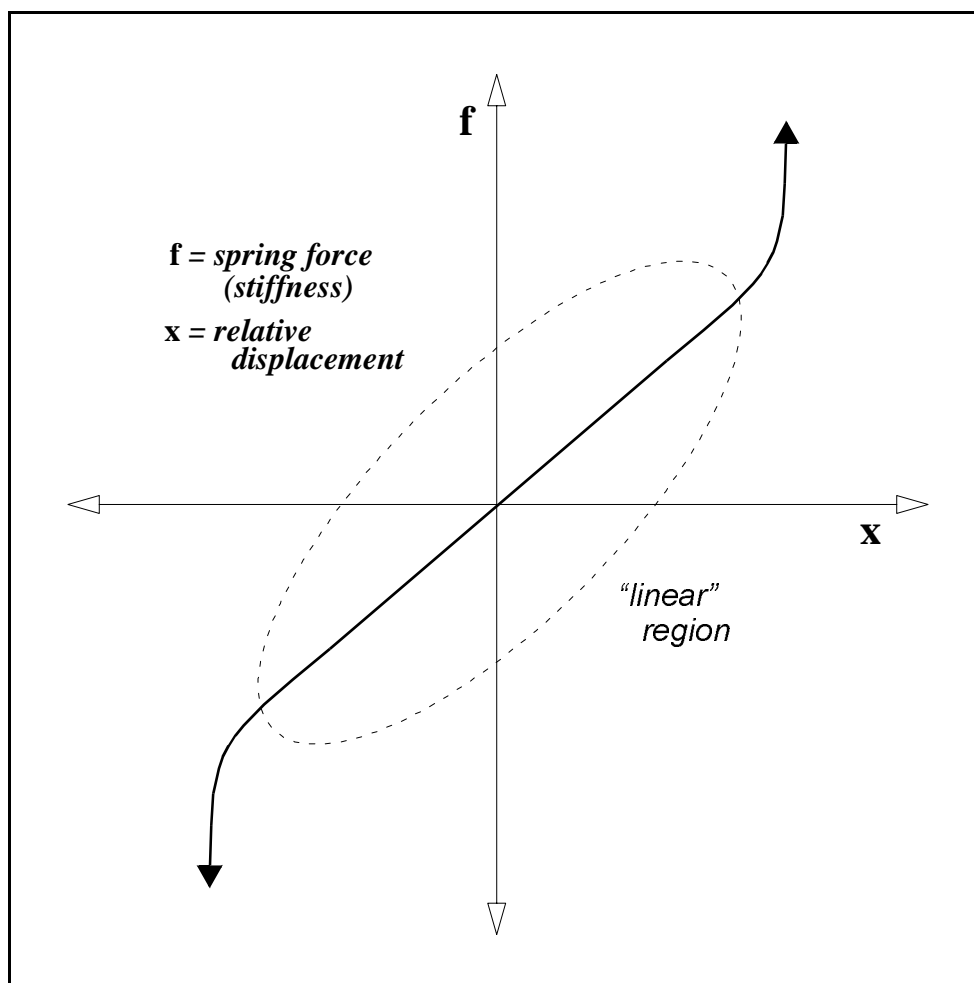


Figure 1.5: The classical fundamental mode compliance approximation.

The classical compliance model, characterised by Hooke’s Law, relates the strain of a flexible body to its stress. It is recognised that this is only true for a limited amount of strain, after which permanent, *plastic* or *yield* deformation will occur; however, within this

region the static compliance is linearly proportional to the force or torque applied to the body. A sketch of the classical model is shown in Figure 1.5 on the preceding page. This figure shows the effect with spring which is stretched to the edge of its elastic range, after which the additional force necessary to produce plastic deformation becomes apparent. Other possibilities also exist, for example, springs which deform substantially with little increase in applied force after some critical amount of stretch. In either case, the point is merely to recognise that the spring force cannot be assumed to remain linear beyond a reasonable range of compliant motion.

The classical model, which is a good approximation for limited strains and strain rates, is the type found in W. Voigt's (physicist, 1850–1919) classical second-order viscoelastically-damped system. The spring constant  $k$  describing Hooke's Law is typically determined via a mild static loading experiment.

### 1.1.3.3 The Modern Compliance Model.

A revised model is needed to address compliance in dynamic systems. Hooke's classical spring constant for a flexible body has the limitations that:

- it is accurate only under static conditions; and
- it is only valid for small strains and strain rates.

A complete model will include the nonlinear regions of compliance when vibrations are high in amplitude or dynamic in frequency. What the classical model describes is the fundamental mode shape and frequency of the compliant structure in question.

Extending the classical model to include dynamic contributions from higher structural modes is natural, and is encapsulated by the normal mode summation theory. This theory presumes that since each structural mode can be treated as distinct under harmonic excitation, the observed structural shape under vibration at any instant in time can be expressed as a weighed linear summation of the mode shapes. This theory assumes, however, that the internal damping of the structure is minimal, an imposition which with further development of the theory was at best relaxed only so far as to state that the method is approximate when the damping increases with increasing modal frequency. This does not pose a severe limitation on the applicability of modal summation, however, particularly when considering the fact that, when compared with a nonlinear vibrational model, it is usually more easily implementable in real-time systems. Modal summation extends Hooke's Law into the domain of dynamic excitation, whilst retaining the simplicity of the classical formula: instead of a single second-order equation of motion there are now  $n$  equations, where  $n$

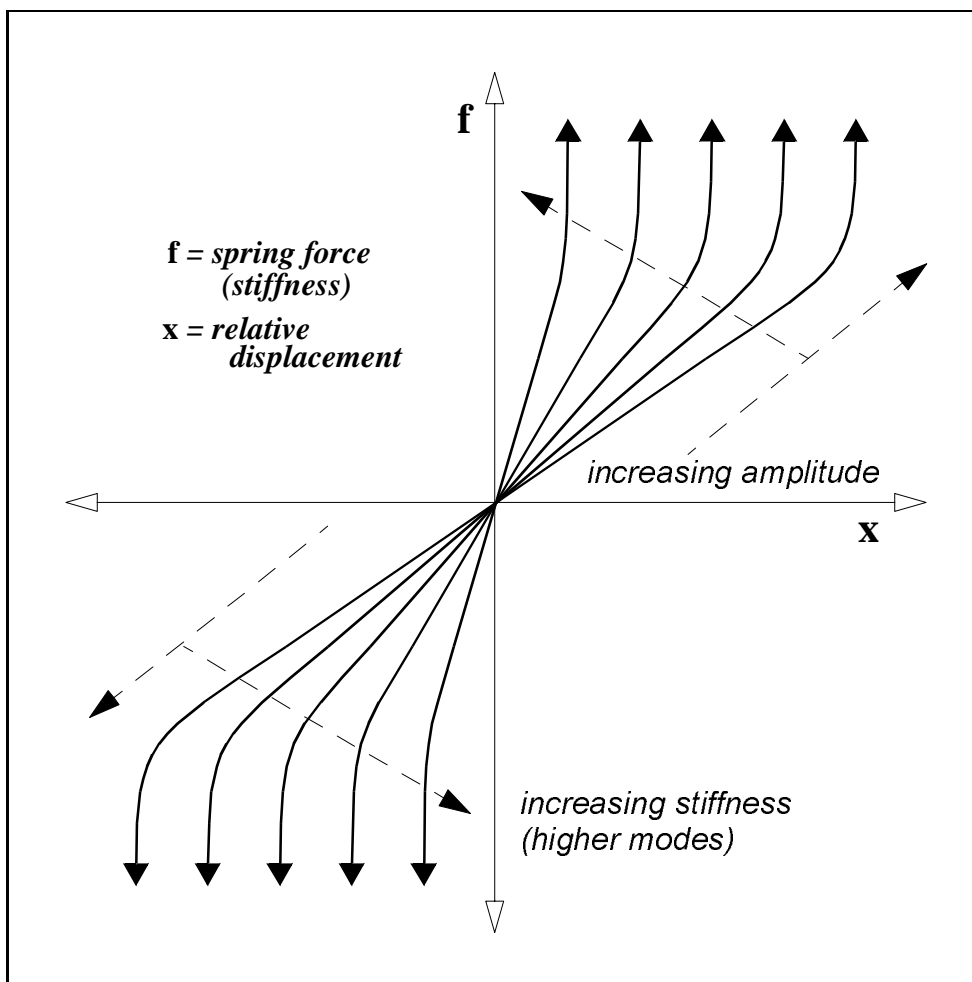


Figure 1.6: Summed modal compliance approximation.

may be truncated at a finite mode number appropriate to the problem at hand (recall that typically the damping increases with every mode).

Modal summation, however, still has limitations when there are large excitation amplitudes acting on the structure, when the modal frequencies are closely-spaced in the natural spectrum of the structure, or when damping couples the modes.<sup>38</sup> To treat this potential problem and thereby further generalise the summation theory, one may consider replacing the linear sum of  $n$  *linear* second-order equations with a linear sum of  $n$  *nonlinear* second-order equations. Because the modal coupling will always be via the system damping (since this is the only effective “cross-term” in the second-order mathematical rendition), allowing the damping term to be nonlinear will allow the rest of the equation to be effectively

<sup>38</sup>Damping will couple the modes when there is much of it, because damping “spreads” out each modal peak in the structure’s spectrum.

linearised. This manipulation is disclosed in detail in the next chapter.

The modern nonlinear compliance model may thus be viewed as a linear summation over nonlinear mode shapes which depend on relatively static variables, for example the excitation amplitude at a given frequency. In other words, the harmonic vibration of a conservative structure may be approximated reasonably well by a linear  $n$ -degree-of-freedom system of nonlinear vibrational modes. The nonlinearity is encompassed by a nonlinear spring constant for each mode, which can be fully characterised by a simple function of excitation frequency and amplitude.

A graphic representation of the nonlinear, dynamic compliance model is shown in Figure 1.6 on the page before. The total compliance is a weighed summation of one or more of the nonlinear mode shapes of the structure at any given point in time.<sup>39</sup>

#### 1.1.4 Motivation for the Study of Friction, Backlash and Compliance.

As discussed at the outset, the study of these three basic nonlinearities is chiefly motivated by the fact that arbitrary combinations of these effects nearly span the gamut of observed behaviour in almost any machine transmission, particularly in the sense of nonlinear disturbances on machine control. Commonly, the mathematical descriptions of machine dynamics are linearised to facilitate the dynamic analysis and control design; in such cases there will almost always be some observable, if not downright unacceptable, levels of nonlinearity caused by friction, backlash and/or compliance. Even in nonlinear systems design, unmodeled, higher-order effects can sufficiently corrupt the desired actions of a machine when the nonlinearity descriptions are mathematically simplified. So in some cases, it is necessary to have a detailed understanding and commensurate model of these basic nonlinearities. As the desired precision of machines is pushed closer towards the boundaries of our design and manufacturing capabilities, for example as in Microelectromechanical Systems (MEMS) design and manufacture, or so-called agile and flexible manufacturing stations, as well as standard machine tools, a better understanding of transmission nonlinearity will be crucial to successful high tolerancing of consumer and industrial products, and hence, the quality and economy of those products.

Further study of these three basic nonlinear phenomena is necessary, and can be facilitated by experimentation on a test bed designed to introduce precisely-quantified combinations of backlash, stiction and compliance to the drive-train system. In particular, research into the effects of combined, rather than individually-isolated, drive train nonlinearities is warranted.

---

<sup>39</sup>It will be shown in the theory that these weights relate to the natural frequencies and frequency of excitation of the system.

#### 1.1.4.1 Understanding Friction.

On a fundamental level, scientists are simply curious to explain the precise phenomena associated with friction—it is still not fully understood, and there remain competing theories of its mechanism on the microscopic scale. Diverse applications of friction control also abound for the general benefit of humanity, for example, as with friction-motivated studies of seismic damage prevention [203]. Friction causes wear in machine joints, severely reducing any machine’s useful lifespan [276]. And friction also causes a good deal of the economy to be lost to it in the form of dissipated (and unrecovered) heat loss. This revelation of the economic detriment associated with friction (and hence, wear) provided a particularly tangible motivation for industry to invest and expand study in the fields of tribology and lubrication at the turn of this century; in 1907, former American Society of Mechanical Engineers president Robert H. Thurston proclaimed:

It is readily seen that in all well-designed machinery friction is the sole cause of lost work. The other possible cause, the permanent deformation of parts, cannot in such cases exist: every piece which is altered in shape by the forces received and transmitted, since it is never sprung beyond the elastic limit, restores by its restoration of form all energy expended in its alteration. Hence, the study of the methods and magnitudes of friction losses, and the laws governing their production, is, next to the theory of pure mechanism, the most important study in relation to the transmission [and “waste”] of energy by machinery. [347, preface]

Increased modern demands on machine tooling precision is currently motivating renewed interest in the control of friction in machines.

#### 1.1.4.2 Understanding Backlash.

Often, the impact is overlooked in machine design and control, with unhappy results. Typical sources of impact include: clearance between cams and followers; backlash or bearing clearances in mechanisms undergoing force or motion reversal; and mechanisms with components having large relative velocities.

The study and control of impact phenomena is especially important for machine designers, since: first all the major stresses in mechanical systems arise as a consequence of impact, and many serious machine failures are generated when impact forces are not properly recognised and controlled;<sup>40</sup> secondly, use-

---

<sup>40</sup>Gear tooth failure (complete or near-complete shearing) will result in a sudden and highly significant increase in backlash, further compromising the mechanism accuracy and possibly causing damage to the machine as a whole.

ful short-duration effects, such as high stresses, rapid dissipation of energy, fast acceleration and deceleration, can be achieved from low energy sources by controlling the impact of bodies at low force levels. [349, p.85]

Better precision, accuracy, speed and agility are demanded of modern machines. The range of precision currently demanded certainly approaches, and sometimes even exceeds, the composite precision of available mechanism components, requiring either a design modification or a special control strategy. The traditional deadband model of backlash fails to address the full issue, so a more complete model must be brought to light.

#### 1.1.4.3 Understanding Compliance.

Most of the time structures built by humans or nature have so many mechanisms built in for dissipating vibrational energy, that the presence of extraneously excited vibrations is rarely noticed. It is for this reason that the need for damping is often not recognized; it has been there often enough to get us out of trouble nearly all the time. Nowadays, as we continue to build ever more efficient and economical structures for various purposes and increase the demands we place on these structures, we also tend to eliminate many of the sources of damping which, though without full recognition, helped such structures to survive their service environments in the past. [236, p.45]

Modern machine tools operate at higher cutting speeds and feed rates to improve productivity. [24, 243] Vibrations at the cutting edge of the tool can cause chatter and may indicate tool damage. Under such situations, especially in high production operations, identification and control of tool compliance can help prevent “catastrophic” failure, and improve workpiece quality during normal operation. Assuming that machine vibrations are intrinsically dissipated is obviously imprudent.

## 1.2 Current Trends in Nonlinear Drive Research.

There is a vast literature on friction especially: the number of journal papers and proceedings presentations add into the thousands world-wide on the subject of friction. Compliance commands a well-understood theory and only in the nonlinear sense of compliance is research by mechanics experts still quietly active. In great contrast, on backlash there are far fewer articles, and many of these are on the subject of hysteresis models by mathematicians, *exempli gratia* [218]; application of backlash identification and control has remained the domain of relatively few investigators. Despite these dedicated efforts, however, a truly comprehensive look at friction or backlash in compliant systems, or backlash

in frictional systems, has been the study of merely a handful of researchers and articles world-wide, if that. This study appears to be one of the very few seeking to address all three nonlinearities together.

### 1.2.1 Shortcomings in Current Research and Technology.

Whereas multibody dynamics, including those of impact as in backlash, are fairly well understood, as are vibrational studies associated with compliance, even at this point in time, scientists are only beginning to better understand the actual mechanisms of friction. Friction, however, acts and reacts intimately with the two other basic nonlinearities as manifested in machine mechanisms large and small. So this lack of understanding is one of the current technological shortcomings. Meanwhile, the urge to smooth over these nonlinearities is not uncommon, and much research effort has been devoted to less than adequate approximations of real system behaviour—nonlinearities are a messy subject! Of course, nonlinearities present mathematical complications and difficulties which make them less convenient and tractable than one might like them to be, so more concerted effort is also required to deal with them. This takes time, and only recently have positive results begun to emerge in the literature in terms of fully nonlinear simulation and control of friction, backlash and/or compliance.

Other shortcomings on social, political and economic levels also exist due to the social construct of science, in some cases hindering the progression of scientific research. Though these variables are of a less technical domain, their effect on the dynamics of conducting research is considerable, if not dominating. These effects would include, for example, the industrial mindset of the American marketplace, which is only recently transiting from quantity-oriented to quality-oriented consumer goods production. Government and industrial sponsorship of certain research programmes also plays into the equation of *which* scientists *where* are funded to perform *what* kind of study, and so on. [322]

#### 1.2.1.1 Social, Economic and Political Factors.

Prior to the popularity of the World Wide Web, the information available, and the ability to coordinate it, must have been more manageable than today: the sheer population of available articles on friction, backlash and compliance, made retrievable through world-wide digital networks connecting every university and research institution, has opened the proverbial floodgates enough to overwhelm even the most focused researcher. The knowledge that other workers half the world over might potentially be conducting concurrent experiments was previously restricted by the few publications dedicated to the field; yet, even the selection of which publication to use for the dissemination of results seems in many

cases to be a political decision as well as a practical one. The landscape of scientific research and remote collaboration has started to change rapidly for the better in recent years, yet there is still the shadow of sparse collaboration and organisation only slowly now drifting away, leaving its (date)mark on the works of researchers prior to the past decade. There now exists an incredible dead weight of literature from the world over, only some of which is particularly insightful or useful, yet all of which must be sifted through, like grading different qualities of ore from within mounds and mounds of earth. I cannot imagine any colleagues on this cusp of the information age who haven't had to grapple with this issue, and certainly the field of drive nonlinearity has suffered a similar history over the years.

Another perspective on the problem makes it apparent that the top-heaviness of the friction literature classifies the dominant scope of interest. In some cases, backlash and compliance are considered design problems best remedied by direct-drive servomotors and stiffer robotic linkages. Friction too may turn this way with the high-tech hope of a perfect dry surface lubricant to emerge sometime in the future. This is largely a philosophical issue, as the simpler and cheaper mechanical systems will surely always remain in use and exhibit some degree of these basic nonlinearities. In the case of the predominant status of machine tools in use, answering the question of arbitrary combinations of friction, backlash and compliance in terms of a software-implementable solution may well be the smartest choice given its relative economy, as well as being the most pragmatic option the machine shop floor manager can implement, and this question is the main motivation inspiring this thesis.

A further obstacle to integrating the world's knowledge on these subjects continues to be the ubiquitous language barrier. This is especially pertinent to those leading research and development in the area of machine tools: the United States, France, Germany and Japan—the world's major industrial powers. To our advantage in the U.S. and the U.K. (England was the home of the industrial revolution, and presently is also leading industrial research, particularly with a mechatronic bent—as is Australia for that matter), we speak the accepted international language of science as natives. However, primarily for reasons of culture and economic competition, it seems France, Germany and Japan, in that order of predilection, publish a significant level of scientific work in their own native tongues. Most engineers in those countries know English fluently, yet conversely, most native speakers of English are unilingual, placing England and America at a potential disadvantage. Duplicated efforts across the oceans have been known to occur, and in the field of research on drive nonlinearities it is no different. Restriction of importation and exportation of high technology are traditional tools of economic protectionism and imperialist isolationism, and further stifle the free trade of scientific progress. Fortunately, new technological freedoms

and abilities to communicate across the globe are beginning to overturn this norm, promoting new opportunities for international collaboration [163]. Researchers in the U.S. who are leading current domestic work on machine tools are predominantly bilingual, and many have strong contacts with other researchers in Europe and Asia working on similar efforts, in part made possible by modern communications technology. Because the research requires interdisciplinary effort, such communication is very salutary. [361]

### 1.2.1.2 Scientific Factors.

Limitations in engineering technology are requiring a deeper understanding of how to control drive nonlinearity to obtain better engineering precisions. Even da Vinci recognised the importance of frictional wear, for example, in terms of precision:

It is impossible to give or make anything of any absolute exactness, for if you desire to make a perfect circle of the movement of one of the points of the compass, and you admit or confirm . . . namely that in the course of long movement this point tends to become worn away, it is necessary to concede that if the whole [of the point] be consumed in a whole of a certain space of time, the part will be consumed in the part of this time, and that the indivisible [microscopic] in the indivisible [infinitesimal] time may give a beginning to such consumption.

And thus the opposite point of these compasses which turns in itself over the centre of this circle, at every stage of movement is in process of being itself consumed and of consuming the place on which it rests; whence we may say that the end of the circle is not joined with its beginning, rather the end of such line is some imperceptible part nearer towards the centre of such circle. [217, p.601]<sup>41</sup>

Understanding friction can certainly aid us to compensate for the imprecisions and inaccuracies of machines requiring higher tolerances.

Stribeck, in concert with da Vinci, remarked how repeated experimentation and the associated bearing wear introduced conflicting data in his investigations [319, p.1346]:

In experiments where the friction would otherwise be constant, increasing lubricant temperature caused the friction to rise, not fall. . . This does not agree with the previous experiments, as evidenced, . . . but suggests that it is

---

<sup>41</sup>*Quod vide* Forster Bequest Manuscripts II 133 r. and 132 v. What da Vinci is trying to say here is that the frictional wear of the pencil inevitably leads to the enscription of what is truly a spiral in the correct, microscopic sense, although by macroscopic observation the ends appear to join exactly and form a complete circle.

caused by the repeated wear and cycling between active use and disuse of the bearings.

[For this reason] I suggest that each experiment be carried out twice at most, possibly thrice. Repetition of experiments at moderate and high speeds verified the traditional observation that at low speeds, friction only agrees qualitatively with its original measurement.<sup>42</sup>

He clearly observed that frictional detritus and the marring of surfaces through extensive use both contributed significantly to the measurement of friction. Thus friction increases over the lifetime of a machine clearly indicate the likelihood of wear in the bearings. This is just one component of the current interest to use friction in monitoring a machine's health over its useful lifetime.

### 1.2.2 Trends in Friction Research.

What then, about friction? The answer is that in spite of both classical studies and recent advances there is hardly a single phase of the subject which is not still in the controversial stage. Authorities are in general agreement as to the nature of heat, the dual character of light, x-rays, radioactivity, and relativity—all topics of comparatively recent origin—but there is no such agreement with regard to friction. [253, p.342]

Though this was written in 1949, recent investigation has reconfirmed, with some chagrin, the fact that friction at low velocities can not be accurately modeled as a constant parameter, much less a consistent one. Friction is known to depend on a variety of specifiable influences at the contact interface, including pressure, geometry, temperature, lubricity, material, transition velocity, lubricating fluid composition, and even the history of prior frictional behaviour at a given point, over time [23]. These factors, each of which may produce a unique or tandem behavioural contribution to the macroscopic interfacial friction, make it very difficult to formulate a comprehensive description to account for all possible friction conditions, even given a very specific machine with specific characteristics.<sup>43</sup> The extent of the problem is critical, and the interdisciplinary component of friction research is particularly evident in a criticism by K. C. Ludema of the University of Michigan:

The lack of good models is surely the result of the complicated nature of friction and wear, but little has been done to plot a rational course through the complexity. [216, p.1]

---

<sup>42</sup>Translation by the author.

<sup>43</sup>Researchers who continue to oversimplify the problem of friction may find themselves without any useful applications of their solutions to real machines!

Understanding of friction and wear is a daunting endeavor also because of the great number of variables that influence friction and wear rate. [For example,] equations for wear in lubricated sliding would include variables from: [216, p.2]

- hydrodynamics, which are mostly those of fluid mechanics plus methods for describing surface topography and contact area;
- contact mechanics, mostly from linear elasticity, sometimes from plasticity but seldom from visco-elasticity;
- materials engineering, relating to (quasi-static) substrate material properties and failure mechanisms, occasionally including fatigue properties;
- chemistry, relating to the function of active chemical species in lubricants.

The point that four different disciplines are active in research is reassuring, but there surely is separation of thought when such distinct disciplines work in the same field.

Friction research continues to evolve within numerous, separate subcategories of specialised research: lubrication theory, material surface science, (nano-)tribology, wear modeling, friction modeling, and control systems theory. In the vast sea of available literature on these subjects, certain researchers and research institutions are nonetheless distinct contributors to the field. It is worthwhile to mention that the majority of friction research (published in English, anyway) is happening in the United States, England, and Japan, with strong contributions from Poland, Italy and Taiwan. The first three are major multinational corporate nations, and the latter, while also major industrialised nations, are particularly major machine tool manufacturing nations.

Friction is well-studied in the literature, and is an effect present to a significant degree in mechanical positioning systems; it is more pronounced in the slowly-moving and discrete position movement or cycling inherent to the smaller, more flexible machine tools currently being developed, and is therefore of particular interest. Traditionally, a dithered control signal is used to provide a mean system excitation greater than the static friction threshold. Adaptive strategies have also been implemented for stiction, but not in conjunction with other non-linearities.

### **1.2.2.1 Transdisciplinary Trends in Machine Lubrication, Material Surface Science, Nanotribology and Wear Modeling.**

In lubrication, among those spearheading a new understanding of various imperial observations of frictional behaviour on the microscopic scale in light of fluid mechanics, is Jacob N. Israelachvili [175]. Very recently, our own John Tichy at Rensselær, collaborating with

his graduate research assistant, has furthered an understanding of friction and lubrication based closely on Israelachvili's results [176]. Bernard Friedland of the New Jersey Institute of Technology (NJIT) has also been contributing to the lubrication theory for some time, especially in conjunction with his colleague (previously also with the NJIT), Young-Jin Park of the Korea Advanced Institute of Science and Technology (KAIST) [14, 129–131, 153, 155]. The same can be said of Andres Soom and his associate Andreas A. Polycarpou from the State University of Buffalo in New York [158, 266, 267]. R. Bell and M. Burdekin in England together helped pioneer the field, and continue to do so [38, 39]. In Japan, Shinobu Kato of the Fukui Institute of Technology has also long been active and continues to contribute [184, 223, 224].

Various specialists have been leading to a better understanding of effects like bearing stiffness (normal force) influence on stiction [204, 345], electrical dependence of stiction [296], sliding friction [196, 259], environmental dependencies of friction [191], boundary lubrication [43, 159, 194, 195], dry lubrication [324], and other surface and lubrication phenomena [3, 40, 228, 274, 382].

Recent major conferences covering lubrication aspects of friction include:

- the 1995 (June) NATO Advanced Research Workshop, hosted by the NATO in Trieste, Italy;
- the 1995 (August) Workshop on Physics and Chemistry Mechanics of Tribology, hosted by the ACS in Bar Harbor, Maine;
- the 1996 (June) NATO Advanced Study Institute, hosted by the NATO in Sesimbra, Portugal.

### 1.2.2.2 Trends in Macroscopic Friction Modeling.

Because of the numerous variables present in modeling friction, the literatures suggests a number of approaches to ease the scope of the problem. Chief among them are dimensional analysis [18, 20] and reduction (parameter “lumping”, usually via perturbation methods) [156]; modeling of individual frictional “régimes” split across one or two salient variables like interfacial velocity [165]; problem reduction by informed mechanical redesign; and comprehensive comparative analysis of the individual and combined contributions of the various influential variables and subsequent model simplification [23]. Brian Feeny, a colleague of Clarke J. Radcliffe, both at Michigan State University, has recently received funding from the National Science Foundation (NSF) to develop nonlinear modeling and extend an understanding of friction to undergraduates in the classroom [113, 114, 208]. F. Pfeiffer of the Technische Universität München (Germany) has modeled multibody

friction dynamics, most recently multicontact stick-slip friction [260]. Finally, the pioneering efforts of Ernest Rabinowicz [275, 276], F. P. Bowden and David Tabor [47, 48], must be duly recognised, because they wrote the first enduring texts to help found the field. Bowden has been active in the field since the late 1930s, and Rabinowicz and Tabor since the '50s.

Proceedings of two major recent conferences on friction modeling present the contributions of numerous other scientists:

- the 1994 (September) Second International Symposium on Contact Mechanics in Carry-le-Rouet, France, published by Plenum Press [279]; and
- the 1995 (September) Biennial Conference on Mechanical Vibration and Noise, hosted by the ASME in Boston [74].

Various research is ongoing towards a better understanding of the chaotic behaviour of stick-slip friction [112, 115, 116, 150, 268–270, 370], the dynamic boundaries and stability of stick-slip friction [1, 16, 30, 41, 42, 54, 55, 149, 164, 179, 180, 193, 209, 232, 278, 283, 284, 287, 288, 291, 302, 353, 360, 363, 364, 379], dwell-time effect on “rising” static friction and subsequent stick-slip cycling [140, 285], multibody stiction [327], and computer simulation of friction [183, 330].

### 1.2.2.3 Trends Towards the Controllability of Friction.

In control systems, Brian Armstrong-Hélouvy of the University of Wisconsin at Milwaukee has notably contributed his long-standing experience by bridging for controls researchers the current germane elements from the tribology and lubrication fields [19]. With two close associates, well-known in their own rights, he recently generated a comprehensive survey on the subject of friction [23], touching upon all important aspects. He also continues to make important individual contributions [17, 18, 21, 22]. Carlos Canudas de Wit of the Laboratoire d’Automatique de l’École Polytechnique à Grenoble, a collaborator on the survey with Armstrong-Hélouvy, has since provided an improved, simpler model than that suggested by Armstrong-Hélouvy which nonetheless captures all the important dynamics. His model, developed in association with Karl Johan Åström of Lund University (well-known for his contributions to adaptive control theory), forms the basis of the model used at the foundation of the work presented herein [58–62]. Pierre E. Dupont of Boston University has worked on models of boundary lubrication in friction, and volunteered methods to aid in its controllability, in addition to assisting on the landmark survey paper with Armstrong-Hélouvy and Canudas de Wit [98–105].

Other detailed surveys are given, among others, by Naomi Elizabeth Ehrich-Leonard’s 1991 Master’s Thesis at the University of Maryland at College Park [106], and also by

J. A. C. Martins and J. T. Oden at the University of Texas at Austin [222, 244]. Friedland and Park have contributed a simultaneous friction-and-velocity observer [131], recently improved by Tafazoli *et alii* [328]. Clarke J. Radcliffe of the Michigan State University, and his previous graduate Steve C. Southward, now with the Lord Corporation in North Carolina, have contributed for some time to stick-slip modeling and control [277, 312], a tradition continued by Feeny. Masayoshi Tomizuka of the University of California at Berkeley has also long been working on controls against friction. His work is discussed in the context of “Trends in Machine Tool Research” in section 1.2.7.

Hundreds of other papers in friction control exist, and are all but ubiquitous: again, their sheer number precludes individual recognition here—the reader is kindly referred to the bibliography for a comprehensive listing. Of particular noteworthiness, however, are recent, major conferences with sessions specifically devoted to friction. These include, in chronological order:

- the 1993 (June) American Controls Conference, hosted by the American Controls Council in San Fransisco [11];
- the 1995 (June) American Controls Conference, hosted by the American Controls Council in Seattle [12];
- the 1995 (December) International Conf. on Decision and Control, hosted by the IEEE in New Orleans [172];
- the 1996 (April) International Conf. on Robotics and Automation, hosted by the IEEE in Minneapolis [174];
- the 1996 (September) International Conf. on Control Applications, hosted by the IEEE in Dearborn, Michigan [173].

These conferences cover all aspects of friction control currently researched.

Many journal articles and books also exist, marking input from many other researchers worldwide. These cover a wide range of applications like proportional + derivative (PD) control [2, 376], proportional+integral+derivative (PID) control [2], fuzzy logic control [178], neural network control [202], hybrid fuzzy-neuro control [186], pseudo-derivative feedback (PDF) control [162], robust control [2, 6, 46, 59, 95], sliding mode control [205, 229], adaptive control [10, 26, 107, 187, 239, 241, 248], hybrid analogue/digital control [28, 125, 152], evolutionary (genetic-algorithm) control [178, 188, 189], and (on-line) numerical simulation of friction for model-reference control [139, 185].

### 1.2.3 Trends in Backlash Research.

Backlash is a highly nonlinear effect, and has the ability to excite high-order modes in a drive train, unlike compliance or friction; with the aforementioned present, drive controllability is further undermined. A number of hysteresis models have been presented for approximating backlash, but further study is advised [218]. Control strategies such as dithering have been applied with some success many years ago [126, 127], but relatively few researchers have pursued a better understanding of mechanical backlash over recent years.

Recently, a state-of-the-art controls perspective was published in book form by the two main researchers in the field, Gang Tao of the University of Virginia and Petar V. Kokotović of the Center for Control Engineering and Computation at the University of California at Santa Barbara [333]. This work is based on numerous articles and proceedings of theirs over the past decade or so, an almost obscene number of which were printed in a small concentration of journals in 1995 alone [331, 334–341, 348]. Particularly revealing is the observation that the titles for this flurry of articles are almost identical except for the random exchange of the key terms, backlash, dead-zone and hysteresis. This casual terminological exchange betrays, in spite of their great efforts, the consistent misrepresentation of backlash as a pure hysteresis or deadzone, as a convenient mathematical simplification necessary to obtain a convenient system-theoretic representation of the phenomenon. Hopefully their results will nonetheless retain some degree of usefulness in real systems, a standing question since they provide not a single example in neither their papers nor text.

The importance of impact phenomena has in recently been exhorted by A. Tornambè of Terza Università di Roma, who ignores the work of Tao and Kokotović completely in his control design and simulations [349–351]; A. Tustin had emphasised the same even as early as 1947 [358, 359]. One objective of this thesis is to resolve the applicability of the algorithms developed by these researchers when used to control an actual system.

Other scientists have made valuable contributions to modeling and control of backlash as well, in the areas of hysteresis modeling [218, 240, 255, 323], phase-plane analysis [250], adaptive control [213, 281, 325, 373], neural control [300], robotic reflexing [369, 380], numerical simulation of plastic collisions [316, 317], impact analysis [96, 97, 137, 141, 154, 206, 210], and even the *advantages* of backlash in control mechanisms [247].

### 1.2.4 Trends in Compliance Research.

Of the three main drive nonlinearities, compliance is the simplest effect to model, and in many cases can be lumped as a parameter within the system it affects; since rotating cutting tools have limited torsional stiffness (especially in the case of miniaturised machine tools), for example, drive-train compliance might be modeled in series with the compliance

of the tool. Cutting-tool vibration is known to adversely affect the quality of the workpiece as well as reduce the lifetime of its spindle bearings [51]. Machine tool feed drives are also suspect of compliance, particularly during the rapid tooling of complex product designs, where there is typically a good deal of back-and-forth cutting motion.

Tool compliance in conjunction with friction at the tool-workpiece interface is analogous to the problems of flexible beams carrying payloads or following (frictional) contours, or rigid elements linked by flexible joints. Hence the field of robotic research has much to offer in the way of understanding compliance. [167–169, 190, 354, 384]

Adaptive control strategies have been developed for the case where the drive-train compliance is not known *a priori* or varies slowly with time [381]. S. Nicosia and P. Tomei of the Seconda Università di Roma, for example, have developed a globally asymptotically stable control law for robots with a single flexible joint [238], and other have followed suit [219]. A more interesting case, however, arises when compliance is present in addition to other non-linear effects.

Various researchers have contributed to compliance research [309, 311], including modeling [86, 128, 132–134, 329], nonlinear compliance control [5, 136, 142, 161, 303, 383], adaptive control [35, 177].

### 1.2.5 Composite Models for Friction, Backlash and Compliance.

A small number of researchers have addressed the more prevalent problem of the three basic drive nonlinearities acting in concert. Realistically speaking, though any one of the nonlinearities described may by itself produce errors in a particular mechanism, it is likely that some significant error from the other nonlinearities will also arise. Specialised mechanisms exist to mechanically limit the manifestation of certain nonlinearities, but this is usually exchanged for an increase in one of the other confounding effects—redesign can thus treat the problem in a limited fashion at best. The counterpart to this realisation is that machines which are *not* specifically designed to mitigate certain nonlinearities may have arbitrary combinations of friction, backlash and compliance never specified by the manufacturer. Worse still, even machines with carefully specified nonlinear drive characteristics will wear with regular use, causing a slow but steady drift from the designed movement of its various mechanisms. For this reason it is particularly important to examine the combined effects of the three basic drive nonlinearities together, as well as their characteristic behaviours when changing throughout the lifespan of the machine tool. The contributions to this area by the literature, however, are as of yet minimal in comparison with theories addressing only the “pure” nonlinearities. Furthermore, there exists almost no work attempting to describe all three of the basic nonlinearities in concert; most efforts

in this direction model at most two of the three at once.

U. Schäfer and Gunther Brandenburg have devoted the past decade to the study of rigid bodies with elastic and frictional transmissions [295]. Their work also includes an analysis, without experimentation, of adaptive compensation for all three of the basic nonlinearities [50]. K. Richter of the University of California at Berkeley, extending collaborative work with F. Pfeiffer on multibody dynamics with elastic elements, generalises the results of flexible beam control to include friction in the actuators [286]. A converse approach has been taken by other researchers investigating the effect of a sudden impact on a slewing flexible beam with friction in the spindle [65, 368].

The only recent attempts to study backlash in conjunction with friction, also the culmination of years of effort, are by D. M. Gorinevsky *et alii* [144], N. Sepehri *et alii* [301], and Jeong-Yul Jeon and Jong-Hwan Kim of the KAIST [178, 188, 189]. Masayoshi Tomizuka of the University of California at Berkeley has devoted some effort to friction control with backlash and saturation [197], predominantly in the context of machine tool control (described in greater detail further on). Before this there was one important two-part work on the same subject by A. Tustin in 1947 [358, 359] and another by K. N. Satyendra in 1956 [293].

Backlash and compliance have recently been studied together in the context of a slewing flexible beam with backlash in the spindle drive, by Nabil G. Chalhoub and Xiaoying Zhang [64]. They assume, since the backlash in their mechanism is relatively stiff compared to the compliance, that the elastic impact effect is ignorable.

Very recently, the AGNC Corp., a U.S. defence contractor, examined fuzzy control of a flexible system with friction and backlash [212].

To use these models on-line, it is necessary to provide the computer with an identification and control structure which can be updated in real time. Because the composite nonlinear models are fairly complex, simple identification methods need to be exploited to make system control viable. One of the currently “hot” topics in nonlinearity modeling is use of the *describing function* method. This method is a hopeful candidate for on-line system identification of nonlinearities because it is well-understood and simple to implement. J. Tou and P. M. Schultheiss in 1953 [352] and K. N. Satyendra in 1956 [293] were concerned with the use of describing functions to model drive nonlinearities, and soon after him C. N. Shen and his graduate research assistants at Rensselaer as well [211, 304–306]. Currently Abílio Azenha and J. A. Tenreiro Machado of the University of Porto [27], José A. Inaudi of the University of California at Berkeley [165, 166], and Michæl Feldman of Technion-Israel Institute of Technology [52, 117–119, 121–123, 145, 146] are further developing this technique. Many others have contributed to the describing function analysis of nonlinearities [50, 245, 295, 307],

but some researchers disagree, stating that describing functions are qualitatively useful, but quantitatively incorrect [23]. One of the objectives of this thesis is to assess the potential and accuracy of the describing method for a nonlinear drive system.

### 1.2.6 The Problem as it Pertains to Machine Tool Technology.

With the increased requirements imposed by higher levels of productivity and increased automation, the demand for increasing accuracy and reliability of products is becoming increasingly stringent. Innovations in manufacturing technology have also been driven by demands to shorten production cycle time and to maintain a consistently high level of product quality in an advanced manufacturing environment. Since the manufacturing accuracy of the machine tools and the accuracy of the finished workpieces are interconnected, no doubt, the performance of a machine tool has a direct influence on the dimensional [tolerance] of the finished workpiece. Therefore, enhancing the accuracy and effectiveness of the machine tool is one of the key requirements for improving product [quality]. [233, p.389]

The above statement was made by researchers investigating the unmodeled effect of tooling error due to frictional heating at the tool-workpiece interface.<sup>44</sup> Their conclusion, however, is as applicable to any other source of machining error, including, of course, friction, backlash and compliance. To wit:

Mechanical systems are distinguished from other controlled plants by several significant nonlinearities such as static friction (stiction) [*sic*], Coulomb friction, backlash and actuator saturation. Among these nonlinearities, the backlash may be reduced at the expense of the increased stiction and Coulomb friction. The actuator saturation primarily affect[s] the transient performance. Stiction may cause... steady-state error, or limit cycle, near the reference position in the linear control of [the] positioning system. [374, p.188]

To understand where the effects of friction, backlash, and compliance come into play with machine tools, it is useful to describe the overall tooling function as a kinematic interaction between the cutting tool and the workpiece. To produce a finished product by cutting away material on the workpiece, the tool and workpiece must move relative to one another, usually in a combination of many possible different directions, speeds, and mutual configurations. Lathes, mills and the like all utilise either rotational or translational drive

---

<sup>44</sup>This is a subject currently under investigation here at Rensselær as well, by Andrew Yoder, working with Richard Smith under the NSF Mechatronics in Machine Tools research initiative—*quod vide* [73, 378].

mechanisms for the feeding and cutting of machine parts. The quality of the finished part is directly related to the quality of the cut: better positioning of the workpiece results in tighter specification tolerances [92]. Positioning and turning are accomplished through the use of a variety drive-train mechanisms, such as gear reducers and lead screws; the more flexible the machine tool, the more complex its drive trains become, and the more such non-linear effects as backlash, stiction and compliance will compromise its tooling quality [225]. This is especially true of mini- and micro-machine tools currently under development for use within the evolving small-scale computer-integrated manufacturing paradigm, whose motions are so deft that these non-linearities more adversely affect them than their larger industrial counterparts [66]. Mechanically-coupled drive-train mechanisms proliferate the machine-tool industry, and are designed to move in various ways.

Traditional milling machines and drill presses have very large, heavy motors which rotate the cutting tool at a specified speed with great stiffness. The stiffness is achieved through a gearing mechanism, and the cutting tool and machine are designed to operate at steady state (without any sudden change in cutting direction). The tool-workpiece interaction is provided by moving a three-degree-of-freedom table to which the workpiece is rigidly clamped, and a fourth degree of freedom is provided by the cutting tool, which can usually be raised or lowered to meet with or withdraw from the workpiece's cutting surface. Because the cutting tool rotates unidirectionally at steady state, there is no backlash effect. The frictional effect is easily overcome under open-loop control, because the motor is so strong (massive and mechanically stiff). The only appreciable effect in the machine spindle is compliance, which if found anywhere, will be in the twist of the cutting tool itself, not in the machine spindle. In fact it is the table which is the real source of error. It is moved side-to-side and up-and-down using lead screws attached to a rotating feed mechanism, which traditionally were turned by hand, but nowadays are controlled by computerised motors, which do the job faster and with better precision and accuracy.<sup>45</sup> The feed motor, which is usually much smaller than the spindle drive motor, must overcome significant friction to move the table, particularly because the lead screws have a large contact area. The screws also cause an appreciable amount of backlash when reversing the table direction, which happens frequently during a typical production run. Lastly, there may be appreciable

---

<sup>45</sup>There is an unfortunate degree of confusion amongst engineers regarding the difference between the meanings of “precision”, “repeatability” and “accuracy”. *Precision* denotes the resolution of a measurement, specifically the smallest attainable *fractional* or *relative uncertainty* or *sensitivity*, whereas *accuracy* describes the repeatability of a correct measurement, equivalently its statistical *standard deviation* [343]. *Repeatability* by itself differs from accuracy in the sense that the standard deviation for both cases is small, although accurate measurements have a mean which is close to the true value represented by the measurements, whereas repeatable measurements may have a significant offset or drift in their mean value. Notice that the precision of a machine can be very coarse while its accuracy may be very good, and *vice-versa*—hence the importance of making the proper distinction.

compliance in the screws as well, especially from torsional vibrations induced in the screws when they are rotated at high velocity to move the table very quickly.

Traditional lathes have a similar operation and set of problems; the only difference is that now it is the workpiece that is rotated on a spindle while the cutting tool is moved about on the table. The number of degrees of freedom are very similar, if not equivalent. What these traditional machines share is that the drive is always the stiff part of the machine, and the table (or feed mechanism, to be more exact) is the part causing all the problems in workpiece quality. However, these types of machines exhibit something of a conundrum: to decrease the backlash, tighter mechanisms are required, yet these introduce more friction; conversely, decreasing the friction allows for more backlash. In general the machines are fairly stiff, and their compliance relatively easy to control—so to reduce the problem of transverse or torsional vibration in the cutting tool or feed screws, it is merely important to provide a mechanism for measuring and modeling its presence, and to then compensate for it.

In contrast to these heavy, dedicated traditional machines, current industry demands for greater efficiency and production throughput have led to the development of what are alternatively called “flexible machining” or “agile manufacturing” stations. [13] These are machine tools with much more functionality, using dynamically interchangeable cutting tools with many redundant degrees of freedom. Such machines are like a decoction of many different traditional machine tools into one “super machine tool”. For example, these machines often have the new ability to move both the cutting tool and worktable simultaneously for increased cutting efficiency. However, the increased functionality and speed comes at the cost of more nonlinearity, introduced precisely by those same benefits gained. To wit: the increased agility of the machines requires more joints, each of which introduces more friction and backlash; the links of the machine must be smaller or it cannot move quickly, hence there is more compliance; the freedom of movement of the cutting tool means it must operate from a smaller drive motor, thereby introducing another source of compliance.

Furthermore, many of the new breed of machine tools are miniaturised versions of their predecessors. [242] These are high-functionality robots the likes of which are used for simultaneous, ultra-high-speed printed circuit board component placement and verification, *in vivo* work on skeletal and bone implants in the surgical theatre, and microelectromechanical systems (MEMS) development. Their smaller size makes them particularly susceptible to the adverse effects of friction, backlash and compliance as they further approach the very characteristic domains of those nonlinearities.

Because newer machine tools cannot meet their primary functional specifications with-

out introducing these undesirable effects to some (usually significant) degree, they must be compensated for using redesigned (nontraditional, usually mechatronic) components, and/or via software compensation. This thesis compares both these potential solutions for the problems as they pertain to machine tools.

### **1.2.7 Trends in Machine Tool Research.**

Among those concentrating their energies in machine tool research specifically related to drive nonlinearity, certain investigators stand out of the crowd. Shinobu Kato, who has touched upon friction in many areas of research, considered stick-slip in the slideways of a workpiece table in 1972 [184]. Masayoshi Tomizuka of the University of California at Berkeley has shown the problems which friction can cause in machine tool contouring accuracy under both low- and high-speed operation [326, 356, 357], and has developed pulse-width modulated (PWM) control techniques to compensate for them [374, 375]. Y. S. Tarn and his associates at the National Taiwan Institute of Technology have since developed and tested controllers for both the stiction [342] and backlash [182] problems individually as found in a computerised numerically-controlled (CNC) drill press and lathe.

Other researchers are involved with a number of machine tool projects, including control [8, 9, 53, 254], and manufacturing [33].

Some investigators are looking at mechatronic solutions to improve machine tool precision and accuracy. A discussion on this is given below, with reference material.

#### **1.2.7.1 How are National Research Institutions Addressing the Problem?**

The National Science Foundation (NSF) has consistently addressed the issue of drive nonlinearity in machine tools for decades. Many of the primary researchers in this field in the United States have produced work in this area through specific funding by the NSF, including Brian Armstrong-Hélouvy of the University of Wisconsin at Milwaukee and Brian Feeny of the Michigan State University.

#### **1.2.7.2 How is Rensselær Addressing the Problem?**

The Rensselær Department of Mechanical Engineering, Aeronautical Engineering and Mechanics (ME, AE & M) has funded this thesis through a Graduate Research Traineeship from the National Science Foundation for Mechatronics in Machine Tool Research [73]. The initiative was first headed by Warren DeVries (who spent some time advising the Foundation after leaving Rensselær), and is now being completed under the directive of Principal Investigator C. James Li.

The ME, AE & M Department has been active in this line of work for many years. C. N. Shen performed intensive research on friction in the late '50s and early '60s [211,304–306]. The late Iradj Tadjbakhsh performed research in the areas of tribology and vibration. Warren DeVries and Stephen Derby have both conducted work in the manufacturing sector [88].

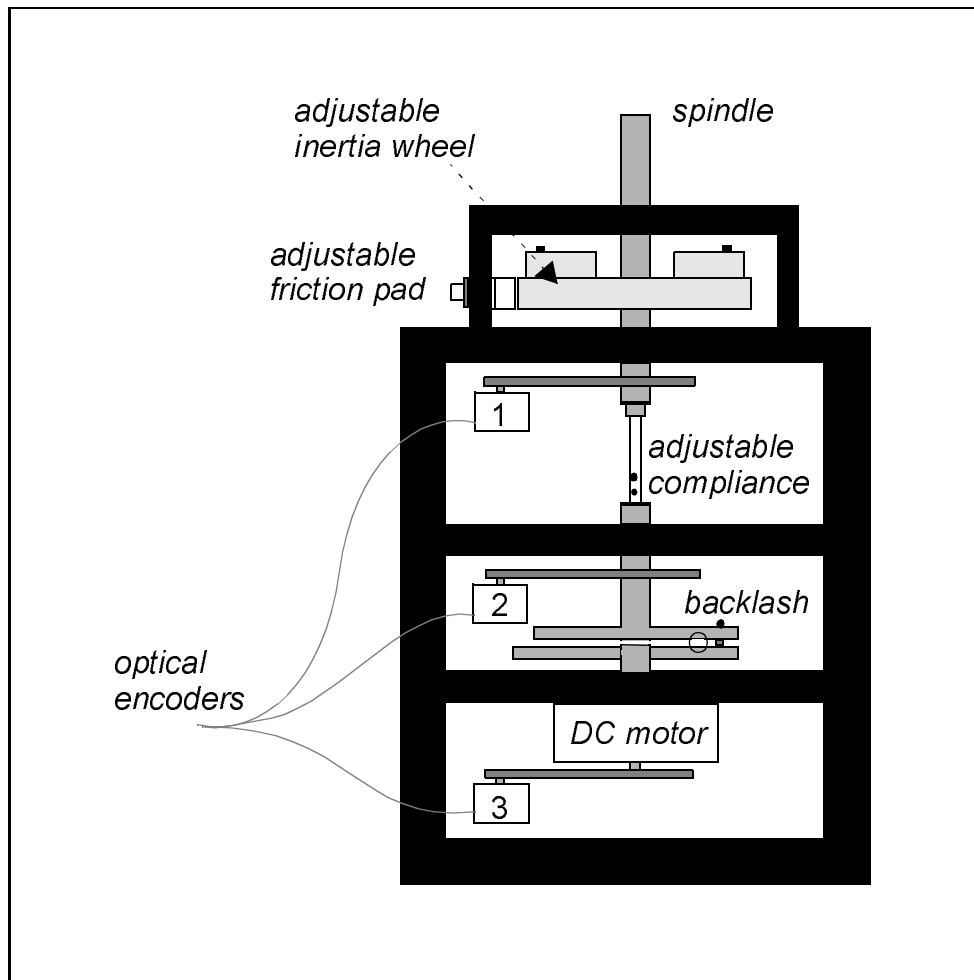


Figure 1.7: The mechanical positioning test bed at Rensselær.

More recently, the foundation for this thesis work was laid in the construction of a mechanical positioning test bed by Rensselær Professor Daniel F. Walczyk, as part of his Master's Thesis in 1991 [367], and by Drs. K-O. Prakah-Asante and Abu Islam at the Active Materials and Smart Structures Laboratory in 1993 [271]. To study the three basic nonlinear drive train phenomena as they interact simultaneously, a special test-bed was designed to introduce precisely-quantified combinations of backlash, friction and compliance to the drive-train system, as shown in Figure 1.7. The test bed was proved successful in

investigating these phenomena [271]. Arbitrary combinations of the three nonlinearities can be mimicked over a continuous range of values, and specific machine tools can be examined by affixing them to the rotating spindle on the test bed. The test bed is design to behave like a wide variety of machine drive mechanisms, including both machine tool spindles with cutting forces and machine tool feed drives with slideway friction.

The investigators on the RPI/NSF Mechatronics in Machine Tool Initiative are also active: Richard Smith and Andrew Yoder are investigating thermal effects at the machine tool-workpiece interface [378]; C. James Li and his graduate assistants are looking at ways to monitor machine tool health and wear to anticipate lifespan and detect catastrophic failure, using dual time-frequency and statistical analysis techniques and neural network system identification; Kevin C. Craig is applying mechatronic system design and active material technologies using real-time, adaptive, nonlinear analogue and digital control [69–73, 77–82, 147, 355, 367, 372]; and John Tichy is supporting research with efforts in tribology and lubrication [176].

The proposal touts Rensselær’s ability to support and lend experience to many areas of research directly related to machine tooling. This thesis addresses two of the five identified machine tool research areas:

- control of servos, robust and adaptive control, .. machine diagnostics and interfaces with other processes, the “open-architecture controller”
- diagnostics, sensor interpretation and fusion for machines and processes, and distributed process planning at the machine tool

The work presented herein is a further contribution to Rensselær’s response to current industry demands. The area of expertise presented, under supervision by Professor Kevin C. Craig, is mechatronic design and dynamic modeling and control.

### 1.2.8 Mechatronic Solutions for Drive Nonlinearity.

Mechatronics is fundamentally a design philosophy spanning many disciplines, as evidenced by Figure 1.8 on the next page [25, 69–71, 82, 257, 258, 344]. It is appropriate that the continued evolution of drive nonlinearity research align with such an interdisciplinary philosophy. As Ludema recommends for the field of friction and wear [216, p.1]:

Inappropriately simple methods are widely used in research, most likely derived from a narrow disciplinary focus . . . The new direction, in both research and in publishing research papers should include the following:

1. covering a very wide range of several variables in all test programs;

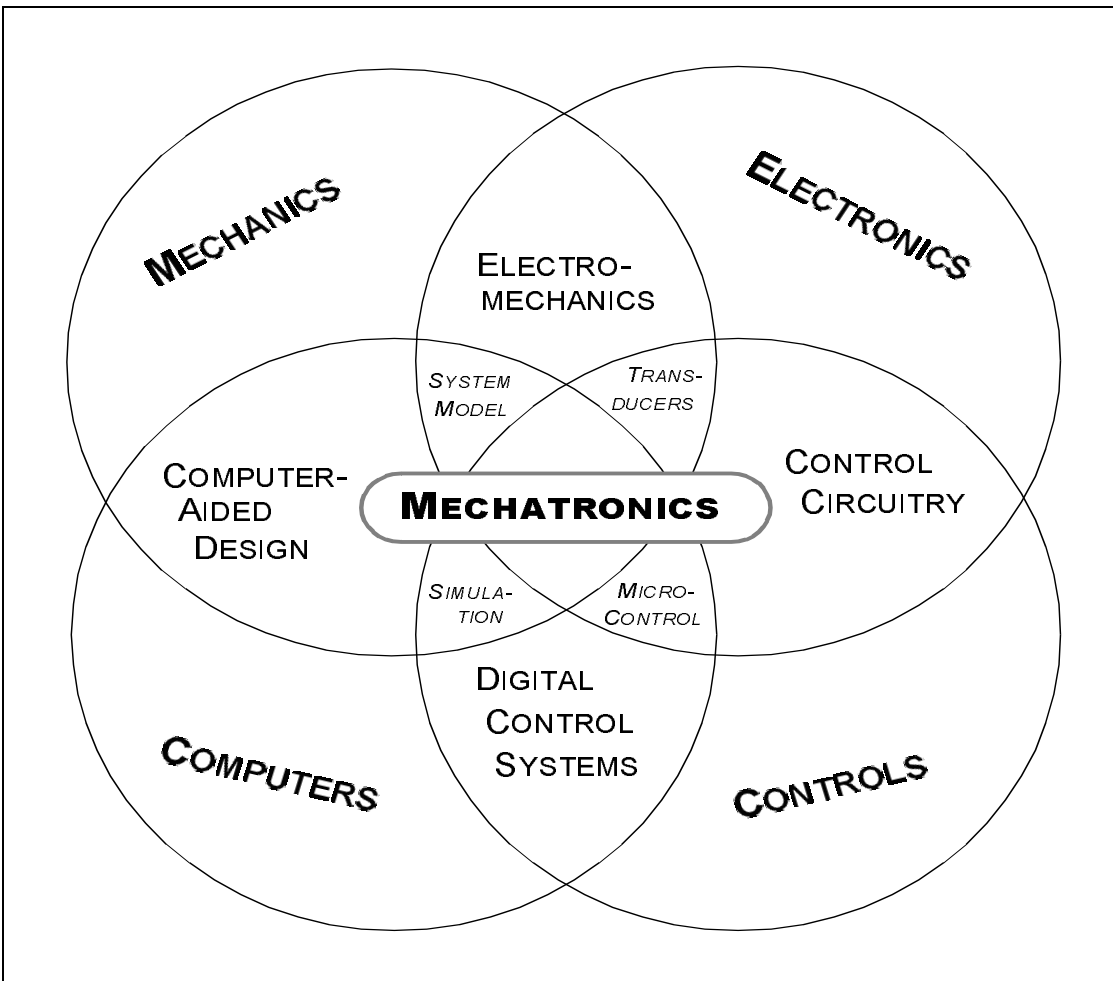


Figure 1.8: The interdisciplinary roots of mechatronic design.

2. describing the conditions of the tests, materials, mechanical dynamics, environment, test geometries *et cetera* completely, so that others can check published information and broaden the range of tentative models;
3. writing equations in terms of operative mechanisms of friction and wear in such a way to reflect actual data;
4. engaging in research with investigators of several disciplines;
5. using some practical machinery as the “point of departure” for the work and as the target for correlation with laboratory work; this will prevent the fruitless efforts to correlate one bench test with another.

Redesign of machines to reduce drive nonlinearity is the most sensible start to eliminating it altogether. [192, 199] However, redesign is usually costly, and fundamentally requires a

high research and capital investment; a much more attractive alternative from an economic perspective provides a simple retrofit instead of outright replacement. Since the subject of drive nonlinearities spans many disciplines, the intelligent redesign solution should be mechatronic in nature; a mechatronic design, though, can also be applied to selected enhancement of retrofitted features. In fact, as research into machine tool redesign progresses (for example, in the area of magnetic bearings), intermediate solutions are nowadays more often mechatronic than not, as a number of examples indicate. [29, 362]

Mechatronic retrofits for machine tools and robotics typically involve replacement of a passive machine element with an active one, providing integral sensing and/or actuating capabilities. Examples of these may be found in references [7, 230, 292].

### 1.3 Unique Contributions of This Work.

This work may be the first to describe an approach for identifying nonlinear friction, impact backlash, and elastic compliance as they act in concert. Of particular significance are the deduction of a comprehensive model for the drive nonlinearities of a wide range of machine tools and other applications, and development of new identification algorithms to characterise asymmetric or nonlinear friction in conjunction with uni- or multimodal compliance. This thesis not only includes detailed analytical formulations of the drive nonlinearities at issue, but also introduces a new model for backlash which includes impact dynamics.

Individually, current methods for friction identification each present certain advantages and drawbacks. The logarithmic decrement method is easy to use, but can only handle unimodal compliance. The Hilbert Transform can potentially resolve backlash and structural damping as well as nonlinear viscous friction, but again in only one natural frequency of interest; furthermore, it requires noise filtering of the results. The wavelet transformation solves the problems of the Hilbert Transform, at the expense of computational complexity. Each of the methods requires harmonic oscillation of the system under investigation. Together, they cover all the nonlinearities under study, so the strengths of each are exploited where they are useful, and the results pieced together. The various methods are explored in detail.

To use the identification methods proposed herein, the systems must be allowed to oscillate freely. This is only possible for underdamped systems, and of those, ones which have a relatively light damping. To allow more heavily and overdamped systems to be diagnosed as well, a novel system identification signal called *parametric harmonic oscillation* is introduced.

Another important contribution is towards identification of asymmetric friction. Fric-

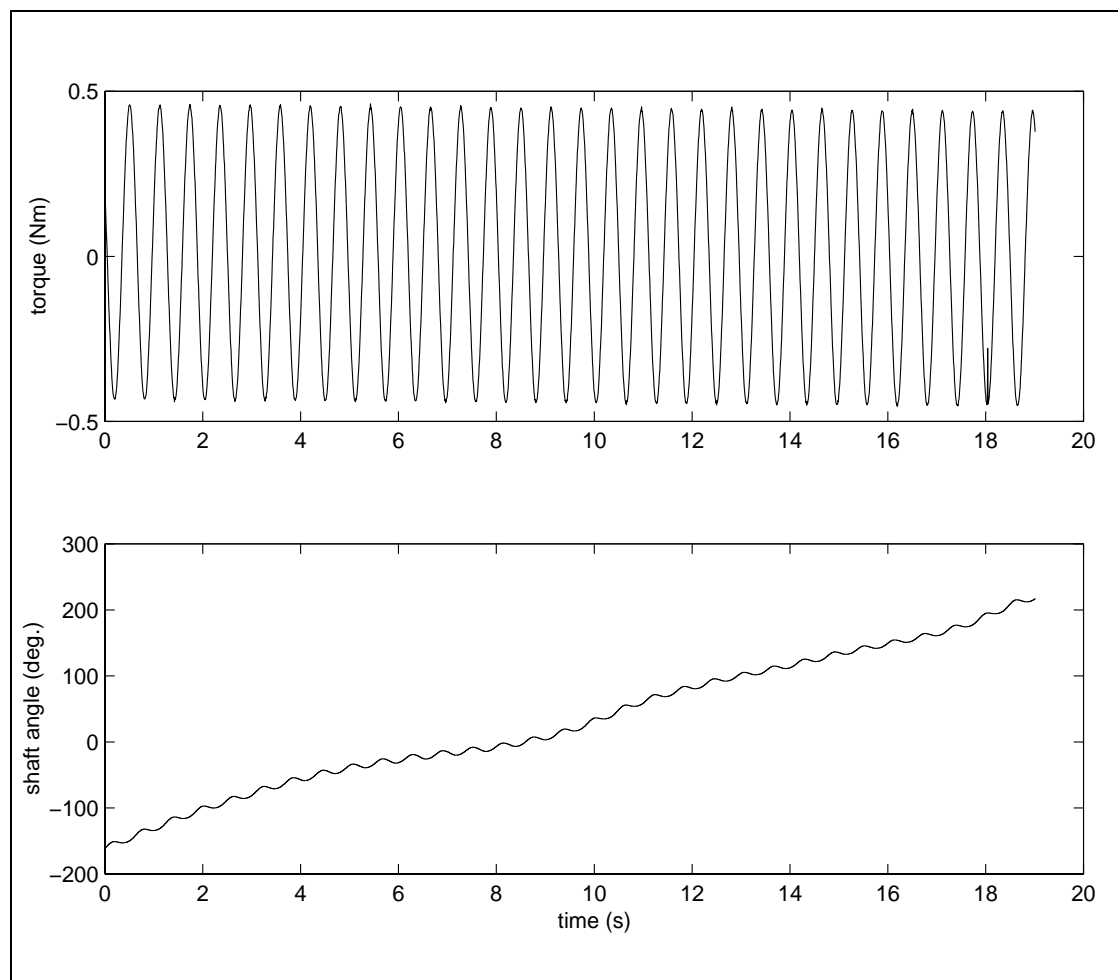


Figure 1.9: Drift caused by asymmetric friction.

tional asymmetry is prevalent in many machines and servosystems, and is typically exacerbated by asymmetric wear on moving parts like shaft bearings and slideways, due to natural operation of the machine. A typical example (taken from the test bed used for the present research) is shown in Figure 1.9: a zero-mean input sinusoid produces a non-zero-mean output sinusoidal motion in the machine. This thesis extends the traditional logarithmic decrement method to include a means for estimating the asymmetry in kinetic and viscous friction for linear second-order system oscillations. Although sequential kinetic and viscous friction identification has been attempted [108, 109], this thesis presents a method for simultaneous identification of these parameters in addition to their respective asymmetries. The concept may be extended to nonlinear and multi-degree-of-freedom systems using the Hilbert Transform and wavelet transformations.

In summary, the problems present in the literature which this thesis addresses directly

are the following:

- lack of sufficient modeling of each of the drive nonlinearities in question;
- poor corroboration of results and synthesis of procedure provided by existing identification methods;
- inability to easily represent asymmetry in the kinetic and viscous frictions;
- inability of overdamped systems to harmonically oscillate when unforced;
- lack of easy-to-use software to simulate and identify drive nonlinearity.

In summary, the contributions of this work are as follows.

1. In the area of system modeling:
  - (a) development of a *realistic*—not merely convenient—lumped-parameter model for the concurrent action of friction, impact backlash and elastic compliance;
  - (b) development of a model highlighting the *interaction* between these basic nonlinearities;
  - (c) development of a simulation to obtain response data for testing the nonlinear model;
  - (d) verification of design parameters for Rensselær’s mechanical positioning test bed and inverted pendulum systems.
2. In the area of system identification:
  - (a) resolution of the applicability of various methods for concurrent friction, backlash and compliance identification;
  - (b) coding of identification algorithms for linear, asymmetric viscous and kinetic friction with unimodal compliance;
  - (c) coding of identification algorithms for nonlinear, symmetric viscous or kinetic friction with multimodal compliance;
  - (d) delineation of possible extensions to nonlinear methods for asymmetric viscous and kinetic friction identification.
3. And in general:
  - (a) extend Rensselær’s usefulness to the needs of basic industry and national economy by directly addressing key points of the NSF/RPI Mechatronics in Machine Tools Research Initiative;

- (b) clarification and bridging of some of the seminal works in the area of nonlinear oscillation identification methodologies.

The journal articles derived from this thesis [77–80] include, respectively: a new model for backlash including impact effects; identification of asymmetric kinetic and viscous friction; producing pseudo-free harmonic oscillations in overdamped systems using the so-called parametric harmonic oscillation method; and corrections and elucidations to published work by others on use of the wavelet transformation for system identification.

## Chapter 2

### **Theory.**

#### **2.1 Models for Drive Nonlinearities.**

Coming up with a complete model for the combined effects of friction, backlash and compliance is one of the unique contributions of this thesis to the developing field of better machine tools—but it is by no means a trivial task. Although the three basic nonlinear elements commonly found in machine tools are by themselves fairly well understood, it is not so simple to just link them together. One of the reasons for this is that they have a certain interdependence. Another is that effects present in one of the phenomena may to some degree also be observable in the other, complicating attribution of its observation to a specific cause. So there are possibilities for models built of the simple composition of each nonlinearity, and for models made of some decoction, so to speak, of the elementary behavioural characteristics among all the combined nonlinearities. In either situation, some prior knowledge of the degree to which each nonlinearity is present will greatly facilitate the proper model selection. The ultimate objective is a model which can be linked to some system identification methodology which allows any, arbitrary interaction of the three basic nonlinearities discussed to be interpreted in real-time.

##### **2.1.1 The State-of-the-Art Friction Model.**

The contact and rubbing of solid bodies: to many it must seem remarkable that an event so common, so intrinsic to the mechanics of everyday life, so important in a multitude of applications of mechanics to engineering problems, and so often the subject of experimental research, has not been satisfactorily depicted by a sound continuum model to date [1985]. However, to those who have taken more than a superficial look at the subject, the absence of a universal continuum model of friction may not be so surprising. The nature of dynamic friction forces developed between bodies in contact is extremely complex and is affected by a long list of factors: the constitution of the interface, the time scales and frequency of contact, the response of the interface to normal forces, inertia and thermal effects, roughness of the contacting surfaces, history of loadings, wear and general failure of the interface materials, the presence or absence of lubricants, and so on. Thus, dynamic friction is not a single phenomenon but is a collection of many complex mechanical and chemical phenomena entwined in a mosaic whose features cannot be grasped through isolated simple experiments.

[244, p.527–528]

The state of the art in understanding friction involves all the empirical effects gathered through the literature on tribology and lubrication [20, p.1483]:

- stribeck friction
- rising static friction
- frictional memory
- presliding displacement
- “normal” friction

The last item is the additional friction connected with the interfacial normal force, which is but mentioned in passing by Armstrong-Hélouvy [23], and remained largely unaddressed until the recent efforts of Dupont [103] and Polycarpou and Soom [267].

#### 2.1.1.1 The Stribeck Effect.

Stribeck friction is shown in Figure 1.2 on page 19 in Chapter 1. Armstrong-Hélouvy states that “Tribology can not yet provide a physically motivated model of Stribeck friction.” However, he agrees with Stribeck that the friction *force versus velocity* curve may be (roughly) divided into four concatenated régimes [20, 319, p.1341]:

- (i) elastic or *presliding* displacement: surface asperities remain in contact without sliding, but yield to applied force on a microscopic level.<sup>46</sup>
- (ii) *boundary* lubrication: the velocity and fluid viscosity are such that dry sliding occurs (dry friction); note that velocity, viscosity, fluid temperature and pressure are all interrelated.
- (iii) *partial* fluid lubrication: some lubricant and small “third-body” particles are drawn into the sliding interface by the increased velocity or non-newtonian viscosity of the fluid, causing partial lubrication and stick-slip problems.
- (iv) *full* fluid lubrication: the bearing is fully supported by an elastohydrodynamic (EHD) lubricant film.

Hess and Soom remark, [158, p.147–148]

---

<sup>46</sup>Presliding displacement is usually very, very small for solid materials in contact.

When examining available models for average (steady-state) friction under different loads, speeds, and lubricant viscosities, it is most natural to begin with the Stribeck diagram, which is often used to delineate the various lubrication régimes from boundary through hydrodynamic.

The functional dependence of the minimum film thickness on load, speed and viscosity is different in each lubrication régime. One cannot, therefore, expect a single dimensionless term, involving these parameters, to accurately describe friction behavior over a wide range of operating conditions.

Stribeck identifies these régimes in both his *friction versus velocity* and *friction versus time* data, and attributes the connection to rising lubricant temperatures under continuous operation. However, most of the interesting effects are transient in nature. The so-called *Stribeck effect* is observed when [319, p.1345–1346]:

- bearing load is increased at low steady velocities; and/or
- velocity is increased under low bearing loads.

A preliminary discussion on Stribeck friction may be found in Chapter 1, § 1.1.1.3 on page 10.

A number of different models have been formed to describe Stribeck friction. One of the first was by Hess and Soom, who examined friction very near zero without actually reversing velocities by exciting their system with a DC-biased sinusoidal velocity. They cast the Stribeck friction into a dimensionless form called the *modified Stribeck parameter* (valid only for non-zero velocities) [158, p.148]:<sup>47</sup>

$$c_S = \frac{\eta \dot{x}}{\sqrt{WE}} \quad \text{where } \dot{x} \neq 0 \quad (2.1)$$

where:  $\eta$  is the lubricant viscosity ( $Pa \cdot s$ );

$x$  is some displacement ( $m$ );

$\dot{x}$  is the sliding velocity ( $m/s$ );

$W$  is the normal contact force ( $N$ );

$E$  is the effective (Young's) modulus of the frictional interface ( $Pa$ ).

According to Hess and Soom,

---

<sup>47</sup>The “original” Stribeck parameter is equivalent to the “modified” parameter presented here if  $E = W$ . The reason the elastic modulus is included here is because without it the Stribeck parameter is only valid in the full-film lubricated régime; including the  $E$  allows a mixed representation valid for the partial (semi-dry) lubrication régime as well. Using the modified representation, it is thus inferred that, at high velocities, the effective modulus  $E \rightarrow W$ .

This approach is equivalent to normalizing the  $\eta\dot{x}$  product by the average contact pressure that would be applied to a Hertzian line contact under the load,  $W$ . This follows from the fact that the contact area of a line contact is proportional to [the denominator] [158, p.148].

They applied this to a dimensionless Coulomb + viscous + Stribeck model [158, eq.(1)],

$$f = \frac{\mu_s}{1 + c_1 c_S^2} + c_2 c_S l \sqrt{\frac{E}{W}} \quad \text{where } \dot{x} > 0 \quad (2.2)$$

where:  $\mu_s$  is the static friction ( $N$ );  
 $c_S$  is the modified Stribeck parameter;  
 $c_1$  is a dimensionless constant;  
 $c_2$  is a constant with units ( $N$ );  
 $l$  is the Hertzian line contact length ( $m$ ).

Here the first term represents Coulomb + Stribeck friction, and the second, viscous friction, in six parameters altogether. The modified Stribeck parameter captures the dependence of friction on the velocity, contact pressure and stiffness (normal load component). Note also the following characteristics:

- increasing (bearing) stiffness causes the friction to drop more rapidly at low velocity;
- the friction at zero velocity is equal to the static friction  $\mu_s$ ;
- above some small critical velocity, the second (viscous) term will dominate the friction.

The *critical Stribeck velocity*  $\dot{x}_S$ , where the Stribeck régime yields to the fully-lubricated viscous régime, will rise with increased contact area and decreased load. When the bearing stiffness (contact pressure) is high the critical Stribeck velocity is reached sooner. Note that Hess and Soom's model does not include a constant, kinetic friction component at higher velocities, however.

Armstrong-Hélouvry, Dupont and Canudas de Wit generalised (2.2) to include the kinetic friction [23, eq.(7)]:

$$f = \mu_k + \frac{(\mu_s - \mu_k)}{1 + (\dot{x}/\dot{x}_S)^2} + \nu \dot{x} \quad \text{where } \dot{x} > 0 \quad (2.3)$$

where:  $\mu_s$  is the static friction ( $N$ );  
 $\mu_k$  is the kinetic friction ( $N$ );  
 $\nu$  is the viscous friction ( $Pa \cdot m \cdot s$ );  
 $\dot{x}_S$  is the critical Stribeck velocity ( $m/s$ ).

Without the kinetic friction component ( $\mu_k = 0$ ) their model is equivalent to Hess and Soom’s representation (2.2) when

$$c_1 = \frac{WE}{(\eta\dot{x}_S)^2} \quad \text{and} \quad c_2 = \frac{\nu W}{\eta l}. \quad (2.4)$$

More importantly, linking the two models shows immediately that the critical Stribeck velocity  $\dot{x}_S$  is simply inversely proportional to the modified Stribeck parameter. When the critical velocity is large, the transition from static to kinetic behaviour is slower, and viscous friction will dominate, so there may be little if any appreciable “negative” friction effect!<sup>48</sup> Conversely, when the critical velocity is small, the transition is faster, producing a significant “negative” friction effect, and with it, potential stiction problems. Thus it is immediately evident that increasing the interface stiffness ( $W$  or  $E$ ) and/or reducing the lubricant viscosity ( $\eta$ ) will improve the stability of low-velocity friction by reducing the effect of Stribeck relative to viscous friction, in direct corroboration with the experimental results presented by Stribeck back in 1902. Stribeck’s work, in fact, suggests the existence of an optimal bearing stiffness for machines under normal operation at a known, steady velocity.

In 1982, Bo and Pavelescu opted for an exponential form [44, eqs.(2)–(3)],

$$f = \mu_k + (\mu_s - \mu_k) e^{-(\dot{x}/\dot{x}_S)^\delta} + \nu\dot{x} \quad \text{where } \dot{x} > 0, \quad (2.5)$$

where  $\delta$  is some empirical constant. When  $\delta$  is large (reported to be the case for boundary lubrication [23, p.1096]), the kinetic friction will be nearly equal to the static friction over all operating velocities, meaning there will be enhanced stability. Armstrong-Hélouvy *et alii* report  $\delta$  to be typically in the range of about 0.5 to 2.0. When  $\delta = 2$ , the model is “Gaussian” and equivalent to (2.3) when the exponential is expanded and truncated as a linear, first-order approximation.<sup>49</sup> Bo and Pavelescu report a quadratic, second-order approximation to be more valid, and necessary to characterise the boundaries of the stiction régime.

Figure 2.1 on the next page shows a comparison of the models proposed by Hess and Soom, Armstrong-Hélouvy *et alii*, and Bo and Pavelescu (equations (2.3) and (2.5)).

---

<sup>48</sup>As Pooh would say, this is a Good Thing.

<sup>49</sup>Notice, however, that according to (2.3) when the velocity equals the critical velocity ( $\dot{x} = \dot{x}_S$ ), the Coulomb friction is the average of the static and kinetic frictions, whereas with (2.5) the relationship is not so convenient, because the critical Stribeck velocity marks a point farther into the lubricated régime.

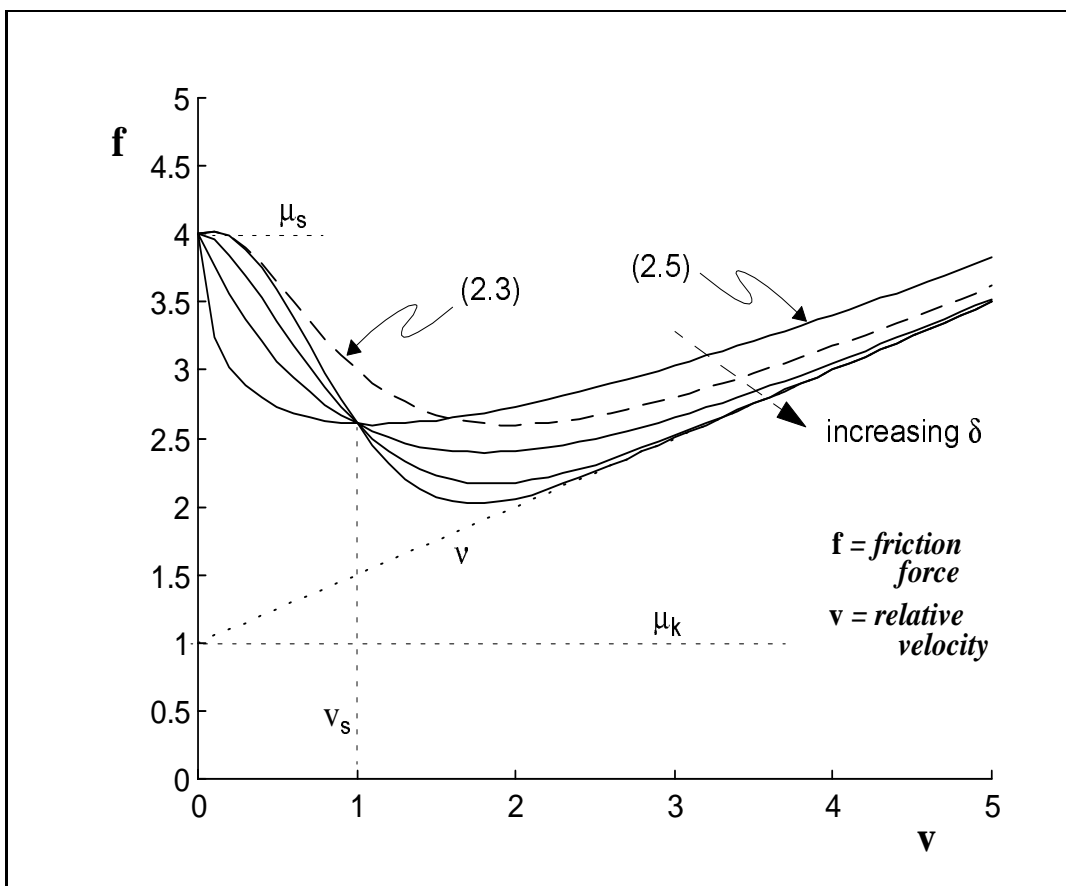


Figure 2.1: A comparison of modern dynamic friction models  
 $(\mu_k = 1, \mu_s = 4, \nu = 0.5, \dot{x}_S = 1)$ .

### 2.1.1.2 Rising and Stick-Slip Frictions.

Kato, Sato and Matsubayashi clarified that “the time-dependence of static friction has a great influence on the behaviour of stick-slip motion.” [184, abstract] Recall that the main cause for stick-slip is attributed to the so-called negative friction present when the static friction exceeds the kinetic friction. So far only the kinetic behaviour of friction has been reviewed.

The behavior of the stick-slip motion depends strongly on both characteristics of static friction during the stick period and kinetic friction during the slip period. Especially the stick-slip motion is intimately associated with static friction. . . When two surfaces are in stationary contact under boundary lubrication, the static frictional force gradually changes with increase of contact time or stick period. [184, p.235]

In order to investigate the mechanism of the time-effect on static friction, it is

necessary to study the contact process between sliding surfaces under boundary lubrication. . . When lubricated metal surfaces are placed in contact under an applied load, the asperities of the surfaces are deformed in supporting the applied load. As a result of this deformation, the lubricant film is trapped between the two metal surfaces and subjected to very high pressure. The pressure, however, may not be uniform over the whole region of contact. In the regions where the pressure is relatively high, local breakdown of the lubricant film can occur and metallic adhesions [or “welds”] may develop. [184, p.239]

Physically, rising static friction arises from the time required to expel the fluid lubricant film from the contact interface. [20, p.1484]

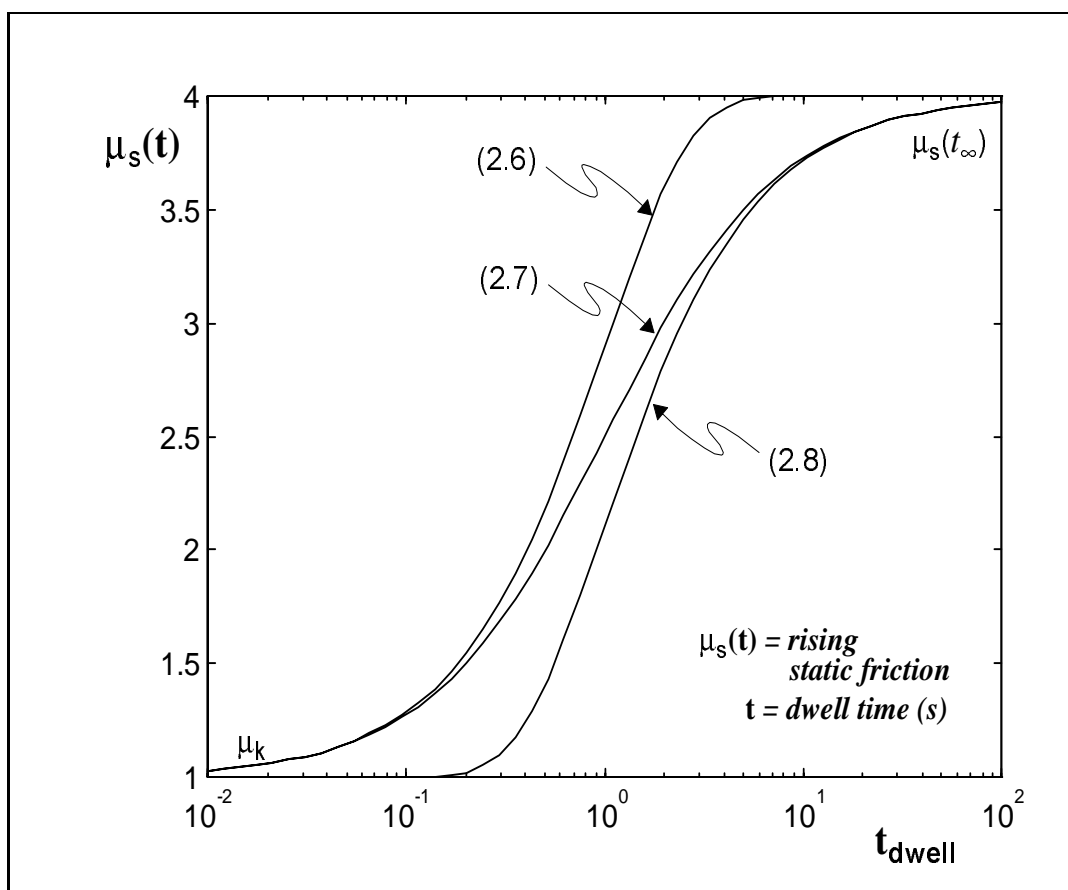


Figure 2.2: Rising static friction ( $\mu_k = 1$ ,  $\mu_s = 4$ ,  $\gamma = \kappa = 1$ ).

With this motivation, Kato *et alii* made careful measurements, and showed that the friction increases sigmoidally from a minimum when the system is just arrested, to a higher value after the system is left to stand for some characteristic duration called the *dwell time*. This behaviour is shown in Figure 2.2. If the dwell time is sufficiently long, that is,

$t_{\text{dwell}} \rightarrow t_{\infty}$ , where typically  $t_{\infty}$  is between 100–1000 s, then the static friction will rise to a plateau, denoted  $\mu_{\infty}$ . A number of different equations have been developed to model this behaviour, and these are reviewed in detail by Kato *et alii* [184, p.238,tab.2/fig.9]. All the models describe the time-dependent static friction using a Coulomb friction term with either an exponential or sigmoidal rising component. Each model is different, demonstrating the faith of different tribologists in one or more different salient parameters and influences. Kato *et alii* find the modification of a model originally proposed by P. G. Howe *et alii* to best fit the acquired data [184, eq.(1)]:

$$\mu_{\text{s}}(t) = \mu_{\text{s}}(t_{\infty}) + [\mu_{\text{k}} - \mu_{\text{s}}(t_{\infty})] e^{-t_{\text{dwell}}^{\kappa}/\gamma} \quad (2.6)$$

where:  $t_{\text{dwell}}$  is the dwell time (time spent stuck) (s);  
 $t_{\infty}$  is the rising time constant (typically 100–1000s);  
 $\kappa$  is a constant, dimensionless lubricant parameter;  
 $\gamma$  is another constant lubricant parameter (s).<sup>50</sup>

Note that  $\mu_{\text{s}}(t_0)$  at the start of sticking is equivalent to the kinetic friction  $\mu_{\text{k}}$  when the dwell time is very brief, and  $\mu_{\text{s}}(t_{\text{dwell}})$  is equivalent to the rising friction constant  $\mu_{\infty}$  when the dwell time  $t_{\text{dwell}}$  is sufficiently long (approaching  $t_{\infty}$ ).

$\gamma$  and  $\kappa$  are empirically determined, though they are observed to be closely correlated to the lubricant boundary film thickness and viscosity  $\eta$ . Kato *et alii* derive  $1/\gamma$  to be roughly in the range of 0.04–0.29 and  $\kappa$  in the range of 0.47–0.67 [184, tbl.2]. Armstrong-Hélouvy obtains  $\gamma \approx 1.66$  and  $\kappa \approx 0.65$  for rough surfaces [19].

This last author also formulated a generalised expression for the rising friction. He extended his earlier dimensional analysis (*quod vide* [18]) to include a frictional memory effect, rising and Stribeck frictions. The rising friction component was [20, eq.(2)]:

$$\mu_{\text{s}}(t) = \mu_{\text{s}}(t - t_{\text{dwell}}) + [\mu_{\text{s}}(t_{\infty}) - \mu_{\text{s}}(t - t_{\text{dwell}})] \frac{t_{\text{dwell}}}{\gamma + t_{\text{dwell}}} . \quad (2.7)$$

Notice this is a linear first-order approximation to (2.6) when  $\kappa = 1$  and the friction at the instant sticking begins  $\mu_{\text{s}}(t - t_{\text{dwell}}) = \mu_{\text{k}}$ , the kinetic friction. So Armstrong-Hélouvy's equation reduces to that of Kato *et alii* when the system sticks after a sufficient duration of continuous sliding (“slipping”)—in other words, the first of any series of stick-slip cycles. What this signifies is that (2.7) extends the work of Kato *et alii* to include multiple successive stiction cycles of shorter duration than  $t_{\infty}$ .

Both equations yield the ultimate static friction  $\mu_{\infty} = \mu_{\text{s}}(t_{\infty})$  when  $t_{\text{dwell}} \rightarrow t_{\infty}$  and the kinetic friction  $\mu_{\text{k}}$  when  $t_{\text{dwell}} \rightarrow 0$ . Furthermore, when  $\gamma$  is near zero, the static

friction will be constant near  $\mu_\infty$ , and when the dwell time is brief, the static friction will remain fairly constant across stick-slip cycles. Different values of  $\gamma$  and  $t_{\text{dwell}}$  adjust the rising friction behaviour between these two extremes. In both cases  $\gamma$  is associated with the sigmoidal rate of change of the static friction with dwell time.

Equation (2.7) is thus an approximation to

$$\mu_s(t) = \mu_s(t - t_{\text{dwell}}) + [\mu_s(t_\infty) - \mu_s(t - t_{\text{dwell}})] e^{-(\gamma/t_{\text{dwell}})} . \quad (2.8)$$

When the dwell time is near zero and/or the rising friction constant is large (slow), the rising friction is fairly constant about the kinetic friction, and when the dwell time is long and/or the rising friction constant small (fast), the rising friction is about equal to the static friction, as expected. This model of rising friction, with  $\mu_s(t - t_{\text{dwell}}) = \mu_k$ , is depicted in Figure 2.2 on page 58.

Armstrong-Hélouvy further produced equivalents of both (2.3) and (2.5) to include rising friction. The first equation is a modification of the model by Hess and Soom [20, eq.(3)]:

$$f = \mu_k + \frac{\mu_s(t)}{1 + (\dot{x}/\dot{x}_s)^2} + \nu\dot{x} \quad \text{where } \dot{x} > 0 . \quad (2.9)$$

The second equation is a modification of the model by Bo and Pavelescu [18, eq.(2)]:

$$f = \left[ \mu_k + \mu_s(t) e^{-(\dot{x}/\dot{x}_s)^2} \right] \text{sgn}(\dot{x}) + \nu\dot{x} \quad \text{where } \dot{x} > 0 . \quad (2.10)$$

In both cases,  $\mu_s$  represents the rising (static) friction parameter, and when rising friction is ignored ( $\gamma = 0$  and  $\mu_s(t) = \text{constant } \mu_s$ ), becomes

$$\mu_s(t) = \mu_s - \mu_k , \quad (2.11)$$

in which case both (2.9) and (2.10) collapse to become, respectively, equivalent to (2.3) and (2.5).

### 2.1.1.3 Frictional Memory.

In their experiments, Hess and Soom confirmed the presence of a delay effect related to the friction. It is basically due to a hysteretic effect in the viscous friction, which is predominantly caused by shearing of the lubricant during motion: when the motion reverses direction, the shear force in the lubricant film is briefly relaxed, and then recovered in the opposite direction. In the words of Armstrong-Hélouvy, [20, p.1484]

In systems ranging from rock mechanics, through lubricated machines, to

numerical analysis of transient partial-elastohydrodynamic lubrication, a time lag, or phase shift, has been observed between a change in the sliding velocity and the corresponding change in friction. When velocity changes, the friction does not change instantly, but adjusts to its new steady-state value only after some time. . . Physically, frictional memory is the result of state in the interface (lubricant film thickness is almost certainly one state variable) which must adjust to the new sliding condition before the friction force will attain its new value.

Hess and Soom propose to model the delay effect by substituting the velocity  $v(t)$  in (2.2) with the velocity one time step in advance,  $v(t + \Delta t)$ , causing the velocity to “lead” the friction by the *frictional memory constant*  $\Delta t$ . They compare two time lag models, one a simple constant time lag, and the other a simple constant equivalent position lag (proportional to the inverse of velocity); the simple time lag is found to compare more favourably with the acquired data.

In the mixed lubrication régime, which is where this lag most significantly affects friction behavior, the lag time increases with normal load and lubricant viscosity. It is shown that the time shift is not associated with a fixed characteristic length [as suggested by Rabinowicz]. The observed delay arises due to entrainment and normal approach, which includes squeeze-films combined with rough surface contact deformations. [158, abstract]

Armstrong simply flips the time shift around to make the friction “lag” the velocity by substituting  $t + \Delta t$  for  $t$  in (2.3), so that [20, eq.(3)]

$$f(t) = f(\dot{x}(t - \Delta t)) . \quad (2.12)$$

This behaviour is shown in Figure 2.3 on the following page. Note that the time lag can be introduced into any of the other elements of dynamic friction presented heretofore simply by substituting  $t - \Delta t$  for  $t$  into the equations.

#### 2.1.1.4 Presliding Displacement.

Armstrong-Hélouvy and Dupont suggest a simple spring-restoring force to represent the presliding displacement, “. . . an approximately linear function of force, up to a critical force, at which breakaway occurs” [22, p.1087,eq.(2)]:

$$\mu_s = -k_s x \quad \text{where } \dot{x} = 0 \quad (2.13)$$

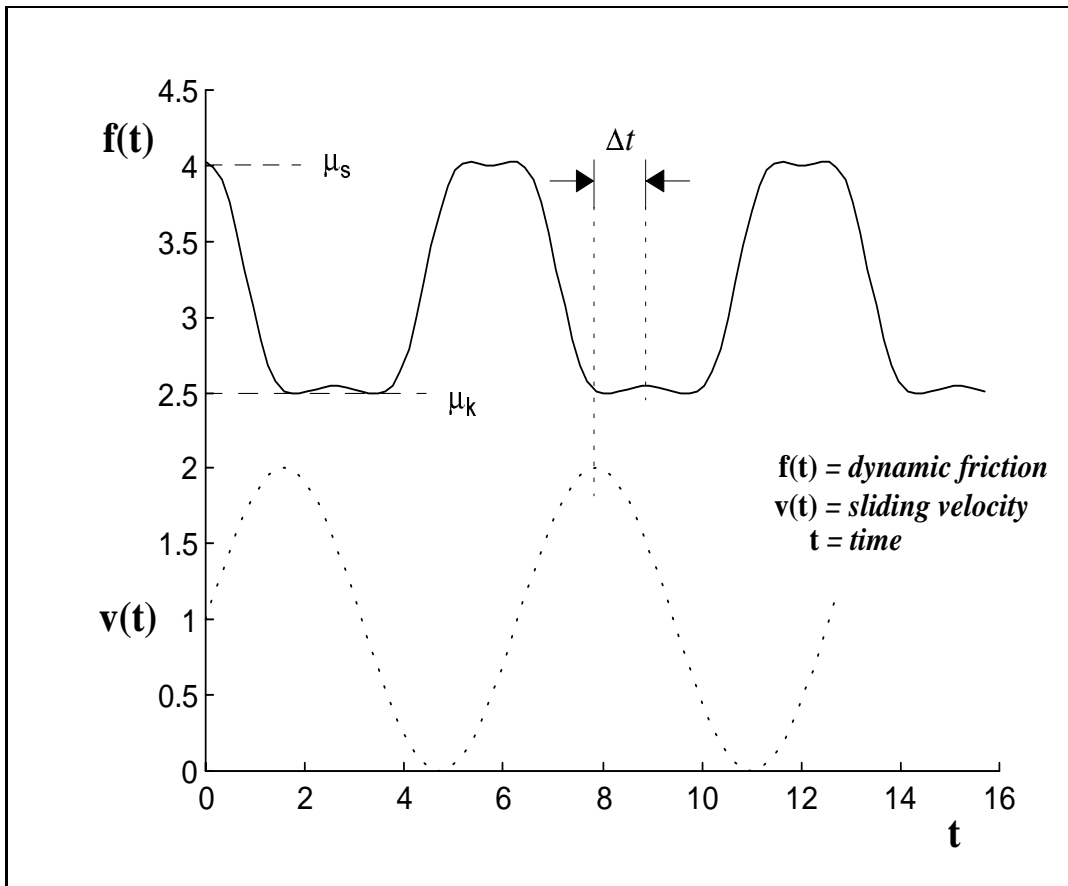


Figure 2.3: Frictional memory ( $\mu_k = 1.5$ ,  $\mu_s = 4$ ,  $\nu = 0.5$ ,  $\dot{x}_S = 1$ ).

where  $k_s$  is the equivalent stiffness under static friction at rest ( $N/m$ ). Note that the displacement  $x$  cannot really change unless  $\dot{x} \neq 0$ , so this equation is ambiguous; by  $\dot{x} = 0$  is meant that the change in displacement is miniscule for the amount of force generated. In other words,  $k_s$  represents a very hefty virtual spring at the contact interface, and  $\dot{x} = 0$  simply denotes the static equilibrium condition of zero *steady-state* sliding. In the words of Armstrong *et alii*,

Polycarpou and Soom [267] have pointed out that static friction is not truly a force of friction, as it is neither dissipative nor a consequence of sliding, but is [rather] a force of constraint [23, p.1087].

The slope represented by this virtual spring constant is simply made to connect the positive and negative static frictions, so technically  $k_s$  is not constant, but rather defined as

$$k_s \triangleq \frac{\Delta\mu_s(t)}{\Delta x_s} = \frac{\mu_{s+}(t) - \mu_{s-}(t)}{x_{s+} - x_{s-}}. \quad (2.14)$$

While it is conceivable that  $\Delta x_s$  too may vary with time (like the rising static friction), it is more likely that it will vary much less than will the static friction. This is because the size of the asperities, and thus the necessary displacement to overcome their interlocking, will not change significantly, whereas their sinking into one another will significantly increase the friction force counteracting motion in the first place.

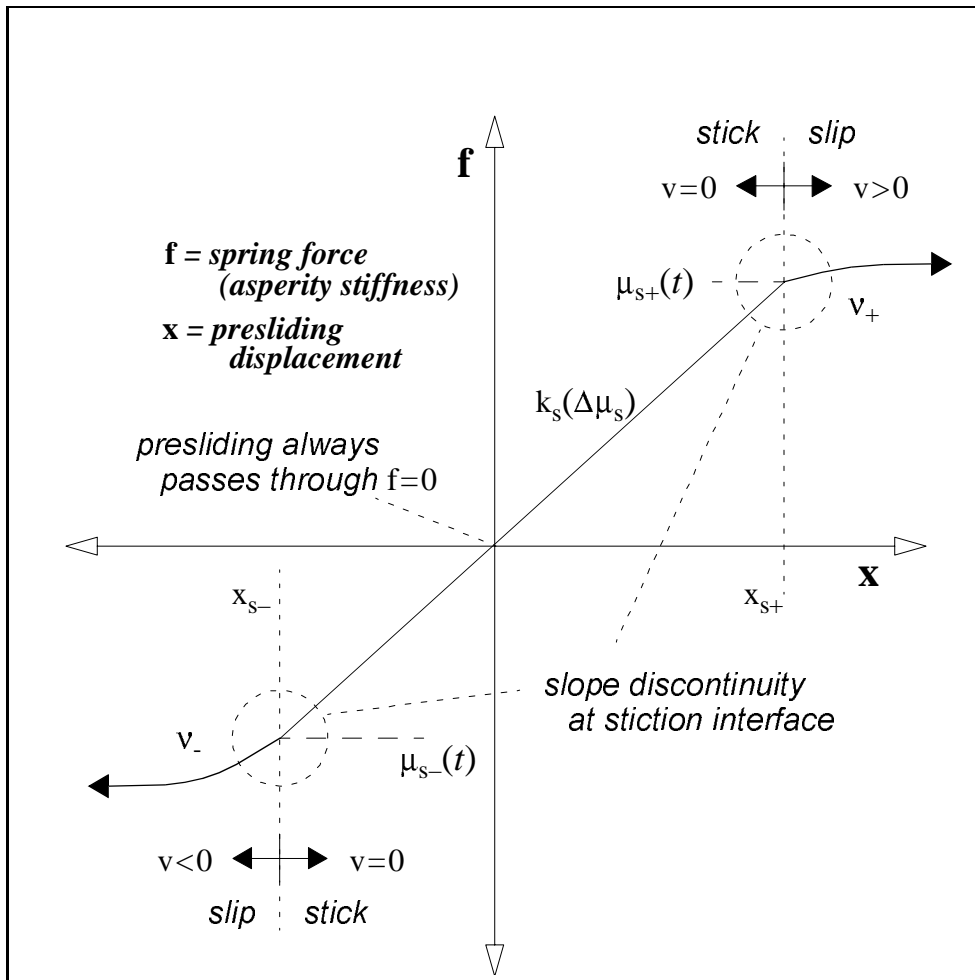


Figure 2.4: Presliding displacement.

Whether or not this presumption holds is largely irrelevant, however, because the primary significance of presliding displacement is merely to describe friction in the neighbourhood of zero velocity as a *continuous* rather than discontinuous function with a bidirectional jump at  $\dot{x} = 0$  due to use of the signum function. The continuum provided by the presliding displacement is shown in Figure 2.4. The function itself is continuous, but the derivative of the function is discontinuous at  $x_{s\pm}$ , where breakaway occurs. This is because the slope in the stick region is  $k_s$ , whereas the slope in the slip region is  $\nu_{\pm}$ , and generally  $k_s \neq \nu$ , leading

to a discontinuity at  $\dot{x} = 0$ . Jang and Tichy here at Rensselær have recently developed a “dual viscous yield” dynamic model which provides continuity across the stiction interface by matching shear stress and rate conditions in the lubricant between sliding rigid bodies. Without considering such microscopic detail, it nonetheless becomes apparent that continuity is assured over a very brief instant right as sliding commences or ends by the physical phenomenon itself. To properly model this behaviour on an empirical level, however, it is probably sufficient to define a quadratic or exponential to join the stiction interface with a continuously-differentiable interpolator.

#### 2.1.1.5 “Normal” Friction.

A number of researchers have shown that the normal force to the line contact of the usual tangential friction actually has a significant effect on the tangential friction for two sliding bodies, with crucial implications for the proper understanding and modeling of stick-slip friction in particular. The normal component is attributed to microscopic changes in the gap distance between the two bodies, the size of which balances the relative contribution from surface asperities *versus* the contribution from elastohydrodynamic sliding conditions (partial fluid lubrication). Usually this gap distance can only change significantly when the interfacial contact is not pre-stressed, that is, the bodies are “resting” upon one another with only moderate force (like that of gravity, for instance). This is the case with some machine tool slideways, where the normal force will determine, to some extent, the boundaries of the stiction régime, since a slideway interface is not prestressed like a bearing is. Furthermore, the slideway normal force may change dramatically during dynamic tool-workpiece interactions (via cutting forces).

In machine tool bearings, the normal friction is dictated by the pressure of the rolling bearings of the rotating spindle, and the heavy weight of the machine tool table on its slideway(s). Under both circumstances, the normal load is high but relatively constant, with small fluctuations attributed to dynamic cutting forces. Since the normal load is a strong contributing factor to the overall friction, yet does not change appreciably during regular machine tool operation, its effect on the overall friction can be implicitly lumped together as static and kinetic friction in the tangential direction without any loss of generality, should the normal displacements be unmodeled explicitly. This is basically the reason classical scientists were able to correlate friction force with normal load. In general the normal force is a strong factor in determining the overall friction, and its effect cannot possibly be observed by modeling friction as a function of tangential motion alone.

Bearing friction is generally increased with increasing bearing stiffness (prestress), but this also limits the normal motion component to a fairly negligible amount. In the case

of the machine tool itself, however, it is a different matter: the tool can flex and therefore bend with reactive force applied at the tool–workpiece interface, even if the tool is rotating at high speed. This bending force at the tool tip is usually much less than that in the bearings holding the tool spindle in place. The tool tip is relatively free to bend since it has only the moderate force constraint of the tool cutting into the workpiece material, hence the normal component can become appreciable to the extent that tool–workpiece stiction, the phenomenon commonly known as tool “chatter”, can arise. Therefore the normal component at the tool–workpiece interface should be included in a complete model, whereas it may be safely ignored when examining the friction in roller bearings.

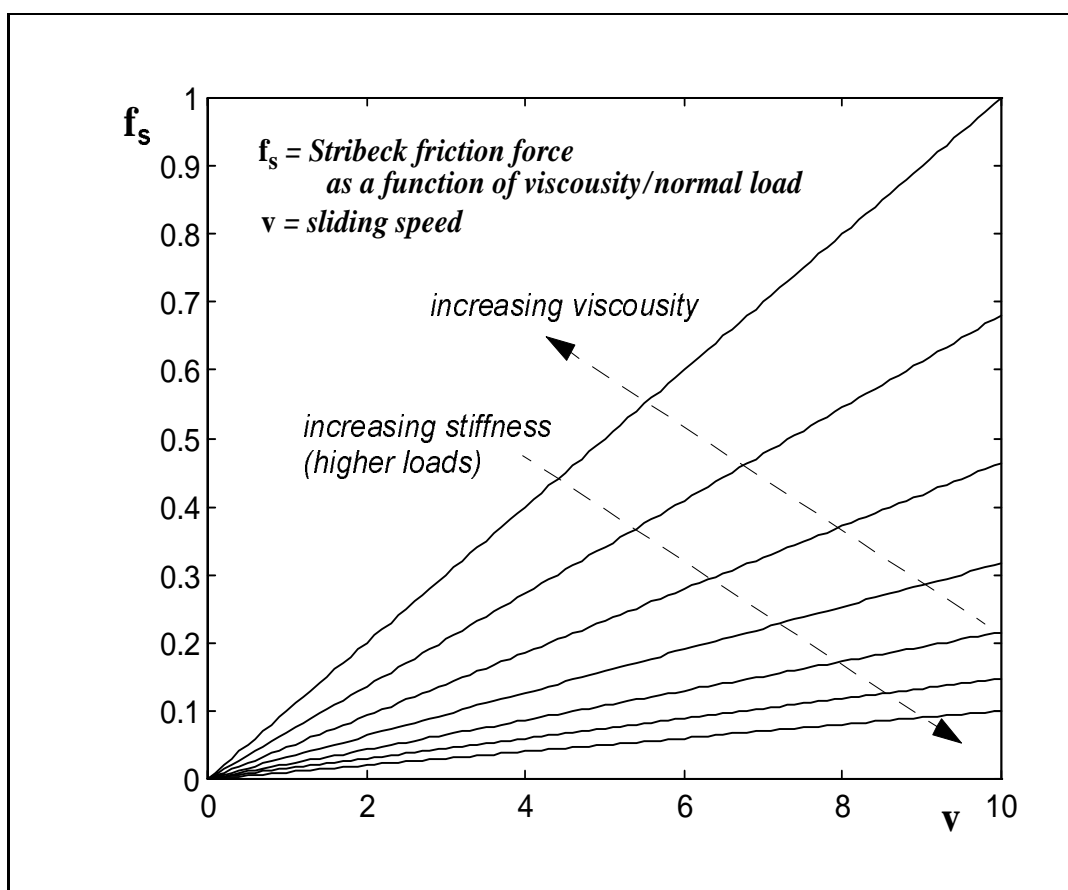


Figure 2.5: Normal friction ( $\eta = 1$ ,  $E = 10$ ).

Stribeck indicates that the normal force or bearing stiffness has a similar influence on the tangential friction as do velocity and duration of continuous operation: that is, there is an optimal bearing stiffness which produces the least friction for some operating velocity. When the modified Stribeck parameter is defined as in (2.1), this is immediately evident and the effect is captured implicitly by all subsequent model equations. The effect of the

contact interface stiffness on friction is shown graphically by Figure 2.5 on the preceding page.

### 2.1.1.6 Full Dynamic Friction Model.

The full friction model will include all the frictional effects discussed so far: Stribeck friction, rising static friction, frictional memory, presliding displacement and normal friction. The first attempt at this was volunteered by Armstrong-Hélouvy and Dupont in 1993, but lacks an interpretation of normal force [22, eqs.(2)–(4)] [23, eqs.(9)–(11)]:

$$f(t) = \operatorname{sgn}\{\dot{x}(t_\Delta)\} \left[ \mu_k + \frac{\mu_s(t_\Delta)}{1 + (\dot{x}/\dot{x}_S)^2} \right] + \nu\dot{x}(t_\Delta), \quad (2.15)$$

where  $t_\Delta \triangleq t - \Delta t$  and the (rising) static friction  $\mu_s(t)$  is given by either (2.6) or (2.7) when  $\dot{x} \neq 0$ , or by the (presliding) static friction (2.13) when  $\dot{x} = 0$ . The first term captures the Stribeck and rising static frictions, and the memory and presliding are contained in  $\Delta t$  and  $k_s$ , respectively. This model is a very straightforward extension of the model (2.5) first introduced by Bo and Pavelescu in 1982, and may be rendered dimensionless by introducing appropriate parameters, and reduced to a function of five variables, as shown by Armstrong-Hélouvy [20].

Around the same time, Canudas de Wit *et alii* considered two other models. The Dahl model, named after the work of Phillip Dahl on internal (material) friction in 1968 [75, 76], assumes a memory lag inversely proportional to the velocity, and is obtained by [62, p.420]

$$\dot{f}(t) = k_s \dot{x}(t_\Delta) \operatorname{sgn} \left\{ 1 - \operatorname{sgn}\{\dot{x}(t_\Delta)\} \frac{f(t_\Delta)}{\mu_k} \right\} \left| 1 - \operatorname{sgn}\{\dot{x}(t_\Delta)\} \frac{f(t_\Delta)}{\mu_k} \right|^\gamma + \nu\dot{x}(t_\Delta) \quad (2.16)$$

where  $\gamma$  is some constant. Most references to the Dahl model take  $\gamma = 1$ . As an alternative, Häessig and Friedland rephrase the Dahl model as [155, p.355]

$$\dot{f}(t) = \gamma_s \dot{x}(t_\Delta) [f(t_\Delta) - f_0(\dot{x}(t_\Delta)) \operatorname{sgn}\{\dot{x}(t_\Delta)\}]^2, \quad (2.17)$$

which is equivalent to (2.16) when  $f_0 = \mu_k$ ,  $\gamma = 2$  and

$$\gamma_s = k_s \mu_k \operatorname{sgn} \left\{ 1 - \operatorname{sgn}\{\dot{x}(t_\Delta)\} \frac{f(t_\Delta)}{\mu_k} \right\}. \quad (2.18)$$

The use of  $\gamma = 2$  produces a “stochastic” or “Gaussian” memory effect, to use the terminology of Canudas de Wit *et alii*.

The second model considered by Canudas de Wit *et alii*, which is more complicated

but allegedly “performs better” than the Dahl model, is written [61, eq.(5)]

$$f(t) = [(1 - g(\dot{x}(t_\Delta)))\mu_s(t_\Delta) + g(\dot{x}(t_\Delta))\mu_k] \operatorname{sgn} \{\dot{x}(t_\Delta)\} + \nu\dot{x}(t_\Delta), \quad (2.19)$$

where  $g(\dot{x})$  describes the Stribeck friction. This relationship is equivalent to (2.15) for  $g(\dot{x}) = [1 + (\dot{x}_S/\dot{x})^2]^{-1}$ , or to (2.5) for  $g(\dot{x}) = 1 - e^{-(\dot{x}/\dot{x}_S)^\delta}$ , though Canudas de Wit *et alii* define the exponential decay according to [61, eq.(6)]

$$\dot{g}(\dot{x}) \triangleq \frac{dg}{dt} = \frac{1}{\Delta t} \left[ 1 - e^{-(\dot{x}/\dot{x}_S)^2} - g(\dot{x}) \right], \quad (2.20)$$

where  $\Delta t$  is the frictional memory constant, during stick  $g(\dot{x}) = 0$  and during slip  $g(\dot{x}) > 0$ . At steady state,  $\dot{g}(\dot{x}) = 0$  so  $g(\dot{x}) = 1 - e^{-(\dot{x}/\dot{x}_S)^2}$ ; in other words, this model is equivalent to (2.5) with  $\delta = 2$  or the first-order approximation (2.15), at steady velocities. However, at unsteady velocities the additional dynamics due to frictional memory are now also captured. This model may be further massaged to obtain the dynamic friction at steady velocities [61, eq.(10)]

$$f(t) = g(\dot{x}) \operatorname{sgn} \{\dot{x}(t_\Delta)\} \mu_s + \nu\dot{x} + (1 - g(\dot{x})) \operatorname{sat} \left\{ \mu_s(t), k_s \dot{x} \Delta t \frac{(1 - g(\dot{x}))}{g(\dot{x})} + \nu_s \dot{x} \right\} \quad (2.21)$$

where the saturation function

$$\operatorname{sat}\{\alpha, \beta\} \triangleq \begin{cases} \alpha \operatorname{sgn} \beta & |\beta| > \alpha \\ \beta & \text{otherwise} \end{cases} \quad (2.22)$$

and:  $g(\dot{x}) = 1 - e^{-\dot{x}/\dot{x}_S^2}$  (as in (2.5));

$k_s$  is the presliding stiffness ( $N/m$ ) as per (2.13);

$\nu_s$  is damping associated with the contact interface.

The saturation function is used here to enforce continuity across the stiction boundary.

The same research team went one step further and have formulated the current state-of-the-art friction model (not encompassing normal force dependency explicitly). This model is based on a concept of interacting “bristles” across the contact interface; the sliding friction is viewed on a macroscopic scale as the average interaction of many infinitesimal elastic bristles interacting between the surfaces. This notion is analogous to the concept of surface asperities elastically yielding at rest and and plastically deforming during dwell times and with velocity. Since often only the macroscopic understanding of friction is of real concern, the “averaged” representation is applicable. The resulting dynamics are very similar to those of the previous model by the same researchers.

Denoting the average deflection of the bristles  $z$  as [62, eq.(1)]

$$\dot{z} = \dot{x} \left[ 1 - \frac{z}{g(\dot{x}) \operatorname{sgn} \dot{x}} \right], \quad (2.23)$$

the friction may then be expressed as [62, eq.(3)]

$$f(t) = k_s z + \nu_s \dot{z} + \nu \dot{x}, \quad (2.24)$$

or, by substituting for  $z$ , as simply

$$f = k_s g(\dot{x}) \operatorname{sgn} \dot{x} + \nu \dot{x} + \left( \nu_s - k_s g(\dot{x}) \frac{1}{|\dot{x}|} \right) \dot{z}. \quad (2.25)$$

If the Stribeck effect is described by [62, eq.(4)]

$$k_s g(\dot{x}) = \left[ \mu_k + (\mu_s(t) - \mu_k) e^{-(\dot{x}/\dot{x}_s)^2} \right] \quad (2.26)$$

then this model is again entirely equivalent to (2.15) at steady velocities, when according to (2.23)  $\dot{z} = 0$  and the latter term vanishes. At unsteady velocities, however, the latter term describes the frictional memory and presliding stiffness effects. The authors further note that this reduces to the Dahl model (2.16) when  $\nu_s = \nu = 0$ ,  $\gamma = 1$ , and  $g(\dot{x}) = \mu_k/k_s$ ; notice this implies  $\dot{x}_s \rightarrow 0$ , or in other words, the Dahl model includes Coulomb and viscous friction, but not the Stribeck effect.

### 2.1.2 The State-of-the-Art Backlash Model.

The complete backlash model includes material resonance and damping during impact, as well as hysteretic deadband. The dynamics include both structural and material vibration, though the structural component is dealt with separately in §2.1.3 on compliance. Material vibration is a function of (internal) material resonance and damping. It can be expressed, to good approximation, as the semi-elastic collision of two masses in one or two damped vibrational modes; if the damping is low (*id est*, the collision is near-elastic), then the unimodal approximation is quite good [206, 294, p.38].

#### 2.1.2.1 Deadband Model.

The deadband in backlash is a region of input motion in a mechanism which results in no appreciable output motion. In this sense it is analogous to the hysteresis described by presliding friction: the deadband is centred about zero velocity (indicating a velocity reversal), and is defined as the backlash gapwidth. The shift in equilibrium does not invali-

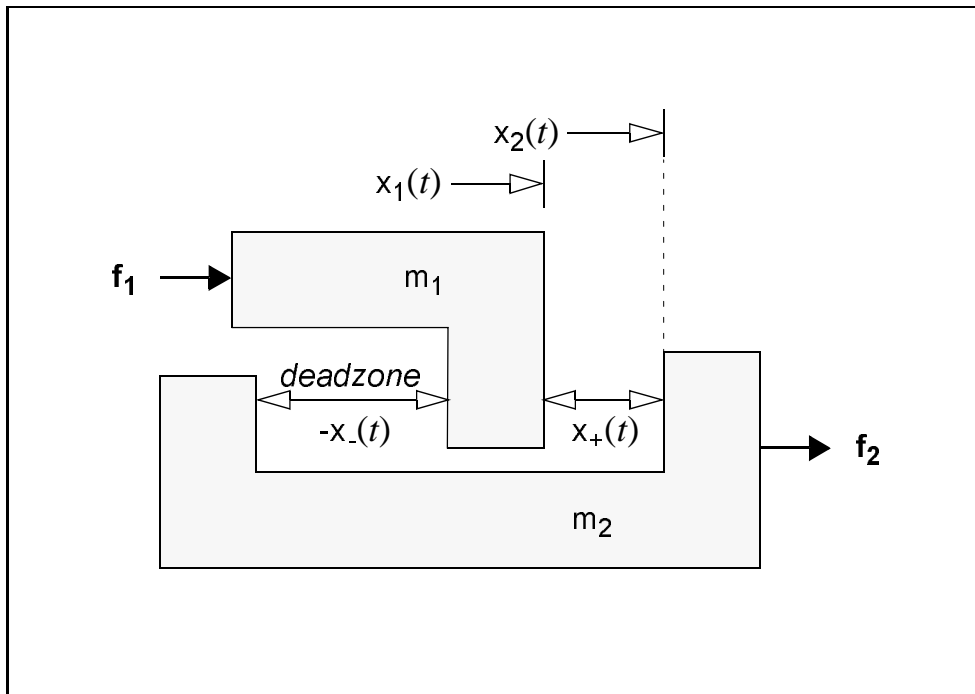


Figure 2.6: Deadband/deadzone model of backlash.

date the deadband model of backlash, since the equilibrium point can always be arbitrarily selected anyway. Tao and Kokotović reserve the terms “deadband” or “deadzone” to mean those strictly centred about zero, and the term “backlash” to denote a shifted deadband; in this thesis, “deadband” is used interchangeably for both situations, and “backlash” is taken to mean the overall deadband effect *including* impact, which the aforementioned authors do not consider. A representation of mechanical deadband is shown in Figure 2.6.

The mathematical description of deadzone is simply [333, eq.(2.2)]

$$\dot{x}_2(t) = \begin{cases} \dot{x}_1(t) & \text{if } \dot{x}_1 > 0 \text{ and } x_2(t) = x_1(t) - x_+(t) \\ \text{or } \dot{x}_1 < 0 \text{ and } x_2(t) = x_1(t) - x_-(t) \\ 0 & \text{otherwise} \end{cases} \quad (2.27)$$

where:  $x_1(t)$  denotes the actuator (the drive or feed motor angle);

$x_2(t)$  denotes the receiver (the tool or feed shaft angle);

$x_+(t)$  denotes the clearance on the “positive” side of the deadband;

$x_-(t)$  denotes the clearance on the “negative” side of the deadband.

This deadzone model acts simply as shown in Figure 1.3 on page 21 in the introductory chapter, where the slope of the input-output relationship is unity on both sides ( $m_- =$

$m_+ = 1$ ).

It is worthwhile to note that Tao and Kokotović’s analysis of deadzone reveals that its inverse, which is constructed for controller development, has the same form as the straightforward classical static + viscous friction model. They describe the backlash as being either “hard” or “soft”; this translates directly to the issue of impact and elastic contact, which “softens” the backlash inherently. It also relates to the discontinuity at zero velocity for static friction, which must naturally have a continuum model (supplied to some extent by the presliding displacement term) although macroscopically speaking, static friction appears to be instantaneous depending on the direction of imminent sliding. These similarities suggest the potential for casting deadzone as a form of friction or *vice-versa*, a notion which may be explored by the ambitious reader.

### 2.1.2.2 Impact Model.

It is crucial to observe that by applying Tao and Kokotović’s model will implicitly encourage a minimum time of traversal of the deadzone, which in turn means maximum acceleration, when the control problem demands the quickest possible elimination of the hysteretic deadzone effect. Although boundary conditions may be imposed when contact is made, there is no assurance in their method that this will be at low velocities (or kinetic energies), because the input-output relationship at the boundaries of the deadzone are assumed to be constant and linear. Anyone will attest from experience that high-energy impact rarely, if ever, produces no rebounding or ringing at the contact interface. It is therefore necessary to include the model of impact dynamics for situations where high-energy traversal of the deadzone may occur (as is the case with fast-moving mechanisms or miniaturised or lightweight mechanisms, or where appreciable compliance is known to exist in the mechanism).

In most cases where backlash arises, such as in gear trains or other transmissions, the two materials making contact are similar, if not the same (often also the contact geometry is symmetric). Assuming that the materials *are* the same, their resonance  $k_1 = k_2$  and damping  $c_1 = c_2$  may be lumped together. The lumped resonance is comprised of the material flexibilities (energy-storing components):

$$k = \frac{k_1 k_2}{k_1 + k_2}. \quad (2.28)$$

The lumped damping is comprised of the material damping (energy-dissipating compo-

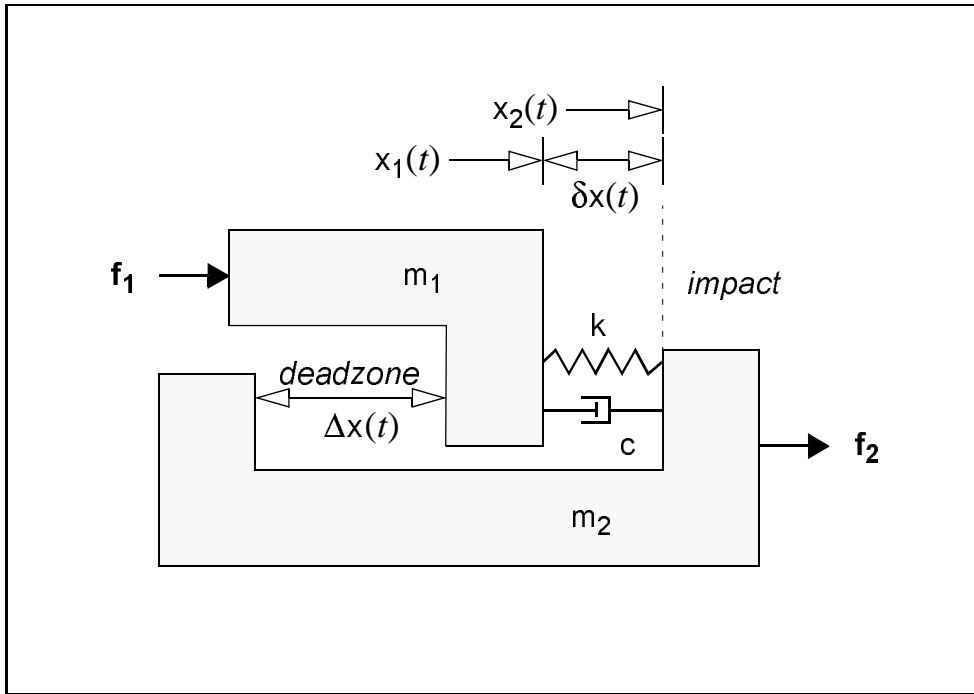


Figure 2.7: Impact with material resonance and damping.

nents):

$$c = c_1 + c_2 . \quad (2.29)$$

A sketch showing these variables during impact is shown in Figure 2.7.

The equations of motion are

$$\mathbf{M}\ddot{\mathbf{x}}(t) + \mathbf{C}\dot{\mathbf{x}}(t) + \mathbf{K}\mathbf{x}(t) = \mathbf{f}(t) \quad (2.30)$$

where

$$\mathbf{M} \triangleq \begin{bmatrix} m_1 & 0 \\ 0 & m_2 \end{bmatrix}, \quad \mathbf{C} \triangleq c \begin{bmatrix} +1 & -1 \\ -1 & +1 \end{bmatrix}, \quad \mathbf{K} \triangleq k \begin{bmatrix} +1 & -1 \\ -1 & +1 \end{bmatrix},$$

$$\mathbf{f}(t) = \begin{bmatrix} f_1(t) \\ f_2(t) \end{bmatrix} \quad \text{and} \quad \mathbf{x}(t) = \begin{bmatrix} x_1(t) \\ x_2(t) \end{bmatrix} .$$

Here  $\mathbf{M}$  is the mass-inertia matrix,  $\mathbf{C}$  the damping matrix,  $\mathbf{K}$  the stiffness matrix,  $\mathbf{x}(t)$  the displacement vector and  $\mathbf{f}(t)$  the forcing vector.

The natural frequency of the impact can be derived from the unforced harmonic equa-

tion where  $\mathbf{f} = \mathbf{0}$ . Taking the Laplace transform<sup>51</sup> of the system in the variable  $s$  and assuming initial conditions to be naught,

$$(\mathbf{M}s^2 + \mathbf{C}s + \mathbf{K})\mathbf{x}(s) = \mathbf{0} . \quad (2.31)$$

Since  $\mathbf{x}(s) = \mathbf{0}$  is trivial,

$$\begin{aligned} |Ms^2 + Cs + K| &= \begin{vmatrix} m_1s^2 + cs + k & -(cs + k) \\ -(cs + k) & m_2s^2 + cs + k \end{vmatrix} \\ &= s^2 [m_1m_2s^2 + (m_1 + m_2)(cs + k)] = 0 . \end{aligned} \quad (2.32)$$

This is called the *impedance transform*, or *characteristic* or *auxiliary* equation of the system, and its roots are the damped eigenvalues of the system, related to its natural frequencies. Let

$$m \triangleq \frac{m_1m_2}{m_1 + m_2} ; \quad (2.33)$$

then

$$s_1^2 = 0 \quad \text{and} \quad s_2 = -\frac{c}{2m} \pm \frac{\sqrt{c^2 - 4km}}{2m} . \quad (2.34)$$

Hence there is a double root  $s_1$  at zero and two complementary roots  $s_2$ . The latter, when the radical term is less than zero, will yield complex conjugate roots; when the radical is zero,  $s_2$  will be a double root; and when the radical term is positive,  $s_2$  will yield complementary real roots. Only the complex solution will result in oscillation during the impact; in other words, when the radical is zero or positive, the impact will be plastic (overdamped). For elastic and semi-elastic collisions, it is convenient to describe the boundary between elastic and plastic collision. This boundary is called the *critical damping*  $c_0$ , and occurs when the term in the radical is identically zero, so that

$$c_0^2 = 4km \quad \text{or} \quad c_0 = 2m\omega_0 , \quad (2.35)$$

---

<sup>51</sup>The variable  $s$  is conventional in the development of control system theory. Other commonly used Laplace variables include  $\lambda$  (when speaking of eigenvalues) and  $\omega$  (when speaking of natural frequencies). Note that the representation is arbitrary, with different conventions in, for example, mathematics or control system theory. In all cases the Laplace variable denotes a time-to-frequency transformation, and here  $s^n$  may be thought of as simply the  $n^{\text{th}}$  temporal derivative operator  $d(n)/dt$  for continuous functions. For the definition of the Laplace variable, see the discussion leading to equation (2.199) in § 2.2.8 on page 112.

where the undamped fundamental (natural) frequency

$$\omega_0 \triangleq \sqrt{\frac{k}{m}}. \quad (2.36)$$

It is convenient to define a dimensionless factor called the *damping ratio* to relate the general damping to  $c_0$ :

$$\zeta \triangleq \frac{c}{c_0} = \frac{c}{2m\omega_0}, \quad (2.37)$$

because now

$$s_2 = \left(-\zeta \pm \sqrt{\zeta^2 - 1}\right) \omega_0. \quad (2.38)$$

During collision, if the two bodies are to separate, there must be a restorative motion. This concept is usually described in terms of a *coefficient of restitution*, the ratio of the release velocity to the contact velocity:

$$\rho \triangleq \frac{v_r}{v_c} \quad (2.39)$$

where:  $v_c = v(t_c)$  at the moment of contact  $t_c$  ( $m/s$ );

$v_r = v(t_r)$  at the moment of release  $t_r$  ( $m/s$ ).

This term must always be negative for elastic collisions, otherwise the two objects stick and the collision is plastic. For  $\rho < 0$ , then, the contact dynamics must have an oscillatory or restorative component, hence  $c < c_0$  or  $\zeta < 1$ . This is called *underdamped* motion, because the damping is sufficiently small to allow at least one oscillation. This requires that  $s_2$  yield a complex conjugate pair of roots

$$s_2 = \left(-\zeta \pm j\sqrt{1 - \zeta^2}\right) \omega_0 = -\zeta\omega_0 \pm j\omega_d \quad \text{where } \zeta < 1, \quad (2.40)$$

$j \triangleq \sqrt{-1}$ , and  $\omega_d \triangleq \omega_0\sqrt{1 - \zeta^2}$  is the damped natural frequency ( $rad/s$ ).

The solution may be written

$$\mathbf{x}(t) = \mathbf{\Lambda}\mathbf{u}(t) \quad (2.41)$$

where the *modal matrix*

$$\mathbf{\Lambda} \triangleq \begin{bmatrix} \boldsymbol{\omega}_1 & \boldsymbol{\omega}_2 \end{bmatrix} = \begin{bmatrix} \omega_{11} & \omega_{12} \\ \omega_{21} & \omega_{22} \end{bmatrix} \quad (2.42)$$

for eigenvectors  $\boldsymbol{\omega}_1$  and  $\boldsymbol{\omega}_2$ , and generalised coordinate vector

$$\mathbf{u} \triangleq \begin{bmatrix} u_1(t) \\ u_2(t) \end{bmatrix}. \quad (2.43)$$

Here  $u_1$  takes the form appropriate for real repeated roots  $s_1$ , and  $u_2$  for complex conjugate roots  $s_2$  [45, ch.8] [346, ch.2]:

$$u_1(t) = (\gamma_{11} + \gamma_{12}t) e^{s_1 t} = \gamma_{11} + \gamma_{12}t \quad (2.44a)$$

$$u_2(t) = \alpha_1 e^{s_2 t} + \alpha_2 e^{s_2^* t}, \quad (2.44b)$$

where  $\gamma$  and  $\alpha$  are constants determined by the initial conditions of system behaviour, and the superscripted  $s_2^*$  denotes the complex conjugate of  $s_2$ . Substituting  $s_2$  from (2.40) and applying Euler's identity,

$$\begin{aligned} u_2(t) &= \alpha_1 e^{(-\zeta\omega_0 + j\omega_d)t} + \alpha_2 e^{(-\zeta\omega_0 - j\omega_d)t} \\ &= e^{-\zeta\omega_0 t} (\alpha_1 e^{+j\omega_d t} + \alpha_2 e^{-j\omega_d t}) \\ &= e^{-\zeta\omega_0 t} [(\alpha_1 + \alpha_2) \cos \omega_d t + j(\alpha_1 - \alpha_2) \sin \omega_d t]. \end{aligned} \quad (2.45)$$

Realising that  $u_2(t)$  must be a real function because the real-life system response  $\mathbf{x}(t)$  can not be complex, let the constants  $\gamma_{21} \triangleq j(\alpha_1 - \alpha_2)$  and  $\gamma_{22} \triangleq (\alpha_1 + \alpha_2)$  be real. When this restriction is stipulated,

$$\alpha_1 = \frac{\gamma_{22} - j\gamma_{21}}{2} \quad \text{and} \quad \alpha_2 = \frac{\gamma_{22} + j\gamma_{21}}{2}, \quad (2.46)$$

which implies that  $\alpha_1 = \alpha_2^*$ ; in other words, the constants  $\alpha$  must be complex conjugates in order that the system response be real. The generalised coordinates may thus be written in a more streamlined form, as

$$u_1(t) = \gamma_{11} + \gamma_{12}t \quad (2.47a)$$

$$u_2(t) = e^{-\zeta\omega_0 t} [\gamma_{21} \sin \omega_d t + \gamma_{22} \cos \omega_d t], \quad (2.47b)$$

where the four constants  $\gamma$  may be discovered via the initial displacement and velocity conditions on  $\mathbf{x}_0 = \mathbf{x}(t_0 = t_c)$ . Notice that the first generalised coordinate  $u_1(t)$  describes the mass centre of the impact pair, and the second,  $u_2(t)$ , the transient vibration between the pair. These coordinates simplify the analysis by separating the rigid body from the vibrational mode and also provide a convenient and natural interpretation of the impact response.

The nontrivial eigenvectors are found by solving the eigenproblem

$$(\mathbf{M}s_i^2 + \mathbf{C}s_i + \mathbf{K}) \boldsymbol{\omega}_i = \mathbf{0} , \quad (2.48)$$

where  $\boldsymbol{\omega}_i \neq \mathbf{0}$ . Substituting  $s_1 = 0$  yields

$$\mathbf{K}\boldsymbol{\omega}_1 = k \begin{bmatrix} +1 & -1 \\ -1 & +1 \end{bmatrix} \begin{bmatrix} \omega_{11} \\ \omega_{21} \end{bmatrix} = \mathbf{0} , \quad (2.49)$$

which in turn specifies the relation  $\omega_{11} = \omega_{21}$ . Either value  $\omega$  is arbitrary, so let

$$\boldsymbol{\omega}_1 = \begin{bmatrix} 1 \\ 1 \end{bmatrix} . \quad (2.50)$$

Substituting  $s_2 \neq 0$  yields

$$[\mathbf{M}s_2^2 + \mathbf{C}s_2 + \mathbf{K}] \boldsymbol{\omega}_2 = \begin{bmatrix} m_1s_2^2 + cs_2 + k & -(cs_2 + k) \\ -(cs_2 + k) & m_2s_2^2 + cs_2 + k \end{bmatrix} \begin{bmatrix} \omega_{12} \\ \omega_{22} \end{bmatrix} = \mathbf{0} , \quad (2.51)$$

which gives the relation  $\omega_{12}/\omega_{22} = -(m_2/m_1)$ . Since again either  $\omega$  is arbitrary, let

$$\boldsymbol{\omega}_2 = \begin{bmatrix} 1 \\ -(m_2/m_1) \end{bmatrix} . \quad (2.52)$$

Then the modal matrix may be written as

$$\boldsymbol{\omega} = [\boldsymbol{\omega}_1 \quad \boldsymbol{\omega}_2] = \begin{bmatrix} 1 & 1 \\ 1 & -(m_2/m_1) \end{bmatrix} , \quad (2.53)$$

and the solution as

$$\begin{aligned} \mathbf{x}(t) &= \boldsymbol{\omega}\mathbf{u}(t) = [\boldsymbol{\omega}_1u_1(t) + \boldsymbol{\omega}_2u_2(t)] \\ &= \begin{bmatrix} \omega_{11}u_1(t) + \omega_{12}u_2(t) \\ \omega_{21}u_1(t) + \omega_{22}u_2(t) \end{bmatrix} = \begin{bmatrix} u_1(t) + u_2(t) \\ u_1(t) - (m_2/m_1)u_2(t) \end{bmatrix} . \end{aligned} \quad (2.54)$$

So the underdamped displacements

$$x_1(t) = \gamma_{11} + \gamma_{12}t + e^{-\zeta\omega_0 t} [\gamma_{21} \sin \omega_d t + \gamma_{22} \cos \omega_d t] \quad (2.55a)$$

$$x_2(t) = \gamma_{11} + \gamma_{12}t - \frac{m_2}{m_1} e^{-\zeta\omega_0 t} [\gamma_{21} \sin \omega_d t + \gamma_{22} \cos \omega_d t] \quad (2.55b)$$

and the underdamped velocities

$$\dot{x}_1(t) = \gamma_{12} + e^{-\zeta\omega_0 t} [-(\gamma_{22}\omega_d + \gamma_{21}\zeta\omega_0) \sin \omega_d t + (\gamma_{21}\omega_d - \gamma_{22}\zeta\omega_0) \cos \omega_d t] \quad (2.56a)$$

$$\dot{x}_2(t) = \gamma_{12} - \frac{m_2}{m_1} e^{-\zeta\omega_0 t} [-(\gamma_{22}\omega_d + \gamma_{21}\zeta\omega_0) \sin \omega_d t + (\gamma_{21}\omega_d - \gamma_{22}\zeta\omega_0) \cos \omega_d t] . \quad (2.56b)$$

Let the reference time of contact be arbitrarily set to zero ( $t_0 = t_c = 0$ ), which simplifies the impact analysis without any loss of generality. The initial displacement conditions are then

$$x_{10} \triangleq x_1(t_c) = \gamma_{11} + \gamma_{22} \quad (2.57a)$$

$$x_{20} \triangleq x_2(t_c) = \gamma_{11} - (m_2/m_1)\gamma_{22} \quad (2.57b)$$

and the initial velocity conditions become

$$\dot{x}_{10} \triangleq \dot{x}_1(t_c) = \gamma_{12} + (\gamma_{21}\omega_d - \gamma_{22}\zeta\omega_0) \quad (2.58a)$$

$$\dot{x}_{20} \triangleq \dot{x}_2(t_c) = \gamma_{12} - (m_2/m_1)(\gamma_{21}\omega_d - \gamma_{22}\zeta\omega_0) . \quad (2.58b)$$

Constants  $\gamma_{11}$  and  $\gamma_{22}$  are derived from the initial displacement conditions given by equation (2.57):

$$\gamma_{11} = \frac{m_1 x_{10} + m_2 x_{20}}{m_1 + m_2} \quad \text{and} \quad \gamma_{22} = \frac{m}{m_2} \delta x_0 , \quad (2.59)$$

where the compression due to impact  $\delta x_0 \triangleq x_{10} - x_{20}$ . Note that  $\gamma_{11}$  is the mass centre of the system, the equilibrium about which oscillation occurs. The constants  $\gamma_{12}$  and  $\gamma_{21}$  are derived from the initial velocity and displacement conditions (2.58):

$$\gamma_{12} = \frac{m_1 \dot{x}_{10} + m_2 \dot{x}_{20}}{m_1 + m_2} \quad \text{and} \quad \gamma_{21} = \frac{m}{m_2 \omega_d} (\delta \dot{x}_0 + \zeta \omega_0 \delta x_0) , \quad (2.60)$$

where  $\delta \dot{x}_0 \triangleq \dot{x}_{10} - \dot{x}_{20}$ . Note that  $\gamma_{12}$  is the velocity of the mass centre, which is constant for all  $t$ , in agreement with the principle of momentum conservation.

The harmonic vibration during the impact is now completely determined in terms of the following quantities: time  $t$ ; initial displacement  $\mathbf{x}_0$  and velocity  $\dot{\mathbf{x}}_0$ ; and system parameters  $m_1$ ,  $m_2$ ,  $c$  and  $k$ .

### 2.1.2.3 Duration of Impact.

Note that the relative displacement  $\delta x(t) = 0$  at both the instant of contact ( $t = t_c$ ) and release ( $t = t_r$ ). Supposing the relative velocity at impact is some constant  $\delta \dot{x}_0 = v_c$ ,

$$\begin{aligned}\gamma_{11} &= \frac{m_1 x_{10} + m_2 x_{20}}{m_1 + m_2} & \gamma_{12} &= \frac{m_1 \dot{x}_{10} + m_2 \dot{x}_{20}}{m_1 + m_2} \\ \gamma_{21} &= \frac{m}{m_2 \omega_d} v_c & \gamma_{22} &= 0 ,\end{aligned}\tag{2.61}$$

which, when substituted into (2.55), gives

$$\begin{aligned}\delta x(t) &= x_1(t) - x_2(t) = \frac{m_2}{m} u_2(t) \\ &= \frac{m_2}{m} e^{-\zeta \omega_0 t} [\gamma_{21} \sin \omega_d t + \gamma_{22} \cos \omega_d t] = \frac{v_c}{\omega_d} e^{-\zeta \omega_0 t} \sin \omega_d t\end{aligned}\tag{2.62a}$$

and

$$\begin{aligned}\delta \dot{x}(t) &= \dot{x}_1(t) - \dot{x}_2(t) = \frac{m_2}{m} \dot{u}_2(t) \\ &= \frac{m_2}{m} e^{-\zeta \omega_0 t} [-(\gamma_{22} \omega_d + \gamma_{21} \zeta \omega_0) \sin \omega_d t + (\gamma_{21} \omega_d - \gamma_{22} \zeta \omega_0) \cos \omega_d t] \\ &= \frac{v_c}{\omega_d} e^{-\zeta \omega_0 t} (-\zeta \omega_0 \sin \omega_d t + \omega_d \cos \omega_d t) .\end{aligned}\tag{2.62b}$$

Notice that the rigid-body mode has no effect on the relative position and velocity during impact, and rather depends solely on the transient vibration. This is one of the conveniences obtained by expressing the system coordinates  $x(t)$  in terms of the generalised coordinates  $u(t)$ , rather than using them directly.

The applied external force  $f_1$  will include both the forcing function and friction forces.  $f_2$  is the friction force on the impacted body. The force  $\Delta f$  transmitted during the impact is equivalent to the viscoelastic forces between the contacting bodies. Substituting equations (2.62) and (2.37),

$$\begin{aligned}\Delta f(t) &\triangleq c \delta \dot{x}(t) + k \delta x(t) \\ &= \frac{v_c}{\omega_d} e^{-\zeta \omega_0 t} [c(-\zeta \omega_0 \sin \omega_d t + \omega_d \cos \omega_d t) + k \sin \omega_d t] \\ &= \sqrt{\frac{km}{1 - \zeta^2}} \cdot e^{-\zeta \omega_0 t} [(1 - 2\zeta^2) \sin \omega_d t + 2\zeta \sqrt{1 - \zeta^2} \cos \omega_d t] .\end{aligned}\tag{2.63}$$

The force delivered “at” the instant of impact  $t_c = 0$  is a constant impulse force with the

value  $\Delta f(t_c = 0) = f_0$ :

$$f_0 = \sqrt{\frac{km}{1-\zeta^2}} \cdot 2\zeta\sqrt{1-\zeta^2} = 2\zeta\sqrt{km} \cdot v_c = cv_c. \quad (2.64)$$

This is the force “lost” during impact due to internal damping; when there is no damping ( $c \equiv 0$ ),  $f_0 = 0$  and the impact is fully elastic. Notice that  $f_0$  is required to satisfy the principle of momentum conservation, which is otherwise only valid for elastic collisions.<sup>52</sup> The impulse phenomenon described is shown in Figure 2.8.

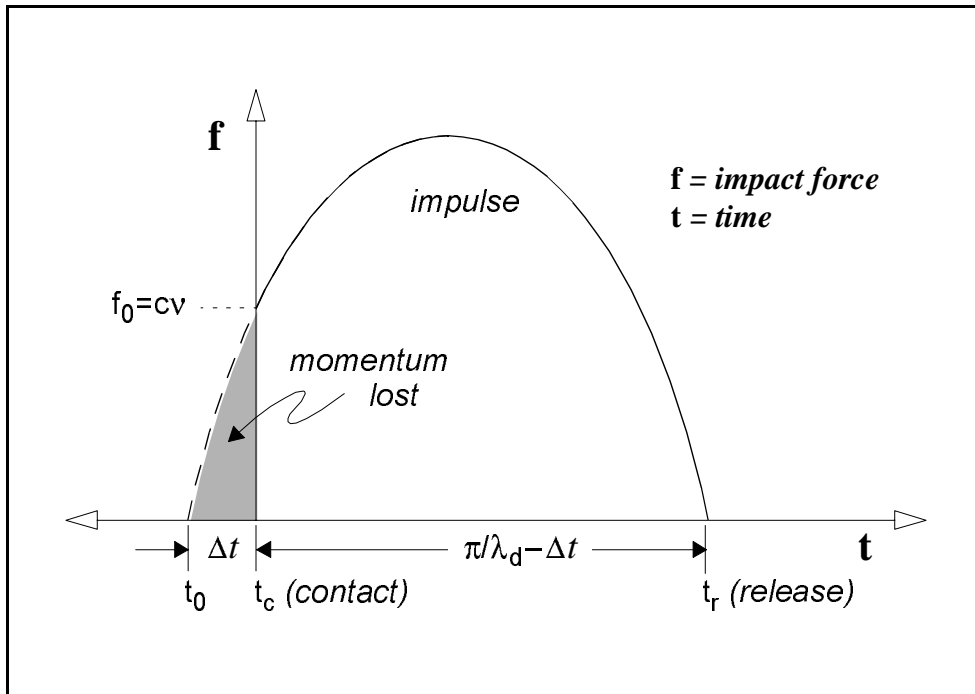


Figure 2.8: Impulse phenomenon at the instant of contact.

Mathematically, the impulse force  $f_0$  may be delivered instantaneously (via the so-called *delta* or *impulse function*), but realistically speaking this is an impossibility: if this could happen, then the model of the collision would be *non-causal, id est*, the impact force would somehow be anticipated before contact was really made.<sup>53</sup> In order that the impact force  $\Delta f(t_0) = 0$  ( $\neq f_0$ ) as must be the case in reality,

$$\Delta f(t_0) = \sqrt{\frac{km}{1-\zeta^2}} \cdot e^{-\zeta\omega_0 t_0} \left[ (1 - 2\zeta^2) \sin \omega_d t_0 + 2\zeta\sqrt{1-\zeta^2} \cos \omega_d t_0 \right] = 0 \quad (2.65)$$

<sup>52</sup>A coefficient of restitution equal to unity is unrealistic, and downright impossible for passive rigid bodies.

<sup>53</sup>Usually the colliding bodies are not sentient enough to exhibit this kind of reflexive action!

at the instant of contact  $t_0$ . This infers that

$$(1 - 2\zeta^2) \sin \omega_d t_0 + 2\zeta \sqrt{1 - \zeta^2} \cos \omega_d t_0 = 0 , \quad (2.66)$$

which is satisfied when

$$\tan \omega_d t_0 = \frac{2\zeta \sqrt{1 - \zeta^2}}{2\zeta^2 - 1} . \quad (2.67)$$

Defining the *resonant frequency* of the second-order response, the frequency where the amplitude of response is greatest, as

$$\omega_r \triangleq \omega_0 \sqrt{1 - 2\zeta^2} \quad \text{where } \zeta \leq \sqrt{2}/2 , \quad (2.68)$$

the condition on  $t_0$  can be expressed as

$$\tan \omega_d t_0 = 2\zeta \frac{\omega_0 \omega_d}{-\omega_r^2} , \quad (2.69)$$

or

$$t_0 = \frac{1}{\omega_d} \arctan \frac{2\zeta \omega_0 \omega_d}{(\zeta \omega_0)^2 - \omega_d^2} \quad \text{where } \zeta \leq \sqrt{2}/2 . \quad (2.70)$$

This value  $t_0$  denotes the *phase lag* of the underdamped system response due to damping, and is always negative for  $\zeta \leq \sqrt{2}/2$ . What this means is that impact actually occurs some time  $t'_c = t_0 \neq 0$  *before* the instant  $t_c$  originally assumed. Fortunately, this need not invalidate all the foregoing mathematics, because recall that the instant of impact  $t_c$  may be selected arbitrarily as any convenient reference point. Because  $t_c = 0$  is so very convenient, let this remain so by setting  $t'_c = 0$ , and instead shift the remainder of the original timescale by the phase lag. Without any loss of generality, then, let the new timescale  $t' = t + t_0$ .

Separation will then occur at release time  $t'_r$ , when the relative displacement  $\delta x(t'_r)$  returns to zero:<sup>54</sup>

$$\delta x(t'_r) = \frac{v_c}{\omega_d} e^{-\zeta \omega_0 t'_r} \sin \omega_d t'_r = 0 , \quad (2.71)$$

This can only be satisfied when  $\sin \omega_d t'_r = 0$ , so  $\omega_d t'_r = n\pi$  where  $n$  is an integer denoting the  $n^{\text{th}}$  contact and separation cycle: when  $n$  is even,  $t' = t'_c$  is the contact time, and when

---

<sup>54</sup>This is equivalent to the standard impulse response for a second-order system with forward gain  $v_c/\omega_0^2$ , *quod vide* [91, eq.(4.11)].

$n$  is odd,  $t' = t'_r$  is the release time. The first separation will then be given by  $n = 1$ , so<sup>55</sup>

$$t'_r = \frac{\pi}{\omega_d} = \frac{\pi}{\omega_0 \sqrt{1 - \zeta^2}} = \frac{2m\pi}{\sqrt{4mk - c^2}}. \quad (2.72)$$

Translating this back into the original timescale  $t = t' - t_0$  this gives (for  $\zeta \leq \sqrt{2}/2$ ):

$$t_r = t'_r - t_0 = \frac{1}{\omega_d} \left( \pi - \arctan \frac{2\zeta\omega_0\omega_d}{(\zeta\omega_0)^2 - \omega_d^2} \right) \quad (\geq t'_r). \quad (2.73)$$

Thus it is evident that ignoring the effect of damping will underestimate the duration of impact.

### 2.1.3 The State-of-the-Art Compliance Model.

Compliance consists of damped resonance at many frequencies. Unlike the impact problem, which is adequately modeled by its fundamental mode of vibration, compliance can consist of contributions from higher modes. In underdamped structures (those which vibrate), normally the higher modes incur more damping, so it may be sufficient to approximate the vibration in terms of a truncated summation of the weighted system modes. For an  $n$ -degree-of-freedom system, then, the total free vibration may be considered as a linear superposition of the eigenvalues (the *modes*) multiplied by the eigenvectors (the *mode shapes*), provided the modes are *well-spaced* (not all bunched together in the low-frequency domain) and the forcing function has a known and deliberate upper frequency bound. Many flexible systems can be successfully approximated using this technique in conjunction with an analytical model for the vibrations [346, § 6.10].

The actual state-of-the-art model would include an *experimental modal analysis* of actual machine tool drive or feed vibrations to determine its true mode shapes and frequencies. If the frequencies are well-spaced, then, the summed normal mode approximation can still be used with good justification. Complex modal interactions, however, can be modeled accurately only by using nonlinear equations of motion, making the problem far more difficult to tackle. A solution to this is to cast the problem as  $n$  uncoupled nonlinear equations, instead of  $n$  coupled linear equations. This is possible using the concept of a nonlinear spring force for every linearly summed mode, in conjunction with the method of proportionally-damped, summed modal approximation.

---

<sup>55</sup>Note that typically repeated impacts occur at very high frequencies (a phenomenon known as *bouncing*), and under certain conditions the time  $t'_r$  may be sufficiently short that it cannot be observed at low digital (discrete) sampling and control rates.

### 2.1.3.1 Summed Normal Mode Approximation.

If the modes are well-spaced, then, each may be approximated by the usual second-order function

$$\mathbf{M}\ddot{\mathbf{x}} + \mathbf{C}\dot{\mathbf{x}} + \mathbf{K}\mathbf{x} = \mathbf{f} , \quad (2.74)$$

with mass, damping and stiffness matrices  $\mathbf{M}$ ,  $\mathbf{C}$  and  $\mathbf{K}$ , respectively, and forcing vector  $\mathbf{f}(t)$ . The solution is written in terms of generalised coordinates  $u(t)$  as

$$\mathbf{x}(t) = \begin{bmatrix} x_1(t) \\ \vdots \\ x_n(t) \end{bmatrix} = \boldsymbol{\omega}\mathbf{u}(t) , \quad (2.75)$$

where

$$\boldsymbol{\omega} \triangleq [\boldsymbol{\omega}_1 \quad \dots \quad \boldsymbol{\omega}_n] \quad (2.76)$$

is the modal matrix.

The *generalised mass matrix* can be expressed as

$$\mathbb{M} \triangleq \boldsymbol{\omega}^T \mathbf{M} \boldsymbol{\omega} = \begin{bmatrix} m_{11} & 0 & \dots & 0 \\ 0 & m_{22} & \ddots & \vdots \\ \vdots & \ddots & \ddots & 0 \\ 0 & \dots & 0 & m_{nn} \end{bmatrix} \quad (2.77)$$

where

$$m_{ii} \triangleq \boldsymbol{\omega}_i^T \mathbf{M} \boldsymbol{\omega}_i , \quad (2.78)$$

and the *generalised stiffness matrix* as

$$\mathbb{K} \triangleq \boldsymbol{\omega}^T \mathbf{K} \boldsymbol{\omega} = \begin{bmatrix} k_{11} & 0 & \dots & 0 \\ 0 & k_{22} & \ddots & \vdots \\ \vdots & \ddots & \ddots & 0 \\ 0 & \dots & 0 & k_{nn} \end{bmatrix} \quad (2.79)$$

where

$$k_{ii} \triangleq \boldsymbol{\omega}_i^T \mathbf{K} \boldsymbol{\omega}_i . \quad (2.80)$$

Defining *orthnormal* modes

$$\tilde{\omega}_i \triangleq \omega_i/m_{ii} \quad (2.81)$$

along with orthonormal modal matrix

$$\tilde{\mathbf{\Lambda}} \triangleq \begin{bmatrix} \tilde{\omega}_1 & \dots & \tilde{\omega}_n \end{bmatrix}, \quad (2.82)$$

the orthonormal generalised mass matrix is

$$\tilde{\mathbf{M}} \triangleq \tilde{\mathbf{\Lambda}}^T \mathbf{M} \tilde{\mathbf{\Lambda}} = \mathbf{I} \quad (2.83)$$

and the orthonormal generalised stiffness matrix

$$\tilde{\mathbf{K}} \triangleq \tilde{\mathbf{\Lambda}}^T \mathbf{K} \tilde{\mathbf{\Lambda}} = \begin{bmatrix} \omega_1^2 & 0 & \dots & 0 \\ 0 & \omega_2^2 & \ddots & \vdots \\ \vdots & \ddots & \ddots & 0 \\ 0 & \dots & 0 & \omega_n^2 \end{bmatrix} \quad (2.84)$$

is equal to the diagonal matrix of the eigenvalues squared.

Substituting (2.75) into (2.74) and premultiplying by  $\omega^T$  yields

$$\mathbf{M}\ddot{\mathbf{u}} + \mathbf{C}\dot{\mathbf{u}} + \mathbf{K}\mathbf{u} = \omega^T \mathbf{f}. \quad (2.85)$$

Alternatively, applying instead the orthonormal modal matrix with

$$\mathbf{x}(t) = \tilde{\mathbf{\Lambda}}\mathbf{u}(t), \quad (2.86)$$

the normalised equation

$$\ddot{\mathbf{u}}(t) + \tilde{\mathbf{C}}\dot{\mathbf{u}}(t) + \tilde{\mathbf{K}}\mathbf{u}(t) = \tilde{\mathbf{f}}(t) \quad (2.87)$$

is obtained, where

$$\tilde{\mathbf{f}} \triangleq \begin{bmatrix} \tilde{f}_1 \\ \vdots \\ \tilde{f}_n \end{bmatrix} = \tilde{\mathbf{\Lambda}}^T \mathbf{f}. \quad (2.88)$$

Notice that the generalised mass and stiffness matrices are pure diagonal, whereas typically the damping matrix  $\mathbf{C}$  (or  $\tilde{\mathbf{C}}$ ) is *not* diagonal, but instead couples the  $n$  mass and spring components. Realising that the eigenvalues  $\omega_i$  denote the undamped natural frequencies of the system and are composed of the mass and stiffness terms only, this means

that the damping matrix couples the system modes.  $\mathbf{C}$  (or  $\tilde{\mathbf{C}}$ ) cannot become uncoupled unless it is made diagonal.

### 2.1.3.2 Proportional Damping.

Proportional damping (known also as *Rayleigh* or *classical* damping) provides one way to uncouple the damping matrix. Suppose the damping matrix can be expressed as a linear combination of mass and stiffness,

$$\mathbf{C} = \alpha\mathbf{M} + \beta\mathbf{K} , \quad (2.89)$$

where  $\alpha$  and  $\beta$  are constants. Applying the orthonormal modal matrix  $\tilde{\mathbf{\Lambda}}$  gives

$$\tilde{\mathbf{C}} \triangleq \tilde{\mathbf{\Lambda}}^T \mathbf{C} \tilde{\mathbf{\Lambda}} = \alpha\mathbf{I} + \beta\tilde{\mathbf{K}} . \quad (2.90)$$

Substituting into (2.87),

$$\ddot{\mathbf{u}}(t) + \left[ \alpha\mathbf{I} + \beta\tilde{\mathbf{K}} \right] \dot{\mathbf{u}}(t) + \tilde{\mathbf{K}}\mathbf{u} = \tilde{\mathbf{f}} , \quad (2.91)$$

which describes the  $n$  second-order equations

$$\ddot{u}_i(t) + (\alpha + \beta\omega_i^2) \dot{u}_i(t) + \omega_i^2 u_i(t) = \tilde{f}_i(t) . \quad (2.92)$$

The modal damping can then be defined according to

$$2\zeta_i\omega_i = \alpha + \beta\omega_i^2 , \quad (2.93)$$

and the  $i^{th}$  equation expressed in terms of the damping as the uncoupled second-order system

$$\ddot{u}_i(t) + 2\zeta_i\omega_i\dot{u}_i(t) + \omega_i^2 u_i(t) = \tilde{f}_i(t) . \quad (2.94)$$

Note that

$$\tilde{f}_i(t) = \sum_{j=1}^n \tilde{\omega}_{ji} \cdot \mu_j(t) \quad (2.95)$$

where  $\tilde{\omega}_{ji}$  represents the  $j^{th}$  element of eigenvector (or mode shape)  $\tilde{\omega}_i$ . The factor

$$\sum_{j=1}^n \tilde{\omega}_{ji} \quad (2.96)$$

is called the *modal participation factor* for mode  $\tilde{\omega}_i$ , and denotes the relative presence of the  $i^{\text{th}}$  orthonormal mode in the frequency composition of forcing function  $\mathbf{f}(t)$ .

Brandon and Al-Shareef note:

The advantage of the proportional damping model is that the mode shapes of the damped structure are identical to those of the undamped structure.<sup>56</sup> . . . The use of a proportional damping assumption in the analysis of spindle-bearing systems is difficult to justify. The dissipative mechanisms are difficult to model accurately, and are concentrated primarily at the bearings and the tool-workpiece interface [51, p.141].

However, if the damping is non-proportional, a nonlinear damping  $\zeta$  as a function of frequency may still be applied using the same method.

### 2.1.3.3 Shaft Boundary Conditions.

Machine tool feed drives consist of long ball screws which exhibit marked compliance at high feed rates. These types of shafts are always connected at one end to the drive motor, but the effective length of the compliant section in question changes with the position of the workpiece table. Hence the modes and mode shapes will vary as a function of the table position. The boundary at the motor may be considered a pure moment applied by the motor itself, while the other end will exhibit a dynamic friction torque where it is fixed by a lubricated bearing. Somewhere in the middle, the workpiece table will ride along the ball screw via two “clamps” set a fixed length apart; these clamps ride within the grooves of the ball screw, allowing the table to slide along its slideway. The clamped points will act as semi-rigid, frictional nodes counteracting torsional vibration in the screw, and the table will also exhibit a nonlinear slideway friction varying with the screw rotational velocity.

In the case of machine tool cutting, two situations with compliance in the tool may define the type of forcing function: if the tool is free from the workpiece, there is no torque acting at the tool tip and the problem becomes one of the tool torqued at one end and vibrating freely at the other; on the other hand, if the tool is in contact with the workpiece then there will be a reactive friction torque at the free end of the tool and a forcing function at the controlled end.

The net torque in either circumstance may be defined in terms of the difference between the boundary torques at either end of the shaft. Given this net torque applied to the ends of the shaft, the action of that torque at any point along the length of the shaft may be

---

<sup>56</sup>—although the modal *frequencies* of the undamped structure will only conservatively approximate those of the damped structure.

separated in terms of the net torque as modified by some function distributing it along the tool length. Thus the forcing function may be written as

$$\mathbf{f}(t) \triangleq \boldsymbol{\gamma}(x)f(t) \quad (2.97)$$

where  $f(t)$  is the net force acting at the boundaries, and

$$\boldsymbol{\gamma} \triangleq \begin{bmatrix} \gamma_1 \\ \vdots \\ \gamma_n \end{bmatrix} \quad \text{where } 0 < \gamma_i < 1 \quad (2.98)$$

is a vector describing the action of  $f(t)$  at displacement  $x$ . With this observation the participation factor for the  $i^{\text{th}}$  mode shape becomes

$$\sum_{j=1}^n \tilde{\omega}_{ji} \cdot \gamma_i(x), \quad (2.99)$$

so that now the modal summation is linearly separated in the variables  $x$  and  $t$ :

$$\tilde{f}_i(t) = f(t) \sum_{j=1}^n \tilde{\omega}_{ji} \cdot \gamma_i(x). \quad (2.100)$$

#### 2.1.3.4 Nonlinear Fundamental Mode Approximation.

Brandon and Al-Shareef note that the stiffness of the bearings holding the machine tool spindle has little effect on the fundamental or second and third mode shapes of the spindle, but an increasingly significant effect on higher modes. This bearing stiffness can be modeled by the boundary conditions specifying the vibrational behaviour of the spindle, as a moment at either of its ends. They make a case for disregarding the higher modes because:

In the higher modes . . . the modal displacement is nodal, or near nodal, at the cutting zone. Thus these modes are unlikely to affect the chatter sensitivity markedly, even where the frequency spectrum of the cutting force contains significant content in the vicinity of the modal resonant frequency. [51, p.144]

The summed-mode approximation can thus justifiably be truncated to a manageable, primary number of modes to consider. Brandon and Al-Shareef

. . reinforce the generally-held view that the stability of the cutting process . . .

is dominated by the response characteristics of a single mode of the spindle-bearing systems. [51, abstract]

The mode shapes do much to reinforce the common perception that the... process should concentrate on the first mode, since this mode is the only mode shape which has its peak displacement at the cutting zone, while the other three modes have small deflections within the cutting zone.<sup>57</sup> Thus the... cutting zone, most commonly studied in performance assessment of machine tools, will depend strongly on the first mode and only contain relatively minor contributions from the higher modes. [51, p.144–145]

Thomson notes that in such cases where the maximum peak deflection is of primary interest, an acceptable truncated summation of modes can be used [346, eq.(6.10-7)]:

$$\max |x_i| \approx |\omega_1(x_i) \max(u_1(t))| + \sqrt{\sum_{j=2}^n [\omega_j(x_i) \max(u_j(t))]^2}, \quad (2.101)$$

where typically  $n = 2$  or  $n = 3$ .

Brandon and Al-Shareef suggest taking only the first mode as an approximation, in which case the distributed compliant system can be modeled as an equivalent second-order, nonlinear, viscoelastic, lumped-parameter system similar to that described by the impact model in § 2.1.2.2 on page 70 and the harmonic oscillator described in § 2.2.3 on page 101.

#### 2.1.4 A Lumped Model for Drive Nonlinearities.

Brandon and Al-Shareef conducted a study of a lathe spindle and its modal representation, and also argued for a lumped model representation of second-order subsystems acting about an equilibrium point located at the centre of action of the distributed system.

The model approach used by the authors was designed for versatility rather than as a practical design tool. Thus in each segment of the shaft the inertia distribution was modeled in terms of a lumped mass at the centre of the segment.<sup>58</sup> Similarly the dissipative effects were modeled as lumped elements. The use of point-lumped dampers, effectively ‘earthed’, would be regarded as inadmissible for general structures but is, however, consistent with much of the research in vibration attenuation of machine tool spindles... [51, p.142]

---

<sup>57</sup>Brandon and Al-Shareef model the cutting tool as either a prismatic beam or rod.

<sup>58</sup>The geometric and mass centre of each segment was collocated because each segment of their lathe spindle was radially symmetric.

Noting that the effects of backlash and compliance can be approximated by second-order terms, and that in friction there are only two nonlinear terms (Stribeck friction and the velocity sign-dependency) at every subsystem (the drive motor, shaft, bearings and tool), using a lumped second-order representation seems justified, especially for the sake of problem tractability and straightforward industrial implementation. The nonlinearities in the shaft and/or tool compliance can be reflected by a (single or summation of) nonlinear spring(s) to further simplify the overall mechanism.

A figure showing the transfer-function block diagramme of the lumped system is given in Figure 2.9 on the following page. Notice that this diagramme directly correlates with the behaviour of many real systems, including: the action of the test bed (see Figure 1.7 on page 45); the model of a typical rotating machine tool, like a lathe or drill press; the model of a workpiece feed table with flexible drive shaft; or a flexible robot carrying or pushing a payload.

#### 2.1.4.1 Drive Motor Subsystem.

Neither the tool nor feed drive models have yet been discussed, so they will be treated with some detail here.

Drive motors in typical machine tool spindles use alternating three-phased current (AC) to produce high power rotational torques. Additionally, they are usually quite massive, and thus have much inertia. These qualities are both part of the “passive” design of the tool, selected to reduce sensitivity to such adverse effects as drive nonlinearity or initial workpiece roughness or mass, by maximising the mechanical “stiffness” of the machine. The transfer function for a typical AC motor is simpler than that for a direct-current (DC) motor, which must alternate the power itself using brushes or special control circuits. When the motor mass is very large, the transfer function approaches a constant.

The transfer function for a two-phase AC motor, for example, is given by [91, tbl.2.6.7]

$$\theta_m(s) = \frac{k_m}{s(t_m s + 1)} v_c(s) \quad (2.102)$$

where:  $\theta_m$  is the motor output angle;  
 $v_c$  is the applied control voltage;  
 $k_m$  is the motor constant,

and the motor time constant

$$t_m \approx J_m / (\nu_m - p) \quad (2.103)$$

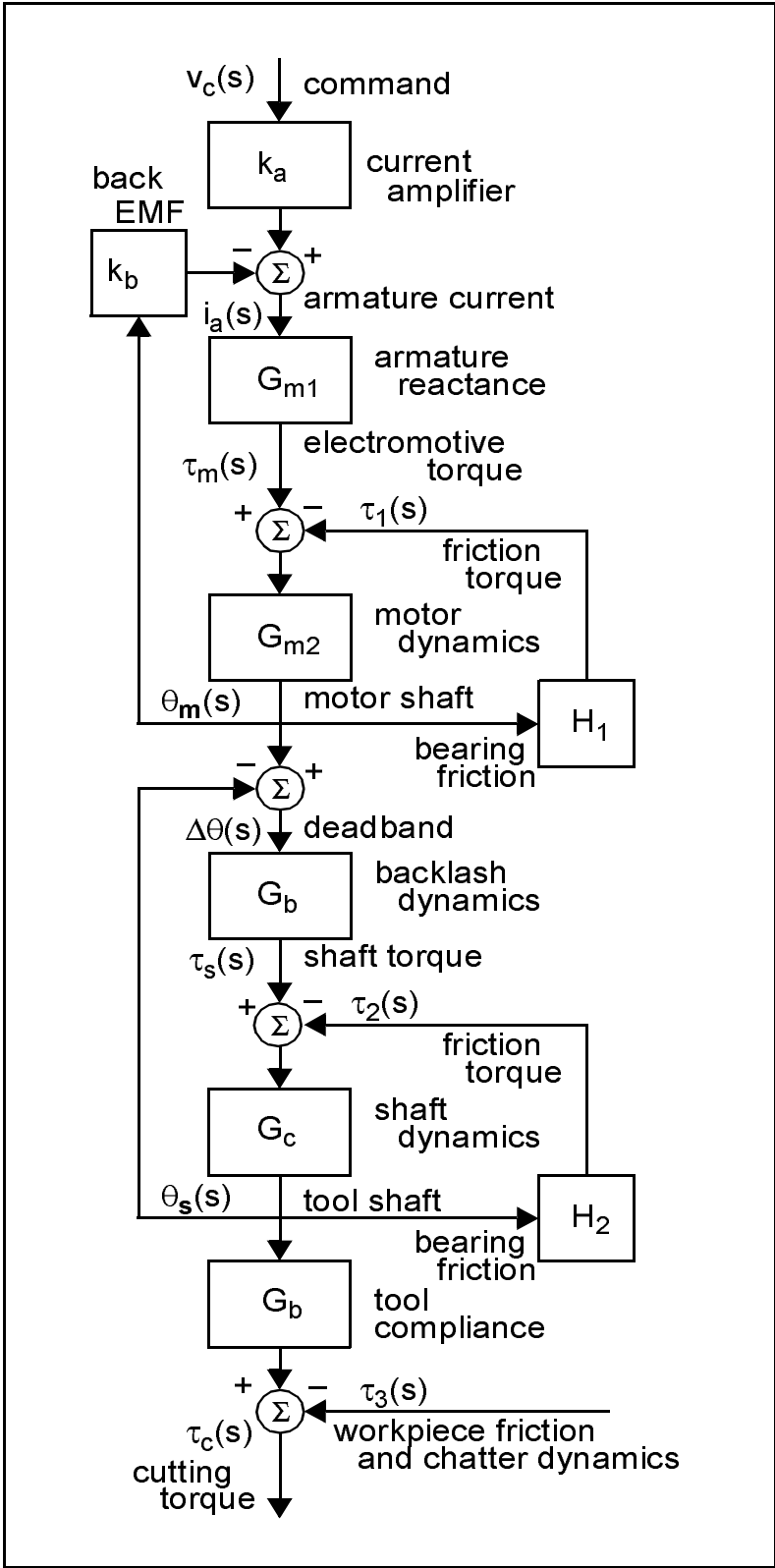


Figure 2.9: Total system block diagramme.

where:  $J_m$  is the motor inertia;  
 $\nu_m$  is the motor shaft viscous friction;  
 $p$  is a linearised torque-speed curve usually supplied by the manufacturer.

Notice that when the motor inertia is significantly large, the motor transfer function tends to simply

$$\theta_m(s) = \frac{k_m}{t_m s^2} v_c(s), \quad (2.104)$$

which, interpreting the Laplace variable  $s$ , means that the motor acceleration is proportional to the control voltage. For a constant control, then, the acceleration will reach a plateau countered by frictional forces and rotate with considerable inertia, meaning that small disturbances will not significantly affect normal operation.

The mechanical positioning test bed uses a high-torque, low-inertia DC servomotor, which is especially designed to have a very low time constant.<sup>59</sup> The low motor inertia means that small disturbances can only be eliminated using large dynamic control currents, whereas typical machine tool motors will retain a fair insensitivity to small disturbances even with brief periods of low control currents, when in steady, high-speed operation. So the test bed motor does not effectively model the operation of large machine tools which rotate at steady speeds, but does better to model the dynamics of smaller machine tools, feed drives, and manufacturing line pick-and-place robots which change direction often. The disturbance forces on the test bed must therefore take on proportionally-reduced values to effectively replicate large machine tool operations like cutting.

Since the test bed is used to develop and test the identification theory, its model is presented here. The high power of the servomotor is achieved by using both low inertia and the method of armature current control, rather than field current control. Although in theory “the field-current controlled motor . . . provides substantial power amplification” [91, p.49], and is of simpler construction than the armature-controlled version, it requires many rotor windings on the motor shaft, increasing its inertia and thereby, slowing its dynamic response. By using a printed-circuit armature, the armature-controlled motor can yield fast dynamic response with lower inertia, and achieve similar power amplifications as the field-controlled version, though it requires a somewhat more complex mechanical design.

The transfer function for the current-controlled DC servomotor is

$$\theta_m(s) = \frac{k_m(L_m s + R_m)}{s[(J_m s + \mu_m(s))(L_m s + R_m) + k_m k_{EMF}]} i_a(s) \quad (2.105)$$

---

<sup>59</sup>Such servomotors are sometimes called *printed-circuit (PCB)*, *pancake* or *disc* motors, because they have the armature “coils” printed on or sandwiched within a flat, circular disc.

where:  $\theta_m(s)$  is the motor output angle (*rad*);  
 $i_a(s)$  is the applied armature current (*A*);  
 $k_m$  is the motor torque constant (*N · m/A*);  
 $J_m$  is the motor inertia (*N · m · s<sup>2</sup>*);  
 $R_m$  is the armature resistance ( $\Omega$ );  
 $L_m$  is the armature inductance (*H*);  
 $k_{EMF}$  is the “back-electromotive” force (*V · s*);  
 $\mu_m(s)$  is the motor dynamic friction (*N · m · s*).

Traditionally,  $\mu_m(s)$  is taken to be simply the constant viscous friction  $\nu_m$ , but here the full dynamic friction (as discussed in §2.1.1.6) is used, which includes the viscous term along with other nonlinear effects. Note that  $\mu_m(s)$  is itself a (nonlinear) first-order function of  $s$ . Also, it can be shown that  $k_{EMF} \approx k_m$  [91, p.52]<sup>60</sup>, which simplifies the problem somewhat, as does the observation that the servomotor inductance  $L_m$  is very low compared with its resistance  $R_m$ . If the ratio is negligible ( $L_m \approx 0$ ), and  $k_{EMF} \approx k_m$ , then the subsystem becomes

$$\theta_m(s) \approx \frac{k_m R_m}{s [(J_m s + \mu_m(s)) R_m + k_m^2]} i_a(s), \quad (2.106)$$

which is evidently a second-order system with input  $v_c(s)$  and output  $\theta_m(s)$ , and their associated derivatives in  $s$ . Note, however, that this is a nonlinear system, due to the dynamic friction  $\mu_m(s)$ . The system is of second order because  $\mu_m(s)$  is a first-order (nonlinear) function of  $s$ .

The electronic motor amplifier typically has a much higher bandwidth than the mechanical system, and can therefore be considered constant over the operating range of the system. In this case,

$$\theta_m(s) = \frac{k_a k_m (L_m s + R_m)}{s [(J_m s + \mu_m(s))(L_m s + R_m) + k_m k_{EMF}]} v_c(s), \quad (2.107)$$

or

$$\theta_m(s) \approx \frac{k_a k_m R_m}{s [(J_m s + \mu_m(s)) R_m + k_m^2]} v_c(s), \quad (2.108)$$

where  $k_a$  is the motor amplifier constant (*A/V*).<sup>61</sup>

Splitting the domain of  $\dot{\theta}_m$  at  $\dot{\theta}_m = 0$ , three second-order functions can be continuously

<sup>60</sup> *Nm/A* and *Vs* both denote units of energy flux.

<sup>61</sup> *A/V* may also be written as *S*, known as “Siemens” after the pioneering German electronic physicist.

defined for the two resulting domains and the boundary, as follows:

$$\theta_m(s) \approx \frac{k_a k_m R_m}{s} v_c(s) \cdot \begin{cases} 1/[(J_m s + \mu_m^+(s))R_m + k_m^2] & \dot{\theta}_m > 0 \\ 1/\mu_m^0(s) & \dot{\theta}_m = 0 \\ 1/[(J_m s + \mu_m^-(s))R_m + k_m^2] & \dot{\theta}_m < 0 \end{cases} \quad (2.109)$$

where:  $\mu_m^+$  is the dynamic friction for “positive” motions;  
 $\mu_m^0$  is the presliding friction when there is no motion;  
 $\mu_m^-$  is the dynamic friction for “negative” motions.

#### 2.1.4.2 Shaft Subsystem.

At the other end of the motor shaft there is the compliant shaft and tool, or alternately the complaint feed drive and workpiece table. It has already been noted that the fundamental mode of the tool, modeled by a restoring torque with a nonlinear dependency on forcing frequency, is sufficient to characterise most machine tool cutting operations. The torsional mode is of interest to this study, because of its effects on machine tool chatter. This produces the rotational analogue of the nonlinear viscoelastic model previously presented in (2.94), considering only the fundamental mode ( $i = 1$ ):

$$s^2 \theta_t(s) + 2\zeta_t \omega_t s \theta_t(s) + \omega_t^2 \theta_t(s) = \tau_t(s) \quad (2.110)$$

where:  $\theta_t$  is the angular displacement of the tool (*rad*);  
 $\omega_t$  is the fundamental mode of the tool (*rad/s*);  
 $\zeta_t$  is the internal damping of the tool;  
 $\tau_t$  is the forcing function (*N · m*).

Note that the fundamental mode and mode shape will depend on the material the tool is made of, its shape, and the boundary conditions. This information can be obtained analytically for simple boundary conditions and tool geometry.

The simplest geometry to consider analytically is a torsioned prismatic rod with constant circular cross-section, a good approximation to most machine tool drive and feed shafts.<sup>62</sup> The torque produced for a given angle of twist is [138, ch.3] [272, ch.7]

$$\Delta \tau_t(t) = \frac{G_t K_p}{l_t} \Delta \theta_t(t) \quad (2.111)$$

---

<sup>62</sup> *Prismatic* rods and beams have a uniform cross section along their entire length.

where:  $\Delta\tau_t$  is the net torque required to generate the tool twist;  
 $G_t$  is the shear modulus of elasticity of the tool material;  
 $K_p$  is St. Venant's constant for the tool geometry;  
 $l_t$  is the length of the tool;  
 $\Delta\theta_t$  is the net angle of tool twist.

Coulomb first developed the theory for torsioned rods, and made the assumption that the value  $K_p \equiv I_p$ , the polar moment of inertia of the rod's cross section, for all cross-sectional geometries. B. de St. Venant in 1855 extended the work of Coulomb to include the cross-sectional distortion due to twisting, providing significantly corrected results for non-circular cross sections (Coulomb's result was shown to be valid only for the special case of circular cross sections). [314]

The polar moment of inertia of the circular tool cross section

$$I_p = \pi d_t^4 / 32, \quad (2.112)$$

where  $d_t$  is the tool diameter. Note also the relation

$$G_t = \frac{E_t}{2(1 + \sigma_t)} \quad (2.113)$$

where:  $E_t$  is the (Young's) modulus of elasticity of the tool;  
 $\sigma_t$  is Poisson's ratio [265]<sup>63</sup> of the tool material.

A prismatic rod model thus describes a net torque proportional to the net angle of twist.

Considering as an alternative the model of a prismatic rod with rectangular cross section (which is the type used to introduce compliance to the mechanical positioning test bed transmission), [272, eq.(7.104)]

$$\Delta\tau_t(t) = a^3 \frac{G_t}{l_t} \left\{ \frac{b}{3} - a \left( \frac{4^3 \pi^5}{3} \right) [\tanh \rho + 3^{-5} \tanh \rho + \dots] \right\} \Delta\theta_t(t) \quad (2.114)$$

where:  $a$  is the shorter side of the rectangular cross-section;  
 $b$  is the longer side of the rectangular cross-section;  
 $\rho = (\pi b) / (2a)$ .

Notice that  $\tanh \rho$  approaches unity very quickly as  $\rho$  increases. If  $b > 3a$ , as is the case with the mechanical positioning test bed ( $b = 6.25a$ ), then "the hyperbolic tangents can differ only in the fourth significant figure" and the torque reduces to [272, eq.(7.107)] [367, eq.(A.3)]

$$\Delta\tau_t(t) \approx \frac{G_t}{3l_t} a^3 (b - 0.630a) \Delta\theta_t(t) . \quad (2.115)$$

The *stiffness*  $k_t$  of the tool is defined as the spring coefficient  $\Delta\tau_t/\Delta\theta_t$ , and the tool *compliance* as its inverse,  $1/k_t$ . The stiffness has the form

$$k_t = \frac{K_p G_t}{l_t} \quad (2.116)$$

where St. Venant's constant is

$$K_p \approx a^3 (b - 0.630a) / 3 . \quad (2.117)$$

The preceding equations describe the spring “constants” of the tool under static deflection, which is directly related to the fundamental mode. For hard-to-analyse tool geometries the fundamental mode and mode shape are relatively easy to determine via a static deflection experiment. In the sense that the springiness of the tool is expected to change with frequency due to damping at different velocities, the static deflection experiment will yield a linear approximation to the nonlinear tool compliance, which considers the tool stiffness to be a function of frequency as well as geometry, material stiffness, and boundary conditions.

It is useful to examine the vibrational modes of the compliant shaft to determine what natural frequencies may be excited during the machine's operation. The undamped modes and mode shapes may be obtained via the classical wave equation [346, § 9.3 ] [272, ch.10]. Consider a unit length of the shaft  $dx$  subjected to a unit twist  $d\theta$ . The twist per unit length is then simply  $d\theta/dx$ . Generalising equation (2.111), it is easy to see that therefore

$$\frac{d\theta}{dx} = \frac{d\tau}{K_p G} . \quad (2.118)$$

The net torque across this infinitesimal element

$$\begin{aligned} d\tau &= \left( \tau + \frac{\delta\tau}{\delta x} dx \right) - \tau = \frac{\delta\tau}{\delta x} dx \\ &= K_p G \frac{d\theta}{dx} = K_p G \frac{\delta^2\theta}{\delta x^2} dx . \end{aligned} \quad (2.119)$$

This torque is equivalent to the product of the polar mass moment of inertia  $\rho I_p dx$  and the angular acceleration of the element  $\delta^2\theta/\delta t^2$ , where  $\rho$  is the mass density of the shaft, so

$$K_p G \frac{\delta^2\theta}{\delta x^2} dx = \rho I_p dx \frac{\delta^2\theta}{\delta t^2} \quad (2.120)$$

or using the classical representation for the wave equation,

$$\frac{\delta^2\theta}{\delta t^2} = \alpha^2 \frac{\delta^2\theta}{\delta x^2}, \quad (2.121)$$

where

$$\alpha^2 = \frac{K_p G}{\rho I_p}, \quad (2.122)$$

and it becomes evident that for circular rods, the St. Venant's constant and polar moment of inertia cancel out to become unity.<sup>64</sup> For the rectangular shaft, on the contrary, substitution of (2.117) along with the polar moment of inertia for a rectangular cross section, [138, appx.D]

$$I_p = \frac{ab}{12} (a^2 + b^2), \quad (2.123)$$

yields the value

$$\alpha^2 \approx \frac{G}{\rho} \cdot \frac{4a^2(b - 0.630a)}{b(a^2 + b^2)} \quad \text{where } b \geq 3a, \quad (2.124)$$

which is less than unity for all  $b \geq 3a > 0$ . The value  $\alpha$  denotes the torsional wave propagation velocity through the shaft, so the wave velocity along a circular rod is unaffected by its dimension, whereas that along a rectangular bar is always slower than that for a circular rod, an interesting result to observe. For the value  $b = 6.25a$  of the test bed compliance element, substitution reveals that

$$\alpha^2 \approx 0.3^2 \cdot \frac{G}{\rho}, \quad (2.125)$$

which shows that vibrations in the test bed shaft propagate at just under a third the speed they would along a circular rod.

Presuming that it is possible to linearly separate the variables in the description of the twist angle along the length of the shaft at any point in time,

$$\theta(x, t) = \phi(x) \cdot \gamma(t), \quad (2.126)$$

where:  $\phi(x)$  is some function depending only on the shaft displacement  $x$ ;

$\gamma(t)$  is some function depending only on time.

This representation is entirely equivalent to that used to introduce the method of modal summation via proportional damping in § 2.1.3.2 on page 83; here  $\phi(x)$  denotes the torsional

---

<sup>64</sup>—Thus explaining why Coulomb's result for circular rods happened to be correct.

mode shape of the shaft and  $\gamma(t)$  the modal participation factor. Taking derivatives,

$$\frac{\delta^2\theta}{\delta t^2} = \phi(x) \cdot \frac{d^2\gamma(t)}{dt^2} \quad \text{and} \quad \frac{\delta^2\theta}{\delta x^2} = \gamma(t) \cdot \frac{d^2\phi(x)}{dx^2} . \quad (2.127)$$

Substituting these into (2.121),

$$\frac{1}{\alpha^2\gamma} \cdot \frac{d^2\gamma}{dt^2} = \frac{1}{\phi} \cdot \frac{d^2\phi}{dx^2} . \quad (2.128)$$

Notice the temporal and spacial components are now completely decoupled, which is valid if the modes are well-spaced and the damping is sufficient, as discussed under the modal summation method. Because the left-hand side depends only on time, and the right-hand side only on space, for the equation to hold true, both sides must be constant. Let this constant, for the sake of convenience, be equal to  $-(\omega/\alpha)^2$ , where  $\omega \triangleq \dot{\theta}$  and the propagation velocity  $\alpha$  is defined as before. Two differential equations are then produced:

$$\ddot{\gamma} + \omega^2\gamma = 0 \quad \text{and} \quad \phi'' + (\omega/\alpha)^2\phi = 0 , \quad (2.129)$$

where the dots (·) denote derivation with respect to time  $t$ , and the dashes (") derivation with respect to space  $x$ . The general solutions are then

$$\phi(x) = A \sin\left(\frac{\omega}{\alpha}x\right) + B \cos\left(\frac{\omega}{\alpha}x\right) \quad (2.130a)$$

$$\gamma(t) = C \sin(\omega t) + D \cos(\omega t) , \quad (2.130b)$$

where  $A$  and  $B$  are constants determined by the boundary conditions, and  $C$  and  $D$  by the initial conditions of the system.

When the tool end is clamped,  $\Delta\tau_t(t)$  will appear at the tool end of the backlash element, because the end cannot rotate. When the tool is free,  $\Delta\tau_t(t)$  will describe the forced vibration of the tool at the end of the backlash element. Friction at the tool-workpiece interface will introduce damped rotation to the boundary condition. The lumped compliance model for the shaft and tool is then described by equation (2.110), where the modal frequency  $\omega_t$  and damping  $\zeta_t$  depend on the tool characteristics as derived analytically using geometry and material properties, or experimentally via modal analysis and static deflection tests.

A conservative estimate of the modal response (the lower bound for the second mode) may be obtained by considering the shaft vibration where one end is fixed and the other free to rotate. If the fixed end of the shaft is where  $x = 0$ , then its rotation  $\phi(x = 0) = 0$ , because in general  $\gamma(t) \neq 0$ . If the free end is where  $x = l$ , the shaft length, then its strain

$\phi'(x = l) = 0$ . Thus

$$\phi(x = 0) = B = 0 \quad \text{and} \quad \phi'(x = l) = A \frac{\omega}{\alpha} \cos\left(\frac{\omega}{\alpha} l\right) = 0, \quad (2.131)$$

so

$$\omega = \frac{\alpha}{l} \cdot \frac{(2n - 1)}{2} \pi, \quad (2.132)$$

where  $n > 0$  is the mode number. This relationship between the modal frequency  $\omega$  and the propagation velocity  $\alpha$  shows that the test bed's rectangular compliance element will have thrice the flexibility of a circular rod with like dimension. Substitution of the material parameters and shaft length easily give the undamped modal frequencies. A liberal estimate of the modal frequencies will be given by fixed-fixed boundary conditions, which can be analytically shown to lead to modes at double the frequency of the fixed-free modes. In reality, the frictional torque provided between, alternately, the workpiece table and slideway, or the cutting tool and workpiece, will result in modal frequencies between the conservative and liberal estimates outlined above.

#### 2.1.4.3 Transmission Subsystem.

The transmission subsystem is considered to be composed of one backlash element, although in gearboxes, for example, many backlash elements are present which sum up to one total backlash between the input and output. Detailed identification of gear trains is not examined in this thesis. The backlash element is rather described as a simple linkage between the motor and tool subsystems: when the two shafts are not in contact, the tool subsystem moves freely, and when they are in contact, the tool is torqued by the motor.

Consider the second-order motor model

$$\theta_m(s) \approx \frac{k_a k_m R_m}{s [(J_m s + \mu_m(s)) R_m + k_m^2]} v_c(s). \quad (2.133)$$

Here  $\theta_m$  denotes the controlled angular position of the motor. Let  $\theta_t$  denote the angular position of the tool chuck, attached to the rigid transmission spindle after the backlash element. These values correspond, respectively, to the angular equivalents of  $x_1$  and  $x_2$  in

Figure 2.3 on page 62. Rephrasing this equation in terms of the motor torque yields

$$\begin{aligned}
 \tau_m(s) &= \frac{k_m(J_m s + \mu_m(s))(L_m s + R_m)}{(J_m s + \mu_m(s))(L_m s + R_m) + k_m k_{EMF}} i_a(s) \\
 &= \frac{k_a k_m (J_m s + \mu_m(s))(L_m s + R_m)}{(J_m s + \mu_m(s))(L_m s + R_m) + k_m k_{EMF}} v_c(s) \\
 &\approx \frac{k_a k_m R_m (J_m s + \mu_m(s))}{(J_m s + \mu_m(s)) R_m + k_m^2} v_c(s).
 \end{aligned} \tag{2.134}$$

The second-order tool compliance model is given by (2.110).

The deadzone can now be written as

$$\Delta\tau_t(t) = \begin{cases} \tau_m(t) + \tau_w(t) & \text{if } |\dot{\theta}_m| \geq |\dot{\theta}_t| \\ & \text{and } \Delta\theta_m(t) = 0 \text{ or } \Delta\theta_m^0 \\ \tau_w(t) & \text{otherwise} \end{cases} \tag{2.135}$$

where:  $\tau_w(t)$  is the tool-workpiece friction;

$\Delta\theta_m(t)$  is the dynamic clearance between the shafts;

$\Delta\theta_m^0$  is the maximum static clearance (the deadzone gapwidth).

Note that  $\tau_w(t) = 0$  if the tool end is free and  $\tau_w(t) = \tau_m(t)$  if it is clamped, though the boundary conditions for either situation will lead to different modes and mode shapes for the tool.

Impact occurs when at the moment of contact  $t_c$ , the difference in velocities (the net impact velocity) is appreciable. This will typically occur only when the backlash is itself appreciable, or when the motor is faster than the shaft and tool. Impact is modeled only when the two shafts first make contact. At this moment, the impact model can be used to compute the relative velocities after impact and determine the net amount of transmitted torque during contact. Within the scheme of the overall motion, this is assumed to occur nearly instantaneously, and repeated impacts (“bouncing”) are anticipated before “permanent” contact is maintained. The transmitted torque during impact will excite the modal frequencies of the tool in a manner depending on the tool boundary conditions. The problem is completely analogous to the impact of a flexible beam at its tip, with an optional tip mass and/or friction moment, a matter studied extensively within the robotics research community. [31, 32, 37, 65, 84, 94, 124, 137, 220, 221, 261, 349, 350, 368, 369, 377, 380]

## 2.2 Identification of Drive Nonlinearities.

In this section, some identification methods will be investigated to determine those best suited to the various subsystem identifications. The system as a whole can be classified into a collection of subsystems, each performing a specific function, which leads to an overall “divide-and-conquer” system identification strategy. Taking this approach, it may additionally be possible to identify the type of machine tool being used via an expert-systems approach, by comparing the known salient behaviours of common machine tools. This might further provide a means for “blueprinting” the normal operating characteristics of a particular type of machine tool, along with its parameter sensitivities, thereby yielding a template against which to judge the performance or health of individual machine tools. The identification procedures outlined in Chapter 4 may suggest to the interested reader how such a template might be constructed from the salient machine behavioural patterns identified using the techniques described in this section.

### 2.2.1 System Identification Methods.

For linear, time-invariant, second-order, uni- or multimodal systems, such as machine tools with only slowly-varying system parameters, the free-vibration response can be a sufficient form of system identification because the free vibration occurs at the (damped) natural frequency of the system. When free vibration is not feasible, system identification is performed by exciting the system with a control signal designed to elicit characteristic system responses. Because many systems, including the ones examined by this thesis, can be described in terms of their reactivity to frequency- and amplitude-modulated signals, usually such signals are used in a manner which ensures that no one frequency or amplitude is biased above any other. One of the contributions of the present work is a novel method for obtaining the free vibration response for any second-order system (including overdamped ones).

Time-invariant linear systems exhibit a linear dependence on the amplitude of an excitation, so for these systems only the frequency need be modulated to ensure that the entire range of possible responses is properly examined. The traditional approach involves a so-called *sine sweep*, where the relevant frequency range is traversed in a quasi-steady-state manner (the window of response data sampled at any instantaneous frequency is sufficiently representative of a steady-state response); in other words, the sweep through the frequency range is “slow enough” such that the response for a given frequency within the range may be properly discerned. With the advent of high-speed digital minicomputers, even the analysis of transient (non-steady-state) data may be performed so quickly that the identification signal (the sweep) sounds like (and is commonly known as) a “chirp”. This old stand-

by has all the advantages of simplicity, but is complicated by requiring a transformation between the time and frequency domains.

Statistical (stochastic) analysis has suggested the use of a *white noise* signal, a random signal with a specified, constant standard deviation for all frequencies. In reality, it is impossible to guarantee a constant deviation because theoretically this requires a signal of infinite duration.

A recent improvement on both the chirp and white noise signals is named the *Schröder-phased* waveform, after its inventor. [34,298,372] The Schröder-phased signal is formulated within the frequency domain itself, and then transformed back into the time domain, with the advantage that the *phase* transformation (as well as the magnitude) at any given frequency is weighed equally within the time-domain signal. The chirp signal has a constant magnitude at all frequencies, though its phase is distorted when transformed into the frequency domain; the Schröder-phased waveform solves this problem. Furthermore, unlike the white noise signal, the Schröder-phased waveform is specified only at discrete frequencies, and therefore can accomplish the same task in a finite amount of time using a digital computer, whilst guaranteeing a uniform excitation at each of the frequencies of interest. The Schröder-phased signal is therefore the signal of choice when the linear system is to be controlled or identified digitally, and the delays of the system are important.

Unlike various frequency-based methods, the logarithmic decrement method, developed by Lord Rayleigh in the late 1800s, uses the time-domain oscillation response directly. [280] The advantage of this approach is its simplicity, as will become evident in the sections following.

These conveniences do not render the same simplifications to nonlinear systems, unfortunately, which may exhibit wild response fluctuations to different excitation amplitudes at any one frequency. For these systems it is necessary to modulate both the frequency and amplitude of the identification signal. [214]

One way this can be efficiently accomplished is by the use of *harmonic excitation*, where two independent chirp-type signals are fed into the system simultaneously. The two simultaneous signals are represented in an analytic form known as the *describing function* representation. [308] This allows the input-output response, which need not be linear, to be mapped in the Hilbert space. A Hilbert Transform is used to decode the mapping into a representation of the frequency- and amplitude-dependent natural frequencies and damping of the system, similar to the way amplitude-modulated (AM) radiowaves may be decoded. [151] Promising aspects of the describing function approach include its simplicity and potential for real-time applications. [117, 118, 226, 262]

A second nonlinear identification scheme employs the wavelet transformation, [56,315]

which for good reason has lately come very much into vogue (and also come of age) within the signal-processing community. The wavelet transformation has the remarkable capability of achieving both a good time resolution and a good frequency resolution. If one considers that at low frequencies of oscillation, the timeline is inherently more resolvable, and that for long timelines, the frequency is inherently more resolvable, it would seem reasonable to focus efforts on identifying more accurately the less resolvable of the two, depending on the characteristics of a given data segment. This is precisely what the wavelet can do well, allowing it to perform localised time-domain analysis for nonlinear oscillations, as well as the localised frequency-domain analysis proffered by traditional techniques like the Fourier Transform. [249]

Other possible identification methods might employ wavelet or Schröder-phased representations of the describing function. In this manner, the identification might be performed in a shorter amount of time, possibly even in real time during normal machine operation.

### 2.2.2 Simple Harmonic Motion

Consider the forced oscillation of the piecewise linear (time-invariant) second-order system

$$J\ddot{\theta}(t) + C\dot{\theta}(t) + K\theta(t) + \tau_c = \tau(t) . \quad (2.136)$$

Coulomb friction torque [67] is a piecewise constant function defined in terms of static and kinetic friction:

$$\tau_c = \begin{cases} \mu_s & \dot{\theta}(t) = 0 \\ \mu_k \operatorname{sgn}(\dot{\theta}) & \dot{\theta}(t) \neq 0 \end{cases} , \quad (2.137)$$

where due to the nature of friction  $\mu_s \geq \mu_k$  (ergo, the counter-intuitive phenomenon of stick-slip friction, or *stiction*).

Substituting  $\ddot{\theta}(t) = \dot{\theta}(t) = 0$  into (2.136), the static friction satisfies

$$\theta(t) \leq \theta_s \quad \text{where} \quad \theta_s \triangleq \mu_s / K . \quad (2.138)$$

This describes a region of possible positions  $\theta$  for which the spring force  $K\theta$  is insufficient to produce movement by overcoming the static friction  $\mu_s$ .<sup>65</sup> The static friction is important, and we will return to it later on, but let us now first consider the dynamics of the kinetic friction on the system.

---

<sup>65</sup>Notice also the correspondence of the friction stasis  $\theta_s$  to the presliding stiffness (2.14).

Notice that equation (2.136) is linear when either  $\dot{\theta} < 0$  or  $\dot{\theta} > 0$ . Defining

$$\theta_k \triangleq \mu_k/K, \quad (2.139)$$

we can thus reformulate the problem in terms of the linear equation

$$J\ddot{\gamma}(t) + C\dot{\gamma}(t) + K\gamma(t) = \tau(t), \quad (2.140)$$

where

$$\gamma(t) \triangleq \theta(t) + \theta_k \operatorname{sgn} \dot{\theta}(t) \quad (2.141a)$$

$$\text{and } \dot{\gamma}(t) \equiv \dot{\theta}(t), \quad (2.141b)$$

within regions of unidirectional motion ( $\dot{\theta}$  does not change sign).

### 2.2.3 Transient (Unforced) Harmonic Oscillation

The transient response is that observed when the system is unforced (when  $\tau(t) \equiv 0$ ). The so-called *free* oscillation may be expressed as

$$\gamma(t) = Ae^{-\sigma t} \sinh(\omega_d t - \phi_0) \quad (2.142)$$

where the *rate of decay*

$$\sigma \triangleq \frac{C}{2J}, \quad (2.143)$$

which relates the *damped natural frequency*

$$\omega_d \triangleq \sqrt{\sigma^2 - \omega_0^2} \quad (2.144)$$

to the (*undamped*) *natural frequency*

$$\omega_0 \triangleq \sqrt{\frac{K}{J}}. \quad (2.145)$$

The oscillation has an *amplitude* (also called *envelope*)

$$A^2 = \frac{\dot{\gamma}_0^2 + 2\sigma\dot{\gamma}_0\gamma_0 + \omega_0^2\gamma_0^2}{\omega_d^2} \quad (2.146)$$

and *phase*

$$\tanh \phi_0 = -\frac{\omega_d \gamma_0}{\dot{\gamma}_0 + \sigma \gamma_0}, \quad (2.147)$$

given the initial conditions on position and velocity

$$\gamma_0 \triangleq \gamma(t_0) \quad \text{and} \quad \dot{\gamma}_0 \triangleq \dot{\gamma}(t_0). \quad (2.148)$$

These equations are valid for *all* real first- and second-order oscillations, regardless of damping or stiffness, provided that the physical quantities  $J > 0$ ,  $C \geq 0$  and  $K \geq 0$ .

### 2.2.3.1 Overdamped Response

The system is *overdamped* when  $\sigma^2 > \omega_0^2$ . In this case equation (2.142) may be applied without modification. The special case when  $K = 0$  ( $\omega_0 = 0$ ) results in an equivalent first-order system, which has no static restoring (spring) force. Usually this first-order response is analysed in terms of a first-order system, for example

$$J\dot{z}(t) + Cz(t) = \tau(t), \quad (2.149)$$

from which the response is recovered by integrating the solution  $z(t) \triangleq \dot{\theta}(t)$ . However, the very same response may be obtained simply by substituting  $K = 0$  directly into equations (2.142) through (2.148).

### 2.2.3.2 Critically-damped Response

For systems with non-zero stiffness  $K > 0$ , the nondimensional *damping coefficient* is written as one of the standard equations

$$\zeta \triangleq \frac{\sigma}{\omega_0} = \frac{C}{C_c} = \frac{C}{2J\omega_0} = \frac{C}{2\sqrt{JK}}. \quad (2.150)$$

The meaning of the damping coefficient  $\zeta$  as the ratio between the viscous damping coefficient  $C$  to the *critical damping coefficient*  $C_c$  is that the critical value  $C = C_c$  demarcates the oscillatory and non-oscillatory system responses. For underdamped systems,  $0 \leq \zeta < 1$ .

When  $\sigma^2 = \omega_0^2$  ( $\zeta = 1$ ) the system is *critically damped*. In this case, both  $\omega_d = 0$  and  $\phi_0 = 0$ . Observing that

$$\lim_{\omega_d \rightarrow 0} \frac{\sinh \omega_d t}{\omega_d} = \lim_{\omega_d \rightarrow 0} \frac{\sin \omega_d t}{\omega_d} = t, \quad (2.151)$$

substitution into equation (2.142) results in the familiar expression for the critically-damped

response,

$$\gamma(t) = te^{-\sigma t} \sqrt{\dot{\gamma}_0^2 + 2\sigma\dot{\gamma}_0\gamma_0 + \omega_0^2\gamma_0^2}. \quad (2.152)$$

Notice that since  $\sigma = \omega_0$ , either may be used interchangeably in the final expression.

### 2.2.3.3 Underdamped Response

The system is *underdamped* when  $\sigma^2 < \omega_0^2$ . In this case,  $\omega_d$  (as defined) will be an imaginary number,<sup>66</sup> so it is customarily redefined to be the complex conjugate of equation (2.144). Thus, using  $j\omega_d$  and  $j\phi_0$  instead of  $\omega_d$  and  $\phi_0$ , respectively, in equations (2.146) and (2.147), and then substituting into (2.142),

$$\gamma(t) = -jAe^{-\sigma t} \sinh(j\omega_d t - j\phi_0). \quad (2.153)$$

This can be rewritten via the identity  $-j \sinh(jx) = \sin(\theta)$ , to reveal the familiar equation for underdamped oscillation,

$$\gamma(t) = Ae^{-\sigma t} \sin(\omega_d t - \phi_0). \quad (2.154)$$

The overdamped and underdamped equations are therefore mathematically equivalent; redefining the damped natural frequency to maintain its realness for underdamped oscillations is generally a matter of convenience for educational and interpretive purposes, since usually people are more intimately familiar with the behaviour of regular sines and cosines than of their hyperbolic equivalents.

### 2.2.4 Asymmetric Harmonic Motion

Many real systems exhibit appreciable asymmetric Coulomb and viscous friction, which can be defined as

$$\mu_s = \bar{\tau}_s + \Delta\mu_s \operatorname{sgn} \tau(t) \quad (2.155a)$$

$$\mu_k = \bar{\tau}_k + \Delta\mu_k \operatorname{sgn} \dot{\theta}(t) \quad (2.155b)$$

$$C = \bar{C} + \Delta C \operatorname{sgn} \dot{\theta}(t) \quad (2.155c)$$

where the terms with a *bar* denote the mean frictional values, and those with the  $\Delta$  denote their variation depending on the direction of applied force  $\tau(t)$  or motion  $\dot{\theta}(t)$ .

The asymmetric Coulomb friction can be expressed in terms of the parameters  $\theta_s$  and  $\theta_k$  as before, in which case the asymmetries give rise to a constant offset in the displacement

---

<sup>66</sup>The imaginary number  $j \triangleq \sqrt{-1}$  is used, in keeping with the nomenclature adopted by the electrical engineering and control systems community.

response  $\theta(t)$  as per (2.141). The system's displacement may thus be written in the more general form

$$\begin{aligned}\gamma(t) &\triangleq \theta(t) + \theta_k \operatorname{sgn} \dot{\theta}(t) = \theta(t) + \theta_k \operatorname{sgn} \dot{\gamma}(t) \\ &= \theta(t) + [\bar{\theta}_k + \Delta\theta_k \operatorname{sgn} \dot{\gamma}(t)] \operatorname{sgn} \dot{\gamma}(t) \\ &= \theta(t) + \bar{\theta}_k \operatorname{sgn} \dot{\gamma}(t) + \Delta\theta_k ,\end{aligned}\tag{2.156}$$

the solution of which now also contains the asymmetric rate of decay

$$\sigma \triangleq \bar{\sigma} + \Delta\sigma \operatorname{sgn} \dot{\gamma}(t) ,\tag{2.157}$$

where of course  $\dot{\gamma}(t) \equiv \dot{\theta}(t)$  as before, within regions of unidirectional motion.

## 2.2.5 The Logarithmic Decrement Method

The logarithmic decrement method is a popular way to identify an underdamped system by examining the envelope and frequency of its oscillation. It has its roots in work pioneered over a century ago by Lord Rayleigh [280]; recently it was revisited by Feeny and Liang [114] to include estimation of Coulomb friction in addition to the usual viscous vibration damping. In the following logical extension it is further shown how asymmetric Coulomb and viscous friction too may be estimated.

### 2.2.5.1 The Logarithmic Decrement

Given an underdamped oscillation (2.154), its velocity may be written

$$\dot{\gamma}(t) = Ae^{-\sigma t} [\omega_d \cos(\omega_d t - \phi_0) - \sigma \sin(\omega_d t - \phi_0)] ,\tag{2.158}$$

which is nil ( $\dot{\gamma}(t) = 0$ ) when the displacement  $\gamma(t)$  is at a maximum or minimum (at a *peak*). Denoting the  $n^{\text{th}}$  peak displacement as  $\gamma_n(t)$ , and the corresponding velocity  $\dot{\gamma}_n(t) = 0$ , the angle of oscillation  $\omega_d t - \phi_0$  at peak  $n$  can be written as

$$\tan(\omega_d t - \phi_0) = \frac{\omega_d}{\sigma} = \frac{\sqrt{1 - \zeta^2}}{\zeta} .\tag{2.159}$$

The (modified) form of (2.147) for underdamped oscillation at the  $n^{\text{th}}$  peak is

$$\tan \phi_0 = - \frac{\omega_d \gamma_n}{\dot{\gamma}_n + \sigma \gamma_n} ,\tag{2.160}$$

which when substituted into the trigonometric expansion of (2.159) yields

$$\tan \omega_d t = \frac{\omega_d \dot{\gamma}_n}{\sigma \dot{\gamma}_n + \omega_0^2 \gamma_n}. \quad (2.161)$$

This expression is always nil because  $\dot{\gamma}_n = 0$  by definition, and thus  $\omega_d t = n\pi$ , from which it follows that

$$\sigma t = \zeta \omega_0 t = n\pi \frac{\zeta}{\sqrt{1 - \zeta^2}} = n\pi \frac{\sigma}{\omega_d} \quad (2.162)$$

and

$$\sin \omega_d t = \sin n\pi = 0 \quad (2.163a)$$

$$\cos \omega_d t = \cos n\pi = (-1)^n \quad (2.163b)$$

at the  $n^{\text{th}}$  oscillation peak.

Substituting  $\dot{\gamma}_n = 0$  into equations (2.146) and (2.160) further yield, respectively,

$$A = \frac{\omega_0}{\omega_d} \gamma_0, \quad \sin \phi_0 = -\sqrt{1 - \zeta^2}, \quad \text{and} \quad \cos \phi_0 = \zeta. \quad (2.164)$$

Substituting the results of equations (2.162) - (2.164) into the trigonometric expansion of (2.154) finally gives the  $n^{\text{th}}$  peak displacement

$$\gamma_n = (-1)^n \gamma_0 e^{-n\pi\beta} = -\gamma_{n-1} e^{-\pi\beta} \quad \forall \quad n > 0, \quad (2.165)$$

where the *logarithmic decrement* is defined as the logarithm of the ratio between successive peaks,

$$\pi\beta \triangleq -\ln \frac{-\gamma_n}{\gamma_{n-1}} = -\frac{\pi\zeta}{\sqrt{1 - \zeta^2}} = -\frac{\pi\sigma}{\omega_d}, \quad (2.166)$$

which, incidentally, is the equivalent of  $(-\pi \cot \phi_0)$  at the oscillation peaks.

### 2.2.5.2 Asymmetric Friction Estimation

Asymmetric viscous friction can be expressed in terms of two values  $\beta^+$  and  $\beta^-$  such that equation (2.165) becomes

$$\gamma_n = -\gamma_{n-1} e^{-\pi\beta}, \quad (2.167)$$

where either  $\beta = \beta^+$  or  $\beta = \beta^-$  depending on whether  $n$  is even or odd (exactly which is unimportant, as long as the user is consistent with the adopted notation). For symmetric  $\beta = \beta^+ = \beta^-$  this collapses once again into equation (2.165).

When the asymmetric dry and viscous friction of equations (2.156) and (2.157) are

substituted at the oscillation peaks given by (2.167) and (2.166), the frictional asymmetry of the oscillation becomes visible:

$$\theta_n + \theta_{n-1}e^{-\pi\beta^+} = - \left(1 + e^{-\pi\beta^+}\right) [\Delta\theta_k + (-1)^n\bar{\theta}_k] \quad (2.168a)$$

$$\theta_{n-1} + \theta_{n-2}e^{-\pi\beta^-} = - \left(1 + e^{-\pi\beta^-}\right) [\Delta\theta_k + (-1)^{n-1}\bar{\theta}_k] , \quad (2.168b)$$

with the substitution  $\text{sgn } \dot{\gamma} = \text{sgn } \dot{\theta} = (-1)^n$ , where  $n$  is *odd* if motion starts in the negative direction (either  $\gamma_0 > 0$  and/or  $\dot{\gamma}_0 < 0$ ), and *even* if motion starts in the positive direction (either  $\gamma_0 < 0$  and/or  $\dot{\gamma}_0 > 0$ ). The (+) and (−) superscripts on  $\beta$  denote the direction of motion ( $\text{sgn } \dot{\gamma}$ ) between oscillation peaks, and the associated positive or negative viscous friction bias introduced by the asymmetric damping of equation (2.157).

It is important to note that the  $\text{sgn } \dot{\gamma}$  term in equations (2.156) and (2.157) is constant for all motion between points  $n$  and  $n - 1$ ; in other words, the signum function changes sign only *in-between* the oscillation peaks, not *at* the peaks themselves, where instead it equals zero. Successive peak displacements are used to infer information about the motion between those peaks, not at the peaks themselves, hence the correct sign of the signum function as applied to the frictional term  $\bar{\theta}_k$  at those peaks should be that of the velocity between the same. This explains why the  $(-1)^n\bar{\theta}_k$  term can be gathered with the  $\Delta\theta_k$  term on the right hand sides of equations (2.168).

Notice furthermore that the expression solved for  $\theta(t)$  in equation (2.156) is equivalent to the solution for  $\gamma(t)$  as defined, but for the sign reversal of the kinetic friction terms. Because of this similarity in the solution form,  $\gamma_n$  may be substituted for  $\theta_n$  in (2.168) by reversing the sign on the right-hand sides of the equations. In this manner the friction can be estimated from the actual data points  $\gamma(t)$  (since the friction-free displacements  $\theta(t)$  are unknown before the friction is estimated).

Solving for the decrement ratios,

$$e^{-\pi\beta^+} = -\frac{\gamma_n - \gamma_{n-2}}{\gamma_{n-1} - \gamma_{n-3}} \quad \text{and} \quad e^{-\pi\beta^-} = -\frac{\gamma_{n-1} - \gamma_{n-3}}{\gamma_{n-2} - \gamma_{n-4}} . \quad (2.169)$$

These results are an extension of equation (2.166) which take advantage of the observation that  $\gamma_n - \gamma_{n-2} = \theta_n - \theta_{n-2}$  to remove the kinetic friction contribution from the viscous friction estimation.

Solving (2.168) for the kinetic friction parameters, the kinetic friction is given by

$$\bar{\theta}_k = \frac{1}{2(-1)^n} \left( \frac{\gamma_n + \gamma_{n-1}e^{-\pi\beta^+}}{1 + e^{-\pi\beta^+}} - \frac{\gamma_{n-1} + \gamma_{n-2}e^{-\pi\beta^-}}{1 + e^{-\pi\beta^-}} \right) \quad (2.170a)$$

$$\text{and } \Delta\theta_k = \frac{1}{2} \left( \frac{\gamma_n + \gamma_{n-1}e^{-\pi\beta^+}}{1 + e^{-\pi\beta^+}} + \frac{\gamma_{n-1} + \gamma_{n-2}e^{-\pi\beta^-}}{1 + e^{-\pi\beta^-}} \right). \quad (2.170b)$$

The asymmetric kinetic friction may be determined directly from the logarithmic decrement and oscillation peaks as per equations (2.170). Using the logarithmic decrement values in equations (2.169), the respective viscous damping ratios may also be determined from equation (2.166):

$$\zeta^\pm = \sqrt{\frac{(\beta^\pm)^2}{\pi^2 + (\beta^\pm)^2}}, \quad (2.171)$$

from which

$$\bar{\zeta} = \frac{\zeta^+ + \zeta^-}{2} \quad \text{and} \quad \Delta\zeta = \left| \frac{\zeta^+ - \zeta^-}{2} \right|. \quad (2.172)$$

### 2.2.5.3 Identification Procedure

When the viscous friction is asymmetric ( $\Delta\zeta \neq 0$ ), the oscillation will also be asymmetric, complicating the natural frequency estimation. Whereas the natural frequency of the system is of course constant, the damped natural frequency, as evident in the asymmetric response, takes one of two values depending on the direction of motion:

$$\omega_d^\pm = \frac{\pi}{\Delta t^\pm}, \quad (2.173)$$

where the  $\Delta t$  denotes the time difference between successive oscillation peaks:

$$\Delta t^+ \triangleq t_n - t_{n-1} \quad \text{and} \quad \Delta t^- \triangleq t_{n-1} - t_{n-2}. \quad (2.174)$$

The natural frequency of the system is then given by

$$\omega_0 = \frac{\omega_d^\pm}{\sqrt{1 - \zeta^\pm}}. \quad (2.175)$$

(Naturally, if the theoretically equivalent +/- terms are averaged, the numerical estimation can thereby be improved against noise in the data.)

Note lastly that the equations presented in this section are first-order approximations, using the fewest number of data for each estimation. The approximations may be extended to higher dimensions by further combining the successive terms defined in equations (2.168).

### 2.2.6 Forced Harmonic Oscillation

A complement to the pseudo-“free” vibration response exhibited by the parametric harmonic oscillation is a forced oscillatory response produced by an external harmonic force  $\tau(t)$ . After the transient response of the system has subsided ( $Ae^{-\sigma t}$  in equation (2.142) is acceptably small for some  $t \gg t_0$ ), the *steady-state* response  $\gamma(t \gg t_0)$  will be an oscillation of the same frequency as that of the input  $\tau(t)$ .

For example, let the *forcing function* be defined as

$$\tau(t) \triangleq A_1 \sin(\omega t - \phi_1) . \quad (2.176)$$

The persistent system response to this force is then

$$\gamma_p(t \gg t_0) = A_2 \sin(\omega t - \phi_2) , \quad (2.177)$$

where

$$\omega_0^2 = \omega^2 + \frac{R \cos \rho}{J} \quad (2.178a)$$

$$\text{and} \quad \sigma = \frac{R \sin \rho}{2J\omega} , \quad (2.178b)$$

and the *relative amplitude* and *relative phase (lag)* are

$$R \triangleq \frac{A_1}{A_2} \quad \text{and} \quad \rho \triangleq \phi_2 - \phi_1 , \quad (2.179)$$

respectively, both of which are measured experimentally and used to estimate the natural frequency and damping coefficient. By slowly sweeping the excitation across a range of frequencies  $\omega$ , the traditional “sine sweep” identification procedure is performed, from which the Bode plot of the output amplitude and phase can be constructed; only the relative amplitude and phase (lag) need to be known for any given frequency.

### 2.2.7 Parametric Harmonic Oscillation Using PD Feedback

The ultimate objective of system identification is to discover the physical parameter values from which the system’s behaviour is derived. For the systems described in this treatment, the values of mass  $J$ , viscous friction coefficient  $C$ , and spring constant  $K$  should be estimated. It is difficult to measure precisely the values of these parameters when they differ greatly in relative scale. For example, when there is very little damping ( $\zeta \approx 0$ ), the behaviour is predominantly oscillatory and  $C$  will be difficult to estimate with good confidence. Similarly,  $K$  is nearly impossible to estimate when the natural frequency of the system is close to naught ( $\omega_0 \approx 0$ ). The system mass  $J$  is also hard to determine when it

is small relative to  $C$  and  $K$ . Ideally, therefore, each of these parameters should be close to one another in relative scale. However, this is impossible to achieve physically if the system parameters are for some reason unchangeable, and the problem is that oscillatory motion is required to implement most available time-domain identification techniques with reasonable precision.

The parametric harmonic oscillation method resolves this problem by artificially modulating the energy dissipation and storage of the system. Consider the forced second-order system

$$J\ddot{\gamma}(t) + C\dot{\gamma}(t) + K\gamma(t) = \tau(t) = - [D_j\dot{\gamma}(t') + P_i\gamma(t')] , \quad (2.180)$$

where  $D$  is a derivative feedback constant with the same units as  $C$ , and  $P$  is a proportional feedback with the same units as  $K$ . The PD feedback is presumed to include a time delay  $\Delta t \triangleq t - t'$ , due to any of a number of realistic factors, such as the mechanical or electrical time constant of the motor and amplifier providing the feedback force.<sup>67</sup>

Because the whole idea behind parametric harmonic oscillation is to produce an artificially underdamped system, we can assume that the displacements have the form described in § 2.2.3.3 on page 103. Therefore

$$\begin{aligned} \gamma(t') &= Ae^{-\sigma t'} \sin(\omega_d t' - \phi_0) = Ae^{-\sigma(t-\Delta t)} \sin[\omega_d(t - \Delta t) - \phi_0] \\ &= Ae^{-\sigma t} e^{\Delta t} [\cos(\Delta\phi) \sin(\omega_d t - \phi_0) - \sin(\Delta\phi) \cos(\omega_d t - \phi_0)] , \end{aligned} \quad (2.181)$$

where the phase lag caused by time delay  $\Delta t$

$$\Delta\phi \triangleq \omega_d \Delta t . \quad (2.182)$$

It is convenient for the sake of synthesis to write  $\gamma(t')$  and its derivative in terms of  $\gamma(t)$  and the phase shift  $\Delta\phi$ . From equations (2.154) and (2.158) it is evident that

$$Ae^{-\sigma t} \cos(\omega_d t - \phi_0) = \frac{\dot{\gamma} + \sigma\gamma}{\omega_d} . \quad (2.183)$$

From the same two equations, the derivative of equation (2.158) can be written as

$$\begin{aligned} \ddot{\gamma}(t) &= Ae^{-\sigma t} [(\sigma^2 - \omega_d^2) \sin(\omega_d t - \phi_0) - 2\sigma\omega_d \cos(\omega_d t - \phi_0)] \\ &= - [\omega_0^2 \gamma(t) + 2\sigma\dot{\gamma}(t)] , \end{aligned} \quad (2.184)$$

---

<sup>67</sup>Note that this  $\Delta t$  is not the same as in § 2.2.5.3 on page 107.

from which, after substituting equation (2.144), we can see that

$$\ddot{\gamma} + \sigma\dot{\gamma} = -(\omega_0^2\gamma + \sigma\dot{\gamma}) . \quad (2.185)$$

Substituting equations (2.183)–(2.185) into (2.181),

$$\gamma(t') = e^{\sigma\Delta t} \left[ \gamma \cos(\Delta\phi) - \frac{\dot{\gamma} + \sigma\gamma}{\omega_d} \sin(\Delta\phi) \right] = \alpha_1\gamma(t) - \alpha_2\dot{\gamma}(t) \quad (2.186a)$$

$$\dot{\gamma}(t') = e^{\sigma\Delta t} \left[ \dot{\gamma} \cos(\Delta\phi) + \frac{\omega_0^2\gamma + \sigma\dot{\gamma}}{\omega_d} \sin(\Delta\phi) \right] = \omega_0^2\alpha_2\gamma(t) + \alpha_1\dot{\gamma}(t) , \quad (2.186b)$$

where

$$\alpha_1 \triangleq e^{\sigma\Delta t} \left[ \cos(\Delta\phi) - \frac{\sigma}{\omega_d} \sin(\Delta\phi) \right] \quad \text{and} \quad \alpha_2 \triangleq e^{\sigma\Delta t} \frac{1}{\omega_d} \sin(\Delta\phi) . \quad (2.187)$$

Now, gathering the terms of equation (2.180) yields the homogenous form

$$J\ddot{\gamma}(t) + C_i\dot{\gamma}(t) + K_i\gamma(t) = 0 , \quad (2.188)$$

where

$$C_i \triangleq C + D_i\alpha_{1i} - P_i\alpha_{2i} \quad \text{and} \quad K_i \triangleq K + P_i\alpha_{1i} + \omega_0^2 D_i\alpha_{2i} , \quad (2.189)$$

with a solution of the same form as equation (2.154). Using the parametric feedback parameters  $P_i$  and  $D_i$ , the system's harmonic oscillation may be controlled as if the feedback parameters were built into the physics of the system itself.

Notice that in the absence of a time delay ( $\Delta t = 0$ ),  $\alpha_1 = 1$  and  $\alpha_2 = 0$ , so that  $C_i$  depends only on  $D_i$  and  $K_i$  only on  $P_i$ .

### 2.2.7.1 (Pseudo-) Free Parametric Harmonic Oscillation

The significance of the parametric harmonic oscillation technique is that, for example, heavily overdamped systems ( $C \gg K$ ) can be identified using methods requiring oscillations, and heavily underdamped systems ( $C \ll K$ ) can be identified more quickly by introducing appropriate damping. The harmonic oscillation is now controlled by appropriate selection of values for  $P_i$  and  $D_i$ .

Using the parametric values  $C_i$  and  $K_i$ , equations (2.143) and (2.145) yield

$$C_i = 2\hat{J}\sigma_i = 2\hat{J}\zeta_i\omega_{0i} , \quad (2.190a)$$

$$\text{and} \quad K_i = \hat{J}\omega_{0i}^2 . \quad (2.190b)$$

The estimates  $\zeta_i$  and  $\omega_{0i}$  (and therefore  $\sigma_i$ ) are determined via system identification of the response  $\gamma(t)$  (as described in the following sections). Taking any two distinct responses  $i$  and  $j$ , the mass-based system parameters can be estimated using the mass-normalised parameter identification of the  $i^{th}$  and  $j^{th}$  parametric harmonic oscillations, as follows.

The mass, viscous friction, and spring constant can be estimated as, respectively,

$$\hat{J} = \frac{(D_i\alpha_{1i} - P_i\alpha_{2i}) - (D_j\alpha_{1j} - P_j\alpha_{2j})}{2(\sigma_i - \sigma_j)} \quad (2.191a)$$

$$\text{and} \quad \hat{C} = \frac{\sigma_j(D_i\alpha_{1i} - P_i\alpha_{2i}) - \sigma_i(D_j\alpha_{1j} - P_j\alpha_{2j})}{\sigma_i - \sigma_j}. \quad (2.191b)$$

Similarly,

$$\hat{J} = \frac{(D_i\alpha_{2i}\omega_{0i}^2 + P_i\alpha_{1i}) - (D_j\alpha_{2j}\omega_{0j}^2 + P_j\alpha_{1j})}{\omega_{0i}^2 - \omega_{0j}^2} \quad (2.192a)$$

$$\text{and} \quad \hat{K} = \frac{\omega_{0j}^2(D_i\alpha_{2i}\omega_{0i}^2 + P_i\alpha_{1i}) - \omega_{0i}^2(D_j\alpha_{2j}\omega_{0j}^2 + P_j\alpha_{1j})}{\omega_{0i}^2 - \omega_{0j}^2}. \quad (2.192b)$$

If both  $D_i \neq D_j$  and  $P_i \neq P_j$ , both above estimations can be used to estimate  $J$ ,  $C$ , and  $K$ . Using the mass-based estimates, the actual damping and natural frequency can be estimated by solving equations (2.145) and (2.154) for  $\hat{\omega}_0$  and  $\hat{\zeta}$ , respectively. Note that since the damping will presumably be small (as this is a primary objective of the parametric harmonic oscillation method), the frequency  $\omega_0$  will usually be easier to estimate with good numerical confidence than will the damping  $\zeta$ . In practise, therefore, equations (2.192) are generally recommended over (2.191). However, either equation can be expressed in an alternate manner depending on which equation for the mass estimate  $\hat{J}$  is substituted when deriving the solution for  $C$  or  $K$ . In conclusion, the parametric harmonic oscillation method is shown to provide a succinct way to estimate the physical system parameters of a system when a method for estimating  $\zeta$  and  $\omega_0$  is available.

### 2.2.7.2 Forced Parametric Harmonic Oscillation

For any two excitation frequencies  $\omega_i$  and  $\omega_j$ , expressions for the mass-based system parameters may be determined as

$$\hat{J} = \frac{(P_i - R_i \cos \rho_i) - (P_j - R_j \cos \rho_j)}{\omega_i^2 - \omega_j^2}, \quad (2.193a)$$

$$\hat{C} = \frac{(R_i \sin \rho_i - D_i) \omega_j + (R_j \sin \rho_j - D_j) \omega_i}{2\omega_i \omega_j}, \quad (2.193b)$$

$$\text{and} \quad \hat{K} = \frac{(P_i - R_i \cos \rho_i) \omega_j^2 - (P_j - R_j \cos \rho_j) \omega_i^2}{\omega_i^2 - \omega_j^2}, \quad (2.193c)$$

where  $R$  and  $\rho$  are defined as per (2.179). Notice that unlike the case of free parametric oscillation, these forced parametric oscillation results are also valid when  $P_i = P_j$  and/or  $D_i = D_j$ , and furthermore circumspect the need to directly measure the frequency  $\omega_0$  or damping  $\zeta$ . If, alternatively,  $\omega_{0i}$  and  $\zeta_i$  are already known for the respective feedback values  $P_i$  and  $D_i$ , one can alternatively apply

$$\hat{J} = \frac{1}{\omega_{0i}^2 - \omega_i^2} R_i \cos \rho_i = \frac{1}{2\sigma_i \omega_i} R_i \sin \rho_i, \quad (2.194a)$$

$$\hat{C} = \frac{1}{\omega_i} R_i \sin \rho_i - D_i, \quad (2.194b)$$

$$\text{and} \quad \hat{K} = \frac{\omega_{0i}^2}{\omega_{0i}^2 - \omega_i^2} R_i \cos \rho_i - P_i \quad (2.194c)$$

to obtain the same estimations.

### 2.2.8 Analytic Signals and Describing Functions.

A *describing function* simply refers to the function describing the nonlinear sensitivity of a response to amplitude and frequency simultaneously. [308, ch.5] The Hilbert Transform is one example of identification techniques which provide estimates for the describing function, and is therefore classifiable within the group of so-called describing function “methods”. Among the kinds of systems which can be studied using the describing function method are “almost-linear” systems containing one *hard nonlinearity* like backlash, and/or algebraically nonlinear elements like nonlinear damping or compliance. The system model studied herein falls into both of these categories, suggesting the application of describing function analysis as one possible means of estimating the system nonlinearities.

Restrictions on use of this technique specify that the forcing function and/or response be periodic in nature, and that only one nonlinearity be present at once. For this reason, the Hilbert Transform is not promising for systems with multiple degrees of freedom, unless

each degree-of-freedom can be analysed independently. In situations where measurements are available at the physical location of each nonlinearity, this may be possible, but many “black-box” systems may not afford this luxury. Nonetheless, the Hilbert Transform, as a particularly straightforward implementation of describing function analysis, can be shown to be a good point of departure for the investigation of the system nonlinearities at issue, and indeed has been used to identify numerous actual systems as reported in the literature. [52, 119, 120, 145, 146]

To introduce the concept of describing function analysis, consider the definition of the complex *analytic signal* [151, § 1.13 ]<sup>68</sup>

$$\theta_a(t) = A(t)e^{j\phi(t)} , \quad (2.195)$$

where the *instantaneous amplitude*

$$A(t) \triangleq A_0 \exp \int_0^t -\sigma(t) dt \quad (2.196)$$

and the *instantaneous phase*

$$\phi(t) \triangleq \int_0^t \omega(t) dt + \phi_0 . \quad (2.197)$$

The analytic signal (2.195) may now be written

$$\theta_a(t) = A_0 e^{j\phi_0} \exp \int_0^t \{-\sigma(t) + j\omega(t)\} dt = A_0 e^{j\phi_0} \exp \int_0^t s(t) dt , \quad (2.198)$$

where the *complex angular frequency* <sup>69</sup>

$$s(t) \triangleq -\sigma(t) + j\omega(t) . \quad (2.199)$$

The analytical signal theory has its roots in complex-valued functional analysis as pioneered by Cauchy, Johann Carl Friedrich Gauss (mathematician, 1777–1855), George Green (mathematician, 1793–1841),<sup>70</sup> and, in particular, G. F. Bernhard Riemann (mathematician, 1826–1866).

In essence, using the complex-valued functional analysis introduces an additional degree-of-freedom in the identification which can then be used to capture the nonlinearity dependent upon the two dimensions of frequency and amplitude, as opposed to frequency by

<sup>68</sup>In their paper, Ruzzene *et alii* [289] confuse the nomenclature, as elaborated in [79].

<sup>69</sup>—Also known as the Laplace operator  $s$ .

<sup>70</sup>Green’s work was independently achieved by Mikhail Ostrogradski (mathematician, 1801–1861), though largely overlooked until rediscovered by Lord Kelvin in 1846.

itself (which is the restriction inherent to linear frequency analysis). This two-dimensional space is called the *Hilbert Space*, hence the connection between the Hilbert Transformation and the describing function method.

### 2.2.9 Hilbert Transform.

Describing function theory has been used extensively to determine the individual characteristics of friction, backlash and compliance [52,63,85,117–123,145,146,151,165,166,245,293,307]. A describing function is simply a single-frequency pair of sinusoids, phase-shifted in such a way as to form a pair of basis functions, and subsequently used to test the system modes and mode shapes. To this end, it is ideal for measuring either nonlinear compliance or friction in a drive train. Pseudo-linear friction and backlash elements are known to enter limit cycles when driven by harmonic signals; hence, describing functions can also be used to identify these additional properties.<sup>71</sup>

The *analytic* describing function for an excitation torque may be written as

$$\tau_a(t) = \tau_m(t) + j\tilde{\tau}_m(t), \quad (2.200)$$

where the complex component is denoted by  $j \triangleq \sqrt{-1}$ , and the effective motor torque is

$$\tau_m = \tau_m^{\mathbb{R}} + j\tau_m^{\mathbb{I}}, \quad (2.201)$$

with a Hilbert Transform  $\tilde{\tau}_m$  defined by the (temporal) convolution

$$\tilde{\tau}_m(t) \triangleq \mathcal{H}\{\tau_m(t)\} \triangleq \tau_m(t) * -\frac{1}{\pi t}. \quad (2.202)$$

Here the  $\mathbb{R}$  and  $\mathbb{I}$  superscripts denote the real and imaginary arguments, respectively. In the frequency domain, the Fourier Transform of the envelope  $-1/(\pi t)$  is simply  $j \operatorname{sgn} \omega$ ,

$$\tilde{\tau}_m(s = j\omega) = j \operatorname{sgn} \omega \tau_m(s). \quad (2.203)$$

This property provides the orthogonalisation required to make the analytic function representation a basis for the Hilbert Space.

Let the system identification excitation signal be the analytic signal  $\tau_a(t)$  given above in (2.200). In polar form this can be written according to Euler's identity

$$\tau_a(t) = A(t)e^{j\phi_\tau(t)} = A(t) [\cos \phi_\tau(t) + j \sin \phi_\tau(t)] \quad (2.204)$$

---

<sup>71</sup>Friction and backlash may be considered pseudo-linear because they are linear in steady-state operation.

so that

$$\tau_m(t) = A(t) \cos \phi_\tau(t) \quad \text{and} \quad \tilde{\tau}_m(t) = A(t) \sin \phi_\tau(t) , \quad (2.205)$$

where the *instantaneous amplitude* is

$$A(t) = \sqrt{\tau_m^2(t) + \tilde{\tau}_m^2(t)} \quad (2.206)$$

and the *instantaneous phase*

$$\phi_\tau(t) = \arctan \frac{\tilde{\tau}_m(t)}{\tau_m(t)} . \quad (2.207)$$

Note that

$$\tau_m(t) = \frac{\tau_a(t) + \tau_a^*(t)}{2} , \quad (2.208)$$

where  $\tau_a^*$  denotes the complex conjugate of  $\tau_a$ .

Now consider a generic second-order viscoelastic system

$$\ddot{\theta}_m(t) + 2\zeta\omega_0\dot{\theta}_m(t) + \omega_0^2\theta_m(t) = \frac{1}{J} \tau_m(t) \quad (2.209)$$

where:  $\theta_m(t)$  is the motor rotation (*rad/s*);

$\zeta$  is its proportional, symmetric damping;

$\omega_0$  is its undamped natural frequency (*rad/s*);

$\tau_m(t)$  is the applied system identification torque ( $N \cdot m$ ).

Assuming the Hilbert Transform is a (quasi-)linear operator for the given system,<sup>72</sup> transforming both sides of the equation of motion yields

$$\ddot{\tilde{\theta}}_m(t) + 2\zeta\omega_0\dot{\tilde{\theta}}_m(t) + \omega_0^2\tilde{\theta}_m(t) = \frac{1}{J} \tilde{\tau}_m(t) , \quad (2.210)$$

which when multiplied by  $j$  and added to (2.209) yields

$$(\ddot{\theta}_m + j\ddot{\tilde{\theta}}_m) + 2\zeta\omega_0(\dot{\theta}_m + j\dot{\tilde{\theta}}_m) + \omega_0^2(\theta_m + j\tilde{\theta}_m) = \frac{1}{J} (\tau_m + j\tilde{\tau}_m) , \quad (2.211)$$

or simply

$$\ddot{\theta}_a(t) + 2\zeta\omega_0\dot{\theta}_a(t) + \omega_0^2\theta_a(t) = \frac{1}{J} \tau_a(t) , \quad (2.212)$$

where the subscript “a” denotes the analytic signal formulation.

---

<sup>72</sup>According to Bedrosian’s Theorem [36] the Hilbert Transform is commutative with respect to derivatives, that is,  $\mathcal{H}\{\dot{\theta}\} = \dot{\mathcal{H}}\{\theta\} = \dot{\tilde{\theta}}$  when the frequencies of the commuted elements are non-overlapping, *id est*, they are sufficiently “well-spaced” in the frequency domain.

Note that the first and second derivatives of the instantaneous amplitude given in equation (2.196) are, respectively,

$$\dot{A}(t) = -\sigma A(t) \quad \text{and} \quad \ddot{A}(t) = (\sigma^2 - \dot{\sigma}) A(t). \quad (2.213)$$

The derivatives of the instantaneous phase given in equation (2.196) are somewhat simpler,

$$\dot{\phi}(t) = \omega(t) \quad \text{and} \quad \ddot{\phi}(t) = \dot{\omega}(t). \quad (2.214)$$

Combining these into equation (2.195), the derivatives of the analytic signal can be written as

$$\dot{\theta}_a(t) = -s\theta_a(t) \quad \text{and} \quad \ddot{\theta}_a(t) = (s^2 - \dot{s})\theta_a(t). \quad (2.215)$$

In other words, the Laplace operator  $s(t)$  allows the derivatives to be written in algebraic terms of the original analytic signal itself.

Substituting equations (2.195) and (2.215) into equation (2.212),

$$(s^2 + 2\zeta\omega_0 s + \omega_0^2)\theta_a(t) = \frac{1}{J}\tau_a(t). \quad (2.216)$$

The characteristic equation of this (forced) analytic oscillation is the solution of the parenthetical term:

$$s^2 + 2\zeta\omega_0 s + \omega_0^2 = \frac{\tau_a(t)}{J\theta_a(t)}. \quad (2.217)$$

The inverse of this characteristic equation is the describing function of the system—“the complex ratio of the fundamental component of the nonlinear element [response] by the input [excitation] sinusoid” [308, p.168]—and reveals that the solutions for  $s$  (the roots of the characteristic equation) in fact denote the *poles* of the system (as expected from the usual Laplace-domain representation). This also demonstrates quite clearly that the analytical signal representation formed by applying the Hilbert Transform is an apt form for performing the describing function analysis on the original system.

The square of the Laplace variable (the angular complex frequency) as defined in equation (2.199) is

$$s^2 = (\sigma + j\omega)^2 = (\sigma^2 - \omega^2) + 2j\omega, \quad (2.218)$$

and its derivative is

$$\dot{s}(t) = \dot{\sigma}(t) + j\dot{\omega}(t). \quad (2.219)$$

Substituting these terms into (2.215) and separating real and imaginary components, the

dual solution emerges as

$$\sigma^2 - \omega^2 + 2\zeta\omega_0\sigma + \omega_0^2 + \dot{\sigma} = \left\{ \frac{\tau_a(t)}{J\theta_a(t)} \right\}^{\mathbb{R}} \quad (2.220)$$

$$\text{and} \quad 2\omega(\sigma + \zeta\omega_0) + \dot{\omega} = \left\{ \frac{\tau_a(t)}{J\theta_a(t)} \right\}^{\mathbb{I}}. \quad (2.221)$$

Solving for the natural frequency and decay rate,

$$\omega_0^2 = (\sigma^2 + \omega^2) + \frac{\sigma\dot{\omega} - \dot{\sigma}\omega}{\omega} + \left[ \left\{ \frac{\tau_a(t)}{J\theta_a(t)} \right\}^{\mathbb{R}} - \frac{\sigma}{\omega} \left\{ \frac{\tau_a(t)}{J\theta_a(t)} \right\}^{\mathbb{I}} \right] \quad (2.222a)$$

and

$$\zeta\omega_0 = - \left( \sigma + \frac{\dot{\omega}}{2\omega} \right) + \frac{1}{2\omega} \left\{ \frac{\tau_a(t)}{J\theta_a(t)} \right\}^{\mathbb{I}}. \quad (2.222b)$$

Noting that  $C = 2J\zeta\omega_0$  and  $K = J\omega_0^2$ , and that equation (2.213) yields

$$\sigma(t) = - \frac{\dot{A}(t)}{A(t)}, \quad (2.223)$$

substitution into (2.222) results identically in the solution which is published by Feldman [118, eq.(3)].<sup>73</sup> When the excitation torque  $\tau_a(t) \equiv 0$ , the solution reduces to and agrees with the free response of Feldman [117, eq.(6)]. The instantaneous frequency and amplitude can thus be solved simply by using the Hilbert Transform and the first and second derivatives of the instantaneous amplitude and instantaneous phase of the free vibration response, or for that matter the forced response as well, provided the inertia  $J$  (or mass) is known. Note that the necessity of first- and second-order derivatives, however, will in practise typically increase the noise level in the estimations because of precision errors inherent to the numerical evaluation of derivatives using digital computers.

In a typical system identification procedure the inertia of the system will *not* be known *a priori*, however, so the forced vibration analysis requires further information about the system. Feldman proposes to estimate the mass (or inertia) by solving equation (2.222) for  $J$  with the assumption that  $\omega_0(t)$  varies negligibly over short time intervals. The inertia may be obtained by expressing equation (2.222) for two consecutive time instants  $t_1$  and  $t_2$  which are close enough to one another that  $\omega_0(t_2) \gtrsim \omega_0(t_1)$ , and then solving for  $J$  [118, eq.(5)]; the approximation is technically a finite difference approximation to the derivative obtained

---

<sup>73</sup>Note that Feldman uses mass  $m$  instead of inertia  $J$ , and also a different notation for the rate of decay, denoted in his paper by the variable  $h_0$ .

in the calculus when  $(t_2 - t_1) \rightarrow 0$ , however, instantaneous differentiation is discouraged by Feldman because it exacerbates machine precision errors when numerically evaluated on a digital computer.

### 2.2.9.1 Evaluation of the Instantaneous Amplitude and Phase

Solving equation (2.214) for the definition of the complex angular frequency given in (2.199),

$$s(t) = -\sigma(t) + j\omega(t) = -\frac{\dot{\theta}_a(t)}{\theta_a(t)}, \quad (2.224)$$

from which it follows that

$$\sigma(t) = \frac{\dot{\theta}_a(t)^{\mathbb{R}}}{\theta_a(t)} \quad \text{and} \quad \omega(t) = -\frac{\dot{\theta}_a(t)^{\mathbb{R}}}{\theta_a(t)}. \quad (2.225)$$

Now the expressions (2.213) for the instantaneous amplitude and (2.214) for the instantaneous phase may be written in terms of the analytical system response:

$$\dot{A}(t) = A(t) \frac{\dot{\theta}_a(t)^{\mathbb{R}}}{\theta_a(t)} \quad \text{and} \quad \ddot{A}(t) = A(t) \left( \frac{\ddot{\theta}_a(t)^{\mathbb{R}}}{\theta_a(t)} + \frac{\dot{\theta}_a(t)^{\mathbb{I}}}{\theta_a(t)^2} \right) \quad (2.226a)$$

and

$$\dot{\phi}(t) = \frac{\dot{\theta}_a(t)^{\mathbb{R}}}{\theta_a(t)} \quad \text{and} \quad \ddot{\phi}(t) = \frac{\ddot{\theta}_a(t)^{\mathbb{I}}}{\theta_a(t)} - 2 \frac{\dot{\theta}_a(t)^{\mathbb{R}}}{\theta_a(t)} \frac{\dot{\theta}_a(t)^{\mathbb{I}}}{\theta_a(t)}. \quad (2.226b)$$

With the appropriate substitutions now the frequency and damping of eqs. (2.222) can be expressed purely in terms of the analytic signal representation of the system response and excitation, and their derivatives.

### 2.2.9.2 Application to Linear and Quasi-Linear Second-Order Systems

When the frequency and damping are constant (linear and time-invariant), or slowly-varying (quasi-linear), the instantaneous radial velocity (more commonly called the *rate of (amplitudinal) decay*) can be written in the familiar way,

$$\sigma(t) = \zeta\omega_0, \quad (2.227)$$

and the instantaneous phase as

$$\phi(t) = \omega_d t + \phi_0, \quad (2.228)$$

where the instantaneous angular velocity  $\omega(t) \equiv \omega_d$  is now the (constant) damped natural frequency. The resulting time-invariant, second-order oscillation can thus be expressed as

$$\theta_a(t) = A_0 e^{j\phi_0} e^{\int_0^t s(t) dt} = A_0 e^{-\zeta\omega_0 t} e^{j(\omega_d t + \phi_0)}, \quad (2.229)$$

which has the familiar form for linear second-order systems. For this kind of system, equations (2.222) may be simplified to read

$$\omega_0^2 = (\sigma^2 + \omega_d^2) + \left[ \left\{ \frac{\tau_a(t)}{J\theta_a(t)} \right\}^{\mathbb{R}} - \frac{\sigma}{\omega} \left\{ \frac{\tau_a(t)}{J\theta_a(t)} \right\}^{\mathbb{I}} \right] \quad (2.230a)$$

and

$$\zeta\omega_0 = \frac{1}{4\omega_d} \left\{ \frac{\tau_a(t)}{J\theta_a(t)} \right\}^{\mathbb{I}}. \quad (2.230b)$$

## 2.2.10 Wavelet Transformation.

Authors M. Ruzzene *et alii* [289] present in their article a very useful bridge from the Hilbert Transform method for vibration analysis to the Wavelet Transform method. The conceptual relationship between the two is made in a refreshingly lucid manner.<sup>74</sup> The independent article by Huang Dishan [89] is also a useful guide bridging the Hilbert and wavelet transforms. Together with the article by Ruzzene, a formidable signal processing method is presented.

As mentioned before, the wavelet transform is an attractive alternative to the Hilbert Transform because it provides inherent temporal localisation which the latter method is incapable of doing. The result is a comparable analysis, with the additional (and significant) advantages of reduced noise and true multimodal (or multiple degree-of-freedom) analysis capability.

### 2.2.10.1 The Morlet Wavelet

The Morlet Wavelet is used as the basis function for the considered wavelet transformation. Morlet's Wavelet is a specific instance of the general function

$$g(t) \triangleq A \exp \{ - (\alpha t^2 + \beta t + \gamma) \}, \quad (2.231)$$

---

<sup>74</sup>Nonetheless some small technical *errata* exist; the reader should be especially cautious regarding interpretation of their nomenclature, as the authors confuse the distinction between instantaneous phase and instantaneous angular velocity in a number of places throughout the paper. Please refer to [79] for a complete discussion.

where  $A$ ,  $\alpha$ ,  $\beta$ , and  $\gamma$  are some constants. When this function is first translated (time-shifted) by some amount  $b$ , and then dilated (scaled) by some amount  $a$ , we can write

$$\begin{aligned} g\left(\frac{t-b}{a}\right) &= A \exp\left\{-\left[\alpha\left(\frac{t-b}{a}\right)^2 + \beta\left(\frac{t-b}{a}\right) + \gamma\right]\right\} \\ &= A \exp\left\{-\left[\alpha\left(\frac{t}{a}\right)^2 + \left(\beta - \frac{2\alpha b}{a}\right)\left(\frac{t}{a}\right) + \left(\alpha\frac{b^2}{a^2} - \beta\frac{b}{a} + \gamma\right)\right]\right\}. \end{aligned} \quad (2.232)$$

Selection of the values  $a = 1$  and  $b = 0$  suppress the dilation and translation properties of the wavelet, respectively, yielding the so-called *mother wavelet*. Both Ruzzene *et alii* [289, eq.(2)] and Dishan [89, eqs.(8), (10)] use the Morlet Wavelet mother obtained by first substituting the parameter values

$$A = 1/\sqrt{a}, \quad \alpha = 1/2, \quad \beta = -j\omega_c, \quad \gamma = 0 \quad (2.233)$$

into equation (2.232), yielding

$$g\left(\frac{t-b}{a}\right) = \frac{1}{\sqrt{a}} \exp - \left[ \left\{ \frac{1}{2} \left(\frac{t}{a}\right)^2 - \left(j\omega_c + \frac{b}{a}\right) \frac{t}{a} + \left(j\omega_c + \frac{b}{2a}\right) \frac{b}{a} \right\} \right], \quad (2.234)$$

and then setting  $a = 1$  and  $b = 0$  to ultimately produce

$$g(t) = e^{j\omega_c t} e^{-t^2/2}, \quad (2.235)$$

where  $\omega_c$  is the *centre frequency* of the wavelet.<sup>75</sup>

### 2.2.10.2 The Morlet Wavelet Transformation

The wavelet transformation under consideration is proportional to the convolution of this *analysing wavelet*  $g((t-b)/a)$  with some signal  $x(t)$ .<sup>76</sup> As demonstrated by Ruzzene *et alii* [289, eq.(3)], this convolution may be performed either directly or, alternatively, via the convolution theorem of the Fourier Transform, which defines the (inner product) transform pair (*exempli gratia* [273, eq.(12.0.9)])

$$\text{Conv}(x, g) = \langle x(t), g(t) \rangle = x(t) \star g(t) \iff X(\omega) \cdot G(\omega). \quad (2.236)$$

---

<sup>75</sup>Ruzzene *et alii* use the symbol  $\omega_0$  for the centre frequency, which is avoided here to prevent confusion with the undamped natural frequency of the system. Also note that the value of  $A$  used by Ruzzene (as defined in (2.233)) differs from that used by Dishan in [89, eq.(11)].

<sup>76</sup>Note that Dishan uses the variables  $h$  and  $f$ , respectively, in place of  $g$  and  $x$ .

Furthermore, the correlation theorem of the Fourier Transform defines the transform pair (*exempli gratia* [273, eq.(12.0.10)])<sup>77</sup>

$$\text{Corr}(x, g) \iff X(\omega) \cdot G(-\omega) = X(\omega) \cdot G^*(\omega), \quad (2.237)$$

which estimates the similarity of the frequency content between  $X(\omega)$  and  $G(\omega)$ . Since the wavelet has a Gaussian window (embodied by its exponential envelope), the frequency correlation is also localised in time. This dual time-frequency localisation is the essential usefulness provided by signal processing using the wavelet transformation.

The wavelet transformation can thus be written in terms of the inverse Fourier Transform of the spectra  $X(\omega)$  and  $G^*(\omega)$ :<sup>78</sup>

$$W \triangleq \mathcal{F}^{-1} \{ \mathcal{F} \{x(t)\} \cdot \mathcal{F}^* \{g(t)\} \} = \mathcal{F}^{-1} \{ X(\omega) G^*(\omega) \} \quad (2.238)$$

$$= \frac{1}{\sqrt{2\pi}} \int_{-\infty}^{+\infty} X(\omega) \cdot G^*(\omega) e^{j\omega t} d\omega, \quad (2.239)$$

where  $G^*$  is the complex conjugate of the Fourier Transform

$$G(\omega) \triangleq \frac{1}{\sqrt{2\pi}} \int_{-\infty}^{+\infty} g\left(\frac{t-b}{a}\right) e^{-j\omega t} dt. \quad (2.240)$$

Using the Gaussian Fourier pair [151, §1.7.1] [313, #15.75]

$$\int_{-\infty}^{+\infty} A \exp \{ - (px^2 + qx + r) \} dx = A \sqrt{\frac{\pi}{p}} \exp \left\{ \frac{q^2 - 4pr}{4p} \right\} \quad (2.241)$$

and substituting equation (2.232) into (2.240), it can be shown that

$$G(\omega) = \frac{aA}{\sqrt{2\alpha}} \exp \left\{ \frac{(\beta + j\omega a)^2}{4\alpha} \right\} \exp \{ -(\gamma + j\omega b) \}. \quad (2.242)$$

The conjugate of the Fourier Transform of equation (2.234) is now

$$G^*(\omega) \triangleq \sqrt{a} \exp \left\{ -\frac{1}{2}(a\omega - \omega_c)^2 \right\} e^{+j\omega b}. \quad (2.243)$$

---

<sup>77</sup>The equality on the right-hand side is possible because  $x$  is real-valued and  $g$  is composed of an even real component and an odd imaginary component. [273, §12.0]

<sup>78</sup>We use the *symmetric* form of the Fourier Transform definition, which premultiplies both the *forward* and *inverse* transformations by a factor of  $1/\sqrt{2\pi}$ , *exempli gratia* [318, eq.(4.3.12)].

In tandem, equation (2.238) becomes

$$W = \sqrt{\frac{a}{2\pi}} \int_{-\infty}^{+\infty} X(\omega) \exp \left\{ -\frac{1}{2} (a\omega - \omega_c)^2 \right\} \exp \{j\omega(t+b)\} d\omega, \quad (2.244)$$

where the signal spectrum  $X(\omega)$  is typically computed via the fast Fourier Transform algorithm.<sup>79</sup>

### 2.2.11 Wavelet Transformation of an Analytic Signal

When the mathematical form of the signal  $x(t)$  under analysis is known (or assumed), a closed analytical form of the wavelet transformation may be derived by evaluating the (correlation) convolution integral directly: [289, eq.(1)] [89, eq.(1)]

$$W = \int_{-\infty}^{+\infty} x(t) g \left( \frac{t-b}{a} \right) dt. \quad (2.245)$$

However, generally the Fourier Transform of the conjugate is not necessarily equivalent to the complex conjugate of the Fourier Transform.

Dishan shows that the wavelet transformation can be used to construct a passband of Hilbert Transformers across the frequency range of interest. Ruzzene *et alii* show that, alternatively, the wavelet transformation can be used to “focus in” on frequencies of interest, by tuning the wavelet centre frequency  $\omega_c$ . The necessary stipulation is that the dilation

$$a \longrightarrow \omega_c/\omega(t) = \omega_c/\dot{\phi}(t). \quad (2.246)$$

Observing that the wavelet transformation

$$\begin{aligned} W &= \sqrt{ak}(t) \exp \left\{ -\frac{1}{2} (a\omega_d - \omega_c)^2 \right\} \exp \{j\omega_d(t+b)\} \\ &= \sqrt{ak}(t) \exp \left\{ -\frac{1}{2} (a\dot{\phi} - \omega_c)^2 \right\} \exp \{j\dot{\phi}(t+b)\}, \end{aligned} \quad (2.247)$$

now the dilation tuning described by equation (2.246) is evident. In practise, a first iteration of equation (2.247) with some dilation  $a$  will yield a fair estimate of  $\phi$  for the frequency with the highest correlation for that initial value of  $a$ , which can be used in (2.246) above to iterate  $a$ . In practise, only two numerical iterations are generally needed to focus the

---

<sup>79</sup>Note that this result differs from [289, eq.(3)], which neglects the exponential term  $e^{j\omega t}$  inherent to the inverse Fourier Transform, the scaling factor  $\sqrt{a}$ , and also the factor of  $\sqrt{2\pi}$  from one or the other of the transform  $G(\omega)$  or  $W$  (these factors are, however, evident in Dishan [89, eq.(11)]). More importantly, all references to  $G(\omega)$  in the original work by Ruzzene *et alii* should have the relevant exponential *halved*, in accordance with other references on the Morlet wavelet.

dilation almost precisely onto the nearest frequency.

The phase relation is given by

$$\angle W = \dot{\phi}(t) (t + b) = \omega_d(t + b) , \quad (2.248)$$

and is equal to  $\omega_d t$  when the time shift  $b = 0$ . Thus the time derivative of the phase angle of the wavelet yields the damped natural frequency  $\omega_d$  of the mode focused by dilation parameter  $a$ . The magnitude of this mode is then simply

$$A(t) = \frac{1}{\sqrt{a}} |W| = \sqrt{\frac{\dot{\phi}}{\omega_c}} |W| = \sqrt{\frac{\omega_d}{\omega_c}} |W| = \frac{1}{\sqrt{\omega_c}} |W| \frac{d}{dt} \angle W . \quad (2.249)$$

The negative slope of the natural logarithm of amplitude  $k(t)$  is then equal to the decay rate  $\sigma$ . Once the decay rate and damped natural frequency are known, the damping ratio  $\zeta$  and undamped modal frequency  $\omega_0$  may be determined via the relations given in (2.143) and (2.150), analogous to the Hilbert Transform analysis.

### 2.3 Summary

Each method as presented has its own set of particular strengths (and, of course, shortcomings too). The experiences of the author in this regard are summarised here.

The logarithmic decrement method is the simplest in concept, and is familiar to researchers working in the area of vibration analysis and control. It does not require any time-frequency transformations, instead extracting significant information from the displacement history alone. The log decrement method has been extended for the first time to asymmetric friction, but can only be used to process free vibrations (of underdamped systems). Also, a minimum number of oscillations are necessary and the procedure is sensitive to noise. The log decrement can furthermore only be used for linear, second-order systems, or ones with very slowly-varying parameters.

The Hilbert Transform is the simplest analysis to compute, algorithmically speaking, but does involve a more complicated approach. It has the advantage of being able to handle quasi-linear systems with some amplitudinal dependence, as well as the usual frequency dependence. It can also be applied to systems under forced harmonic oscillation. Unfortunately, the need for derivatives of the Hilbert Transform in the analysis tends to worsen the signal-to-noise ratio of the information extracted from the system displacement history.

The work of Ruzzene *et alii*, together with that of Dishan, bridge the relationship between the Hilbert Transform and Morlet Wavelet Transformation in a manner most useful for the modal analysis of linearly separable, multimodal oscillatory systems. Nonlinear vis-

cous damping and frequency, or distributed linear frequencies and associated modal damping, are both made possible in a computationally fast manner using the Hilbert Transform, or alternatively in a clean, noiseless manner of signal processing by the wavelet transformation. In spite of some minor discrepancies within the literature cited, both methods are shown to be very relevant and indeed useful.

The wavelet transformation offers the best of all possible solutions in the following sense: it has all the advantages of the Hilbert Transform method, with none of the drawbacks. The analysis is relatively noise-free and accurate, and can be used in parallel to extract multi-modal information from the same response data. If there is any disadvantage then it is the relatively high computation intensity required to perform the analysis. Still, on modern hardware (*id est*, a digital signal processor) this issue is not a hampering concern. The wavelet analysis further shows promise of being able to distinguish either asymmetric friction or kinetic and viscous damping, although this is not shown in this thesis; the concept involves examining the periodic “flutter” evident in the envelope and phase of the transformed oscillation signal.

The choice of which analysis to use obviously depends on the extent of nonlinearity present in the system, but if the system is quasi-linear, then a case can be made to apply the logarithmic decrement if asymmetry is of interest, which otherwise is not known to be possible with the other methods.

Lastly, and most importantly, the parametric harmonic oscillation method allows one to obtain the kind of response that is necessary to apply any of the discussed analytical techniques. Using PD feedback, it has been shown that even in the presence of a time delay in the feedback loop, it is easily possible to produce any kind of harmonic oscillation which may be deemed necessary to produce representative response data for subsequent analysis.

Although not all nonlinearities are examined in full—dynamic friction effects and impact backlash, though modeled heavily, are not evaluated together with the servo friction and nonlinear compliance identification methods presented—nonetheless this work represents solid ground from which to extend studies in the direction of identifying, and eventually, controlling these machine tool drive train nonlinearities as they act in concert to confound machining precision and accuracy between, and across, tooling runs.

## Chapter 3

### **Experimental Apparata.**

The experiment is designed to assess the validity and usefulness of asymmetric viscous and kinetic friction identification as predicted by theory and simulation. To verify the extended logarithmic decrement method in conjunction with the technique of parametric harmonic oscillation, two systems known to have measurable degrees of both viscous and kinetic friction were used for the experimentation. One system moves rotationally and the other translationally, allowing the techniques to be proved for the two fundamental types of machine motion. More importantly, these two motions are both manifest in common machine tools, providing a germane link to the study of machine tool dynamics. The first system studied was the mechanical positioning test bed which will be used for continued work in the area of nonlinearity identification and control of machine tool spindles and cutting tools; the second system was the inverted pendulum used for mechatronics education at Rensselaer, and represents the motions present in machine tool workpiece positioning tables.

#### **3.1 Hardware.**

The mechanical positioning test bed is a unique device allowing the user to independently adjust kinetic friction, backlash and compliance in the rotating spindle between a motor and an end effector. The nonlinearities can be arbitrarily combined to mimick the dynamics of a number of realistic machine tools. The test bed was designed with this purpose in mind, and therefore has parameter variability similar to friction in common servo systems, backlash in common gear mechanisms, and compliance in common linkages and effectors. The spindle can rotate continuously and can be used to control any of a variety of attachments; one previous experiment used the test bed to examine the effect of drive nonlinearities on the precise positioning of a flexible beam affixed to the end of the spindle. [82].

The inverted pendulum system is basically a stick-balancing device originally constructed for educational purposes. The pendulum swings about a pivot point attached to a cart which can move back and forth on a linear track. A DC motor applies a linear force to the cart to maintain a central displacement whilst keeping the stick from falling over.

Both systems use optical encoders to measure displacement with excellent accuracy and as little noise as possible.

### 3.1.1 Equipment.

Two dynamic systems were investigated to verify the parametric harmonic oscillation method for system identification, one with a rotating shaft, and the other with a linear track. Either system represents a typical machine motion, and either is known to exhibit asymmetric friction characteristics, as inferred by the observation of drift in the displacement output when excited with a zero-mean sinusoidal input. The mechanical positioning test bed shown in Figure 1.7 is the rotational system used; the other is a newer system, an inverted pendulum shown in Figure 3.1.1.

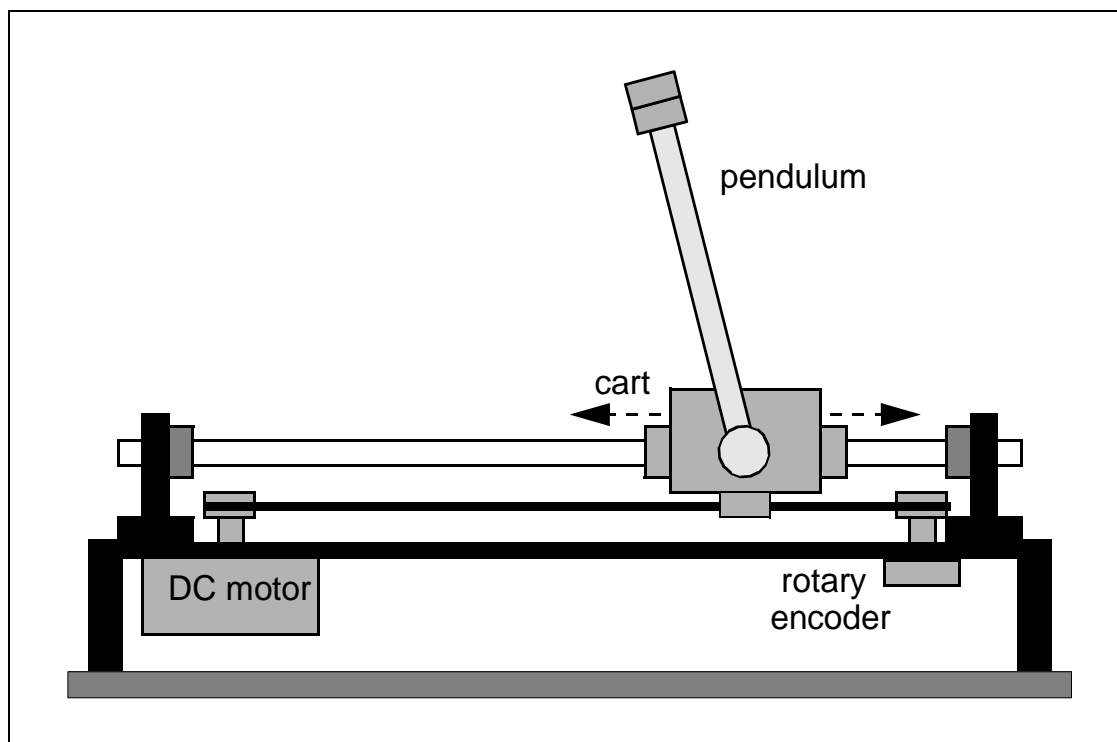


Figure 3.1: The linear inverted pendulum system at Rensselaer.

The inverted pendulum system rides on a cart which traverses a linear track, as shown, and is described in detail in [355].

### 3.1.2 Hardware Interface.

In order to acquire the oscillation response data and also provide the real-time PD feedback required for the parametric harmonic oscillation method, a data acquisition and control hardware interface must be interposed between the computer providing the data storage and system feedback capabilities and the systems under investigation. The equipment consists of an IBM<sup>®</sup>-compatible minicomputer (the so-called *personal computer*, or

*PC*), containing a quadrature decoder board and a data acquisition card, and a low-pass analogue filter bank used for high-frequency noise reduction and anti-aliasing. The particular computer used for the experiments presented herein was a GateWay 2000<sup>®</sup> Pentium II, the decoder card a Technology 80<sup>®</sup> TE5312B, the data acquisition card a National Instruments<sup>®</sup> Lab-PC+, and the filter bank an Avens Signal Equipment<sup>®</sup> model 4000.

### 3.1.3 Signal Wiring.

Appropriate wiring and auxiliary hardware must be used between the systems and the computer interface. The PMI ServoDisc motors' current, in both the pendulum and test bed systems, is modulated by PMI Servo amplifiers, carried by Gaussian-shielded heavy-gauge wiring. The wiring must be shielded to reduce noise from the 40-kHz switching action of the amplifiers, and it must be grounded at the amplifier end *only*, to prevent turning the shield into a noise antenna by way of creating a ground loop. Optical encoders for both the test bed and the pendulum system can be directly connected to the decoder board's quadrature inputs. The motor command and current feedback signals are each passed through the low-pass filter to prevent high-frequency noise and signal aliasing, respectively. All analogue signals are passed through coaxial cables to preserve a high signal-to-noise ratio. A wiring diagramme showing all these connections is shown in Figure 3.1.3.

Figure 3.2: Equipment Wiring Diagramme.

## 3.2 Software.

### 3.2.1 Data Acquisition Interface.

Data acquisition code was written to acquire real-time data from the dynamic systems under investigation. This software runs on the computer and coordinates the data

acquisition and feedback control. The code itself is described in detail in Appendix C.

### **3.2.2 Simulation.**

Simulation code was developed in collaboration with Jeongmin Lee (M.S.) to provide a means for comparing the actual test bed motion with the analytical model structure used in the identification procedures. The simulator integrates the model structure for a given set of parameter values, producing a simulated time response for the displacement and velocity of each of the three subsystems “A”, “B”, and “C” of the test bed.

The simulation has some important abilities which can assist in the development of a working model of the system and/or evaluation of control system designs to mitigate the system nonlinearities. One is the ability to “lock” into place any or all of the three subsystems, so that they cannot move. Another is to excite subsystem “A”, the backlash arm, with an arbitrary forcing function; this applied torque can be a function of the system states, and thus be used to simulate a feedback control system based on displacements and velocities. The simulation also allows specification of a backlash function which can include impact dynamics based on system states; this could be as simple as a coefficient-of-restitution impact, or as comprehensive as the impact dynamics described by this thesis in §2.1.2.

The simulation constitutes a complete model of the mechanical positioning test bed and is thus a very useful tool for verifying identification and control algorithms developed for that system. It also can simulate various more generic motions like forced or unforced harmonic oscillations with single or multiple degrees of freedom.

## Chapter 4

### Method of Procedure.

#### 4.1 System Identification Methodology.

The overarching philosophy for identifying the system properly is to subdivide the overall system into as many decoupled, independently-acting components as possible. Such separability will always occur at the couplings between the various subsystems, if and when it is possible. In some cases only a “lumped” identification will be possible, though this need not necessarily compromise the controllability of the identified system. Nonetheless, a detailed understanding of each nonlinear element in the drive will naturally aid the process.

At relatively high steady velocities, the elements of backlash and stiction are eliminated, and the lumped motor and shaft dynamics can be identified as a second-order system with linear friction (kinetic + viscous). A simple step response method can be used to identify the second-order characteristics, with a low-frequency, DC-biased square-wave identification signal; the overshoot and speed-of-response to the square wave will determine the damping and damped natural frequency of the system, and the data can be fit to determine the system inertia and fundamental compliance. The viscous and kinetic frictions can be found by a simple linear fit to the obtained data at different steady-state velocities. By subsequently reducing the DC bias so that the modulated speed at its minimum is very near zero, but still positive, the static friction and critical Stribeck velocity may be determined. At this point the dynamic friction and rigid-body dynamics are both fully determined. Variations in the identified parameters may be fit to a periodic function to check whether there is any correlation between the rotational angle and friction force, which in many machines will often be the case. [234]

The method of parametric harmonic oscillation described in §2.2.7 has an advantage over producing a fit with the step response data, because oscillations can be produced for even overdamped systems; oscillating the system allows estimation of the frequency as well as the damping.

The rising static and presliding frictions can be determined from a purely static test where the applied torque is ramped up in a quasi-steady-state manner. The breakaway force and rate of ramping are used to determine the rising friction time constant, and refine the static friction estimate. The full dynamic friction model is then available.

Backlash can be determined by applying some constant torque and measuring the relative shaft displacements. The nonlinear backlash and compliance characteristics may be determined using a describing function method like the Hilbert Transform over a range

of frequencies and amplitudes.

If the motor can be decoupled from the shaft then it is possible to separately identify the motor and shaft dynamics. Note, however, that if there is no backlash then such a procedure would be moot. The most challenging aspect to separate friction and dynamics identification for the motor and shaft will be when a small backlash gapwidth exists which cannot be removed for the sake of identification. In this case, either a lumped model approximation must be used, or identification attempted with very small signal amplitudes, which under some circumstances may be meaningless in terms of the macroscopic system response.

What is interesting and useful about the lumped system is that with careful analysis, certain parameters can be rendered trivial under particular operating conditions. For example, when the system is at rest, all the velocity terms cancel and what is left is a static deflection and force problem, which can be easily evaluated to render the static terms. Similar simplifications emerge with sufficiently large steady-state speeds. These may be subsequently used to facilitate further identification of the remaining parameters of import. Once rough estimates of the system parameters are obtained, the machine can be brought “on-line” and an on-going, adaptive estimation may be implemented in the background, to constantly monitor and track the machine’s operating characteristics. The identification procedure should be simple and automatable to ease its implementation on the machine tool shop floor, and it must be accurate enough to provide marked improvements in tooling quality and machine health monitoring.

Substituting the obtained values into the full model, the parameters can be updated on-line during regular operation using an adaptive strategy. This now allows a comprehensive control strategy to be developed using the full model in situations where the subsystems are dynamically coupled during normal use. The decoupling strategy of the initial, off-line identification phase now acts as a baseline against which to compare the adaptively-measured machine characteristics, providing the possibility of machine health monitoring as well as improved controllability.

## 4.2 Procedural Motivation.

The reason for identifying macroscopic friction effects is the immediate applicability to industrial servosystems. Before microscopic effects like the dynamic friction models discussed at length in §2.1.1 can be of use, the macroscopic frictional behaviour should be understood. Similarly, the parametrically oscillated responses described allow for (multimodal) compliance estimation in addition to viscous and/or kinetic friction estimation. Between the methods expounded in this thesis, the only “missing” nonlinearity is that of

backlash. However, backlash in and of itself is somewhat less challenging to study than friction, because the dynamics are relatively straightforward to estimate in the absence of other nonlinearities. Since a number of new contributions are made for friction identification within the present work, other nonlinearities are surveyed with mathematical detail, but not investigated experimentally. This provides a solid departure point for future contributions in those areas.

### 4.3 Verification of the Proposed Identification Techniques.

Aiding the verification procedures were previous analyses of the two systems studied. For both systems, the motor inertias and frictions were published in the manufacturer's specifications. [263,264] The pendulum system mass was measured using a scale, and the friction in that system was observed to be almost completely dominated by the motor friction, implying that little difference should be found between the pendulum system identification with and without the cart mass. The test bed inertias and frictions were both computed using the material properties and geometries, and also identified by Prakah-Asante *et alii* [271] using the auto-regressive moving average with exogenous input (ARMAX) method. These previous results provided a solid set of information for testing the validity of the proposed identification method.

Furthermore, the identification techniques proposed were first proved in simulation, with very good results. The experimental data would therefore be anticipated to have an identification accuracy on the order of, but certainly not better than, that afforded by the simulation results (about five per cent).

## Chapter 5

### Experimental Results.

In most cases, only about 4-12 oscillation peaks were available per oscillation for estimation using the log decrement method. (A representative oscillation is shown in Figure 5.1.) The more accurate results are therefore obtained for lightly-damped parametric oscillations, highlighting again the usefulness of derivative feedback for reducing the system damping. Generally speaking, the more oscillations, the better the log decrement estimation. On the other hand, the method works fairly well even with the minimum of two to four oscillation peaks.

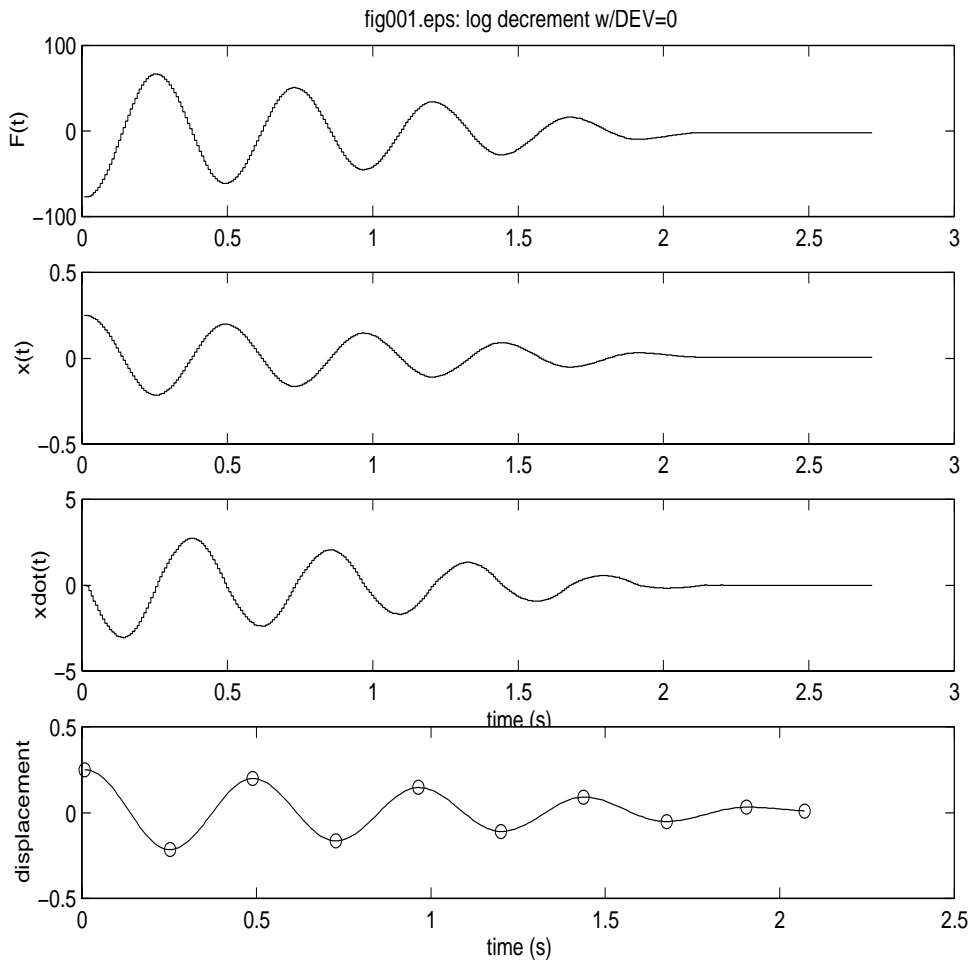


Figure 5.1: A Representative Parametric Harmonic Oscillation.

Table 5.1 shows the simulation parameters identified using the proposed methods on

systems with various combinations of viscous and kinetic friction. Since the estimation of parameters using the simulated response has an accuracy only on the order of about five per cent, this would be the anticipated baseline accuracy for analysis using experimental data. Unlike some other methods, the logarithmic decrement method uses only a fraction of the information available in the data (the peak times and values). This has the advantage of allowing parameter estimation in the presence of noise, however this is traded off for a moderate loss in accuracy. It is nonetheless also one of the few methods available for determining the friction asymmetry in such a straightforward manner.

When the estimation for  $K$  is corrected with the information that there should be no spring force in the system, the mass estimate is greatly improved (this is how the pendulum system information in Table 5.3 on page 138 is corrected). This shows that quality of the mass estimation depends directly on the quality of the frequency and damping data measured during oscillation. In practise, the frequency estimation is quite accurately accomplished by examining the zero- (or mean-) crossings of the oscillation; it is the damping estimates determined by the log decrement method which generally exhibit the larger of the estimation errors.

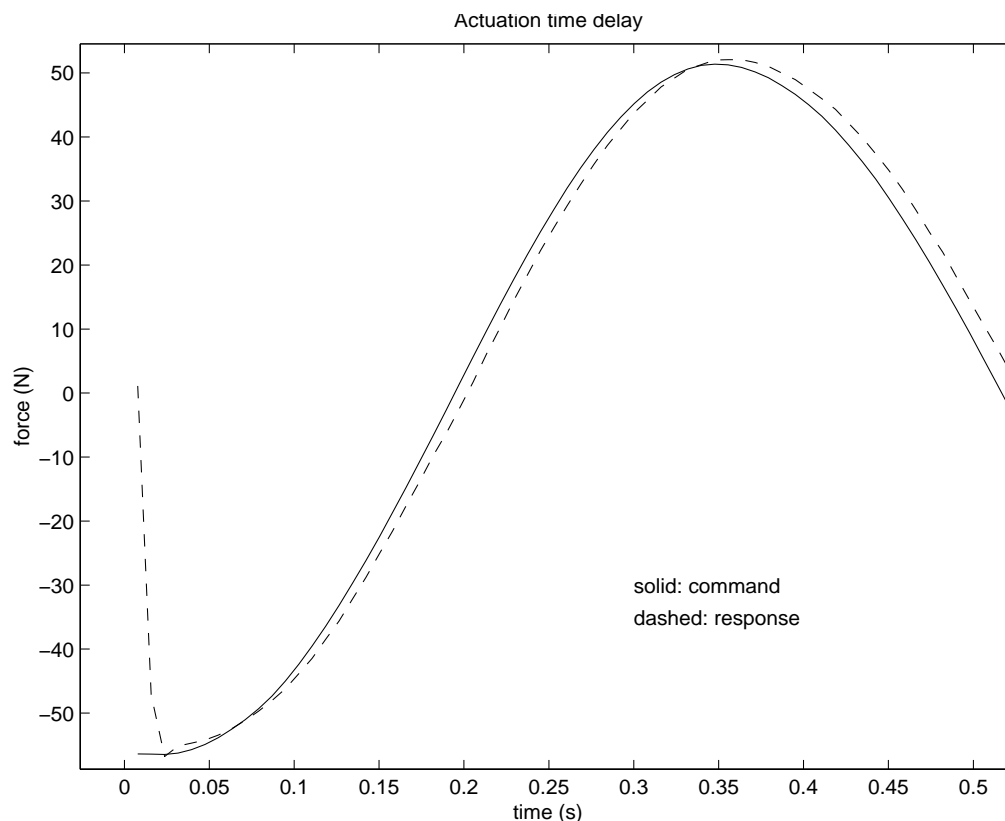


Figure 5.2: Time Delay in the PHO Feedback Loop.

Table 5.1: Simulation: Log-Decrement Identification.

	$\omega_0$ (rad/s)	$\bar{f}_k \pm \Delta f_k$ (Nm)	$\bar{c} \pm \Delta c$ (Nms/rad)
simulated	3.162	$0.2000 \pm 0.5000$	$0.4000 \pm 0.3000$
estimated	3.277	$0.2148 \pm 0.5370$	$0.4140 \pm 0.3109$
% error	3.6%	$7.4\% \pm 7.4\%$	$3.5\% \pm 3.6\%$
simulated	4.000	$0.2000 \pm 0.5000$	$0.3000 \pm 0.4000$
estimated	4.129	$0.2130 \pm 0.5326$	$0.3095 \pm 0.4129$
% error	3.2%	$6.5\% \pm 6.5\%$	$3.2\% \pm 3.2\%$
simulated	4.000	$0.0700 \pm 0.1300$	$0.3000 \pm 0.0000$
estimated	4.023	$0.0715 \pm 0.1352$	$0.3015 \pm 0.0002$
% error	0.6%	$2.1\% \pm 4.0\%$	$0.5\% \pm 0.2\%$
simulated	4.000	$2.0000 \pm 2.0000$	$0.6250 \pm 0.1250$
estimated	4.024	$2.0098 \pm 2.0316$	$0.6155 \pm 0.1134$
% error	0.6%	$0.5\% \pm 1.6\%$	$1.5\% \pm 9.3\%$
simulated	2.000	$0.0000 \pm 0.0000$	$0.4000 \pm 0.3000$
estimated	2.094	$0.0000 \pm 0.0000$	$0.4184 \pm 0.3141$
% error	4.7%	$0.0\% \pm 0.0\%$	$4.6\% \pm 4.7\%$
simulated	2.000	$0.2000 \pm 0.0000$	$0.5000 \pm 0.0000$
estimated	2.015	$0.2030 \pm 0.0001$	$0.5034 \pm 0.0000$
% error	0.8%	$1.5\% \pm 0.1\%$	$0.7\% \pm 0.0\%$
simulated	4.000	$6.2500 \pm 5.7500$	$0.6250 \pm 0.1250$
estimated	4.026	$6.3193 \pm 5.7178$	$0.6293 \pm 0.1288$
% error	0.7%	$1.1\% \pm 0.6\%$	$0.7\% \pm 3.0\%$
simulated	4.000	$0.4000 \pm 0.3000$	$0.1000 \pm 0.0000$
estimated	4.114	$0.4213 \pm 0.2836$	$0.1013 \pm 0.0008$
% error	2.9%	$5.3\% \pm 5.5\%$	$1.3\% \pm 0.8\%$

In the actual parametric harmonic oscillation implementation, there is a measurable time delay between the PD feedback command and the actual PD current fed back through the motor, as seen in Figure 5.2 on the page before. Here both the constant time delay is visible, as well as the initial slew required for the amplifier and motor to rise to the initial command current.

The viscous friction estimation suffers in the experimental situation when there is a time delay in the PD-feedback loop used for parametric harmonic oscillation. The severity

of this problem depends on the length of the delay relative to the period of each harmonic oscillation. Because larger system masses produce slower oscillations, it is typically the systems with smaller mass which exhibit this adverse effect. The estimation error due to this problem is evident in the friction values shown for the test bed in Table 5.2 on page 137. Generally, it may therefore be advisable to add some constant mass to the system during identification, and then subtract this known value from the final estimation, in order to circumvent the time delay effect, unless the time delay can be measured directly and compensated for. Mass estimation is, fortunately, relatively insensitive to the inaccuracies in the friction estimation, and depends more significantly on the frequency estimation. The kinetic friction estimation is independent of any system dynamics, and is therefore also unaffected by the presence of a time delay in the feedback loop.

Lastly, it is worth noting that an interesting phenomenon occurs when the kinetic friction is high and the viscous friction is low. When the maximum oscillation velocity is such that the maximum viscous friction is always less than the kinetic friction, it is possible to oscillate the system with negative damping and still achieve a stable response. In such a situation, the parametric damping coefficient  $C_i < 0$ , and the envelope of the oscillation will have an accelerated slope, rather than a decelerated slope as for an exponential decay (the envelope will be bullet shaped!).<sup>80</sup> For systems with a high kinetic friction this means that even negative damping can be used to obtain the system parameters. Normally, in the absence of kinetic friction, negative damping causes exponential instability, and therefore negative damping should be used with caution. However, if the kinetic friction is high, then negative damping will be the only way to obtain sufficient oscillation for successful identification using the parametric harmonic oscillation method.

### 5.1 System ID Results from the Mechanical Positioning Test Bed.

The mechanical positioning test bed was identified in three sections corresponding to its three nonlinear junctions. Since the test bed was fairly well characterised by previous calculations and identification on the part of Walczyk [367] and Prakah-Asante *et alii* [271], this system provides a good test of the proposed system identification methods against expected results.

The results shown in Table 5.2 were obtained before the time-delay compensation was developed and included towards the very end of the research for this thesis. Therefore the nefarious effect of the time delay is still present in the data, and clearly seen to decrease as the system inertia increases. It can also be seen clearly that the time delay, which is

---

<sup>80</sup>—See Figure 5.3 for an example of this balance between negative viscous damping yet positive kinetic damping.

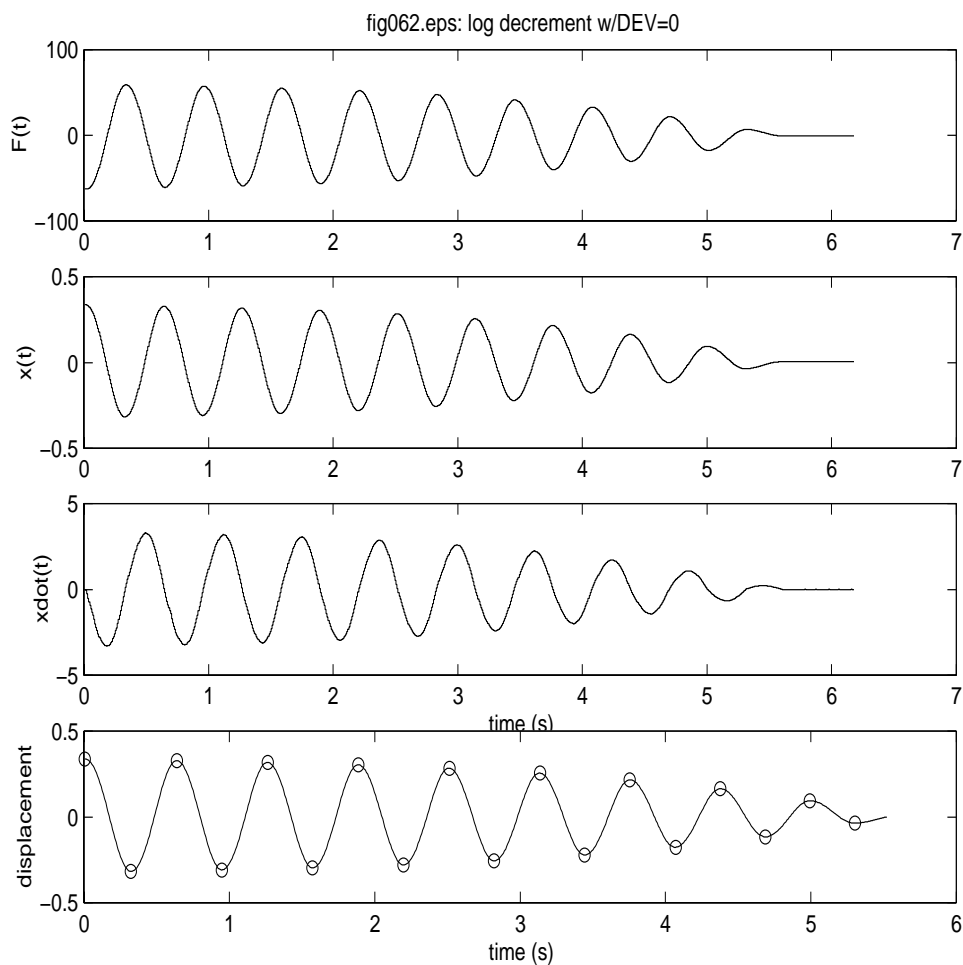


Figure 5.3: Negative Viscous Damping in the Presence of Kinetic Friction.

interpreted as a phase lag by the system identification, gives the identification algorithm the false impression that the friction is greater than it really is, as if the system were slowed by additional friction forces which in fact are not present. These reasons account for the discrepancies in the friction estimation, and it is evident that the time delay has a significantly confounding effect on the accuracy of viscous friction estimation.

Since three separate sections are identified independently, the differences in parameter estimations between successive parts of the machine yield the information about each part itself, in sequence. The identification results were in this regard very good, however bodies A and B each exhibited some offset from the expected value as published by Walczyk and later by Prakah-Asante. The reason for this is because the published values in both of those previous references were made for the test bed system prior to the addition of an important modification made (by Walczyk) after those publications were already released.

To understand this, a brief synopsis of the history of the test bed is in order: the test bed as originally built contained an imbalance in the lower and upper backlash arms (see Walczyk, [367, dwg.32 & 35]), which caused the test bed to wobble perilously when the spindle was rotated at high speeds; to remedy this situation, the backlash arms were modified to include counterbalances, although the new calculations were not published (until now—see Appendix C). The difference between the identification results here and the published values correspond neatly with the previously undocumented modifications, as shown in the data. Presumably, the modifications had not yet been made between the time of Walczyk’s thesis in 1991 and Prakah-Asante’s initial journal submission in 1992, both of which document the original test bed configuration, without the counterbalance improvements. The reader should be made aware of this when referencing the aforementioned works for comparison against the parameters estimated by the techniques in this thesis.

Table 5.2: Test Bed System Identification (without time-delay compensation).  
(Published values from [264], [367], and [271].)

	A only		A + B		A + B + C	
	published	measured	published	measured	published	measured
$\Delta t$ (ms)	13.77	12.24	–	10.76	–	10.63
$J$ (Nms <sup>2</sup> )	0.0115355	0.01194	0.0150626	0.01744	0.0339399	0.03136
$k$ (Nm)	0 (nil)	0.001034	0 (nil)	0.1492	nil (0)	-0.01168
$\bar{c}$ (Nms)	0.0007457	0.002355	0.0018657	0.001233	0.0029857	0.004514
$\Delta c$ (Ns/m)	–	0.0002458	–	0.000848	–	0.000858
$\bar{f}_k$ (Nm)	0.109456	-0.07233	0.1416169	-0.1921	0.1711679	-0.1968
$\Delta f_k$ (Nm)	–	0.008622	–	0.0243	–	0.005588
$\bar{f}_s$ (Nm)	–	0.6098	–	-0.5152	–	-2.49
$\Delta f_s$ (Nm)	–	0.08057	–	0.5208	–	0.5377

## 5.2 System ID Results from the Inverted Pendulum System.

The inverted pendulum system was identified in two stages, once with the driving motor by itself, and a second time with the linear cart attached. One reason for this was to verify the suspicion that the dominant frictional component is not in the linear track, but in the driving motor. Because less friction information was previously available on this system (particularly for the linear bearings), performing two tests in this manner afforded the possibility of better evaluating the system identification accuracy by comparing the

results against empirically observed differences between the system with and without the linear cart included.

Table 5.3: Pendulum System Identification (corrected for  $K = 0$ ).  
(Published values from [263] and [355].)

	motor only			motor + cart		
	published	measured	error	published	measured	error
$\Delta t$ (ms)	10.84	9.2838	14%	–	10.548	–
$m$ (kg)	1.4250	1.6466	16%	2.3900	2.4223	1.4%
$k$ (N/m)	0 (nil)	2.8790	9.3%	0 (nil)	+8.9827	–
$\bar{c}$ (Ns/m)	0.3656	0.3727	1.9%	–	0.8043	–
$\Delta c$ (Ns/m)	0 (nil)	-0.0096	–	–	+0.3268	–
$\bar{f}_k$ (N)	3.7330	-5.1676	38%	–	7.9340	–
$\Delta f_k$ (N)	0 (nil)	1.5043	–	–	+0.7163	–
$\bar{f}_s$ (N)	–	8.3029	–	–	20.2141	–
$\Delta f_s$ (N)	–	4.3673	–	–	10.9196	–

## Chapter 6

### **Discussion and Conclusions.**

Nonlinear drive train modeling, identification and control is a complicated, yet important subject for understanding the potential improvements to machine tool control under faster operating conditions with higher precision demands. By first developing a comprehensive model of these nonlinearities and then focusing on the firstmost significant aspect of the same, the parametric harmonic oscillation method and extended logarithmic decrement method together provide a powerful and easy-to-use means for identifying asymmetric kinetic and viscous friction in drive trains.

Parametric harmonic oscillation can be applied to any system which must be oscillated for identification purposes. Even forced parametric harmonic oscillation provides a means for redundancy in the response measurements which is not possible using the traditional sine sweep or white noise identification approaches by themselves; however, parametric harmonic oscillation can be used to complement these traditional methods without any direct modification to said methods themselves. By including the realistic effect of a time delay in the PD feedback path, pseudo-free harmonic oscillations can also be analysed accurately using traditional techniques, even for overdamped systems not previously analysable using these methods. The new method is thus a versatile asset to the set of traditional system identification tools.

The extended logarithmic decrement method extends a commonly-used traditional technique to include the important aspect of asymmetric friction identification. The method is well-known to most researchers and industry professionals dealing with vibration control, and can therefore be straightforwardly applied by most researchers in the field. Although the new log decrement method can only handle a single degree of freedom at a time, with a sensor displacement at each rigid body it is possible to use the difference in displacements of successive bodies to identify the friction and compliance for each degree of freedom in turn.

The Hilbert Transform and wavelet transformation methods as published in the literature [89, 117, 118, 121–123, 146, 165, 208, 235, 237, 289] have also been verified as useful methods for damping and frequency estimation. The advantage of these methods over the logarithmic decrement method is that they can handle multimodal rather than unimodal frequencies in-between successive rigid bodies. Insofar as multiple modes may be termed generalised coordinates, thereby representing unique degrees of freedom, these methods are thus also capable of analysing multiple degree-of-freedom systems. Furthermore, the back-

ground research presented herein shows that these nonlinear methods are also promising candidates for asymmetric friction identification.

The new methods are developed in theoretical detail and proven in simulation. Experimental results corroborate preceding analyses and verify the applicability and usefulness of these methods on systems representing typical machine tool dynamics. Asymmetric friction identification represents a significant contribution to industry, in the sense that precise servo control requires a reasonable knowledge of asymmetric friction. The author knows of no prior work which identifies asymmetric friction in a single identification manoeuvre. The parametric harmonic oscillation method can be used as a front end for a number of traditional identification procedures requiring either free or forced harmonic oscillation data to work. This new method now allows any nonlinear, multi-degree-of-freedom second-order system (not merely underdamped ones) to be analysed using the popular methods.

The work performed on friction identification therefore embodies one of the crucial first steps in identifying the combined action of friction, compliance and backlash in machine tools. Identification of the other nonlinearities will be aided by this cornerstone of research now completed by this thesis.

## 6.1 Recommended Future Work.

The work expounded upon in this thesis constitutes a solid base of departure for future work. A number of different areas of groundwork have been laid, including:

- historical literature review and comprehensive bibliography
- comprehensive description of the current state of the art
- comprehensive analytical modeling of drive train nonlinearities
- direct connection to machine tool drive nonlinearities
- comprehensive and flexible simulation of mechanical positioning test bed
- corroboration of analytically predicted test bed and pendulum system parameters
- a clear set of options outlined for continuation of this research

The subject under study is extensive in scope. Many interesting possibilities lend themselves naturally to continuation of the present work, including:

- extension of the Hilbert Transform and/or wavelet transformation method to simultaneous and/or asymmetric viscous and kinetic friction ID

- on-line, adaptive identification and tracking of asymmetric kinetic and viscous friction
- prove identification on an actual machine tool feed drive mechanism performing a standard circular countour test
- fully automate the identification procedure
- track parameter drifts adaptively and on-line during normal operation
- improve the machine precision and accuracy during use via feedback control
- monitor the general “health” of the machine’s dynamic components
- delineation of a methodology for machine tool classification according to drive train nonlinearity and operational function

## References.

- [1] George G. Adams. Self-excited oscillations in sliding with a constant friction coefficient. In Cudney [74], pages 1171–1177.
- [2] John Adams and Shahram Payandeh. Methods for low-velocity friction compensation: Theory and experimental study. *J. Rob. Sys.*, 13(6):391–404, 1996.
- [3] M. J. Adams. Theoretical and computational methods in friction, lubrication and wear. *Tribology Int.*, 29(8):625–626, 1996.
- [4] Josef Adolfsson and Jeanette Karlsén, editors. *Proceedings of the 6<sup>th</sup> UK Mechatronics Forum International Conference (Mechatronics '98)*, New York City, September 9-11, 1998. UK Mechatronics Forum Centre for Intelligent Automation, Pergamon Press.
- [5] Amit Ailon, Rogelio Lozano-Leal, and Michael Gil'. Point-to-point regulation of a robot with flexible joints including electrical effects of actuator dynamics. *IEEE Trans. Auto. Control*, 42(4):559–564, April 1997.
- [6] R. Aimar *et alii*. Experiments on robust friction compensation: the inverted pendulum case. In *Proc. Amer. Control Conf. ACC* [12], pages 3303–3305.
- [7] Gürsel Alıcı and Ron W. Daniel. Static friction effects during hard-on-hard contact tasks and their implications for manipulator design. *Int. J. Robot. Res.*, 13(6):508–520, December 1994.
- [8] D. M. Alter and Tsu-Chin Tsao. Control of linear motors for machine tool drives: Design and implementation of  $h_\infty$  optimal feedback control. *ASME J. Dyn. Sys., Meas., and Control*, 118:649–656, December 1996.
- [9] David M. Alter and Tsu-Chin Tsao. Control of linear motors for machine tool feed drives: Experimental investigation of optimal feedforward tracking control. *ASME J. Dyn. Sys., Meas., and Control*, 120:137–142, March 1998.
- [10] Jose Alvarez-Ramírez, Ruben Garrido, and Ricardo Femat. Control of systems with friction. *Phys. Rev.-E*, 51(6):6235–6238, June 1995.
- [11] American Control Council. *Proc. Amer. Control Conf. ACC*. American Control Council, June 1993.
- [12] American Control Council. *Proc. Amer. Control Conf. ACC*. American Control Council, June 1995.
- [13] American Society of Mechanical Engineers. *Japan-USA Symp. on Flex. Auto.*, 1996.
- [14] Jayesh Amin, Bernard Friedland, and Avraham Harnoy. Implementation of a friction estimation and compensation technique. *IEEE Control Sys. Mag.*, 17(4):71–76, August 1997. See also Friedland, Harnoy *et alii* [129–131, 153, 155].

- [15] Guillaume Amontons. De la resistance causée dans les machines. *Mém. de l'Acad. Roy. Sci. de Paris*, pages 206–222, 1699.
- [16] J. R. Anderson and A. A. Ferri. Behavior of a single-degree-of-freedom system with a generalized friction law. *J. Sound and Vib.*, 140(2):287–304, 1990.
- [17] Brian Armstrong[-Hélouvry]. Friction: Experimental determination, modeling and compensation. In *J. IEEE Trans. Rob. Auto.* [169], pages 1422–1427. See also Armstrong-Hélouvry & Dupont [100].
- [18] Brian Armstrong-Hélouvry. Stick-slip arising from stribek friction. In *J. IEEE Trans. Rob. Auto.* [170], pages 1377–1382. See also Armstrong-Hélouvry & Dupont [100].
- [19] Brian Armstrong-Hélouvry. *Control of Machines with Friction*. Kluwer Academic Publishers Group, Dordrecht, Nederland, 1991. See also Armstrong-Hélouvry & Dupont [100].
- [20] Brian Armstrong-Hélouvry. Stick slip and control in low-speed motion. *IEEE Trans. Auto. Control*, 38(10):1483–1496, October 1993. See also Armstrong-Hélouvry & Dupont [100].
- [21] Brian Armstrong[-Hélouvry] and Bimal Amin. PID control in the presence of static friction: A comparison of algebraic and describing function analysis. *Automatica*, 32(5):679–692, 1996. See also Armstrong-Hélouvry & Dupont [100].
- [22] Brian Armstrong-Hélouvry and Pierre [E.] Dupont. Friction modeling for control. In *Proc. Amer. Control Conf. ACC* [11], pages 1905–1909. See also Armstrong-Hélouvry & Dupont [100].
- [23] Brian Armstrong-Hélouvry, Pierre [E.] Dupont, and Carlos Canudas de Wit. A survey of models, analysis tools and compensation methods for the control of machines with friction. *Automatica*, 30(7):1083–1138, 1994. Survey paper; see also Armstrong, Dupont & Canudas de Wit [58–62, 98–105].
- [24] Steven Ashley. High-speed machining goes mainstream. *Mech. Eng. Mag.*, 117(5):56–61, May 1995.
- [25] Steven Ashley. Getting a hold on mechatronics. *Mech. Eng. Mag.*, 119(5):60–63, May 1997.
- [26] Karl J[ohan] Åström and Björn Wittenmark. *Adaptive Control*. Addison-Wesley Series in Electrical and Computer Engineering: Control Engineering. Addison-Wesley, Reading, Massachusetts, second edition, 1995. See also Åström, Wittenmark, *et alii* [61, 62, 248, 323].
- [27] Abílio Azenha and J. A. Tenreiro Machado. Variable structure control of robots with nonlinear friction and backlash at the joints. In *J. IEEE Trans. Rob. Auto.* [174], pages 366–371.
- [28] Er-Wei Bai. Parametrization and adaptive compensation of friction forces. *Int. J. Adaptive Control Sig. Proc.*, 11:21–31, February 1997.

- [29] Avram Bar-Cohen. Mechanical engineering in the information age. *Mech. Eng. Mag.*, 117(12):64–70, December 1995.
- [30] V. M. Baranov, E. M. Kudryavtsev, and G. A. Sarychev. Modelling of the parameters of acoustic emission under sliding friction of solids. *Wear*, 203:125–133, 1997.
- [31] Alan A. Barhorst. Modeling contact/impact in hybrid-parameter multiple body mechanical system—extensions for higher-order continuum models. In Cudney [74], pages 99–107.
- [32] Alan A. Barhorst. Contact/impact in hybrid parameter multiple body mechanical systems— extensions for higher-order continuum models. *ASME J. Dyn. Sys., Meas., and Control*, 120:142–144, March 1998.
- [33] Niels Bay. Testing of friction and lubrication in cold forging and extrusion. Rensselær Dept. of ME, AE & M graduate colloquium series, October 11, 1996.
- [34] D. S. Bayard. Statistical plant set estimation using Schröder-phased multisinusoidal input design. In *Proc. Amer. Control Conf. ACC*, FA12, pages 2988–2995. American Control Council, American Control Council, 1992.
- [35] A. Baz and Jong-Tai Hong. Adaptive control of flexible structures using modal positive position feedback. *Int. J. Adaptive Control Sig. Proc.*, 11:231–253, May 1997.
- [36] E. Bedrosian. A product theorem for Hilbert transforms. *Proc. IEEE*, 51(5):868–869, May 1963.
- [37] C. J. Begley and L. N. Virgin. Impact response and the influence of friction. *J. Sound and Vib.*, 211(5):801–818, April 16, 1998.
- [38] R. Bell and M. Burdekin. Dynamic behaviour of plain slideways. *Proc. IMechE*, 181 i(8):169–184, 1966–1967.
- [39] R. Bell and M. Burdekin. A study of the stick-slip motion of machine tool feed drives. *Proc. IMechE*, 184 i(30):543–560, 1969–1970.
- [40] M. T. Bengisu and A. Akay. Relation of dry-friction to surface roughness. *J. Eng. Mech.*, 119:18–25, January 1997.
- [41] Edward J. Berger, Charles M. Krousgrill, and Farshid Sadeghi. Stability of sliding in a system excited by a rough moving surface. In Cudney [74], pages 553–563.
- [42] Raymond J. Black. Self-excited multi-mode vibrations of aircraft brakes with nonlinear negative damping. In Cudney [74], pages 1241–1245.
- [43] K. A. Blencoe and J. A. Williams. Friction of sliding surfaces carrying boundary films. *Wear*, 203–204:722–729, 1997.
- [44] Li Chun Bo and D. Pavelescu. The friction-speed relationship and its influence on the critical velocity of stick-slip motion. *Wear*, 82:277–289, 1982.

- [45] Mary L. Boas. *Mathematical Methods in the Physical Sciences*. John Wiley & Sons, New York–London–Sydney, second edition, 1983.
- [46] B. Bona and M. Indri. Friction compensation and robustness issues in force/position controlled manipulators. *IEE Proc. Control Th. App.*, 142(6):569–574, November 1995.
- [47] F. P. Bowden and D[avid] Tabor. The sliding of metals, frictional fluctuations, and vibrations of moving parts. *Engineer*, 168:214, 1939.
- [48] F. P. Bowden and D[avid] Tabor. *Friction and Lubrication*. Methuen's Monographs on Physical Subjects. Methuen & Co., London, revised edition, 1967.
- [49] Carl B. Boyer. *A History of Mathematics*. John Wiley & Sons, New York–London–Sydney, second edition, 1991.
- [50] G[ünther] Brandenburg and U. Schäfer. Influence of adaptive compensation of simultaneously acting backlash and Coulomb friction in elastic two-mass systems of robots and machine tools. In *J. IEEE Proc. Control App.*, WA–4–5, pages 1–3, New York City, 1989. Institute of Electrical and Electronics Engineers, Institute of Electrical and Electronics Engineers.
- [51] J. A. Brandon and K. J. H. Shareef. On the applicability of modal and response representations in the dynamic analysis of machine tool spindle bearing systems. *Proc. IMechE*, 205:139–145, 1991.
- [52] Simon [G.] Braun, Michæl Feldman, and Asif Grushkevich. Identification of electromagnetic damping force for a rotating system. In *14<sup>th</sup> International Modal Analysis Conference (IMAC)* [311], pages 1–5. See also Feldman *et alii* [117–119, 121–123, 145, 146].
- [53] N[eil] Brown and R[obert] M. Parkin. A mechatronics system for the improvement of surface form in planed and moulded timber components. In Adolfsson and Karlsén [4], pages 173–179.
- [54] E. Budak and Y. Altıntaş. Analytical prediction of chatter stability in milling—Part I: General formulation. *ASME J. Dyn. Sys., Meas., and Control*, 120:22–30, March 1998.
- [55] E. Budak and Y. Altıntaş. Analytical prediction of chatter stability in milling—Part II: Application of the general formulation to common milling systems. *ASME J. Dyn. Sys., Meas., and Control*, 120:31–36, March 1998.
- [56] C. Sidney Burrus, Ramesh A. Gopinath, and Haitao Guo. *An Introduction to Wavelets and Wavelet Transforms: A Primer*. Prentice-Hall, Upper Saddle River, New Jersey, 1998.
- [57] Florian Cajori. *A History of Physics*. MacMillan, New York City, second edition, 1929.

- [58] C[arlos] Canudas de Wit and P[ablo] Lischinsky. Adaptive friction compensation with partially known dynamic friction model. *Int. J. Adaptive Control Sig. Proc.*, 11:65–80, February 1997. See also Canudas de Wit *et alii* [23].
- [59] C[arlos] Canudas de Wit and V. Seront. Robust adaptive friction compensation. In *J. IEEE Trans. Rob. Auto.* [170], pages 1383–1388. See also Canudas de Wit *et alii* [23].
- [60] C[arlos] Canudas de Wit *et alii*. Adaptive friction compensation in robot manipulators: Low velocities. *Int. J. Robot. Res.*, 10(3):189–199, June 1991. See also Canudas de Wit *et alii* [23].
- [61] C[arlos] Canudas de Wit *et alii*. Dynamic friction models and control design. In *Proc. Amer. Control Conf. ACC* [11], pages 1920–1926. See also Canudas de Wit, Åström *et alii* [23, 26, 62, 248, 323].
- [62] C[arlos] Canudas de Wit *et alii*. A new model for control of systems with friction. *IEEE Trans. Auto. Control*, 40(3):419–425, March 1995. See also Canudas de Wit, Åström *et alii* [23, 26, 61, 248, 323].
- [63] Danilo Capecchi, Renato Masiani, and Fabrizio Vastroni. Dynamical behaviour of hysteretic systems under harmonic forces. In Cudney [74], pages 799–806.
- [64] Nabil G. Chalhoub and Xiaoying Zhang. Modeling and control of backlash in the drive mechanism of a radially rotating compliant beam. *ASME J. Dyn. Sys., Meas., and Control*, 118:158–161, March 1996.
- [65] B. V. Chapnik, G. R. Heppler, and J. D. Aplevich. Modeling impact on a one-link flexible robotic arm. *J. IEEE Trans. Rob. Auto.*, 7(4):479–488, August 1991.
- [66] J. Constance. Intelligent processing of materials. *Mech. Eng. Mag.*, pages 37–40, November 1991.
- [67] Charles Augustin Coulomb. Théorie des machines simples, en ayant égard au frottement de leur parties, et à la roideur du cordages. *Mém. des Math. Phys.*, 10:161–342, 1785.
- [68] J. J. Craig. *Adaptive Control of Mechanical Manipulators*. Addison-Wesley, Reading, Massachusetts, 1987.
- [69] Kevin C. Craig. Mechatronics at Rensselær: Integration through design. In *ASME Int. Conf. on Comp. and Eng.*, pages 247–252, New York City, August 1992. American Society of Mechanical Engineers, American Society of Mechanical Engineers. See also Craig *et alii* [77–82, 147, 355, 367, 372, 378].
- [70] Kevin C. Craig. Mechatronic system design at Rensselær. In Edward Carryer, editor, *Workshop on Mechatronics Education*, Stanford, California, July 1994. Stanford University. See also Craig *et alii* [77–82, 147, 355, 367, 372, 378].
- [71] Kevin C. Craig and Julian A. de Marchi. Mechatronic system design at Rensselær. In Memiş Acar, editor, *Int. Conf. Recent Advances in Mechatronics*, volume 1 of

- Mechatronics Education and Training*, pages 293–302, Istanbul, Turkey, August 1995. Boğaziçi Üniversitesi. See also Craig, de Marchi *et alii* [77–82, 147, 355, 367, 372, 378].
- [72] Kevin C. Craig and Julian A. de Marchi. Mechatronic system design at Rensselær. *J. Comp. App. Eng. Ed.*, 4(1):67–78, 1996. See also Craig, de Marchi *et alii* [77–82, 147, 355, 367, 372, 378].
- [73] Kevin [C.] Craig *et alii*. NSF grant no. 9354913: Graduate research traineeships for mechatronics in machine tool research. Rensselær Dept. of ME, AE & M proposal to the NSF, 1993. This proposal originated the NSF funding which supported the research conducted under the auspices of this thesis. See also Craig *et alii* [77–82, 147, 355, 367, 372, 378].
- [74] H. H. Cudney, editor. *ASME Proc. Eng. Tech.*, New York City, September 1995. American Society of Mechanical Engineers, American Society of Mechanical Engineers.
- [75] Philip R. Dahl. Solid friction damping of mechanical vibrations. *AIAA J.*, 14(12):1675–1682, December 1976.
- [76] Phillip R. Dahl. A solid friction model. Unclassified military document, Defense Logistics Agency, Defense Technical Information Center (DTIC), Cameron Station, Alexandria, VA 22304-6145 U.S.A., May 1968. Contract No. AF04695-67-C-0158, Report No. TOR-0158(3107-18)-1.
- [77] Julian A. de Marchi and Kevin C. Craig. Asymmetric viscous and kinetic friction identification via the extended logarithmic decrement method. *ASME J. Dyn. Sys., Meas., and Control*. An article submitted in 1998 for publication; see also de Marchi, Craig *et alii* [69–73, 147, 355, 367, 372, 378].
- [78] Julian A. de Marchi and Kevin C. Craig. Comments on: “Natural frequencies and dampings identification using wavelet transform: Application to real data”. *J. Mech. Sys. and Sig. Proc.* A letter with commentary submitted in 1998 to the editor for publication; see also de Marchi, Craig *et alii* [69–73, 147, 355, 367, 372, 378].
- [79] Julian A. de Marchi and Kevin C. Craig. Identification of arbitrarily overdamped second-order systems via parametric harmonic oscillation. *ASME J. Dyn. Sys., Meas., and Control*. An article submitted in 1998 for publication; see also de Marchi, Craig *et alii* [69–73, 147, 355, 367, 372, 378].
- [80] Julian A. de Marchi and Kevin C. Craig. A model for backlash and compliance with viscoelastic impact effects. *J. Mech. Sys. and Sig. Proc.* An article submitted in 1998 for publication; see also de Marchi, Craig *et alii* [69–73, 147, 355, 367, 372, 378].
- [81] Julian A. de Marchi and Kevin C. Craig. Mechatronics in machine tools. In Parkin *et al.* [257]. See also de Marchi, Craig *et alii* [69–73, 147, 355, 367, 372, 378].
- [82] Julian A. de Marchi, Jun Ma, and Kevin C. Craig. Experimental degradation of flexible beam control in the presence of drive-train non-linearities. In Li [207]. See also de Marchi, Craig *et alii* [69–73, 147, 355, 367, 372, 378].

- [83] Dan Deitz. Educating engineers for the digital age. *Mech. Eng. Mag.*, 117(9):77–80, September 1995. See also Kuttner & Deitz [199].
- [84] Dan Deitz. Impact codes for the virtual laboratory. *Mech. Eng. Mag.*, 117(5):66–70, May 1995. See also Kuttner & Deitz [199].
- [85] J[acob] P[ieter] den Hartog. Forced vibrations with combined Coulomb and viscous friction. *ASME Trans.*, 53:107–115, 1930.
- [86] J[acob] P[ieter] den Hartog. *Mechanical Vibrations*. Dover Publications, New York City, fourth edition, 1985. Originally published in 1934 by McGraw-Hill, reprinted by Dover.
- [87] John W[arren] Dettman. *Applied Complex Variables*. Dover Publications, New York City, first edition, 1984. Originally published by Macmillan in 1965, reprinted by Dover.
- [88] Warren R. DeVries. A dynamic model for simulating orthogonal turning. Internal report, Rensselaer Polytechnic Institute, Troy, New York, April 1987. As part of a consultation to the General Motors Research Laboratories, Engineering Mechanics Department.
- [89] Huang Dishan. A wavelet-based algorithm for the Hilbert transform. *J. Mech. Sys. and Sig. Proc.*, 10(2):125–134, 1996.
- [90] S. J. Dokos. Sliding friction under extreme pressures. *J. App. Mech.*, 13:A148–A156, 1946.
- [91] Richard C. Dorf. *Modern Control Systems*. Addison-Wesley Series in Electrical and Computer Engineering: Control Engineering. Addison-Wesley, Reading, Massachusetts, fifth edition, 1990.
- [92] U. Dorndorf, V. S. B. Kiridena, and P. M. Ferreira. Optimal budgeting of quasistatic machine tool errors. *American Society of Mechanical Engineers Journal Engineer for Ind.*, 116:42–53, February 1994.
- [93] John C. Doyle, Bruce A. Francis, and Allen R. Tannenbaum. *Feedback Control Theory*. MacMillan, New York City, 1992.
- [94] S. J. Drew and B. J. Stone. Impact excitation of torsional vibration systems. In *13<sup>th</sup> International Modal Analysis Conference (IMAC)* [310], pages 1432–1436.
- [95] Hongliu Du and Satish S. Nair. Low-velocity friction compensation. *IEEE Control Sys. Mag.*, 18(2):61–69, April 1998.
- [96] S[teven] Dubowsky and F. Freudenstein. Dynamic analysis of mechanical systems with clearances—Part I: Formation of dynamic model. *American Society of Mechanical Engineers Journal Engineer for Ind.*, 93:305–309, February 1971. See also Morel & Dubowsky [230].

- [97] Steven Dubowsky and F. Freudenstein. Dynamic analysis of mechanical systems with clearances—Part II: Dynamic response. *American Society of Mechanical Engineers Journal Engineer for Ind.*, 93:310–316, February 1971. See also Morel & Dubowsky [230].
- [98] Pierre E. Dupont. Friction modeling in dynamic robot simulation. In *J. IEEE Trans. Rob. Auto.* [170], pages 1370–1376. See also Dupont *et alii* [22, 23].
- [99] Pierre [E.] Dupont. Avoiding stick-slip through PD control. *IEEE Trans. Auto. Control*, 39(5):1094–1097, May 1994. See also Dupont *et alii* [22, 23].
- [100] Pierre [E.] Dupont and Brian Armstrong-Hélouvry. Compensation techniques for servos with friction. In *Proc. Amer. Control Conf. ACC* [11], pages 1915–1919. See also Armstrong-Hélouvry *et alii* [17–21, 23, 100].
- [101] Pierre [E.] Dupont and D. Bapna. Stability of sliding frictional surfaces with varying normal force. *J. Vib. Acoustics*, 116:237–242, April 1994. See also Dupont *et alii* [22, 23].
- [102] Pierre E. Dupont and Eric P. Dunlap. Friction modeling and control in boundary lubrication. In *Proc. Amer. Control Conf. ACC* [11], pages 1910–1914. See also Dupont *et alii* [22, 23].
- [103] Pierre E. Dupont and Prakash S. Kasturi. Experimental investigation of frictional dynamics associated with normal load. In Cudney [74], pages 1109–1115. See also Dupont *et alii* [22, 23].
- [104] Pierre [E.] Dupont and Ann Stokes. Semi-active control of friction dampers. In *J. IEEE Proc. Dec. Control* [172], pages 3331–3336. See also Dupont *et alii* [22, 23].
- [105] Pierre E. Dupont and Serge P. Yamajako. Stability of rigid-body dynamics with sliding frictional contacts. In *J. IEEE Trans. Rob. Auto.* [174], pages 378–384. See also Dupont *et alii* [22, 23].
- [106] Naomi E[izabeth] Ehrich[-Leonard]. An investigation of control strategies for friction compensation. Master’s thesis, The University of Maryland at College Park, College Park, Maryland, 1991. P. S. Krishnaprasad, advisor.
- [107] Naomi [Elizabeth] Ehrich-Leonard and P. S. Krishnaprasad. Adaptive friction compensation for bi-directional low-velocity position tracking. In *J. IEEE Proc. Dec. Control* [171], pages 267–273.
- [108] M. R. Elhami and D. J. Brookfield. Sequential identification of Coulomb and viscous friction in robot drives. *Automatica*, 33(3):393–401, 1997.
- [109] M. R. Elhami and D. J. Brookfield. Sequential identification of coulomb and viscous friction in robot drives. *Automatica*, 33(3):393–401, March 1998.
- [110] P. Eschmann. *Ball and Roller Bearings Theory, Design and Application*. John Wiley & Sons, New York–London–Sydney, second edition, 1985.

- [111] Leonhard Euler. Sur le frottement des corps solides. *Histoire de l'Acad. Roy. Sci. et Belles Lettres*, page 122, 1750.
- [112] Brian [F.] Feeny. A nonsmooth Coulomb friction oscillator. *IEEE Trans. Auto. Control*, 37(10):1609–1612, October 1992. See also Liang & Feeny [208, 209].
- [113] B[rian] F. Feeny and J.-W. Liang. Phase-space reconstructions of stick-slip systems. In Cudney [74], pages 1049–1059. See also Liang & Feeny [208].
- [114] B[rian] F. Feeny and J.-W. Liang. A decrement method for the simultaneous estimation of Coulomb and viscous friction. *J. Sound and Vib.*, 195:149–154, August 8, 1996.
- [115] B[rian] F. Feeny and F. C. Moon. Autocorrelation on symbol dynamics for a chaotic dry-friction oscillator. *Phys. Letters–A*, 141(8/9):397–400, November 20, 1989. See also Liang & Feeny [208, 209].
- [116] B[rian F.] Feeny and F. C. Moon. Chaos in a forced dry-friction oscillator: Experiments and numerical modeling. *J. Sound and Vib.*, 170(3):303–323, 1994. See also Liang & Feeny [208, 209].
- [117] Michæl Feldman. Non-linear system vibration analysis using Hilbert transform – [Part] I: Free vibration analysis method "FREEVIB". *J. Mech. Sys. and Sig. Proc.*, 8(2):119–127, 1994. See also Gottlieb *et alii* [145, 146].
- [118] Michæl Feldman. Non-linear system vibration analysis using Hilbert transform – [Part] II: Forced vibration analysis method "FORCEVIB". *J. Mech. Sys. and Sig. Proc.*, 8(3):309–318, 1994. See also Gottlieb *et alii* [145, 146].
- [119] Michæl Feldman and Yakov Ben-Haim. Experimental investigation of lap-joint dynamics. In *13<sup>th</sup> International Modal Analysis Conference (IMAC)* [310], pages 1826–1831. See also Gottlieb *et alii* [145, 146] and Freund & Ben-Haim [128].
- [120] Michæl Feldman and Simon [G.] Braun. Nonlinear vibration analysis of a robot arm. In *12<sup>th</sup> International Modal Analysis Conference (IMAC)* [309], pages 1692–1697. See also Gottlieb *et alii* [145, 146].
- [121] Michæl Feldman and Simon [G.] Braun. Identification of non-linear system parameters via the instantaneous frequency: Application of the Hilbert transform and wigner-ville techniques. In *13<sup>th</sup> International Modal Analysis Conference (IMAC)* [310], pages 637–642. See also Gottlieb *et alii* [145, 146].
- [122] Michæl Feldman and Simon [G.] Braun. Non-linear spring and damping forces estimation during free vibration. In Cudney [74], pages 1241–1248. See also Gottlieb *et alii* [145, 146].
- [123] Michæl Feldman and Simon [G.] Braun. Processing for instantaneous frequency of two-component signal: Use of the Hilbert transform. In *13<sup>th</sup> International Modal Analysis Conference (IMAC)* [310], pages 776–781. See also Gottlieb *et alii* [145, 146].

- [124] G. Ferretti, G. Magnani, and A. Zavala Río. Impact modeling and control for industrial manipulators. *IEEE Control Sys. Mag.*, 18(4):65–71, August 1998.
- [125] Gene F. Franklin, J. David Powell, and Michael L. Workman. *Digital Control of Dynamic Systems*. Addison-Wesley Series in Electrical and Computer Engineering: Control Engineering. Addison-Wesley, Reading, Massachusetts, second edition, July 1994. Originally published in 1980.
- [126] E. A. Freeman. An approximate transient analysis of a second-order position-control system when backlash is present. *IEE Mono.*, (254M):61–68, September 1957.
- [127] E. A. Freeman. The stabilization of control systems with backlash using a high-frequency on-off loop. *IEE Mono.*, (31):150–154, February 1960.
- [128] Yotam Freund and Yakov Ben-Haim. Selectively sensitive identification of connectivity matrices in linear elastic systems. In *13<sup>th</sup> International Modal Analysis Conference (IMAC)* [310], pages 1474–1478. See also Feldman & Ben-Haim [119].
- [129] Bernard Friedland and Amos El-Roy. Precision single-axis motion control system with friction compensation. In *Proc. Amer. Control Conf. ACC* [12], pages 3299–3302. See also Friedland *et alii* [14, 130, 131, 153, 155].
- [130] Bernard Friedland, Sofia Mentzelopoulou, and Young-Jin Park. Friction estimation in multimass systems. In *Proc. Amer. Control Conf. ACC* [11], pages 1927–1931. See also Friedland, Park *et alii* [14, 129, 131, 153, 155].
- [131] Bernard Friedland and Young-Jin Park. On adaptive friction compensation. *IEEE Trans. Auto. Control*, 37(10):1609–1612, October 1992. See also Friedland, Park *et alii* [14, 129, 130, 153, 155].
- [132] Rong-Fong Fung. Dynamic responses of the flexible connecting rod of a slider-crank mechanism with time-dependent boundary effect. *Comp. and Struc.*, 63(1):79–90, 1997.
- [133] Rong-Fong Fung and H-H. Chen. Steady-state response of the flexible connecting rod of a slider-crank mechanism with time-dependent boundary condition. *J. Sound and Vib.*, 199(2):237–251, January 16, 1997.
- [134] Rong-Fong Fung and F-Y. Lee. Dynamic analysis of the flexible rod of a quick-return mechanism with time-dependent coefficients by the finite element method. *J. Sound and Vib.*, 202(2):187–201, May 1, 1997.
- [135] Galileo Galilei. *Discorsi e dimostrazioni matematiche*. *Leiden*, 1638. *Quod vide* [215, note.1].
- [136] S. S. Ge, T. H. Lee, and G. Zhu. A nonlinear feedback controller for a single-link flexible manipulator based on a finite-element model. *J. Rob. Sys.*, 14(3):165–178, 1997.
- [137] J. Christian Gerdes and Vijay Kumar. An impact model of mechanical backlash for control system analysis. In *Proc. Amer. Control Conf. ACC* [12], pages 3311–3315.

- [138] James M. Gere and Stephen P. Timoshenko. *Mechanics of Materials*. PWS-Kent Series in Engineering. PWS-Kent Publishing Company, Boston, third edition, 1990.
- [139] Roland Glowinski and Anthony J. Kearsley. On the simulation and control of some friction constrained motions. *SIAM J. Opt.*, 5(3):681–694, August 1995.
- [140] Chao Goa, Doris Kuhlmann-Wilsdorf, and David D. Makel. The dynamic analysis of stick-slip motion. *Wear*, 173:1–12, 1994.
- [141] M. Farid Golnaraghi, DerChyan Lin, and Paul Fromme. Gear damage detection using chaotic dynamics techniques: A preliminary study. In Cudney [74], pages 121–127.
- [142] F. R. Goma. Vibration control using complex modal damping. In *13<sup>th</sup> International Modal Analysis Conference (IMAC)* [310], pages 1263–1269.
- [143] Michel Goossens, Frank Mittelbach, and Alexander Samarin. *The L<sup>A</sup>T<sub>E</sub>X Companion*. Addison-Wesley, Reading, Massachusetts, 1994. L<sup>A</sup>T<sub>E</sub>X 2<sub>ε</sub> advanced reference manual.
- [144] D. M. Gorinevsky, A. V. Lensky, and E. I. Sabitov. Feedback control of a one-link flexible manipulator with gear train. *J. Rob. Sys.*, 8(5):659–676, October 1991.
- [145] Oded Gottlieb, Michæl Feldman, and Solomon C. S. Yim. Analysis of a nonlinear friction damping mechanism in a fluid-structure interaction system. In Cudney [74], pages 1083–1090. See also Feldman *et alii* [52, 117–119, 121–123, 146].
- [146] O[ded] Gottlieb, M[ichæl] Feldman, and S[olomon] C. S. Yim. Parameter identification of nonlinear ocean mooring systems using the Hilbert transform. *J. Offshore Mech. and Arctic Eng.*, 118:29–36, February 1996. See also Feldman *et alii* [52, 117–119, 121–123, 145].
- [147] Scott A. Green, Robert S. Hirsch, and Kevin C. Craig. Mechatronics and digital control design at Rensselær. In Li [207]. See also Craig *et alii* [69–73, 77–82, 355, 367, 372, 378].
- [148] J. A. Greenwood. Analysis of elliptical hertzian contacts. *Tribology Int.*, 30(3):235–237, 1996.
- [149] Fredrik Gustafsson. Monitoring tire-road friction using the wheel slip. *IEEE Control Sys. Mag.*, 18(4):42–49, August 1998.
- [150] Ramesh S. Guttalu and Henryk Flashner. A study of bifurcations in periodic systems. In Cudney [74], pages 715–726.
- [151] Stefan L. Hahn. *Hilbert Transforms in Signal Processing*. Artech House, Norwood, Massachusetts, 1996.
- [152] K. Hamiti, A. Voda-Besançon, and H. Roux-Buisson. Position control of a pneumatic actuator under the influence of stiction. *J. Control Eng. Practice*, 4(8):1079–1088, 1996.

- [153] A[vraham] Harnoy and B[ernard] Friedland. Dynamic friction model of lubricated surfaces for precise motion control. *Tribology Trans.*, 37(3):608–614, October 1994. See also Harnoy, Friedland *et alii* [14, 129–131, 155].
- [154] Cyril M. Harris and Charles E. Crede, editors. *Shock and Vibration Handbook*. Number §9 in McGraw-Hill Handbooks. McGraw-Hill, New York City, 1961.
- [155] D. A. Hässig, Jr. and B[ernard] Friedland. On the modeling and simulation of friction. *ASME J. Dyn. Sys., Meas., and Control*, 113:354–362, September 1991. See also Friedland *et alii* [14, 129–131, 153].
- [156] B. S. Heck and A. A. Ferri. Model reduction of Coulomb friction-damped systems using singular perturbation theory. *ASME J. Dyn. Sys., Meas., and Control*, 118:84–91, March 1996.
- [157] Heinrich R. Hertz. *J. Reine u. Ang. Math.*, 92:156–171, 1881.
- [158] D[aniel] P. Hess and A[ndres] Soom. Friction at a lubricated line contact operating at oscillating sliding velocities. *ASME J. Trib.*, 112:147–152, January 1990. Survey paper; see also Polycarpou & Soom [267].
- [159] D. M. Heyes. Molecular aspects of boundary lubrication. *Tribology Int.*, 29(8):627–629, 1996.
- [160] Robert Hooke. De potentia restitutiva. *London*, 1678. *Quod vide* [215, note.2].
- [161] Jung Hua-Yang, Feng Li-Lian, and Li Chen-Fu. Nonlinear adaptive control for flexible-link manipulators. *J. IEEE Trans. Rob. Auto.*, 13(1):140–148, February 1997.
- [162] Chih-Jung Huang, Jia-Yush Yen, and Shu-Shung Lu. Stability of PDF controller with stick-slip friction device. In *Proc. Amer. Control Conf. ACC* [12], pages 3289–3293.
- [163] W. Hübner and G. Fleischer. Tribology in eastern germany – a retrospective editorial. *Tribology Int.*, 29(3):177–179, 1996.
- [164] M. S. Hundal. Response of a base-excited system with Coulomb and viscous friction. *J. Sound and Vib.*, 64(3):371–378, 1979.
- [165] José A. Inaudi and James M. Kelly. Linear hysteretic damping and the Hilbert transform. *J. Eng. Mech.*, 25:529–545, 1995.
- [166] José A. Inaudi and Nicos Makris. Time-domain analysis of linear hysteretic damping. *J. Earthquake Eng. and Struc. Dyn.*, 25:529–545, 1996.
- [167] Institute of Electrical and Electronics Engineers. *J. IEEE Trans. Rob. Auto.*, New York City, 1986. Institute of Electrical and Electronics Engineers.
- [168] Institute of Electrical and Electronics Engineers. *J. IEEE Trans. Rob. Auto.*, New York City, 1987. Institute of Electrical and Electronics Engineers.

- [169] Institute of Electrical and Electronics Engineers. *J. IEEE Trans. Rob. Auto.*, New York City, 1988. Institute of Electrical and Electronics Engineers.
- [170] Institute of Electrical and Electronics Engineers. *J. IEEE Trans. Rob. Auto.*, New York City, 1990. Institute of Electrical and Electronics Engineers.
- [171] Institute of Electrical and Electronics Engineers. *J. IEEE Proc. Dec. Control*, New York City, December 1992. Institute of Electrical and Electronics Engineers.
- [172] Institute of Electrical and Electronics Engineers. *J. IEEE Proc. Dec. Control*, New York City, December 1995. Institute of Electrical and Electronics Engineers.
- [173] Institute of Electrical and Electronics Engineers. *J. IEEE Proc. Control App.*, New York City, September 1996. Institute of Electrical and Electronics Engineers.
- [174] Institute of Electrical and Electronics Engineers. *J. IEEE Trans. Rob. Auto.*, New York City, April 1996. Institute of Electrical and Electronics Engineers.
- [175] Jacob N. Israelachvili, Patricia M. McGuiggan, and Andrew M. Homola. Dynamic properties of molecularly thin liquid films. *Science*, 240:189–190, April 8, 1988.
- [176] Siyoul Jang and John Tichy. Rheological models for stick-slip behaviour. Internal report, Rensselaer Polytechnic Institute, Troy, New York, 1997.
- [177] Mrdjan Jankovic. Observer-based control for elastic-joint robots. *J. IEEE Trans. Rob. Auto.*, 11(4):618–623, August 1995.
- [178] Jeong-Yul Jeon, Jong-Hwan Kim, and Kwangill Koh. Experimental evolutionary programming-based high-precision control. *IEEE Control Sys. Mag.*, 17(2):66–74, April 1997. See also Jeon, Kim *et alii* [188, 189, 205].
- [179] V. I. Johannes, M. A. Green, and C. A. Brockley. The role of the rate of application of the tangential force in determining the static friction coefficient. *Wear*, 24:381–385, 1973.
- [180] R. E. Kalman. Physical and mathematical mechanisms of instability in nonlinear automatic control systems. In *ASME/AIEE Conf. Nonlinear Control Sys.*, IRD-3, pages 553–566, New York City, March 1956. American Society of Mechanical Engineers, American Society of Mechanical Engineers.
- [181] Thomas R. Kane and David A. Levinson. *Dynamics: Theory and Applications*. McGraw-Hill Series in Mechanical Engineering. McGraw-Hill, New York City, 1985.
- [182] J. Y. Kao *et alii*. A study of backlash on the motion accuracy of CNC lathes. *Int. J. Mach. Tools and Manuf.*, 36(5):539–550, 1996. See also Tarng & Cheng [342].
- [183] Dean Karnopp. Computer simulation of stick-slip friction in mechanical dynamic systems. *ASME J. Dyn. Sys., Meas., and Control*, 107:100–109, March 1985.
- [184] S[hinobu] Kato, N. Sato, and T. Matsubayashi. Some considerations on characteristics of static friction of machine tool slideway. *ASME J. Lub. Tech.*, 93:234–247, February 1972. (New journal name is *ASME J. Trib.* .) See also Kato, Marui *et alii* [223, 224].

- [185] Howard Kaufman, Izhak Bar-Kana, and Kenneth Sobel. *Direct Adaptive Control Algorithms: Theory and Applications*. Springer-Verlag Communications and Control Engineering Series. Springer-Verlag, Berlin, 1994.
- [186] Kazuo Kiguchi and Toshio Fukuda. Fuzzy-neural friction compensation method of robot manipulation during position/force control. In *J. IEEE Trans. Rob. Auto.* [174], pages 372–377.
- [187] Sun Kim and Karl B. Ousterhout. The development of a real-time recursive frequency-based active chatter controller. In Cudney [74], pages 129–137.
- [188] Jong-Hwan Kim *et alii*. High-precision control of positioning systems with nonsmooth nonlinearities. In Tao [332], pages 4375–4380. See also Lee & Kim [205].
- [189] Jong-Hwan Kim *et alii*. Identification and control of systems with friction using accelerated evolutionary programming. *IEEE Control Sys. Mag.*, 16(4):38–47, August 1996. See also Lee & Kim [205].
- [190] Nenad M. Kircanski and Andrew A. Goldberg. An experimental study of nonlinear stiffness, hysteresis and friction effects in robot joints with harmonic drives and torque sensors. *Int. J. Robot. Res.*, 16(2):214–239, April 1997.
- [191] D. Klaffke. On the repeatability of friction and wear results and on the influence of humidity in oscillating sliding tests of steel-steel pairings. *Wear*, 189:117–121, 1995.
- [192] Uri Klement. A global network for plant design. *Mech. Eng. Mag.*, 118(12):52–54, December 1996.
- [193] H. J. Klepp *et alii*. On the determination of the solutions for the kinetic state of single-freedom multi-body systems with friction. *Z. Angew. Math. Mech.*, 77(1):53–58, 1997.
- [194] K. Komvopoulos, N. Saka, and N. P. Suh. The mechanism of friction in boundary lubrication. *ASME J. Trib.*, 107:452–462, October 1985.
- [195] E. M. Kopalinsky and A. J. Black. Metallic sliding friction under boundary lubricated conditions: Investigation of the influence of lubricant at the start of sliding. *Wear*, 190:197–203, 1995.
- [196] E. M. Kopalinsky and P. L. B. Oxley. Explaining the mechanics of metallic sliding friction and wear in terms of slipline field models of asperity deformation. *Wear*, 190:145–154, 1995.
- [197] Tomoaki Kubo, George Anwar, and Masayoshi Tomizuka. Application of nonlinear friction compensation to robot arm control. In *J. IEEE Trans. Rob. Auto.* [167], pages 722–727. See also Tomizuka *et alii* [326, 356, 357, 374, 375].
- [198] Max Kurtz. *Handbook of Applied Mathematics for Engineers*. McGraw-Hill, New York City, 1991. Reference.
- [199] Brian Kuttner and Dan Deitz. Reviewing designs in cyberspace. *Mech. Eng. Mag.*, 118(12):56–58, December 1996. See also Deitz [83, 84].

- [200] Jean J. Labrosse.  *$\mu C/OS$ : The Real-Time Kernel*. R & D Publications, Inc., Lawrence, Kansas, 1992. Software revision v1.09. See <http://www.rdbooks.com> for information on obtaining software updates.
- [201] Leslie Lamport. *L<sup>A</sup>T<sub>E</sub>X: A Document Preparation System*. Addison-Wesley, Reading, Massachusetts, second edition, 1994. L<sup>A</sup>T<sub>E</sub>X 2 <sub>$\epsilon$</sub>  user's guide and basic reference manual.
- [202] G. A. Larsen, S[abri] Cetinkunt, and A. Donmez. CMAC neural network control for high precision motion control in the presence of friction. *ASME J. Dyn. Sys., Meas., and Control*, 117:415–420, September 1995.
- [203] Debra S. Larson and Apostolos Fafitis. Slip-stick steady-state solution for simple Coulomb-damped mass. *J. Eng. Mech.*, 121(2):289–298, February 1995.
- [204] Rong-Tsong Lee, Chii-Rong Yang, and Yuang-Cherng Chiou. A procedure for evaluating the positioning accuracy of reciprocating friction drive systems. *Tribology Int.*, 29(5):395–404, 1996.
- [205] Seon-Woo Lee and Jong-Hwan Kim. Robust adaptive stick-slip friction compensation. *IEEE Trans. Ind. Elec.*, 42(5):474–479, October 1995. See also Kim *et alii* [178, 188, 189].
- [206] Yau-Shing Lee. *Dynamic Hardness Testing*. PhD thesis, Rensselaer Polytechnic Institute, Troy, New York, August 1995. Henry A. Scarton, advisor.
- [207] C. Jim Li, editor. *ASME Int. Mech. Eng. Congress and Exposition*, New York City, September 1995. American Society of Mechanical Engineers, American Society of Mechanical Engineers.
- [208] J.-W. Liang and B[rian] F. Feeny. Wavelet analysis of stick-slip in an oscillator with dry friction. In Cudney [74], pages 1061–1069. See also Feeny & Liang [113].
- [209] J.-W. Liang and B[rian] F. Feeny. Dynamical friction behavior in a forced oscillator with a compliant contact. *J. App. Mech.*, 65:250–257, March 1998. See also Liang & Feeny [113, 208].
- [210] C. T. Lim and W. J. Stronge. Frictional torque and compliance in collinear elastic collisions. *Int. J. Mech. Sci.*, 36(10):911–930, 1994.
- [211] Cheng Sheng Lin. Second-order system with dry and Coulomb friction under ramp input. Master's thesis, Rensselaer Polytechnic Institute, Troy, New York, June 1962. C. N. Shen, advisor.
- [212] Ching-Fang Lin, Tie-Jun Yu, and Xu Feng. Fuzzy control of a nonlinear pointing testbed with backlash and friction. In Tao [332], pages 4363–4368.
- [213] Zongli Lin. Global control of linear systems with saturating actuators. In Tao [332], pages 4357–4362.

- [214] Lennart Ljung. *System Identification: Theory for the User*. Prentice-Hall PTR Information and System Sciences Series. Prentice-Hall, Upper Saddle River, New Jersey, 1987.
- [215] A. E. H. Love. *A Treatise on the Mathematical Theory of Elasticity*. Dover Publications, New York City, fourth edition, 1944. No ISBN available.
- [216] K. C. Ludema. Mechanism-based modeling of friction and wear. *Wear*, 200:1–7, 1996.
- [217] Edward MacCurdy, editor. *The NoteBooks of Leonardo da Vinci*. Reynal & Hitchcock, New York City, 1939.
- [218] Jack W. Macki, Paolo Nistri, and Pietro Zecca. Mathematical models for hysteresis. *SIAM Rev.*, 35(1):94–123, March 1993. Survey paper.
- [219] Heidar A. Malki *et alii*. Fuzzy PID control of a flexible-joint robot arm with uncertainties from time-varying loads. *IEEE Trans. Control Sys. Tech.*, 5(3):371–378, May 1997.
- [220] Dan B. Marghitu. Frictional impact of an elastic body. In Cudney [74], pages 191–201.
- [221] Dan B. Marghitu and Yildirim Hurmuzlu. Nonlinear dynamics of an elastic rod with frictional impact. *Nonlinear Dyn.*, 10:187–201, June 1996.
- [222] J. A. C. Martins, J. T. Oden, and F. M. F. Simões. A study of static and kinetic friction. *Int. J. Eng. Sci.*, 28(1):29–92, 1990. Survey paper; see also Oden & Martins [244].
- [223] Etsuo Marui and Shinobu Kato. Forced vibration of a base-excited single-degree-of-freedom system with Coulomb friction. *ASME J. Dyn. Sys., Meas., and Control*, 106:280–285, December 1984. See also Marui, Kato *et alii* [184, 224].
- [224] Etsuo Marui *et alii*. Some considerations of slideway friction characteristics by observing stick-slip vibration. *Tribology Int.*, 29(3):251–262, 1996. See also Marui, Kato *et alii* [184, 223].
- [225] F. Mason. Multipart fixturing delivers speed and flexibility. *Amer. Machinist*, (10):51–53, January 1994.
- [226] A. S. McCormack, K. R. Godfrey, and J. O. Flower. Design of multilevel multiharmonic signals for system identification. *IEE Proc. Control Th. App.*, 142(3):247–252, May 1995.
- [227] Jean L. McKechnie, editor. *[Merriam] Webster's New Universal Unabridged Dictionary*. Simon and Schuster, New York City, fourteenth edition, 1983.
- [228] Anil Misra. Mechanistic model for contact between rough surfaces. *J. Eng. Mech.*, 123(5):475–484, May 1997.

- [229] Samir Mittal and C. H. Menq. Robust compensation techniques for DC servomechanisms subject to stiction and parametric uncertainties using sliding mode estimation. In *Proc. Amer. Control Conf. ACC* [12], pages 3306–3310.
- [230] Guillaume Morel and Steven Dubowsky. The precise control of manipulators with joint friction: A base force/torque sensor method. In *J. IEEE Trans. Rob. Auto.* [174], pages 360–365. See also Dubowsky & Freudenstein [96, 97].
- [231] A. J. Morin. Nouvelles expériences sur le frottement. *Inst. de France Acad. Roy. des Sci.*, 4:1–128, 1831–1834.
- [232] Naser Mostaghel and Todd Davis. Representations of Coulomb friction for dynamic analysis. *J. Earthquake Eng. and Struc. Dyn.*, 26:541–548, 1997.
- [233] J. Mou and C. R. Liu. An adaptive methodology for machine tools error correction. *American Society of Mechanical Engineers Journal Engineer for Ind.*, 117:389–399, August 1995.
- [234] M. Nakano *et alii*. Elimination of position-dependent disturbances in constant-speed-rotation control systems. *J. Control Eng. Practice*, 4(9):1241–1248, September 1996.
- [235] Sharath M. Narayana *et alii*. Interpolation/extrapolation of frequency-domain responses using the Hilbert transform. *IEEE Trans. Microwave Th. Tech.*, 44(10):1621–1626, October 1996.
- [236] Ahid D. Nashif, David I. G. Jones, and John P. Henderson. *Vibration Damping*. Wiley-Interscience Series. John Wiley & Sons, New York–London–Sydney, 1985.
- [237] David E. Newland. Progress in the application of wavelet theory to vibration analysis. In Cudney [74], pages 1313–1322.
- [238] S. Nicosia and P. Tomei. Design of global tracking controllers for flexible-joint robots. *J. Rob. Sys.*, 10(6):835–846, 1993.
- [239] P. N. Nikiforuk and K. Tamura. Design of a disturbance-accomodating adaptive control system and its application to a DC-servo motor system with Coulomb friction. *ASME J. Dyn. Sys., Meas., and Control*, 110:343–349, December 1988.
- [240] Mattias Nordin, Johann Galić, and Per-Olof Gutman. New models for backlash and gearplay. *Int. J. Adaptive Control Sig. Proc.*, 11:49–63, May 1997.
- [241] W. Nuninger, B. Balaud, and F. Kratz. Disturbance rejection using output and input estimation: Application to the friction compensation of a DC motor. *J. Control Eng. Practice*, 5:477–483, April 1997.
- [242] Leo O’Conner. Micromachines tap actuating principles. *Mech. Eng. Mag.*, 116(8):58–60, August 1994.
- [243] Leo O’Conner. Machining with super-fast spindles. *Mech. Eng. Mag.*, 117(5):62–64, May 1995.

- [244] J. T. Oden and J. A. C. Martins. Models and computational methods for dynamic friction phenomena. *Computer Meth. App. Mech. and Eng.*, 52:527–634, 1985. Survey paper; see also Martins *et alii* [222].
- [245] James R. O'Donnell, Jr. *Nonlinear Control System Design Using Sinusoidal-Input Describing Function Methods*. PhD thesis, Rensselaer Polytechnic Institute, Troy, New York, June 1992. Dean K. Frederick and James H. Taylor, advisors.
- [246] Hans C. Ohanian. *Physics*, volume 1. W.W. Norton, New York City, 1985.
- [247] N. Olgac and V. R. Iragavarapu. Sliding mode control with backlash and saturation laws. *Int. J. Robot. Auto.*, 10(2):49–55, 1995.
- [248] Henrik Olsson and Karl J. Åström. Observer-based friction compensation. In Tao [332], pages 4345–4350. See also Åström *et alii* [26, 61, 62, 248, 323].
- [249] Alan V. Oppenheim and Ronald W. Shafer. *Digital Signal Processing*. Prentice-Hall, Upper Saddle River, New Jersey, 1975.
- [250] Earle W. Owen. A phase-space and analogue computer study of some feedback control systems containing backlash and compensating nonlinearities. Master's thesis, Rensselaer Polytechnic Institute, Troy, New York, June 1959. C. H. Dunn, advisor.
- [251] Frederic Palmer. What about friction? – Part I: Classical laws. *Amer. J. Math.*, 17(6):181–187, September 1949.
- [252] Frederic Palmer. What about friction? – Part II: Friction as a result of molecular forces. *Amer. J. Math.*, 17(6):327–335, September 1949.
- [253] Frederic Palmer. What about friction? – Part III: Friction saw / electrical theory / lubrication. *Amer. J. Math.*, 17(6):336–342, September 1949.
- [254] G. Pan *et alii*. Modeling and intelligent chatter control strategies for a lathe machine. *J. Control Eng. Practice*, 4(12):1647–1658, 1996.
- [255] M. C. Pan *et alii*. Diagnosis of the joint backlash of a mechanism: Wigner-ville distribution combined with correlation techniques. In Cudney [74], pages 1405–1412.
- [256] Antoine Parent. Mémoire qui contient tout ce qui se fait sur les plans inclinés. *Mém. de l'Acad. Roy. Sci. de Paris*, page 173, 1704.
- [257] R[obert] M. Parkin, E. Kallenbach, and E[ugen] Saffert, editors. *Control and Configuration Aspects of Mechatronics*, Institute of Microsystems Technology, Mechatronics and Mechanics, Postfach 100565, D-98684 Ilmenau, Thuringia, Deutschland, September 21-26, 1997. Euro Conference in Focused Aspects of Mechatronics, Tech. Uni.-Ilmenau, Faculty of Mech. Eng.
- [258] Greg Paula. Process control takes to the net. *Mech. Eng. Mag.*, 118(12):55, December 1996.

- [259] B. N. J. Persson and Zhenyu Zhang. Theory of friction: Coulomb drag between two closely-spaced solids. *Phys. Rev. B: Cond. Matter*, 57(12):7327–7334, March 15, 1998.
- [260] F[riedrich] Pfeiffer. Complementarity problems of stick-slip vibrations. *J. Vib. Acoustics*, 118:177–183, April 1996.
- [261] Friedrich Pfeiffer and Christoph Glocker. Impacts with friction. In Cudney [74], pages 171–180.
- [262] C. Pierre, A. A. Ferri, and E. H. Dowell. Multi-harmonic analysis of dry-friction-damped systems using an incremental harmonic balance meethod. *J. App. Mech.*, 52:558–964, December 1985.
- [263] PMI Motion Technologies. *U12M4T ServoDisc*. Kollmorgen Corporation, 49 Mall Drive, Commack, NY 11725-5703, March 1986. Reference.
- [264] PMI Motion Technologies. *U16M4T ServoDisc*. Kollmorgen Corporation, 49 Mall Drive, Commack, NY 11725-5703, March 1986. Reference.
- [265] Siméon-Denis Poisson. Mém. sur l'équilibre et le mouvement des corps élastique. *Mém. de l'Acad. de Paris*, 1829. Treatise 8. *Quod vide* Love [215, p13].
- [266] Andreas A. Polycarpou and Izhak Etsion. Comparison of the static friction subboundary lubrication model with experimental measurements on thin-film disks. *ASME J. Trib.*, 41(2):217–224, 1998.
- [267] A[ndreas] A. Polycarpou and A[ndres] Soom. Application of a two-dimensional model of continuous sliding friction to stick-slip. *Wear*, 181:32–41, 1995. See also Hess & Soom [158].
- [268] K. Popp, N. Hinrichs, and M. Östreich. Dynamical behaviour of a friction oscillator with simultaneous self and external excitation. *Sādhanā*, 20(2–4):627–654, April–August 1995.
- [269] K. Popp and P. Stelzer. *Nonlinear Dynamics in Engineering Systems*. Springer-Verlag, Berlin, 1990.
- [270] K. Popp and P. Stelzer. Stick-slip vibrations and chaos. *Phil. Trans. R. Soc. of London–A*, 332:89–105, 1990.
- [271] K[waku] O[ppong] Prakah-Asante *et alii*. Design, construction and testing of a singe-axis servomechanism for control experiments involving Coulomb friction, backlash and joint compliance. *J. Eng. Design*, 4(4):305–329, 1993. See also Craig, Walczyk *et alii* [69–73, 77–82, 147, 355, 367, 372, 378].
- [272] John Prescott. *Applied Elasticity*. Dover Publications, New York City, reprinted edition, 1961. “..an unabridged and unaltered republication of the work first published by Green & Co. in 1924.”.

- [273] William H. Press *et alii*. *Numerical Recipes in C: The Art of Scientific Computing*. Cambridge University Press, Cambridge, England, second edition, 1992. See also Vetterling *et alii* [366].
- [274] Michæl Puttré. Surface modeling for multiaxis machining. *Mech. Eng. Mag.*, 116(10):58–60, October 1994.
- [275] Ernest Rabinowicz. Resource letter F-1 on friction. *Amer. J. Math.*, 31(12):1–4, December 1963.
- [276] Ernest Rabinowicz. *Friction and Wear of Materials*. John Wiley & Sons, New York–London–Sydney, second edition, 1995.
- [277] Clark J. Radcliffe and Steve C. Southward. A property of stick-slip friction models which promotes limit cycle generation. In *Proc. Amer. Control Conf. ACC*, TA6, pages 1198–1203. American Control Council, American Control Council, 1990. See also Radcliffe & Southward [312].
- [278] A. Rantzer. Friction analysis based on integral quadratic constraints. In Tao [332], pages 3948–3952.
- [279] M. Raous, M. Jean, and J. J. Moreau, editors. *Proc. Second Contact Mech. Int. Symp.*, New York City; London, September 1994. Plenum Press. Compiled and published in 1995.
- [280] Lord Rayleigh. *The Theory of Sound*, volume 1. Dover Publications, New York City, 1877. Reprinted by Dover in 1945.
- [281] D. A. Recker. Indirect adaptive non-linear control of discrete time systems containing a dead-zone. *Int. J. Adaptive Control Sig. Proc.*, 11:33–48, February 1997.
- [282] M. Osborne Reynolds. On the theory of lubrication. *Phil. Trans. R. Soc. of London*, 1, 1886.
- [283] J[ames] R. Rice and A[ndy] L. Ruina. Stability of steady frictional slipping. *J. App. Mech.*, 50:343–349, June 1983. See also Ruina [288].
- [284] James R. Rice and Simon T. Tse. Dynamic motion of a single degree-of-freedom system following a rate- and state-dependent friction law. *J. Geophys. Res.*, 91(B1):521–530, January 10, 1986. (Volume on Physics and Chemistry).
- [285] R. S. H. Richardson and H. Nolle. Surface friction under time-dependent loads. *Wear*, 37:87–101, 1976.
- [286] K. Richter. Noncollocated feedback for the control of elastic structures with friction in the actuators. *ASME J. Dyn. Sys., Meas., and Control*, 117:645–649, 1995.
- [287] Ronald A. L. Rorrer. Friction-induced vibration of multi-degree-of-freedom sliding subsystems. In Cudney [74], pages 1179–1186.
- [288] Andy [L.] Ruina. Slip instability and state variable friction laws. *J. Geophys. Res.*, 88(B12):10359–10370, December 10, 1983. (Volume on Physics and Chemistry). See also Rice & Ruina [283].

- [289] M. Ruzzene *et alii*. Natural frequencies and dampings identification using wavelet transform: Application to real data. *J. Mech. Sys. and Sig. Proc.*, 11(2):207–218, 1997.
- [290] Z. Rymuza. Energy concept of the coefficient of friction. *Wear*, 199:187–196, 1996.
- [291] K. Y. Sanliturk, M. Imregun, and D. J. Ewins. Harmonic balance vibration analysis of turbine blades with friction dampers. *J. Vib. Acoustics*, 119:96–103, January 1997.
- [292] Kaiji Sato *et alii*. Control and elimination of lead-screw backlash for ultra-precision positioning. *JSME Int. J.-C*, 38(1):36–41, 1995.
- [293] K. N. Satyendra. Describing functions representing the effect of inertia, backlash, and Coulomb friction on the stability of an automatic control system – [Part] I. *AIAA J.*, 75(ii):243–249, September 1956. Part II appears never to have been published.
- [294] Henry A. Scarton. Dynamic hardness (SDH). Rensselaer Dept. of ME, AE & M graduate colloquium series, October 4, 1996.
- [295] U. Schäfer and G[ünther] Brandenburg. Model reference position control of an elastic two-mass system with compensation of Coulomb friction. In *Proc. Amer. Control Conf. ACC* [11], pages 1937–1941.
- [296] R. Schnurmann and E. Warlow-Davies. The electrostatic component of the force of sliding friction. *Proc. Phys. Soc.*, 54:14, 1942.
- [297] The Graduate School. *Thesis Writing*. Rensselaer Polytechnic Institute, Troy, New York, 1984. Reference.
- [298] M. R. Schröder. Synthesis of low peak-factor signals and binary sequences of low auto-correlation. *IEEE Trans. Info. Th.*, 16:85–89, January 1970.
- [299] Francis W. Sears and Gerhard L. Salinger. *Thermodynamics, Kinetic Theory, and Statistical Thermodynamics*. Addison-Wesley Principles of Physics Series. Addison-Wesley, Reading, Massachusetts, third edition, 1975.
- [300] David R. Seidl *et alii*. Neural network compensation of gear backlash hysteresis in position-controlled mechanisms. *IEEE Trans. App. Ind.*, 31(6):1475–1483, November/December 1995.
- [301] N. Sepeheri, F. Sassani, and P. D. Lawrence. Simulation and experimental studies of gear backlash and stick-slip friction in hydraulic excavator swing motion. *ASME J. Dyn. Sys., Meas., and Control*, 118:463–467, September 1996.
- [302] S. W. Shaw. On the dynamic response of a system with dry friction. *J. Sound and Vib.*, 108(2):305–324, 1986.
- [303] S. W. Shaw and C. Pierre. Normal modes of vibration for non-linear continuous systems. *J. Sound and Vib.*, 169(3):319–347, 1994.

- [304] C. N. Shen. Synthesis of high-order nonlinear control systems with ramp input. *IRE Trans. Auto.*, AC-7(2):22–37, 1962.
- [305] C. N. Shen, H. A. Miller, and N. B. Nichols. Nonlinear integral compensation of a velocity-lag servomechanism with backlash. *ASME Trans.*, pages 585–592, April 1957.
- [306] C. N. Shen and Hubert Wang. Nonlinear compensation of a second- and third-order system with dry friction. *IEEE Trans. App. Ind.*, 83(71):128–136, March 1964.
- [307] M. Y. Silberberg. A note on the describing function of an element with Coulomb, static and viscous friction. *AIEE Trans.*, 75(ii):423–425, January 1957.
- [308] Jean-Jacques E. Slotine and Weiping Li. *Applied Nonlinear Control*. McGraw-Hill, New York City, 1991.
- [309] Society for Experimental Mechanics. *12<sup>th</sup> International Modal Analysis Conference (IMAC)*, Bethel, Connecticut, 1994. SPIE Optical Engineering Press.
- [310] Society for Experimental Mechanics. *13<sup>th</sup> International Modal Analysis Conference (IMAC)*, Bethel, Connecticut, 1995. SPIE Optical Engineering Press.
- [311] Society for Experimental Mechanics. *14<sup>th</sup> International Modal Analysis Conference (IMAC)*, Bethel, Connecticut, 1996. SPIE Optical Engineering Press.
- [312] S[teve] C. Southward, C[lark] J. Radcliffe, and C. R. MacCluer. Robust nonlinear stick-slip friction compensation. *ASME J. Dyn. Sys., Meas., and Control*, 113:639–645, December 1991. See also Radcliffe & Southward [277].
- [313] Murray R. Spiegel. *Mathematical Handbook of Formulas and Tables*. McGraw-Hill, New York City, Schaum’s outline series edition, 1968. Reference.
- [314] B. de St. Venant. Treatise 14. *Mém. des Savant Étrangers*, 1855. *Quod vide* Love [215, p19–20].
- [315] W. J. Staszewski. Wavelet-based compression and feature selection for vibration analysis. *J. Sound and Vib.*, 211(5):735–760, April 16, 1998.
- [316] Jeffrey L. Stein and Churn-Hway Wang. Estimation of gear backlash: Theory and simulation. *ASME J. Dyn. Sys., Meas., and Control*, 120:74–82, March 1998.
- [317] D. E. Stewart and J. C. Trinkle. An implicit time-stepping scheme for rigid body dynamics with inelastic collisions and Coulomb friction. *Int. J. Num. Meth. in Eng.*, 39:2673–2691, 1996. See also Trinkle *et alii* [354].
- [318] Gilbert Strang. *Introduction to Applied Mathematics*. Wellesley-Cambridge Press, Wellesley, Massachusetts, 1986.
- [319] R. Stribeck. Die wesentlichen eigenschaften der gleit- und rollenlager [I]. *Z. Verein. Deutsch. Ing.*, 46(36):1342–1348, September 6, 1902.
- [320] R. Stribeck. Die wesentlichen eigenschaften der gleit- und rollenlager [II]. *Z. Verein. Deutsch. Ing.*, 46(38):1432–1438, September 20, 1902.

- [321] R. Stribeck. Die wesentlichen eigenschaften der gleit- und rollenlager [III]. *Z. Verein. Deutsch. Ing.*, 46(39):1463–1470, September 27, 1902.
- [322] Tim Studt. Basic research: Defining our path to the future. White paper, R&D Magazine, Des Plaines, Illinois (USA), 1997. R&D Magazine is a Cahners Publication (Newton, Massachusetts).
- [323] D. A. Suárez *et alii*. Adaptive control of linear systems with poles in the closed LHP with constrained inputs. In Tao [332], pages 4351–4356. See also Åström, Wittenmark, *et alii* [26, 61, 62, 248, 323].
- [324] Nam P. Suh, Mohsen Mosleh, and Phillip S. Howard. Control of friction. *Wear*, 175:151–158, 1994.
- [325] Xi Sun, Weicun Zhang, and Yihun Jin. Stable adaptive control of backlash nonlinear systems with bounded disturbances. In *J. IEEE Proc. Dec. Control* [171], pages 274–275.
- [326] Akihiro Suzuki and Masayoshi Tomizuka. Design and implementation of digital servo controller for high speed machine tools. In *Proc. Amer. Control Conf. ACC*, TA6, pages 1246–1251. American Control Council, American Control Council, 1991. See also Tomizuka *et alii* [197, 356, 357, 374, 375].
- [327] R. G. Synnestevedt. An effective method for modeling stiction in multibody dynamic systems. *ASME J. Dyn. Sys., Meas., and Control*, 118:172–176, March 1996.
- [328] S. Tafazoli, C. W. de Silva, and P. D. Lawrence. Friction estimation in a planar electrohydraulic manipulator. In *Proc. Amer. Control Conf. ACC* [12], pages 3294–3298.
- [329] K. A. Tahboub and P. C. Müller. A novel model manipulation of elastic-joint robots for control purposes. *Math. and Comp. in Sim.*, 37:221–225, 1994.
- [330] Xi Tan and R. J. Rogers. Simulation of friction in multi-degree-of-freedom vibration systems. *ASME J. Dyn. Sys., Meas., and Control*, 120:144–146, March 1998.
- [331] Gang Tao. Adaptive control of systems with nonsmooth input and output nonlinearities. *IEEE Trans. Auto. Control*, 41(9):1348–1352, September 1996.
- [332] Gang Tao, editor. *J. IEEE Proc. Dec. Control*, New York City, December 1996. Institute of Electrical and Electronics Engineers, Institute of Electrical and Electronics Engineers.
- [333] Gang Tao and Petar V. Kokotović. *Adaptive Control of Systems with Actuator and Sensor Nonlinearities*. Wiley Series on Adaptive and Learning Systems for Signal Processing, Communications, and Control. John Wiley & Sons, New York–London–Sydney, 1996.
- [334] Gang Tao and Petar V. Kokotović. Adaptive control of systems with backlash. Technical report, UC–Santa Barbara, Santa Barbara, California, 1993. Copy of presentation slides from 1993 SIAM conference.

- [335] Gang Tao and Petar V. Kokotović. Adaptive control of systems with backlash. *Automatica*, 29(2):323–335, 1993.
- [336] Gang Tao and Petar V. Kokotović. Adaptive control of plants with unknown dead-zones. *IEEE Trans. Auto. Control*, 39(1):59–68, January 1994.
- [337] Gang Tao and Petar V. Kokotović. Adaptive control of plants with unknown hystereses. *IEEE Trans. Auto. Control*, 40(2):200–212, February 1995.
- [338] Gang Tao and Petar V. Kokotović. Adaptive control of systems with unknown output backlash. *IEEE Trans. Auto. Control*, 40(2):326–330, February 1995.
- [339] Gang Tao and Petar V. Kokotović. Continuous-time adaptive control of systems with unknown backlash. *IEEE Trans. Auto. Control*, 40(6):1083–1087, June 1995.
- [340] Gang Tao and Petar V. Kokotović. Discrete-time adaptive control of plants with unknown output dead-zones. *Automatica*, 31(2):287–291, 1995.
- [341] Gang Tao and Petar V. Kokotović. Discrete-time adaptive control of systems with unknown deadzones. *Int. J. Control*, 61(1):1–17, 1995.
- [342] Y. S. Tarng and H. E. Cheng. An investigation of stick-slip friction on the contouring accuracy of CNC machine tools. *Int. J. Mach. Tools and Manuf.*, 35(4):565–576, 1995. See also Tarng *et alii* [182].
- [343] John R. Taylor. *An Introduction to Error Analysis: The Study of Uncertainty in Physical Measurements*. University Science Series of Books in Physics. Oxford University Press, Oxford; New York City, 1982.
- [344] Charlotte Chandler Thomas. Masters of the universe. *Graduating Engineer*, pages 12–17, March 1997.
- [345] Peter A. Thompson and Mark O. Robbins. Origin of stick-slip motion in boundary lubrication. *Science*, 250:792–794, November 9, 1990.
- [346] William T. Thomson. *Theory of Vibrations with Applications*. Prentice-Hall, Upper Saddle River, New Jersey, fourth edition, 1993.
- [347] Robert H. Thurston. *A Treatise on Friction and Lost Work in Machinery and Millwork*. John Wiley & Sons, New York–London–Sydney, 1907.
- [348] Ming Tian, Gang Tao, and Yi Ling. Adaptive dead-zone inverse for nonlinear plants. In Tao [332], pages 4381–4386. See also Tao *et alii* [331–341].
- [349] A. Tornambè. Modelling and controlling one-degree-of-freedom impacts. *IEE Proc. Control Th. App.*, 143(1):85–90, January 1996.
- [350] A. Tornambè. Modelling and controlling one-degree-of-freedom impacts under elastic/plastic deformations. *IEE Proc. Control Th. App.*, 143(5):470–476, September 1996.

- [351] A. Tornambè and P. Valigi. A decentralized controller for the robust stabilization of a class of mimo dynamical systems. *ASME J. Dyn. Sys., Meas., and Control*, 116:293–304, June 1994.
- [352] J. Tou and P. M. Schultheiss. Static and sliding friction in feedback systems. *J. App. Phys.*, 24(9):1210–1217, September 1953.
- [353] William T. Townsend and J. Kenneth Salisbury, Jr. The effect of Coulomb friction and stiction on force control. In *J. IEEE Trans. Rob. Auto.* [168], pages 833–889.
- [354] J. C. Trinkle *et alii*. On dynamic multi-rigid-body contact problems with coulomb friction. *Z. Angew. Math. Mech.*, 77(4):267–279, 1997. See also Stewart & Trinkle [317].
- [355] Celal S. Tüfekçi *et alii*. Mechatronic design of an inverted pendulum system for engineering education. In Adolfsson and Karlsén [4], pages 685–691. See also Craig, de Marchi, Özçelik *et alii* [69–73, 77–82, 147, 355, 367, 372, 378].
- [356] E. D. Tung, G. Anwar, and M[asayoshi] Tomizuka. Low-velocity friction compensation and feedforward solution based on repetitive control. *ASME J. Dyn. Sys., Meas., and Control*, 115:279–284, June 1993. See also Tomizuka *et alii* [197, 326, 374, 375].
- [357] E. D. Tung, Y. Urushisaki, and M[asayoshi] Tomizuka. Low-velocity friction compensation for machine tool feed drives. In *Proc. Amer. Control Conf. ACC* [11], pages 1932–1936. See also Tomizuka *et alii* [197, 326, 374, 375].
- [358] A. Tustin. The effects of backlash and of speed-dependent friction on the stability of closed-cycle control systems. *IEE J.*, 94(2A):143–151, 1947.
- [359] A. Tustin. A method of analysing the effect of certain kinds of non-linearity in closed-cycle control systems. *IEE J.*, 94(2A):151–160, 1947.
- [360] Y. S. Ünlüsoy and S. T. Tümer. Non-linear dynamic model and its solution for a high-speed cam mechanism with coulomb friction. *J. Sound and Vib.*, 169(3):395–407, 1994.
- [361] Michael Valenti. Engineering across the seas. *Mech. Eng. Mag.*, 117(6):52–58, June 1995.
- [362] Michael Valenti. Machine tools get smarter. *Mech. Eng. Mag.*, 117(11):70–75, November 1995.
- [363] F. van de Velde and P. de Bæts. A new approach of stick-slip based on quasi-harmonic tangential oscillations. *Wear*, 216:15–26, 1998.
- [364] F. van de Velde, P. de Bæts, and J. Degrieck. The friction force during stick-slip with velocity reversals. *Wear*, 216:138–149, 1998.
- [365] Gordon J. van Wijlen and Richard E. Sonntag. *Fundamentals of Classical Thermodynamics*. SI Version. John Wiley & Sons, New York–London–Sydney, third edition, 1985.

- [366] William T. Vetterling *et alii*. *Numerical Recipes: Example Book (c)*. Cambridge University Press, Cambridge, England, first edition, 1988.
- [367] Daniel Francis Walczyk. Design and implementation of an experimental computer-controlled single-axis manipulator. Master's thesis, Rensselaer Polytechnic Institute, Troy, New York, August 1991. Kevin C. Craig, advisor; see also Craig *et alii* [69–73, 77–82, 147, 355, 372, 378].
- [368] Q. F. Wei, P. S. Krishnaprasad, and W. P. Dayawansa. Modeling of impact on a flexible beam. In *J. IEEE Proc. Dec. Control*, WP12, pages 1377–1382, New York City, December 1993. Institute of Electrical and Electronics Engineers, Institute of Electrical and Electronics Engineers.
- [369] Shyh-Woei Weng and Kuu-Young Young. An impact control scheme inspired by human reflex. *J. Rob. Sys.*, 13(12):837–855, 1996.
- [370] M. Wiercigroch. A note on the switch function for the stick-slip phenomenon. *J. Sound and Vib.*, 175(5):700–704, 1994.
- [371] Allan S. Willsky, editor. *Stability of Adaptive Systems: Passivity and Averaging Analysis*. The MIT Press Series in Signal Processing, Optimization, and Control. Massachusetts Institute of Technology, Cambridge, Massachusetts, 1986.
- [372] Andrew B. Wright. *Techniques in Active Noise Control using Active Material-Based Actuators*. PhD thesis, Rensselaer Polytechnic Institute, Troy, New York, August 1996. Kevin C. Craig, advisor; see also Craig *et alii* [69–73, 77–82, 147, 355, 367, 378].
- [373] Jung-Hua Yang and Li-Chen Fu. Nonlinear adaptive control for a manipulator system with gear backlash. In Tao [332], pages 4369–4374.
- [374] Sangsik Yang and Masayoshi Tomizuka. Adaptive pulse-width control for precise positioning under influence of stiction and Coulomb friction. In *Proc. Amer. Control Conf. ACC*, WA6, pages 188–193. American Control Council, American Control Council, 1987. See also Tomizuka *et alii* [197, 326, 356, 357].
- [375] Sangsik Yang and Masayoshi Tomizuka. Adaptive pulse width control for precise positioning under the influence of stiction and Coulomb friction. *ASME J. Dyn. Sys., Meas., and Control*, 110:221–227, September 1988. See also Tomizuka *et alii* [197, 326, 356, 357].
- [376] Y. P. Yang and J. S. Chu. Adaptive velocity control of DC motors with Coulomb friction identification. *ASME J. Dyn. Sys., Meas., and Control*, 115:95–102, March 1993.
- [377] A. S. Yigit. On the use of an elastic-plastic contact law for the impact of a single flexible link. *ASME J. Dyn. Sys., Meas., and Control*, 117:527–533, December 1995.
- [378] Andrew Yoder, Kevin [C.] Craig, and Richard N. Smith. Real-time compensation for thermal expansion in workpieces. In *Proc. Japan-USA Symp. on Flex. Auto.* [13]. See also Craig *et alii* [69–73, 77–82, 147, 355, 367, 372].

- [379] Hsien-I You and Jeng-Hong Hsia. The influence of friction-speed relation on the occurrence of stick-slip motion. *ASME J. Trib.*, 117:450–455, July 1995.
- [380] K. Youcef-Toumi and D. A. Gutz. Impact and force control: Modeling and experiments. *ASME J. Dyn. Sys., Meas., and Control*, 116:89–98, March 1994.
- [381] J. Yuh and D. K. Tissue. Discrete-time adaptive control for mechanical manipulators having a joint compliance. *J. Rob. Sys.*, 8(5):745–765, December 1991.
- [382] Xuejun Zhai, G. Needham, and L. Chang. On the mechanism of multi-valued friction in unsteady sliding line contacts operating in the regime of mixed-film lubrication. *ASME J. Trib.*, 119:149–155, January 1997.
- [383] J. H. Zhang. Spectral analysis for systems with hysteretic restoring force. *J. Mech. Sys. and Sig. Proc.*, 10(1):19–28, 1996.
- [384] Yimin Zhang, Bangcun Wen, and Suhuan Chen. Eigenvalue problem of constrained flexible multibody systems. *Mech. Res. Comm.*, 24(1):11–16, 1997.

## Appendix A

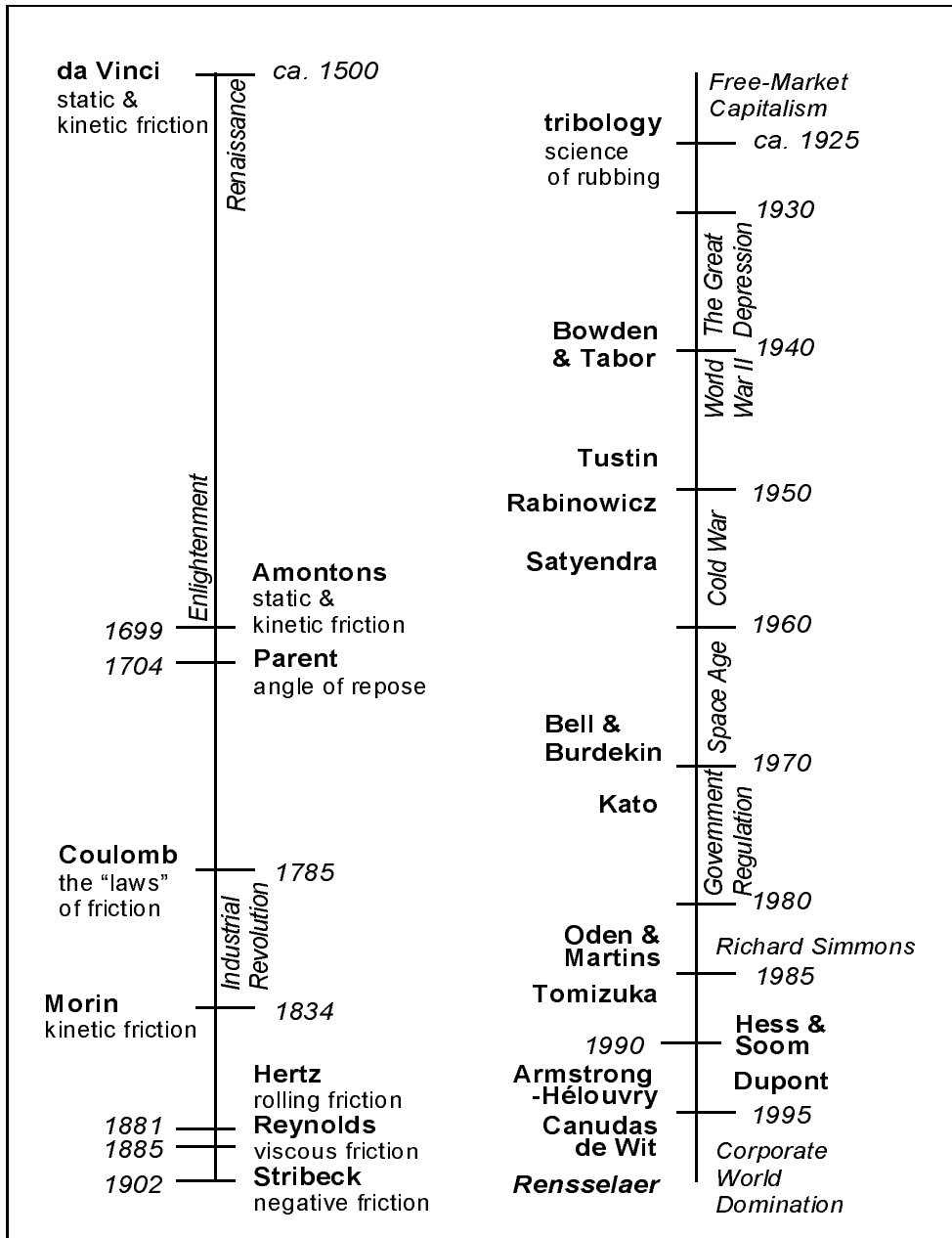


Figure A.1: A timeline of significant discoveries in the history of friction.

## Appendix B

### Software Code.

#### B.1 How to Obtain and Use the Software.

The Simulation code and Matlab<sup>®</sup> software is available via Rensselaer's mechatronics research website, where it can be downloaded using any internet browser. The main address for the website is

<http://www.meche.rpi.edu/research/mechatronics>

The C code is copyrighted by the author and may be licensed for use upon written request.

#### B.2 Simulation Code.

##### B.2.1 Description.

The simulation code was developed using the AutoLev<sup>™</sup> application designed by Thomas Kane and David Levinson to complement Kane's method of dynamics analysis [181]. The AutoLev<sup>™</sup> code listed in §B.2.3 defines the system's generalised coordinates and constraints on those coordinates, and using the laws of rigid-body kinematics then derives the equations of motion for the system. To make the simulation as highly configurable as it is, numerous AutoLev<sup>™</sup> scenarios were developed, each with a different set of constraints describing the various possible types of coupling between the subsystems "A", "B", and "C" of the test bed. AutoLev<sup>™</sup> has the ability to generate FORTRAN or C code to iterate the equations of motion (using a Runge-Kutta integrator) and thereby derive a time response of the system's behaviour. For this work, C code was generated for each scenario, and then all the possible scenarios were amalgamated by hand into one piece of simulation code, by combining the redundant code sections together, and using logic branches to differentiate differing code sections for each of the possible scenarios.

##### B.2.2 Instructions for Use.

The simulation is performed by entering the relevant parameter values into the file named `Simulate.in`. This input file provides the simulation with the necessary configuration information to generate a time response.

Once the input file is updated, the simulation programme `Simulate.exe` can be executed. The executable file is designed to be run under the Microsoft<sup>®</sup> Disk Operating

System (MS-DOS<sup>®</sup>). Basic parameter values will be displayed, along with the simulation time. The simulation is finished once the simulation time reaches the specified simulation end time given in the input file. The time responses will be saved under the filename `Simulate.dat`.<sup>81</sup>

The simulation speed will decrease with increasing system complexity and/or non-linearity, decreasing integration timestep size, and minute displacements. If the system oscillation settles before the specified end time, for example, then the simulation will slow down markedly when the system velocities approach zero. In such circumstances the user may press any key on the keyboard and the simulation will be prematurely ended, and the data up to that point retained in `Simulate.dat`. If the integrator has problems continuing the simulation, the programme will abort itself and display the reason why.

The integrator is sensitive to the timestep size used for any given system with nonlinearities. Generally, a good rule-of-thumb is to decrease the stepsize as the degree of nonlinearity increases. Conversely, simple systems retain sufficient precision with relatively large stepsizes. In any case, be certain to save as few points as possible to retain the analysability of the response data, but no fewer, as this will conserve disk space. For example, accurate peak detection requires that the user should save at least on the order of 20-50 datapoints per oscillation cycle.

### B.2.3 Dynamics Analysis Code (AutoLev<sup>TM</sup>).

- `Simulate.al`: Test bed dynamics analysis.

### B.2.4 Simulation Code (ANSI c).

- `Simulate.c`: Simulation of mechanical positioning test bed behaviour.
- `Simulate.h`: Header file for above C code.
- `Simulate.in`: Input datafile for use with `Simulate.exe`.
- `TestBed.in`: Input datafile containing parameters for Rensselær's mechanical positioning test bed.

## B.3 Data Acquisition Code (c).

### B.3.1 Description.

The data acquisition code allows the user to interface with a dynamic system having a position feedback encoder, and a motor for PD feedback. The proportional and derivative

---

<sup>81</sup>Note that if this file already exists then it will be overwritten!

feedback constants P and D may be changed as necessary to produce a variety of combinations for parametric harmonic oscillation of the dynamic system. The C language was used because of all the higher-level computer languages, C provides the most direct access to the computer's hardware resources (through the use of pointers and in-line assembly code).

Because the parametric harmonic oscillation method requires accurate measurement of velocity for the derivative feedback, a very stable sampling period was necessary. This is confounded on the IBM<sup>®</sup> PC by the MS-DOS<sup>®</sup>, which executes various background tasks to maintain the general functionality of the computer, like refreshing the output display, checking the keyboard for input, and writing data to the hard drive. These processes may be initiated by the programmer, but exactly when they occur, and how long they take, is non-deterministic. The actual timing variability due to these background processes results in timing jitter and data glitches which effectively corrupt the timeline of the data or the data themselves. Furthermore, MS-DOS<sup>®</sup> is configured to perform these functions at a speed of only about 55 Hertz, which is generally (far) too slow for accurate data acquisition and/or system feedback control.

To remediate this problem, the data acquisition programme was first developed around an inexpensive, popular *real-time kernel* called  $\mu\text{C}/\text{OS}$  [200]. The kernel is itself an operating system which can be used to schedule time-critical tasks to ensure that each is accomplished in the available time (assuming this is possible). It does this by executing partial portions of code in turn, according to the priorities assigned to them. In essence, this is the art of *multi-tasking*, and the real-time kernel allows us to perform these multiple tasks all at once, by dividing the computer's attention between them, unlike MS-DOS<sup>®</sup>, which can only perform tasks sequentially. The second key to performing the data acquisition in real time was to then speed up the computer's clock from 55 Hertz to about 140 Hertz or more. This last trick is accomplished by reprogramming the real-time clock on the IBM<sup>®</sup> PC (the so-called "Timer 0" counter) to generate interrupts at some faster rate than the default, and then to run the MS-DOS<sup>®</sup> housekeeper (which performs the required background functions described before) at the expected customary rate of 55 Hz. In this manner, the  $\mu\text{C}/\text{OS}$  kernel can do its job transparently as far as the DOS is concerned, allowing DOS functions (like disk and console writes) to continue to be used, but run the rest of the control loop at a higher pace than is normally possible.

The only caveat to this approach is that the user must be careful not to call any DOS routines in a re-entrant manner, that is, to try to execute the same DOS call more than once before the first call is finished, which would confuse the system and "lock up" the computer. During testing it was found that the data can be corrupted by re-entrancy when writing is performed to the hard drive due to latency in the DOS. To avoid this problem, while

retaining the ease-of-use of DOS write calls used by the likes of C's `fprintf()` function, the data was first acquired to a RAM disk (setup by loading `RAMDrive.sys` in the `Config.sys` file), and then copied over to the hard drive for permanent storage. Writing to the hard drive directly can cause serious damage to the hard drive's file allocation tables, should an unexpected DOS reentrancy occur due during the real-time kernel use. The user is therefore exhorted to write to a RAM disk rather than a hard drive. Using a RAM disk has the further advantage of allowing simple `fprintf()` function calls, even for very large datafiles, rather than requiring an extended memory driver (like `HiMem.sys` and/or `EMM386.exe`) with associated code to write data files exceeding the infamous 640 kB lower memory barrier.

Even with these precautions, the datafiles may contain occasional glitches. In the author's experience, these glitches are limited to either very infrequent and sporadic data corruption for a duration of about 10-100 milliseconds (which occurs perhaps every 100 datafiles), and/or infrequent timeline corruption which occurs for only one datapoint at-a-time (occurring perhaps every 20-30 datafiles). The former error can not be corrected, and the user must discard or repeat the particular oscillation experiment. The latter error is correctable via linear interpolation, and is automatically corrected by the Matlab<sup>®</sup> analysis software presented in §B.5.3.

A final caution applies to the manipulation of the system clock: after running the acquisition code, the user should check the system clock and adjust it to reflect the correct time. This can be done via MS-DOS' `time` utility, or in Windows<sup>®</sup> under `Start -> Settings -> Control Panel -> Date/Time`, and should be done immediately once the operating system is restored and acquisition is finished, in order to avoid confusing make utilities and file copying functions which depend on timestamp comparisons.

### **B.3.2 Instructions for Use.**

Before the acquisition programme is run, the correct hardware connections should be made to interface the computer with the dynamic system under investigation. The National Instruments<sup>®</sup> Lab-PC+<sup>™</sup> is assumed for the actual acquisition; D/A converter channel 0 ("DAC0") is used for the motor feedback, and should be connected to the PMI<sup>®</sup> amplifier's 10-V range command input via a filter (to remove the high frequencies caused by the output quantisation); A/D converter channel 0 ("ACH0") is used to measure the actual current produced by the amplifier, and should run from the amplifier current monitor terminals, again via a filter (to remove any high-frequency interference). The filter used by the author was a configurable eighth-order low-pass Chebychev filter, set for a cut-off frequency of about 120 Hz on both ADC0 and ACH0. The wires between the amplifier and the DC motor should be Gaussian-shielded with a ground at the amplifier end only (to eliminate high-

frequency interference caused by the 40-kHz switching action of the amplifier). Lastly, an encoder to measure displacement should be connected to input channel 0 of the Technology 80<sup>®</sup> TE5312B quadrature decoder board.

The programme itself can be configured for use with different systems by selecting the proper parameter set in C header file `Friction.h`. Two sets pre-defined by the author are the `#pragma` directives `PENDULUM` and `TESTBED`, for the pendulum and test bed systems, respectively, as documented within the header file itself (see §B.3.3). Once the proper set has been selected, the programme must be re-compiled using an ANSI C compiler. The executable must be linked with start-up code, and `CODE` and `DATA` segments (80x86 architecture) for the “large” memory model. The executable should link in the National Instruments library `NI.lib`, and the decoder board library `TE5312.obj`. A project make-file, called `Friction.mak`, which constructs the executable, is available from the author. Executable versions for both the systems studied in this thesis have been compiled, and are called `Pendulum.exe` and `TestBed.exe`. Note that other hardware for the data acquisition can be used by making appropriate changes to the C code and re-compiling for the appropriate platform.

The acquisition programme should be copied to, and run from, a RAM disk as recommended above. The programme uses a National Instruments data acquisition board and therefore the configuration file `ATBrds.cfg` must be located in the root directory of the drive from which the programme is executed (in this case, the configuration file should reside in, or be copied to, the root directory of the RAM disk containing the executable). Since RAM disks are wiped clean with every system (re)boot, these files will need to be copied over afresh after the system is (re)booted.

When the programme is run, it first measures and compensates for any DC offset in the motor command via the current sense feedback. Once this is done, the user is asked to calibrate the displacement range by informing the programme of the displacement extremes. Next, the user is prompted for a filename base under which to save the data acquired; this filename should follow MS-DOS<sup>®</sup> naming conventions, and the three-letter file extension (including the dot) should be omitted (if the extension is entered then the file cannot be created). The first data file will be assigned the extension `.001`, the second `.002`, and so on. Each time a data file is deemed acceptable by the user, the file extension will automatically be incremented. It should lastly be noted that using the [BackSpace] key during entry of the filename will cause a problem because the `scanf()` function used to enter this information in the C programme does not handle this key. If the filename is not typed in correctly the first time around, the user must abort acquisition and run the programme anew.

Once the filename has been entered, the user may carry the proportional and derivative

feedback parameters. When these are set as desired, the [SpaceBar] can be pressed to start parametric harmonic oscillation. The programme automatically detects when the oscillation has settled, and then prompts the user to accept or reject the oscillation. If the oscillation is rejected, the experiment may be repeated. Alternately, pressing the [x] key will exit the programme. During an oscillation, any key may be pressed to abort that oscillation. Lastly, if the motor command exceeds a safe value then the oscillation will abort automatically (this is possible when applying negative damping with a high value for the derivative feedback). A file with the extension .PD will be maintained, summarising the feedback parameters and other information for each oscillation.

The data must be acquired in a specific manner in order to be analysed by the Matlab<sup>®</sup> routines. The proper order involves recording pairs of data files, one for oscillations with a “positive” initial displacement, and the other with a “negative” initial displacement (the order doesn’t matter, as long as the user is consistent). Also, the derivative feedback must be varied in equal steps for each proportional feedback value; after a set of different values for  $D_i$  have been made for a certain value of  $P_i$ , then the proportional feedback may be changed to the next value, for which the set of previous values  $D_i$  is repeated.  $P_i$  can then be changed again, in a step equal to the previous change in  $P_i$ , and so on. This produces a format required by the Matlab<sup>®</sup> files; further details can be found in the Matlab<sup>®</sup> scripts themselves.

### B.3.3 Data Acquisition Code.

- `Friction.c`: Parametric Harmonic Oscillation identification.
- `Friction.h`: Header file for above C code.
- `Friction.mak`: Makefile for generating `Friction.exe`.

## B.4 c Support Code Listings.

### B.4.1 Data-Acquisition Header Files.

- `NI.h`: Definitions for National Instruments<sup>®</sup> data-acquisition products.
- `TE5312.h`: Definitions for Technology 80<sup>®</sup> TE5312B quadrature decoder board.

### B.4.2 System Header Files.

- `ANSI.h`: Header file for American National Standards Institute compliance.
- `Error.h`: Error handler macro.
- `FloatFix.h`: Borland-specific macro to force floating-point format link.

- `IBM-PC.h`: Header file for IBM personal computers (AT, XT and above).
- `Macros.h`: Some handy-dandy macros written by the author.
- `MSDOS.h`: Header file for MS-DOS<sup>®</sup> operating system.
- `PIT8253.h`: Definitions for the Intel<sup>®</sup> 8253 programmable interrupt timer.
- `PPI8255.h`: Definitions for the Intel<sup>®</sup> 8255 programmable peripheral interface.
- `TypeDefs.h`: Common type definitions.

## B.5 Data Analysis Code (Matlab<sup>®</sup>).

### B.5.1 Description.

Data analysis was performed using Matlab<sup>®</sup> because it affords much better flexibility in the revision and debugging process than compiled code does, and has a large library of functions already available for analysis. A number of Matlab<sup>®</sup> scripts (m-files) were written to perform the friction identification described in this thesis. `FreeLID.m` identifies the asymmetric kinetic and viscous friction using the extended logarithmic decrement method, `FreeHID.m` identifies the symmetric viscous friction using the Hilbert Transform, and `FreeWID.m` identifies the symmetric viscous or kinetic friction using the Wavelet transformation. In addition to these files, numerous support routines were written, and are also listed here. All the routines are available from the author, and should eventually be available at MathWorks' FTP archive as well ([www.mathworks.com](http://www.mathworks.com)).

### B.5.2 Instructions for Use.

The Matlab<sup>®</sup> scripts are self-documenting. To learn the implementation for a certain m-file, simply type "help" followed by the name of the m-file at the Matlab<sup>®</sup> user prompt, as with any other Matlab<sup>®</sup> function. The user may need to modify the Matlab<sup>®</sup> path so Matlab<sup>®</sup> knows where to locate the identification and support routines.

Each type of analysis estimates the damped natural frequency of the parametric harmonic oscillation under study, the damping, the undamped natural frequency, and the kinetic friction. Typically the analyses offer estimates with about five per cent error for clean oscillation data.

### B.5.3 Friction Analysis Code.

- `FAnalyse.m`: Analyse a set of parametric harmonic oscillations (PHOs).
- `FMixLR.m`: Mix asymmetric datafiles from a PHO experiment dataset.

- `FProcess.m`: Process PHO experiment dataset for friction identification.
- `FreeHID.m`: Identify friction using the Hilbert Transform.
- `FreeLID.m`: Identify asymmetric kinetic and viscous friction using the logarithmic decrement method.
- `FreeWID.m`: Identify friction using the Morlet Wavelet transformation.

## B.6 Matlab<sup>®</sup> Support Code Listings.

### B.6.1 Control System Design Utilities.

- `Step2.m`: Plot step response of continuous (s-domain) system.

### B.6.2 General Functions.

- `AskPrint.m`: Prompt user whether or not to print current plot.
- `DispLine.m`: Display a line, which can be either blank or some message.
- `DispVar.m`: Display variable and its value on one line.
- `GetDef.m`: Prompts user for input or default acceptance.
- `StrPad.m`: Pad a string with the specified character.
- `Wait4Key.m`: Prompt the user for a keystroke to continue m-file processing.
- `Yes.m`: Answers questions.

### B.6.3 Math Functions.

- `IsEven.m`: Tells whether a number is an even integer or not.
- `IsOdd.m`: Tells whether a number is an odd integer or not.
- `PerDiff.m`: Difference of permuted array elements.
- `PerSum.m`: Summation of permuted array elements.
- `WLSFit.m`: Weighted least-squares fit.
- `WMean.m`: Compute the weighted mean (or center of gravity) of a vector.

### B.6.4 Plotting Functions.

- `Stairs2.m`: Discrete staircase plot.

### B.6.5 Signal Processing Functions.

- `BeatFreq.m`: Finds the beat frequency of the sum of two oscillating functions.
- `Envelope.m`: Finds the envelope of an arbitrary function.
- `FindPeak.m`: Find the peaks (and valleys) of an arbitrary function.
- `OverSht.m`: Finds the per-cent overshoot to a constant reference input.
- `PhDiff.m`: Finds the phase difference between two oscillations.
- `Rising.m`: Finds the rise time for response to constant reference input.
- `Settling.m`: Finds the settling time for a constant-input response.
- `Smooth.m`: Smooth data.
- `Steady.m`: Finds the steady-state region of a given oscillation.
- `ZCross.m`: Find the zero crossings of an arbitrary function.

Appendix C

**Test Bed Counterbalance Modifications.**



